

A REGIONAL APPROACH TO ANALYZING THE ATMOSPHERIC IMPACTS OF
COPPER-NICKEL SMELTING IN NORTHEASTERN MINNESOTA

REGIONAL COPPER-NICKEL STUDY
MINNESOTA ENVIRONMENTAL QUALITY BOARD
MARCH, 1980

A REGIONAL APPROACH TO ANALYZING THE ATMOSPHERIC IMPACTS OF
COPPER-NICKEL SMELTING IN NORTHEASTERN MINNESOTA

A THESIS
SUBMITTED TO THE FACULTY OF THE GRADUATE SCHOOL
OF THE UNIVERSITY OF MINNESOTA

by

INGRID MARIA RITCHIE

IN PARTIAL FULFILLMENT OF THE REQUIREMENTS
FOR THE DEGREE OF
DOCTOR OF PHILOSOPHY

MARCH, 1980

© Copyright by Ingrid Maria Ritchie 1980
All Rights Reserved

TABLE OF CONTENTS

	PAGE
List of Tables	vi
List of Figures	xi
CHAPTER	
1. Summary and conclusions	1
2. Introduction	23
2.1. Background	23
2.2. Issues	25
2.3. Research project	27
3. Application to copper-nickel smelting in northeastern Minnesota	30
3.1. Area of interest	30
3.2. Air quality region receptors and meteorological stations	33
3.3. Regional climatology/meteorology	33
3.3.1. Temperature	36
3.3.2. Wind direction and wind speed	36
3.3.3. Precipitation	38
3.3.4. Atmospheric stability and mixing height	40
3.4. Regional emissions inventory	44
3.4.1. stack parameters	47
3.5. Existing legal framework	49
3.6. Smelter models	56
3.6.1. Sulfur emissions	56
3.6.2. Particulate emissions	67
3.6.3. Elemental constituents	74
3.6.4. Smelter stack parameters	77
4. Health literature review	80
4.1. Total suspended particulates and sulfur oxides	80
4.2. Copper	84
4.3. Cadmium	86
4.4. Lead	87
4.5. Mercury	90
4.6. Arsenic	91
4.7. Nickel	93
4.8. Population at risk	95
5. Modified gaussian model	97
5.1. Introduction	97
5.2. Modified gaussian model flowchart	99
5.3. Theory	106
5.3.1. Wind speed at stack height	106
5.3.2. Plume rise	108
5.3.3. Diffusion	112
5.3.4. Oxidation rate	118
5.3.4.1. laboratory studies	118
5.3.4.2. field studies	123

5.3.4.3.	plume chemistry modeling	125
5.3.5.	Removal processes	127
5.3.5.1.	dry deposition	127
5.3.5.2.	wet removal	133
5.3.6.	Acidity of precipitation	146
5.3.7.	Dynamics of dispersion	148
5.3.7.1.	storm model	151
5.3.7.2.	losses	152
5.3.7.3.	receptor concentration	154
5.3.7.4.	receptor deposition	154
5.3.8.	Cost	155
6.	Model verification and sensitivity analysis	157
6.1.	Accuracy of dispersion models	157
6.2.	Modified gaussian model verification	159
6.2.1.	Introduction	159
6.2.2.	Comparison to Sudbury data	159
6.2.2.1.	description of Sudbury area	159
6.2.2.2.	sources	160
6.2.2.3.	receptors	162
6.2.2.4.	inputs to the model	165
6.2.2.5.	measured deposition	167
6.2.2.6.	predicted deposition	168
6.2.2.7.	measured ambient air quality	174
6.2.2.8.	predicted ambient air quality	175
6.2.3.	Comparison to other models	181
6.2.3.1.	comparison between the standard gaussian model and the modified gaussian model	181
6.2.3.2.	comparison between the numerical model and the modified gaussian model	181
6.2.4.	Summary	185
6.3.	Sensitivity analysis	187
6.3.1.	Rainfall rate	189
6.3.2.	Rainfall duration	189
6.3.3.	Average wind velocity, wind direction, and standard deviation of the wind direction	192
6.3.4.	Washout coefficient	196
6.3.5.	Deposition velocity	196
6.3.6.	Ambient air background concentration	199
6.3.7.	Oxidation rate	203
6.3.8.	Summary	203
7.	Characterization of the copper-nickel study region	207
7.1.	Sulfur oxides	207
7.1.1.	Sources, present and 1985	207
7.1.2.	Ambient SO ₂ concentrations	214
7.1.2.1.	regulatory analysis--annual average SO ₂ concentrations	217
7.1.2.2.	regulatory analysis--maximum 24-hour SO ₂ concentrations	222

7.1.3.	Ambient sulfate concentrations	229
7.1.4.	Sulfate deposition	231
7.2.	Particulates	242
7.2.1.	Sources, present and 1985	246
7.2.2.	Ambient particulate concentrations	251
7.2.2.1.	regulatory analysis--annual average TSP concentrations	253
7.2.2.2.	regulatory analysis--maximum 24-hour TSP concentrations	260
7.2.3.	Particulate deposition	264
8.	Impact analysis for sulfur emissions	271
8.1.	Ambient SO ₂ concentrations	272
8.1.1.	Annual concentrations	272
8.1.2.	24-hour concentrations	285
8.2.	Ambient sulfate concentrations	317
8.3.	Sulfate deposition	320
9.	Impact analysis for particulate emissions	325
9.1.	Ambient particulate concentrations	325
9.2.	Metals	334
9.2.1.	Ambient air concentrations	334
9.2.2.	Deposition	337
10.	Soil and water impacts	341
10.1.	Soil impacts	341
10.2.	Water impacts	348
10.2.1.	Snowpack concentrations	349
10.2.2.	Stream and lake concentrations	353
10.2.3.	Sulfate deposition onto area lakes	357
	Bibliography	362
	Appendix A. Modified gaussian model program	386
	Appendix B. List of abbreviations	393

LIST OF TABLES

TABLE	PAGE
1. Receptor coordinates for the modified gaussian model	35
2. Monthly mean and annual temperatures for 1976-77 compared to the normal temperatures (^o C) at the regional meteorological stations	38
3. Monthly and annual average wind speed (km/hr) for 1976-77 compared to normals at the regional meteorological stations	39
4. Monthly precipitation (cm) for 1976-77 compared to normals at the regional meteorological stations	41
5. Monthly snowfall (cm) for 1976-77 compared to normals at the regional meteorological stations	42
6. Annual stability class occurrences, International Falls	42
7. Mean seasonal and annual morning and afternoon mixing heights and wind speeds at International Falls	43
8. Point sources included in the emissions inventory	46
9. Representative stack data for the regional emissions point source inventory	50
10. Allowable PSD increments for Class I and Class II areas	53
11. Summary of SO ₂ emissions from three smelter configurations producing 100,000 mtpy of copper and nickel metal	65
12. Comparison of sulfur mass balances for the base case, option 1, and option 2 smelters to other domestic smelters	68
13. Stack and fugitive particulate emissions from a smelter complex producing 100,000 mtpy of Cu and Ni metal	75
14. Prioritization of elements in the Duluth-Gabbro ore	76
15. Smelter stack input data	79
16. Ambient air quality standards for sulfur oxides and total suspended particulates	85
17. Population estimates for Cook, Lake, and St. Louis counties, July 1, 1975	95
18. Number of beds in licensed and certified health care facilities in Cook, Lake, and St. Louis counties, 1976	96
19. Smith-Singer diffusion parameters--Brookhaven data	116
20. Plume touchdown distances	119
21. Mechanisms that convert sulfur dioxide to sulfate	120
22. Reported SO ₂ oxidation rates	121
23. Mass median size and dry deposition velocity data	130
24. SO ₂ dry deposition velocity data	132

25.	Washout ratios for particulates used in the modified gaussian model	142
26.	Effective source terms resulting from the localized moving storm	153
27.	Sudbury point source emissions data, 1973-1974	161
28.	Sudbury receptor coordinates	162
29.	Dry deposition velocity and ambient air background concentrations used as input parameters for the Sudbury region modified gaussian model validation	164
30.	Sudbury region meteorological stations and coordinates	164
31.	Analytical reproducibility and detection limits for SO ₄ ⁼ , Cu, Ni, Pb, and Fe	168
32.	Summary statistics, Sudbury validation	169
33.	Student's T-test for receptor locations, Sudbury validation	172
34.	Summary of precision bounds, quantile test	174
35.	SO ₂ receptor-source distances and angular direction of receptors from east	175
36.	Measured and predicted monthly mean and maximum ₃ 24-hour SO ₂ concentrations in the Sudbury airshed, µg/m ³	178
37.	Comparison between the standard gaussian model and the modified gaussian model using stack emissions to predict SO ₂ concentrations for selected single day runs, µg/m ³	182
38.	Atikokan 800 MW power plant emissions used for both the modified gaussian model and numerical model simulations	185
39.	Comparison between numerical model and the modified gaussian model for the proposed 800 MW Atikokan power plant	186
40.	Sensitivity of ambient air concentrations and depositions to ± 15% change in the rainfall rate	190
41.	Sensitivity of ambient air concentrations and depositions to ± 15% change in rainfall duration	191
42.	Sensitivity of ambient air concentrations and depositions to ± 20% change in the average wind direction	193
43.	Sensitivity of ambient air concentrations and depositions to ± 20% change in the average wind velocity	194
44.	Sensitivity of ambient air concentrations and depositions to ± 20% change in the standard deviation of the wind direction	195
45.	Sensitivity of ambient air concentrations and depositions to ± 20% change in the washout coefficient	197
46.	Dry deposition velocity values for sensitivity analysis	199

47.	Sensitivity of ambient air concentrations and depositions to deposition velocity	200
48.	Background concentrations used in the sensitivity analysis compared to the range of values in the literature	201
49.	Sensitivity of ambient air concentrations and depositions to doubling the ambient air background concentrations input	202
50.	Ambient air concentrations and depositions at 2.0%/hr and 0.02%/hr oxidation rates compared to the best guess values	204
51.	Sensitivity of ambient air concentrations and depositions to uncertainties in the rainfall rate, rainfall duration, wind velocity, wind direction, standard deviation of the wind direction, and the washout coefficient	206
52.	Regional SO ₂ emissions inventory used for sources emitting more than 100 mtpy of SO ₂	209
53.	1976 point source SO ₂ emissions inventory summary by source category for the air quality study region and the seven-county metropolitan area	213
54.	Estimated SO ₂ area source emissions for 1976, based on fuel usage (metric tons)	216
55.	Difference between the baseline concentration and the highest and 2nd highest 24-hour concentrations in a Class I area (µg/m ³)	225
56.	Summary of measured sulfur content of atmospheric particulates at eight study area sites, expressed as sulfate	230
57.	Annual sulfate deposition based on bulk deposition data, kg/ha/yr	236
58.	Measured and predicted local sulfate deposition (kg/ha/yr)	238
59.	Calculated dry deposition rates and predicted total sulfate deposition (kg/ha/yr)	239
60.	Predicted wet and dry sulfate deposition from local point sources (kg/ha/30 day)	240
61.	Predicted annual deposition of sulfate at various receptor sites due to point source emissions in the Region (kg/ha/yr)	245
62.	Regional particulate emissions inventory used for sources emitting more than 100 mtpy	247
63.	1976 point source particulate emissions inventory summary by source category for the air quality study region and the seven-county metropolitan area	250

64.	Adjusted annual geometric means at TSP sample sites, 1977	251
65.	The effect of snow cover and mining activity on TSP levels in the study area	252
66.	Percent of predicted 24-hour concentrations that are within a factor of 10 of the measured concentrations	257
67.	Summary of 24-hour TSP measurements during the 1976-77 sampling period which exceeded the primary ($260 \mu\text{g}/\text{m}^3$) and secondary ($150 \mu\text{g}/\text{m}^3$) ambient TSP standards	263
68.	Predicted values exceeding the 24-hour TSP PSD ₃ increment of $37 \mu\text{g}/\text{m}^3$ in Class II areas. Values in $\mu\text{g}/\text{m}^3$.	264
69.	Predicted annual deposition of particulates at various receptor sites due to point source emissions in the region (kg/ha/yr)	270
70.	Summary of SO ₂ annual concentrations at selected sites for the various copper-nickel development cases, with a comparison to 1977 and 1985 predictions without copper-nickel development	286
71.	Summary of 24-hour maximum and second high SO ₂ concentrations at selected sites for copper-nickel development cases in 1985	298
72.	A summary of the predicted concentrations greater than the Class I and Class II 24-hour PSD ₃ increments in 1985 with the various smelter models ($\mu\text{g}/\text{m}^3$)	301
73.	Summary of the number of times the 24-hour SO ₂ Class I PSD increment is predicted to be exceeded by month at all Class I receptor sites based on day-by-day simulations	309
74.	Meteorology for selected single day runs of the modified gaussian model	310
75.	Predicted annual average sulfate concentrations for three smelter models located south of Babbitt and measured sulfate concentrations at selected sites	319
76.	Predicted annual average sulfate deposition rates for three smelter models located south of Babbitt; rates without a smelter are included for comparison	321
77.	Predicted annual sulfate deposition resulting from the three smelter models, 1977 regional sources, 1985 regional sources, kg/ha/yr	324
78.	Comparison between measured and predicted ambient air concentrations of selected metal species, ng/m ³	335
79.	Maximum predicted 24-hour ambient concentrations of metals downwind of the option 1-option 2 smelter model, assuming particulates have the elemental composition of the concentrate, compared to measured values in the region, $\mu\text{g}/\text{m}^3$	337

80.	Mean annual measured and predicted deposition rates for the option 1-option 2 smelter at regional receptors, g/ha/yr	339
81.	Predicted annual metal deposition for the option 1-option 2 smelter, g/ha/yr	340
82.	Comparison between background and predicted Cu and Ni concentrations in soils after 25 years of option 1 smelter operation	347
83.	Susceptibility of lakes and streams to acidification	349
84.	Comparison between measured average snowpack concentrations and predicted snowpack concentrations of selected species	353
85.	Summary comparison between snowpack concentration and stream concentration of selected species at low flow, spring flow, and highest concentrations observed	354
86.	Comparison between measured and predicted deposition rates, stream, and lake concentrations resulting from the option 1 smelter	356
87.	Number of years required to titrate the alkalinity in a low and a high alkalinity lake with strong acid input for selected cases	360

LIST OF FIGURES

FIGURE	PAGE
1. Map of Minnesota's arrowhead region with definitions of various areas used by the regional copper-nickel study	31
2. Mn Cu-Ni development and resource zones within the study region	32
3. Air quality region receptors and meteorological stations	34
4. Annual average wind roses	37
5. Emissions inventory locations	45
6. Principal mining component relationships in the production of copper and nickel metal	55
7. Flowscheme for a copper-nickel smelter using a flash smelter furnace	57
8. Base case model sulfur balance for flash furnace with acid plant control of strong SO ₂ gas to 650 ppm SO ₂ , secondary hooding collection of weak SO ₂ gas to redirect it to the stack discharge	61
9. Option 1 model sulfur balance for flash furnace with acid plant control of strong gas to 650 ppm SO ₂ , secondary hooding collection of weak SO ₂ gas followed by scrubbing to 650 ppm SO ₂	62
10. Option 2 model sulfur balance for flash furnace with acid plant control of strong SO ₂ gas to 300 ppm SO ₂ , secondary hooding collection of weak SO ₂ gas, and scrubbing of acid plant tail gas plus collected weak SO ₂ gas to 143 ppm	63
11. Summary of modeled flash smelter SO ₂ emissions and emissions from other large SO ₂ sources	66
12. Model for stack emissions particulate balance for base case smelter/refinery complex	71
13. Model for stack emissions particulate balance for option 1 and 2	72
14. Summary of modeled flash smelter total particulate emissions and emissions from other large particulate sources	73
15. Flowchart of the modified gaussian model	100
16. Wind angle	102
17. Vertical diffusion	117
18. Horizontal diffusion	117
19. Sulfate removal model	139
20. SO ₂ rain removal model	145
21. Lagrangian coordinate system for dispersion	150

22.	Storm model	154
23.	Sudbury receptors	163
24.	Sudbury SO ₂ monitors and smelters	176
25.	Source category contributions to sulfur dioxide emissions by location	208
26.	1975 annual arithmetic mean SO ₂ concentration for selected measuring stations in the United States	215
27.	Predicted annual average SO ₂ concentration for the 1977 regional baseline case ² (μg/m ³)	218
28.	Predicted annual average SO ₂ concentrations for 1985 (μg/m ³)	219
29.	Predicted annual average SO ₂ concentrations for 1985 without Atikokan power plant (μg/m ³)	221
30.	Predicted maximum 24-hour SO ₂ concentrations for 1977 regional baseline (μg/m ³)	223
31.	Predicted maximum 24-hour SO ₂ concentrations for 1985 (μg/m ³)	224
32.	Box plots of predicted 24-hour ambient SO ₂ concentrations for 1977 and 1985 from local sources	227
33.	Annual frequency distribution of predicted 24-hour ambient SO ₂ concentrations for 1977 and 1985 at selected sites	228
34.	Box plots of 24-hour values predicted for ambient sulfate concentrations from local sources, 1977 and 1985	232
35.	Annual frequency distribution of predicted 24-hour average ambient sulfate concentrations, 1977 and 1985, at selected sites	233
36.	Monthly bulk sulfate deposition and precipitation at sampling sites	235
37.	Box plots of 24-hour values for predicted total sulfate deposition from local sources, 1977 and 1985	243
38.	Annual frequency distribution of predicted 24-hour sulfate deposition from local sources, 1977 and 1985, for selected sites	244
39.	Source category contributions to particulate emissions	248
40.	Geometric mean annual TSP concentrations	254
41.	Predicted annual geometric mean TSP concentrations for 1977 baseline (10 ⁻² μg/m ³)	255
42.	Predicted annual geometric mean TSP concentrations for 1985 (10 ⁻² μg/m ³)	258
43.	Predicted maximum 24-hour TSP concentrations for the 1977 baseline (μg/m ³)	261

44.	Predicted maximum 24-hour TSP concentrations in the region in 1985 ($\mu\text{g}/\text{m}^3$)	262
45.	Box plots of predicted 24-hour TSP concentrations	265
46.	Annual frequency distribution of predicted 24-hour TSP concentrations, 1977 and 1985, at selected sites	266
47.	Box plots of predicted 24-hour TSP deposition values	268
48.	Annual frequency distributions of predicted 24-hour TSP deposition values, 1977 and 1985, at selected sites	269
49.	Hypothetical smelter site and receptor sites used for analysis with modified gaussian model	274
50.	Base case smelter model predicted annual SO_2 concentrations ($\mu\text{g}/\text{m}^3$)	275
51.	Predicted annual SO_2 concentration option 1 smelter model ($\mu\text{g}/\text{m}^3$)	276
52.	Option 2 smelter model annual SO_2 concentration ($\mu\text{g}/\text{m}^3$)	277
53.	Predicted annual Class I, Class II, and regional SO_2 averages with selected smelter cases (based on a hypothetical smelter site 3 miles south of Babbitt)	279
54.	Predicted annual SO_2 concentrations for 1985 with base case smelter ($\mu\text{g}/\text{m}^3$)	281
55.	Predicted annual SO_2 concentrations for 1985 with option 1 smelter ($\mu\text{g}/\text{m}^3$)	282
56.	Predicted annual SO_2 concentration for 1985 with option 2 smelter ($\mu\text{g}/\text{m}^3$)	283
57.	Predicted annual SO_2 concentration for 1985 (without Atikokan) with option 1 smelter ($\mu\text{g}/\text{m}^3$)	284
58.	Predicted maximum 24-hour SO_2 concentrations from the base case smelter ($\mu\text{g}/\text{m}^3$)	288
59.	Predicted maximum 24-hour SO_2 concentrations from the option 1 smelter model ($\mu\text{g}/\text{m}^3$)	289
60.	Predicted maximum 24-hour SO_2 concentrations from the option 2 smelter model ($\mu\text{g}/\text{m}^3$)	290
61.	Predicted maximum 24-hour SO_2 concentrations in 1985 with base case smelter model ($\mu\text{g}/\text{m}^3$)	292
62.	Predicted maximum 24-hour SO_2 concentrations in 1985 with the option 1 smelter model ($\mu\text{g}/\text{m}^3$)	293
63.	Predicted maximum 24-hour SO_2 concentrations in 1985 with the option 2 smelter model ($\mu\text{g}/\text{m}^3$)	294
64.	Predicted maximum 24-hour SO_2 concentrations in 1985 (without Atikokan) with the option 1 smelter model ($\mu\text{g}/\text{m}^3$)	295

65.	Smelter impact areas where the 24-hour maximum SO ₂ concentrations resulting from the various Cu/Ni smelter models are different from 1985, no Cu/Ni development	297
66.	Summary of highest and 2nd highest 24-hour SO ₂ concentration predicted at any receptor in Class I and Class II areas, respectively, for various scenarios	299
67.	24-hour ambient SO ₂ concentrations greater than the Class I PSD increment, 1985 without Cu/Ni development	303
68.	24-hour ambient SO ₂ concentrations greater than the Class I PSD increment, 1985 excluding Atikokan	304
69.	24-hour ambient SO ₂ concentrations greater than the Class I PSD increment, 1985 with base case smelter model	305
70.	24-hour ambient SO ₂ concentrations greater than the Class I PSD increment, 1985 with option 1 smelter model	306
71.	24-hour ambient SO ₂ concentrations greater than the Class I PSD increment, 1985 with option 2 smelter model	307
72.	Maximum predicted 24-hour SO ₂ concentrations along the combined plume centerline for the base case smelter model	311
73.	Maximum predicted 24-hour SO ₂ concentrations resulting from three model smelter cases	313
74.	Smelter siting zones surrounding Class I PSD areas (based on distances where the 24-hour Class I SO ₂ increment is not exceeded by the smelter alone, other applicable regional sources not included)	314
75.	Restrictions on smelter siting in MN Cu/Ni development zones based on SO ₂ concentrations on 5 single worst case days	316
76.	Predicted maximum 24-hour TSP concentrations from the base case smelter model located at a hypothetical site south of Babbitt (µg/m ³)	327
77.	Predicted maximum 24-hour TSP concentrations from the option 1-option 2 smelter model ₃ located at a hypothetical site south of Babbitt (µg/m ³)	328
78.	Predicted stack and fugitive contributions to 24-hour TSP concentrations along a combined plume centerline for the base case smelter model	330
79.	Predicted 24-hour maximum and 2nd high TSP concentrations in Class I and Class II areas for selected receptors	332
80.	Field plot and receptor locations for soil impact analysis	345
81.	Watershed and receptor locations	352

CHAPTER 1. SUMMARY AND CONCLUSIONS

The prospect of a new industrial development in northeastern Minnesota to recover copper and nickel raises the potential for major atmospheric impacts which may be categorized into human health, terrestrial ecosystem, and water quality.

This research project characterized northeastern Minnesota in terms of ambient air concentrations and deposition patterns of selected pollutants (sulfur dioxide, sulfate, total particulate, copper, nickel, arsenic, cadmium, lead, and mercury) for a base year, 1977, and a future year, 1985. These data were then used to assess the potential ambient air impacts of copper-nickel smelting in northeastern Minnesota in terms of the health, environmental, and regulatory issues.

The regional nature of the characterization and impact analysis tasks required an assessment tool that could be used to predict the atmospheric impacts of a mining industry on a several thousand square kilometer area which is already experiencing air quality impacts from existing activity within and outside of the region.

1.1. ATMOSPHERIC DISPERSION MODELING

Well-known short-range atmospheric dispersion models (Climatological Dispersion Model, CDM, and Texas Episodic Model, TEM) were used by Endersen⁶¹ to predict concentrations of SO₂ and particulates within 10 km of hypothetical smelter sites. Because of the distance limitations of the short-range models a longer-range model was developed which predicts concentrations and deposition rates of pollutants at distances up to 150 km from a source.

This model, the modified gaussian model, incorporates the processes of dry deposition, wet scavenging, and oxidation of sulfur dioxide gas to sulfate. Horizontal dispersion is approximated by the gaussian distribution, and vertical dispersion is assumed to be uniform from the ground to the mixing height.

The model can handle 25 sources, 50 receptors, 5 meteorological stations, and 25 pollutants. Required input data for sources include the source coordinates, stack height, source width, heat emissions rate, and pollutant emissions rate. The input data for pollutants include dry deposition velocity, washout ratio, and ambient air background concentration. Receptor data include receptor coordinates and start/stop times for computing.

The modified gaussian model was verified using deposition and ambient air data collected by Kramer^{121, 122, 123} around Sudbury, Ontario. The modified gaussian model was also compared to a well-known gaussian model, CDM, and to a numerical model developed by Ragland.¹⁹³

Generally, the predicted results were within a factor of two of the measured results at Sudbury. The model is not as accurate for single 24-hour events as for monthly or annual averages. The model underestimated the deposition of copper, nickel, iron, and rainfall amount in addition to ambient air concentrations. The results for copper are not conclusive because of high control values in the measured data.

Although the comparison to the standard gaussian model (CDM) and the numerical model were based on limited data, the comparisons are good ($\pm 50\%$) and the results support the modified gaussian model.

The accuracy of modeling predictions depends on the ability of

a model to simulate the physics of the atmosphere and on the input data, primarily meteorological data and pollutant data. Meteorological data are readily available, but they are generally obtained near ground level rather than at stack height where emissions are released. Other sources of error include estimates of pollutant emissions, stack characteristics, and location of sources.

A sensitivity analysis was performed on the primary input and meteorological parameters using 5 sites around Sudbury over a one year period. The meteorological parameters which were tested include the rainfall rate, rainfall duration, wind speed, wind direction, and standard deviation of the wind direction. Other input parameters which were tested include the oxidation rate, dry deposition velocity, washout coefficient, and ambient air background concentrations.

The most sensitive inputs to the model are oxidation rate, background concentration, and deposition velocity because of the large variation in these values reported in the literature.

Uncertainties in the oxidation rate (2 orders of magnitude) resulted in changes of a factor of 2 to 4 in ambient air concentrations of sulfur dioxide and sulfate. Deposition was less sensitive than ambient air concentrations, but varied up to a factor of 4 for wet sulfate. Sensitivity decreased with distance from the source.

Ambient air background concentrations of pollutants are difficult to define, and literature values range widely. Sensitivity of ambient air concentrations and deposition rates to background concentrations increased with distance from the source. A factor of two uncertainty in the background concentration resulted in about a factor of two uncertainty in concentration and deposition at about 45-150 km from

the source. Ambient air background concentrations were not required for the modeling simulations in Minnesota, and the errors due to uncertainty in background concentration do not apply. The factor of 2 to 3 uncertainty in the background concentration literature values, however, is within and greater than the uncertainty of the model making ambient air background values important if they are used in future applications of the model.

Ambient air concentrations are relatively insensitive to changes in deposition velocity. Deposition rates are more sensitive, and sensitivity increases with distance from the source. One to 2 orders of magnitude uncertainty in the deposition velocity resulted in deposition changes ranging up to a factor of 20.

In general uncertainties of \pm (15-20)% in the remaining parameters (rainfall rate, rainfall duration, wind speed, wind direction, standard deviation of the wind direction, and the washout coefficient) do not result in significant uncertainties in ambient air concentrations or depositions. The overall variation is less than \pm 20%.

1.2. REGIONAL CHARACTERIZATION

During the course of the Regional Copper-Nickel Study, two years of air quality data (mid-1976 to mid-1978) were collected in northeastern Minnesota. The results of this monitoring program revealed that the present air quality in the region is good. Sulfur dioxide levels were below the detection limit of $10 \mu\text{g}/\text{m}^3$, and particulate levels in relatively undisturbed areas were about $10 \mu\text{g}/\text{m}^3$, annual geometric mean. Average regional sulfate levels, $1.9 \mu\text{g}/\text{m}^3$, were also low. Elevated particulate levels (2 to 5 times background levels) were measured

close to dust sources such as dirt roads, mining operations, and communities.

A tabulation of major sources within 150 km of the ore body identified 84,820 metric tons of SO₂ emissions per year which were released during the baseline period. An increase of 130% is projected for 1985 (196,700 metric tons per year). For particulates, the baseline emissions, 92,540 mtpy are expected to decline 38% to 57,750 mtpy by 1985. The increases in sulfur dioxide emissions are primarily due to growth in the power generation industry and the conversion of the taconite industry from natural gas to coal. The expected decrease in particulate emissions is attributable to improved control efforts, particularly in the taconite industry.

About 99.5% of the SO₂ emissions estimated from fuel usage are attributed to the industrial use of coal. On this basis it was concluded that area source contributions of SO₂ emissions are minimal, and that SO₂ emissions can be adequately characterized by the point sources in the regional emissions inventory.

The modeling of regional point sources of sulfur dioxide indicates that about 85% of the total measured sulfate deposition (about 15 kg/ha/yr) cannot be accounted for by sources within the region, indicating that long-range transport from outside the region (possibly from as far away as the St. Louis and Ohio valleys, and the east coast area) is an important source of sulfates in the study area.

If national sulfur emissions double by the year 2000 as expected,¹¹¹ sulfate deposition in northeastern Minnesota may increase by a factor of two or more by 1985. Many of the northern lakes are already

experiencing the effects of acidic rain, and any further increases in sulfate deposition will only exacerbate the problem.

Without copper-nickel development in the region there does not appear to be a problem, now or in the immediate future (10 years), which would threaten to exceed the ambient air quality sulfur dioxide standards. Portions of the region are presently experiencing high particulate concentrations for short periods of time which exceed the 24-hour ambient standards. Elevated 24-hour particulate concentrations (20 readings above 150 ug/m^3 which is the secondary standard) were observed during the course of the study's monitoring program, and were generally associated with population centers and mining operations in the Mesabi Iron Range. Although there appears to be a serious sulfate problem, at the present time there are no Federal or State sulfate standards.

Modeling of the particulate point sources indicates that their contribution to observed particulate levels is very small, typically a fraction of a percent. Area sources such as roads and tailings basins, and transport from outside the region appear to dominate the existing particulate levels.

The Minnesota Pollution Control Agency has designated portions of northeastern Minnesota as non-attainment areas in terms of the particulate ambient air quality standards. Any new industrial development in or near these areas which would contribute to particulate concentrations could be restricted unless other sources in the area reduced particulate levels to prevent an increase in overall emissions.

Another air quality regulation which may affect the establishment of a copper-nickel industry is the short-term (24-hour and 3-hour) PSD restriction for sulfur dioxide, with the very stringent Class I requirements posing the greatest limitations. Present development plans in the area, principally from the power generating industry and the taconite industry, indicate that the increased sulfur dioxide emissions projected for 1985 are enough to consume and possibly exceed the 24-hour Class I PSD increment in portions of the Boundary Waters Canoe Area to the northeast of the present development along the Iron Range. This planned development could prevent any new sources of sulfur dioxide emissions such as a copper-nickel smelter from being located in the general corridor from the Iron Range communities (Hoyt Lakes, Biwabik, Gilbert, and so forth) northeast to the BWCA boundary, unless the Class I restrictions are waived by issuance of a variance.

1.3. SMELTER MODELS

The foregoing discussion of sulfur dioxide and particulate concentrations in the region is independent of copper-nickel development. In order to investigate the impacts of copper-nickel smelting, three hypothetical smelter models were used to predict the ambient air concentration and deposition patterns of pollutants resulting from smelting in the region. These models were based on the evaluation of various mining methods and processing options for milling, concentrating, extracting and refining the ore. Final selection of models was predicated on compatibility of the various options, capacity, pollution control, and economic feasibility. Some of the data for the smelter emissions were based on state-of-the-art information which

may be estimated, based on professional judgement of those experienced in the field. In some instances accuracies could range from a factor of 10 to 100.

1.3.1. Sulfur dioxide emissions.

The major source of sulfur dioxide emissions in a copper-nickel development complex is the smelter which processes the concentrated ore into unrefined metal. Point sources of sulfur dioxide result from the discharge of the uncontrolled gas stream. The primary sulfur dioxide control devices are an acid plant which converts the sulfur dioxide gas to sulfuric acid, and a gas scrubber. Both of these control devices produce products which may require disposal; for example, sulfuric acid from the acid plant if there is no market, and sludge from the scrubber.

Fugitive emission sources include leaks in ducts, converters, and refining furnaces. These emissions can be minimized by careful design of the furnace, efficient gas handling equipment, and good housekeeping practices.

A hypothetical copper-nickel smelter with no pollution control equipment could emit 200,000 to 400,000 metric tons of sulfur dioxide emissions each year. Such uncontrolled operations were once standard practice in the United States, and are still operating in many parts of the world. The resulting environmental damage is graphically illustrated by the fact that the area around the Sudbury smelter complex was used to train U.S. astronauts for the moon walks.

1.3.2. Particulate emissions.

Particulate emissions can result from nearly all phases of copper-nickel development. Although the smelter is not the only source of

particulates, there is more concern about these emissions than from other sources because of the high level of metals in the concentrate.

Particulate control in the smelter is primarily accomplished by cyclones, high efficiency electrostatic precipitators, hooding, and ventilation systems. Smelter stack emissions result from drying the concentrate prior to smelting, and from gases passing through the acid plant. A high degree of removal is required before the gas stream can enter the acid plant in order to prevent damage. Carryover from the drying operation is conservatively estimated to be 10%.

If an electric furnace rather than a flash furnace were used for smelting, particulate emissions would be near zero because the electric furnace does not have a dryer.

The major sources of fugitive emissions include leaks in ducts, converters, screening operations, drying, and the refining furnaces. These emissions can be effectively controlled in critical areas, such as the converters, by routing gases to control equipment before final discharge.

Metal particulates were selected for modeling on the basis of quantity of element present in the concentrate, toxicity to either human health or the environment, and the likelihood of release into the environment. The elements selected for the modeling simulations include copper, nickel, arsenic, cadmium, lead, and mercury. Volatile elements such as arsenic and mercury may be carried out of the stack either as a vapor or a particulate. The behavior of these elements is difficult to predict. Because low concentrations are present in the concentrate and a high degree of removal is likely, the potentially

volatile elements were modeled as particulates. This approach, however, should be reconsidered in a specific development proposal based on the composition of materials to be processed, and the technology to be employed.

1.3.3. Models of smelter emissions.

Because a new smelter in the region would have to comply with Federal regulations, the Federal new source performance standards (NSPS) provided the framework for quantifying emissions from hypothetical models. To meet these standards which limit SO_2 in the exit gas stream to 0.065% by volume, a smelter must have the equivalent of double contact acid plant control (99.5% removal by volume) for all process gases from roasters, smelting furnaces, and converters. One problem with the standard is that removal is specified by volume, allowing the possibility of dilution in order to achieve the standard. A standard based on mass would not have this shortcoming. Three pollution control configurations were selected to provide a range of emissions for modeling purposes. The base case smelter model would not meet NSPS, but was included to provide a worst case perspective. All of the smelter models represent a smelter/refinery complex producing 100,000 metric tons per year of refined copper plus nickel metal, and all of the models have a sulfur input of 165,542 mtpy.

Annual sulfur dioxide emissions for the base case, option 1, and option 2 smelters are 12,274 mtpy, 5,502 mtpy, and 1,992 mtpy, respectively. Fugitive emissions are 990 mtpy of SO_2 for each of the models.

Annual particulate emissions are 3,885 mtpy for the base case, and 1,858 mtpy for the option 1-option 2 smelters. Fugitive emissions

are estimated to be 1500 mtpy for each of the particulate models.

There is, of course, a possibility that extremely high concentrations of pollutants can be released during short periods of time as a result of an accident, failure of equipment, or during the course of routine maintenance. Failure of a major piece of equipment such as the acid plant could result in high emissions for up to a few hours before repairs could be made or the smelter operations stopped. It is estimated that the smelter operations could be stopped in 3 to 6 hours. The modified gaussian model is not appropriate for simulating periods less than 24 hours so these upset situations were not modeled. However, two upset cases, low level release of fugitive emissions and stack release were modeled for 3-hour periods by Endersen⁶¹ using short-range models.

1.4. POTENTIAL IMPACTS OF SMELTING

The three hypothetical smelter models were used to predict the ambient air concentrations and deposition patterns of pollutants in the study region. Since it was not possible to model all possible smelter locations, the modeling effort was concentrated near the copper-nickel ore body where atmospheric dispersion patterns are considered to be fairly uniform. The hypothetical smelter was located south of Babbitt for site specific simulations, and non-site specific simulations were also made.

One possible smelter site which would require specialized treatment is along the Duluth lakeshore which is governed by a complex dispersion regime created by Lake Superior and 250 meter bluffs along the lakeshore.

The modeling effort puts the general impact of copper-nickel development on the region's air quality into perspective. Existing ambient air quality standards, which have been developed to protect the public health and welfare, are used to highlight problem areas.

1.4.1. Sulfur dioxide.

The modified gaussian model projects that the annual ambient air quality standards would not be exceeded due to emissions from any of the hypothetical smelter models; the highest predicted annual sulfur dioxide concentrations amount to only 6.0%, 2.6%, about 1.0% of the Federal primary standard for the base case, option 1, and option 2 smelters, respectively. Also, the Federal primary annual standard is not expected to be exceeded by any of the smelter cases even with anticipated 1985 regional development. In fact, the highest annual concentration resulting from the base case smelter coupled with projected 1985 concentrations amounts to only 8.6% of the Federal primary standard.

Although the annual ambient air quality standard is not in jeopardy, there is a possibility that the annual PSD increment for sulfur dioxide could be exceeded by the base case and option 1 smelters alone. Although some PSD siting limitations based on annual averages may exist, the 24-hour PSD requirement will place even more stringent restrictions on smelter siting.

A maximum 24-hour sulfur dioxide concentrations of $120 \mu\text{g}/\text{m}^3$ is predicted for the base case smelter at 5 km from the source. Considering a modeling accuracy of a factor of 2, there is a possibility that the maximum 24-hour State standard will be threatened by the base case

smelter at sites close to the source. The State annual ($60 \mu\text{g}/\text{m}^3$) and maximum 24-hour ($260 \mu\text{g}/\text{m}^3$) standards are more stringent than the Federal standards (annual- $80 \mu\text{g}/\text{m}^3$; maximum 24-hour- $365 \mu\text{g}/\text{m}^3$). The 24-hour standard would not be threatened by either the option 1 or option 2 smelters; ambient concentrations are 50% lower for the option 1 smelter and about 85% lower for the option 2 smelter.

The Class II PSD increment is not predicted to be exceeded even for the smelter model with the least amount of sulfur dioxide control. However, for all three smelter cases the Class I increment could be exceeded out to considerable distances from the smelter as shown in Figure 73 (page 313).

The possibility of a smelter facility being located in the region will be most seriously affected by the short-term PSD restrictions due to the proximity of the BWCA and Voyageurs National Park. Exclusions zones were created around the Class I area for the different smelter cases (Figure 74, page 313). None of the smelter models are expected to meet the allowable 24-hour Class I PSD increment for sulfur dioxide if located within 10 to 20 kilometers of a Class I area. Only the option 2 smelter appears to meet the increment between 10-20 and 30-40 km, and the base case model would require at least 70-80 km.

When these data are applied to the ore development zones, it is seen that none of the smelter models acting alone could be built in zones 1 or 2 (Figure 75, page 316). The option 2 smelter could be built in zones 3 and 4, while the option 1 (and of course option 2) smelter could meet the increment requirements in zones 5, 6, and 7. Within the factor of two accuracy of the model, at worst, none of the

smelters could be located in zones 1, 2, 3, or 4, and only the option 2 smelter could be located in zones 5, 6, or 7.

These results apply only to a smelter facility, and do not factor in the contribution of new or expanded sources other than copper-nickel development. However, it is predicted that these other sources could exceed the 24-hour Class I PSD increment even without copper-nickel development. Taking this into consideration, smelter siting would appear to be excluded in areas that are between the concentrated line of sources along the Iron Range and the Class I areas. For this reason, siting in development zones 1, 2, 3, and possibly 4 and 5 may be precluded. This conclusion is independent of the degree of sulfur dioxide control achieved by a smelter, since the increment may be consumed by other sources. Zones 6 and 7 may then be most promising for smelter siting.

The foregoing analysis of smelter siting is based on ambient air quality considerations not on economics. It is likely that a smelter facility would be located close to the processing facilities, since it is estimated that a 10-15% savings in smelter capital and operating costs could result from shared facilities.¹⁸⁶ Locating the smelter close to the mines and processing facilities would also eliminate risks related to transporting the concentrate.

About 75% of the copper-nickel resource lies in zones 1, 2, and 3. Zone 4 contains about 20% of the resource, and zones 5, 6, and 7 together contain just over 10%.¹⁷⁴ It is clear that when development occurs, the economic potential will be greatest in those zones that would result in the greatest air quality impacts.

The siting question is one that will have to be answered by the appropriate authorities, but it is apparent that the 24-hour PSD increment in a Class I area is one of the standards that will have a major influence on smelter siting in northeastern Minnesota. The effect of other new sulfur dioxide sources is also important since they may consume a portion or all of the increment, potentially excluding a smelter from the region. Clearly, the decisions to be made must involve long-range planning for any future industrial development in the region as a whole.

The possibility of accidental release of sulfur dioxide emissions was not modeled using the modified gaussian model because of the short time periods (3-6 hours) involved. Accidental release was modeled using short-range models by Endersen.⁶¹ It is possible that very high concentrations could result for short periods of time, but the probability of occurrence is difficult to predict.

The three smelter models were also used to predict average regional sulfate deposition. Based on a current average regional deposition of about 15 kg/ha/yr, the modified gaussian model predicts increases of about 15%, 6%, and 2%, respectively, for the base case, option 1, and option 2 smelters. Since ambient sulfate for the region is expected to double by 1985, the increases would be only about half as large. Although the regional sulfate input from a smelter, especially a facility with state-of-the-art control, is expected to be a minor contribution to total sulfate deposition on a regional basis, the contribution close to the smelter may be significant.

For example, sulfate deposition at a site 5 km east of the base case smelter is predicted to increase by about 60% over current levels. Although this increase would be reduced to 25% and 10% for the option 1 and option 2 smelters, respectively, these levels are potentially significant if sensitive lakes are close to the smelter site, or if they receive a large portion of their inflow from areas surrounding the smelter. This may be particularly important during spring runoff when sulfate which has accumulated during the winter is suddenly released into surface waters.

The impact of metals and acid-forming species like sulfate on the area's lakes and streams is of vital interest. Many of the lakes in the area have low buffering capacity and are already susceptible to acidic precipitation. Evidence suggests that some of the lakes in the BWCA are at or near the threshold of acidification which is serious enough to cause decreased productivity of fish and other aquatic life.

1.4.2. Particulates.

The findings for particulate concentrations from smelter emissions are similar to those for sulfur dioxide. Annual ambient concentrations increases due to a smelter are not expected to pose a problem. For 24-hour concentrations under worst case meteorological conditions, values that are about 15% of the primary 24-hour standard may occur at 5 km from the base case smelter; these levels fall to about 2% of the standard at 25 km. However, there is a possibility that the Class I 24-hour increment of $10 \mu\text{g}/\text{m}^3$ could be exceeded if the smelter is located too close to a Class I area. Although some restrictions to smelter siting may exist because of particulate emissions, the

sulfur dioxide emissions would dictate siting on the basis of the PSD regulations.

Ambient air concentrations of Hg, Pb, As and Cd resulting from the option 1-option 2 smelter are predicted to be 2-3 orders of magnitude lower than existing levels which are typical of concentrations measured in remote areas. Concentrations of Cu and Ni, however, are predicted to be the same order of magnitude or higher. Deposition of As, Cd, Pb, and Hg are also expected to be at least 2 orders of magnitude lower. Deposition of Cu and Ni are predicted to be elevated over current levels.

1.4.3. Human health.

During normal operation the projected release of sulfur dioxide, sulfates, total particulates, and metals from the smelter models is not expected to have significant human health consequences. There is a possibility that concentrations of sulfate and particulates may be high enough during normal operation on a few days each year to result in discomfort very close to a smelter controlled only to the level of the base case. During breakdown conditions people who live within a few kilometers downwind of the smelter would be affected. Breakdown episodes would be more of a problem if a smelter were located in a populated area such as Duluth.

Over the long term, the concentration and deposition rate of metals may pose a problem for people living within 10 km of the smelter. Studies have shown that the populations in almost all of the counties in the United States where copper smelters are currently operating are experiencing increased death rates from respiratory cancers,

accidents, and cardiovascular diseases. The actual causes of these increases is not known, but the results do indicate that a potential for human health impacts exists from copper smelting in northeastern Minnesota.

1.4.4. Vegetation and soil.

Northeastern Minnesota is potentially susceptible to impacts on vegetation and soil from smelter emissions. The pine and aspen trees which predominate in the region are sensitive to acute and chronic sulfur dioxide exposure. The soils in the region are relatively thin and poorly buffered, and could, therefore be impacted by deposition of sulfate and metals from a smelter.

During normal operating conditions, vegetation damage is not expected from the release of sulfur dioxide emissions based on the mesoscale modeling results.

The modeling studies suggest that the deposition and accumulation of metals is a potential problem.

Because most of the areas managed for timber by the U.S. Forest Service are managed for conifer species which require mineral soils, the leaf litter layers are often removed for planting. Those forest stands with the least litter will be the most susceptible to metals deposition, and the resultant decreased rates of nutrient recycling may affect subsequent growth and productivity. In addition to reducing forest growth, metals deposition onto the soil may also effect germination and seedling growth.

Little can be done to reclaim areas that have been affected by

widespread chronic air pollution; damage may not even be visible, but may take the form of reduced growth rates. Prevention is, of course, the best solution. Siting of smelters away from young, sensitive conifer plantations and areas having low soil buffering capacity can reduce potential impacts.

1.4.5. Water quality.

Many of the region's lakes are soft water lakes that have limited buffering capacity. This generally includes lakes with the smallest ratio of drainage area to lake volume; lakes at higher elevations may be affected first because more precipitation falls in these areas, resulting in greater deposition. Such lakes are likely to be headwater lakes, and have the least buffering material in their drainage systems.

Data indicate that lakes in the region may already be affected by acidity from atmospheric sources. Atmospheric loadings of sulfate to lakes near the BWCA-VNP are at levels associated with the onset of severe lake acidification in Sweden. However, the association between atmospheric deposition of sulfate to lakes in Minnesota and acidity of these lakes has not been proven.

Potential impacts of acidified lakes include a reduction in the productivity and diversity of aquatic communities with elimination of fish populations in the most susceptible lakes. Increased acidity is also likely to result in detrimental levels of aluminum and other trace metals in lakewater by increasing leaching.

The atmospheric deposition of air pollutants onto surface waters occurs during the summer as rain and during the winter as snow. During the winter months when the ground is frozen and surface runoff is absent,

air pollutants are deposited onto the snow-pack, stored, and later released over a very short interval during the spring melt. The melt-freeze cycles that occur during the snow-melt can result in dramatic increases in the concentrations of pollutants in the meltwater. These increases can be as much as two to three times greater.

The modeling simulations predict that the concentrations of sulfate, copper, and nickel in the snow-pack due to the option 1 smelter will be 10 to 100 times greater than the currently measured levels. If it is assumed that the average concentration in the snow can double or triple in the first 30 to 40% of meltwater, then predicted concentrations would increase accordingly, considering, of course, the factor of two accuracy attributed to the modeling results.

The modeling simulations using the option 1 smelter also show that the predicted contributions of sulfate deposition to regional lakes and streams would be about 10 times greater than currently measured sulfate levels; predicted copper and nickel concentrations would be 10 to 100 times greater than current levels.

The modeling results were also used to predict the length of time required to acidify (to pH 4.5) two regional lakes, one with very little buffering capacity and one with good buffering capacity, by sulfate deposition. The results indicate that a lake with low buffering capacity could be acidified in a short period of time at present sulfate loadings, and that existing point sources, although contributors, are not as significant as sources outside the region. Local sources contribute less than 15% of the total sulfate loading with the rest due to long-range transport from outside the region. The addition of new sources

such as a copper-nickel smelter could be important in determining the the productive life of low alkalinity lakes. Time spans for the acidification of low alkalinity lakes appear to be on the order of less than 10 years at present deposition rates, and perhaps 100 to 200 years for moderately high alkalinity lakes. These results represent a worst case approximation because of assumptions made in the calculations. Even though the absolute values may be inaccurate, present evidence indicates that acidification of northern lakes could be a problem, and any activities which could increase the acidic input into the region's surface waters requires careful evaluation.

For this reason, a research program should be implemented in the near future to better define the identity, sources, and deposition rates of acid-producing compounds in the region.

1.4.6. Summary.

This research project was part of a regional study designed to assess possible environmental impacts resulting from copper-nickel development. There has essentially been a moratorium on copper-nickel mining in Minnesota since 1974 when the Study began. The Copper-Nickel Study report was officially accepted by the Environmental Quality Board in September, 1979, and mining companies can now apply for development permits.

Actual development will probably be different from any of the models used in this assessment. However, the impact assessment tools and baseline data have now been developed that will be used to evaluate future site-specific development proposals. In addition, the Study provides the basis for the development of State policy regulating the

copper-nickel industry in northeastern Minnesota.

CHAPTER 2. INTRODUCTION

2.1. BACKGROUND

Beginning with the discovery of major copper-nickel deposits in northeastern Minnesota in 1948, mining companies have shown considerable interest in developing this resource. By 1974 a major mining company proposed open-pit mining on U.S. forest lands near Ely, Minnesota. Other mining companies also began active exploration in the area.

Concurrently, public apprehension mounted over the possible consequences of the development of a major new base-metal industry in northeastern Minnesota. Although there is major taconite mining in northern Minnesota, copper-nickel development caused concern because it would be located near a prime recreational area. A principal concern was that the open-pit mining proposal was within a few miles of the Boundary Waters Canoe Area (BWCA), a federal designated wilderness area.

This pristine forested region contains numerous interconnecting lakes (over 200) and rivers potentially susceptible to mining and smelting impacts. The strong prospects of a major new mineral industry locating in this sensitive region caused many citizens and environmental groups to push for a major environmental study of the area prior to further exploration and any mining. In late 1974 the Minnesota Environmental Quality Board (MEQB), a State agency responsible for the implementation of the Minnesota Environmental Policy Act, passed a resolution that a regional environmental study be completed prior to the acceptance of any site specific environmental impact statement. Further, all mining exploration programs were required

to include sound preoperational monitoring and environmental assessment programs.

The unique aspects of the 1974 resolution are that: A regional study was implemented which was to be completed prior to any mining proposals; the study would not replace site specific investigations of individual mining proposals; and, a social and economic study was included to interface with the environmental study.

In 1975 the MEQB created a Regional Copper-Nickel Study Task Force, organizationally separate from existing regulatory agencies and under the auspices of the MEQB, to conduct the study. The study began in January, 1976 and was completed in 1979. The cost of the study will be about 4.3 million dollars.

The major objectives of the Regional Copper-Nickel Study were:

- 1) To characterize the region in its pre-copper-nickel development state;
- 2) To identify and describe the probable technologies which may be used to exploit the mineral resource;
- 3) To identify and assess the impacts of primary copper-nickel development and secondary regional growth;
- 4) To conceptualize alternative degrees of development; and
- 5) To assess the cumulative environmental, social, and economic impacts of various hypothetical developments.

Specifically, the Study was designed to provide scientifically developed information so that the State legislature and State agencies can implement any new mining policies they deem necessary.

The Study was organized into six major disciplines: geology and mining technology, water resources, air resources, aquatic biology, terrestrial biology and socio-economics.

This research project developed from the need of the Regional Copper-Nickel Study to assess potential atmospheric impacts of a copper-nickel smelter in northeastern Minnesota on a regional scale.

2.2. ISSUES

The prospect of a major new industrial development in northeastern Minnesota to recover copper and nickel raises the potential for atmospheric impacts. The air quality concerns relating to copper-nickel development can be categorized into human health, terrestrial ecosystems, and water quality. Some of the issues of concern to Minnesotans in each of these areas are outlined below.

Inhalation of airborne sulfur (primarily as gaseous sulfur dioxide, but also as particulate sulfate), copper, nickel, mineral fibers and other particulates is a potential health problem. Other elements of potential concern include arsenic, lead, mercury, and cadmium. The increase of metals uptake by people living near a smelter, acute effects due to upset or breakdown conditions, and potential long-term effects of mineral fibers must be evaluated. The literature relating to identified public health problems resulting from the pollutants selected for the modeling analyses are summarized in Chapter 4.

Ambient concentrations of sulfur dioxide and deposition of airborne metals (primarily copper and nickel) may have direct or indirect effects on terrestrial plants and soil organisms. These changes can affect all other components of the ecosystem. Another concern is the potential for direct vegetation damage by sulfur dioxide close to a smelter should equipment breakdown cause high sulfur dioxide emission rates. The long-term effects due to the deposition of metals,

particularly copper and nickel, are also important in terms of plant productivity.

Atmospheric pollutants can be deposited directly onto water surfaces, or be deposited on land and subsequently washed into rivers and lakes by precipitation. Metals which are potentially toxic to aquatic life include copper, nickel, cobalt, arsenic, lead, mercury, and cadmium. Sulfur in the form of unneutralized sulfate contributes to the acidity of rain which, in turn, can acidify regional waters. Many northern lakes may now be susceptible to increased acidic inputs.

Present air quality standards do not address many of the environmental concerns just listed. However, air quality regulations are also issues that will affect the development of copper-nickel mining and smelting in the State.

The air quality regulations relevant to the development of a copper-nickel industry in Minnesota include standards which limit sulfur dioxide and particulate emissions from a smelter and ambient air quality standards. Ambient standards currently exist for sulfur dioxide, particulates and lead. Trace elements such as copper, nickel, arsenic, mercury, cadmium, zinc and other pollutants such as sulfates, silica and mineral fibers pose potential environmental/health risks, but the ambient air quality standards do not regulate these pollutants at the present time.

In addition to the ambient air standards the region is also subject to the prevention of significant deterioration (PSD) amendments to the Federal Clean Air Act of 1970. The PSD regulations are designed to prevent degradation of air quality by specifying maximum

allowable increases for sulfur dioxide and particulate concentrations above 1977 levels. All of northeastern Minnesota has been designated a Class II PSD area with the exception of the Boundary Waters Canoe Area (BWCA) and the Voyageurs National Park (VNP) which are designated Class I areas and are subject to more stringent regulations.

2.3. RESEARCH PROJECT

The purpose of this research project was to characterize northeastern Minnesota in terms of ambient air concentrations and deposition patterns of sulfur dioxide, sulfate, total particulates, and selected metals for a base year and a future year, and finally, to assess the potential air pollution impacts of copper-nickel smelting in the region in terms of the environmental, health and regulatory issues.

By definition the task was regional in scope and required an assessment tool that could predict atmospheric impacts of a mining industry on a several thousand square kilometer (km^2) area which is already experiencing air quality impacts from existing activity within and outside the area.

The approach to the research project was to first review the literature and determine if predictive air dispersion models were available that could be adapted to model an area of about 5000 km^2 in northeastern Minnesota at a reasonable cost. Because of the problem of acidic rain impacts on streams and lakes the model had to include the following processes: conversion of sulfur dioxide to sulfate, dry deposition and wet scavenging.

Existing models included standard gaussian plume models, puff models, box models, trajectory models, and sophisticated numerical

solutions to the eddy diffusion equation. The gaussian models are limited to application within 10-15 km of the source, existing box model did not include all the required processes, and the numerical models were prohibitively expensive.

A model which was being developed at McMaster University, Hamilton, Ontario by F. Huhn and J.R. Kramer was initially selected for application in northeastern Minnesota. This model included the required processes of chemical conversion, wet scavenging, dry deposition, and, in addition, predicted pollutant concentrations in lakes.

A careful review of the model by Ritchie showed that it would not be appropriate for use in northeastern Minnesota as formulated, and the model was subsequently modified by Ritchie, Bowman, and Burnett for application in Minnesota. The handling of meteorological data and the basic diffusion concepts were retained with some modifications. Major changes were made in the processes of wet scavenging, dry deposition, and losses en route; minor changes were also made in other portions of the model, and the lake model was deleted. The modeling theory is described in Chapter 5.

After the model was developed, it was verified against deposition and concentration data from the Sudbury, Ontario area and two other models. A sensitivity analysis was also performed on the input parameters. Chapter 6 presents the results of the model verification and the sensitivity analysis.

Chapter 3 describes the area that was modeled, rules and regulations that apply to smelter siting, smelter models and the regional sources in the emissions inventory.

Measured data taken by the Regional Copper-Nickel Study are used along with regional modeling simulations to describe the existing air quality in the region, and to make predictions of air quality in 1985 in the absence of copper-nickel mining (Chapter 7).

The smelter models are then used alone and along with the 1985 regional sources to predict the concentration and deposition of pollutants expected from copper-nickel smelting (Chapters 8 and 9).

The impacts of smelter emissions on health, surface waters and soil are discussed in Chapter 10.

CHAPTER 3. APPLICATION TO COPPER-NICKEL SMELTING IN NORTHEASTERN MINNESOTA

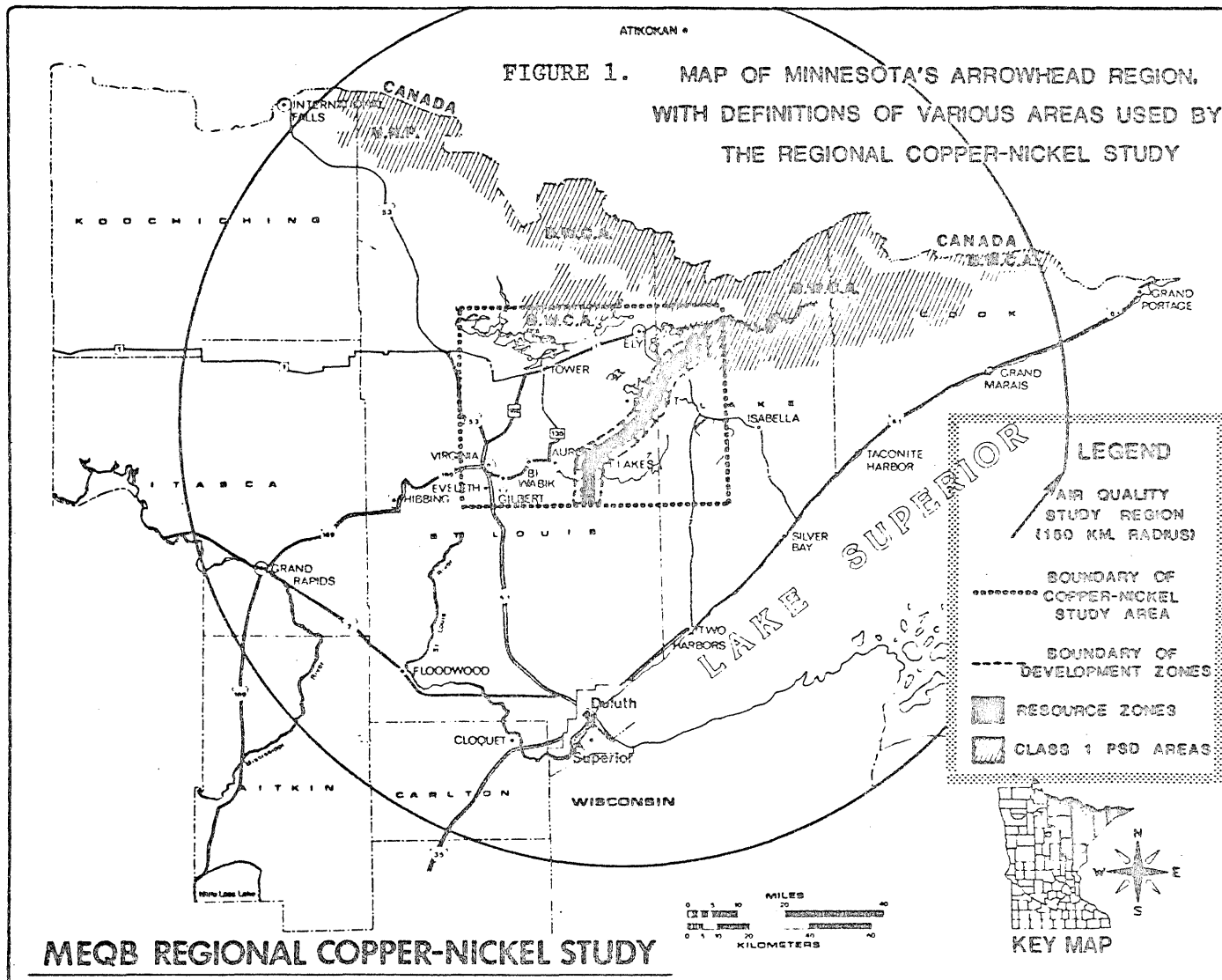
In order to assess the potential air quality impacts from copper-nickel smelting in northeastern Minnesota, it was necessary to identify the types and amounts of air emissions likely to result from a smelter. This chapter discusses the smelter models, the area of interest, regional climatology/meteorology, legal considerations, and introduces the regional emissions inventory.

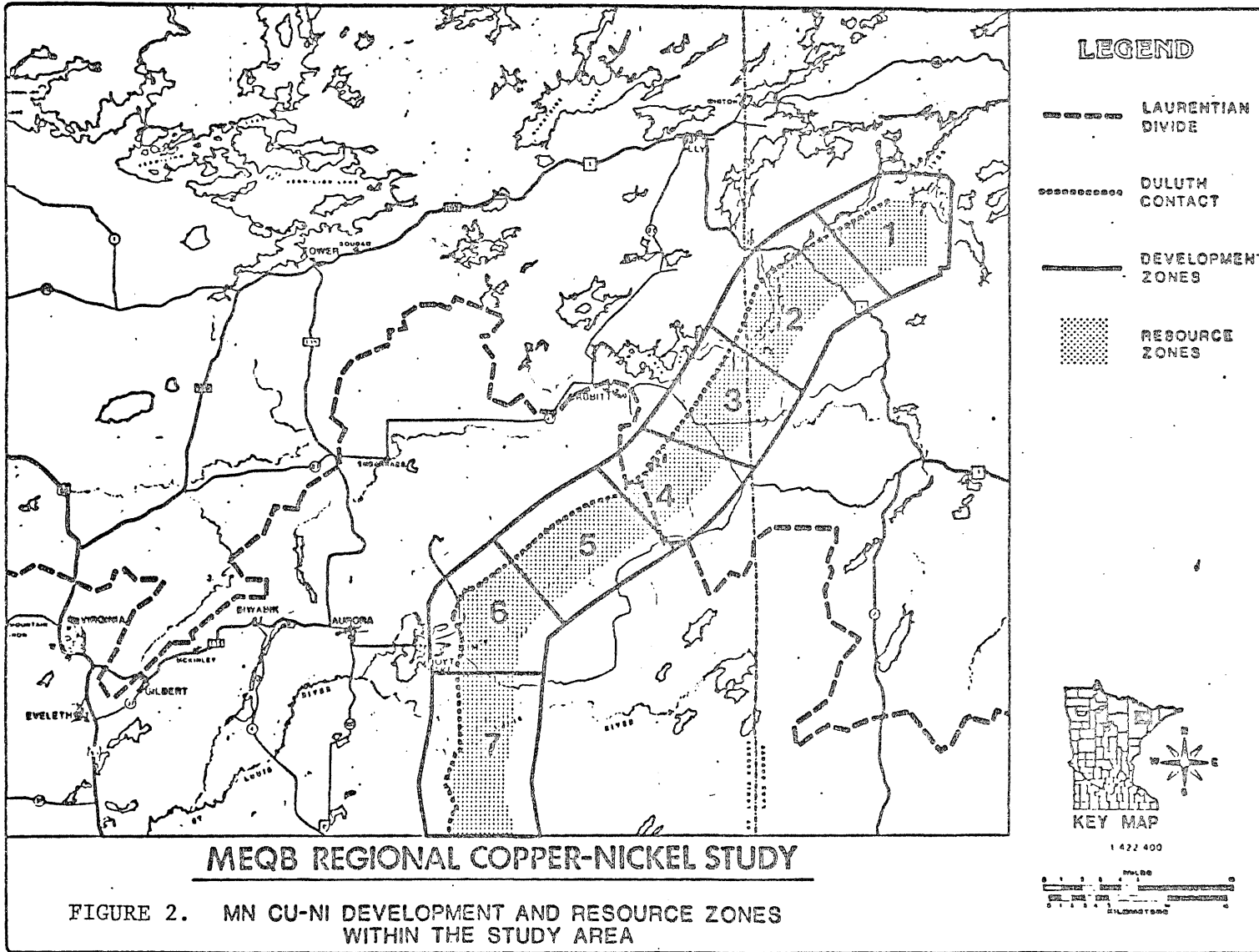
3.1. AREA OF INTEREST

Figure 1 shows a land area of about 10,000 square kilometers encompassing northeastern Minnesota and parts of Canada and Wisconsin. This area is known as the air quality study region or simply as the study region. The study region extends from International Falls in the west to Thunder Bay, Ontario in the east, and is bounded by Atikokan, Ontario to the north and Duluth, Minnesota and Ashland, Wisconsin to the south. Within the larger study region is a smaller area of about 5,000 square kilometers known as the study area. The study area contains the copper-nickel ore body and is actively being considered for mining development.

The zone of the ore body is shown in greater detail in Figure 2. The area most likely to contain any mines, based on available data, has been identified as a set of seven resource zones. The resource zones are surrounded by a larger area called the development zone which should contain most of the facilities needed to serve any mines.

The Boundary Waters Canoe Area and Voyageurs National Park which are Class I prevention of significant deterioration (PSD) areas are also shown in Figure 1.





The study region also contains the receptor sites and regional sources which were included in the modeling simulations.

3.2. AIR QUALITY REGION RECEPTORS AND METEOROLOGICAL STATIONS

Thirty-three receptors (Figure 3) were selected in the study region to be representative of regional watersheds (12 receptors), population centers (11 receptors), rural areas (8 receptors), and mining areas (2 receptors). Table 1 provides the receptors and coordinates.

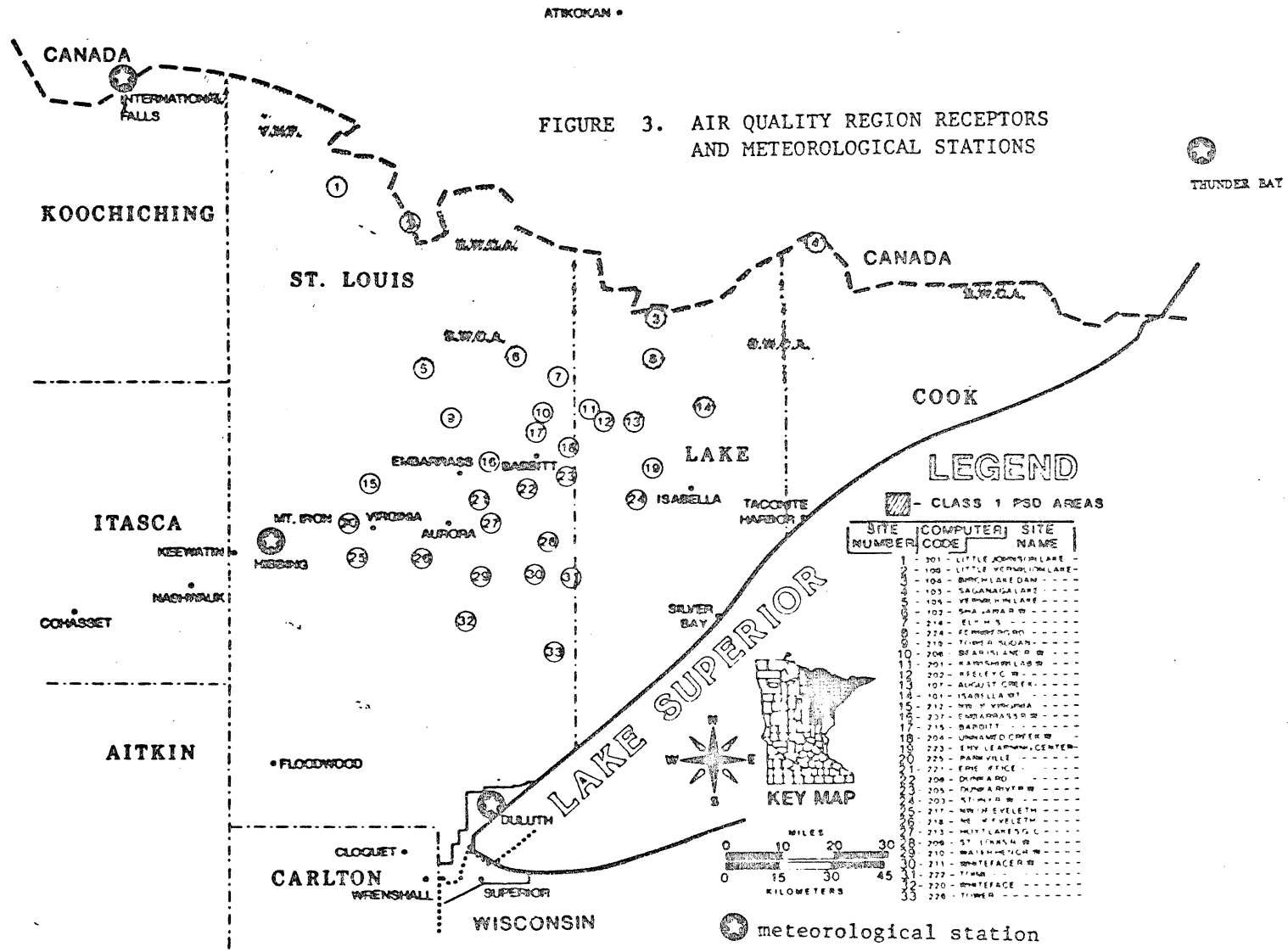
Meteorological data from four stations; Thunder Bay, Duluth, Hibbing, and International Falls; were used to drive the model (Figure 3).

3.3. REGIONAL CLIMATOLOGY/METEOROLOGY

Much of the study region of northeastern Minnesota is heavily wooded with swamplands in low lying areas. The terrain can be characterized as flat to moderately rolling with the exception of the Giants Range. The climate of the region can be considered continental, characterized by cold winters and warm summers. Surface wind patterns are dominated by northwesterlies (about 75% of the time at Hibbing) and southeasterlies.²⁷⁷ Precipitation is moderate; June, July, August, and early September are the months with the highest precipitation. During the winter the ground is snow-covered from November to mid-April; frost may penetrate the ground from a few inches to as many as 60 inches.¹⁴¹

Precipitation averages from 700 to 760 millimeters. Precipitation exceeds lake evaporation by about 200 millimeters, and nearly all of the precipitation that falls on lake surfaces ends up in the lakes.²⁷⁷

Meteorological data from Thunder Bay, Duluth, Hibbing and International Falls were used to drive the modified gaussian model. Data from the four stations during the period November, 1976 through October, 1977 are presented along with normals in the following discussion.



3.4. REGIONAL EMISSIONS INVENTORY

A regional emissions inventory, initially compiled by Bowman²¹ and subsequently refined by Ritchie, provided the basis for both the characterization of present air quality and the evaluation of future development impacts with and without a copper-nickel smelter.

The regional emissions inventory includes point sources emitting more than 100 metric tons per year (mtpy) sulfur dioxide (SO₂) or total suspended particulates (TSP) within a 150 km radius of the copper-nickel ore body (Figure 5) for the base period 1975-76 and the projected year 1985. Other pollutants such as oxides of nitrogen, sulfate, and metals are not included in the inventory. The names and locations of all sources in the inventory are given in Table 8. The source emission rates are given in Chapter 7.

Area sources such as fugitive emissions from tailings basins, unpaved roads, and space heating requirements, and line sources such as traffic are not included, but their contributions to regional ambient air quality are discussed in Chapter 7.

The base year period 1975-76 was selected because it is the most recent year that the State inventory was nearly complete, available in computerized form, and it corresponds closely to the baseline ambient air quality data which were collected during 1976-77. 1985 was the latest year for which emissions projections could be based on expansion plans for industrialization in the region, and 1985 is also the earliest anticipated date that a smelter complex might be operational.

The stability classes at International Falls are used in the dispersion model to calculate the increase in wind speed with stack height according to the power law velocity equation.

Mixing height may be defined as that height above the earth's surface to which pollutants will extend, primarily through the action of atmospheric turbulence.¹⁰³ Estimates of mixing height from International Falls were used in the modified gaussian dispersion model, and are given in Table 7 for various seasons and times of day.

The monthly mixing height equation for the modeling simulations was derived from the seasonal data¹⁰⁶ at International Falls. The average monthly afternoon mixing heights were fit to a sine curve resulting in the equation: $HMAX = 1.000 + 0.510 \sin ((IM-3) \times 0.524)$, where HMAX is the monthly mixing height in km and IM is the month.

An inverse linear relationship exists between pollutant concentration and mixing height.

Table 7. Mean seasonal and annual morning and afternoon mixing heights at International Falls.

<u>Time Period</u>	<u>Morning Mixing Height, meters</u>	<u>Afternoon Mixing Height, meters</u>
Winter	347	656
Spring	411	1646
Summer	337	1747
Fall	513	1146
Annual	402	1299

Maxwell¹⁴¹

Table 5. Monthly snowfall (cm) for 1976-77 compared to normals at the regional meteorological stations

	Thunder Bay ^a		Duluth ^b		Hibbing		International F. ^b	
	1976- 1977	long term	1976- 1977	long term	1976- ^c 1977	long ^d term	1976- 1977	long term
Jan	16.6	51.6	22.4	43.4	32.3	23.6	28.4	29.2
Feb	34.7	31.0	13.0	30.0	15.7	14.4	36.1	21.6
Mar	11.4	35.3	38.9	35.8	17.5	25.1	35.6	25.7
Apr	5.60	20.1	0.25	17.3	trace	14.5	0.51	15.5
May	trace	4.30		2.29		0.50		2.54
Jun				trace				trace
Jul								
Aug				trace				
Sep		trace		trace				0.25
Oct	trace	3.60	4.32	3.05	trace	1.60	trace	3.81
Nov	8.80	30.7	6.86	25.9	8.13	14.5	9.65	26.7
Dec	36.4	45.5	19.8	39.9	25.4	25.2	31.5	27.4
Ann	113.5	222.1	105.5	197.6	99.0	119.4	141.8	152.7

^aFisheries and Environment Canada^{67, 68}

^bNational Oceanic and Atmospheric Administration¹⁶⁴

^cWatson²⁷⁸ ^dWatson²⁷⁷

Table 6. Annual stability class occurrences, International Falls

Stability Class	Year	
	1977 ^a	1970-1974 ^b
A	0.003	0.0045
B	0.034	0.0264
C	0.091	0.0828
D	0.597	0.6235
E-F	0.275	0.2683

^aEndersen⁶¹
^bMaxwell¹⁴¹

Table 4. Monthly precipitation (cm) for 1976-77 compared to normals at the regional meteorological stations.

	Thunder Bay ^a		Duluth ^b		Hibbing		International F. ^b	
	1976- 1977	long term	1976- 1977	long term	1976 ^c - 1977	long ^d - term	1976- 1977	long term
Jan	1.14	4.80	0.91	2.90	1.22	1.63	2.21	2.21
Feb	3.10	3.02	1.19	2.44	1.80	1.48	2.57	1.78
Mar	5.12	4.37	11.3	4.24	2.29	3.51	4.85	2.82
Apr	2.97	5.64	3.23	5.51	3.05	4.16	2.57	4.14
May	6.02	7.47	8.89	7.85	7.75	7.02	14.8	6.68
Jun	10.2	8.28	10.1	10.1	10.8	8.85	10.7	9.93
Jul	9.56	7.11	9.93	9.30	5.56	10.2	5.49	9.75
Aug	16.9	8.79	8.28	8.76	18.5	8.63	7.65	8.48
Sep	28.4	8.33	15.2	8.13	12.5	8.03	17.3	8.43
Oct	5.65	5.69	8.13	5.61	5.97	4.86	2.03	4.39
Nov	1.10	5.72	0.48	4.22	0.48	2.97	0.53	3.30
Dec	2.89	4.60	0.99	2.92	0.81	1.90	1.52	2.31
Ann	93.1	73.9	78.6	72.0	70.7	63.2	72.2	64.2

^aFisheries and Environment Canada^{67, 68}

^bNational Oceanic and Atmospheric Administration¹⁶⁴

^cWatson²⁷⁸

^dWatson²⁷⁷

and precipitation that falls as rain. Snowfall accumulates during the winter. The accumulation is released to the streams and lakes in the area over a short period of time during the spring thaw resulting in potential ecological damage from high concentrations of pollutants that have accumulated in the snow.

Table 5 shows average monthly and annual snowfall at the weather stations. Although total precipitation was above normal during the study period, snowfall was about 51%, 53%, 83%, and 93% of normal at Thunder Bay, Duluth, Hibbing, and International Falls, respectively.

3.3.4. Atmospheric stability and mixing height.

Atmospheric stability and wind speed are the primary meteorological parameters which determine the capacity of the atmosphere to transport and disperse pollutants.

Stability is commonly characterized by categories (first proposed by Pasquill¹⁷⁷) which are determined by wind speed at a height of about 10 meters along with the incoming solar radiation during the day and cloud cover during the night. Table 6 shows the annual stability categories at International Falls for the period 1970-1974¹⁴¹ and for 1977.⁶¹ Category A is the most unstable, D is neutral, and F is the most stable.

Table 3. Monthly and annual average wind speed (km/hr) for 1976-77 compared to normals at the regional meteorological stations.

	Thunder Bay ^a		Duluth ^b		Hibbing		International F. ^b	
	1976-1977	long term	1976-1977	long term	1976 ^d -1977	long ^c term	1976-1977	long term
Jan	16.0	15.0	15.1	19.3	14.4	14.8	12.1	14.8
Feb	15.3	14.6	18.0	19.0	16.0	14.8	14.2	14.6
Mar	15.8	14.3	20.6	19.5	17.6	15.1	15.3	15.3
Apr	11.9	15.8	18.2	21.2	16.0	16.7	13.2	16.9
May	12.3	15.2	17.7	19.8	16.0	16.3	14.0	16.3
Jun	10.0	13.2	15.0	17.4	14.4	14.2	11.7	14.0
Jul	9.2	12.6	14.2	15.9	14.4	13.2	13.2	12.9
Aug	9.3	11.8	14.3	15.6	14.4	12.6	12.4	12.4
Sep	10.8	12.7	16.3	17.1	14.4	13.7	12.2	14.2
Oct	10.7	15.9	17.9	18.3	16.0	15.9	14.6	15.3
Nov	15.5	14.8	15.4	19.5	17.6	15.0	14.8	15.9
Dec	13.8	14.3	15.8	18.3	16.0	14.3	13.5	14.6
Ann	12.6	14.2	16.5	18.3	15.6	14.6	13.4	14.8

^aFisheries and Environment Canada^{67, 68}

^bNational Oceanic and Atmospheric Administration¹⁶⁴

^cMaxwell¹⁴¹

^dWatson²⁷⁸

between December and March. During the study period the general precipitation pattern was one of extreme dryness from July 1, 1976 to February 23, 1977, and was followed by very wet and rainy weather for the remainder of 1977.

Table 4 provides a summary of monthly precipitation recorded at the meteorological stations. Total precipitation for the year of data used in the modeling was 26%, 9%, 12% and 12% higher than normal at Thunder Bay, Duluth, Hibbing, and International Falls, respectively.

It is important to distinguish between precipitation that falls as snow

3.3.3. Precipitation.

The study region has a wet and a dry period which correspond closely to summer and winter seasons, respectively. Watson²⁷⁷ analyzed composite precipitation records from 1894 to 1976, and defined the wet season as beginning on April 14 when a sudden increase in average precipitation begins, and ending on October 15 when a sharp drop in precipitation takes place.

June and July are the wettest months and February is the driest. The region experiences heavy snowfall and the most frequent snow occurs

Table 2. Monthly mean and annual temperatures for 1976-77 compared to normal temperatures (°C) at the regional meteorological stations.

	Thunder Bay ^a		Duluth ^b		Hibbing		International F.	
	1976-1977	long term	1976-1977	long term	1976 ^e 1977	long ^d term	1976 ^c 1977	long ^b term
Jan	-17.9	-14.8	-17.9	-13.1	-19.3	-15.4	-21	-16.7
Feb	-10.0	-13.0	- 8.2	-11.1	- 9.4	-13.3	-10.8	-13.9
Mar	- 1.2	- 6.2	- 0.3	- 4.7	0	- 5.8	- 1.3	- 6.3
Apr	4.3	2.4	6.9	3.7	6.9	2.4	6.1	3.4
May	12.0	8.3	14.1	9.7	15.5	10.2	16.1	10.0
Jun	13.8	13.8	15.6	15.0	16.4	15.2	16.6	15.8
Jul	17.0	17.5	18.8	18.7	19.3	18.7	19.2	15.4
Aug	13.6	16.5	14.8	17.8	14.5	16.5	13.9	17.3
Sep	11.3	11.3	11.8	12.4	11.9	11.8	11.4	11.7
Oct	6.1	6.1	6.8	7.4	6.2	5.0	6.3	6.4
Nov	-5.8	-2.5	-5.5	-2.0	-6.8	-4.2	1.5	5.4
Dec	-17.2	-10.8	-15.3	-9.8	-17.1	-11.7	-19.4	-12.9
Ann	2.2	2.4	3.5	3.7	3.2	6.7	3.2	2.4

^aFisheries and Environment Canada^{67, 68}

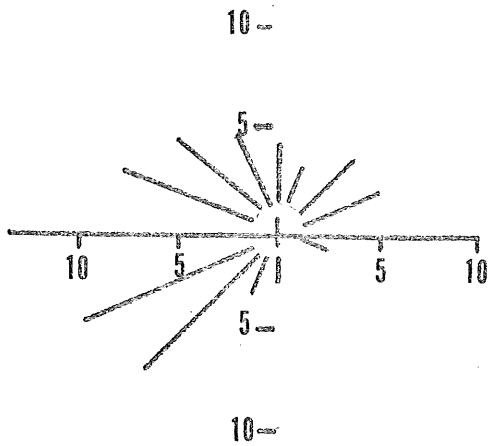
^bNational Oceanic and Atmospheric Administration¹⁶³

^cNational Oceanic and Atmospheric Administration¹⁶⁴

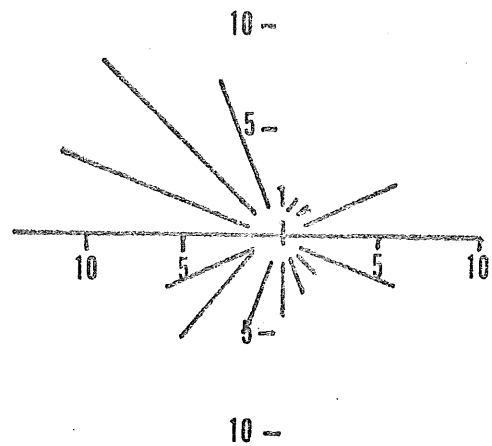
^dWatson²⁷⁷ ^eWatson²⁷⁸

FIGURE 4. ANNUAL AVERAGE WIND ROSES

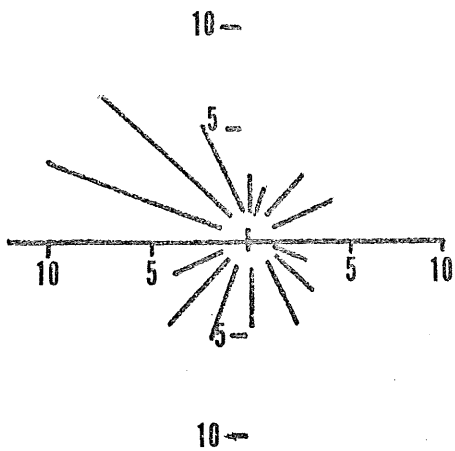
PERCENT OF TIME WIND BLOWS FROM EACH OF
16 MAJOR WIND DIRECTIONS



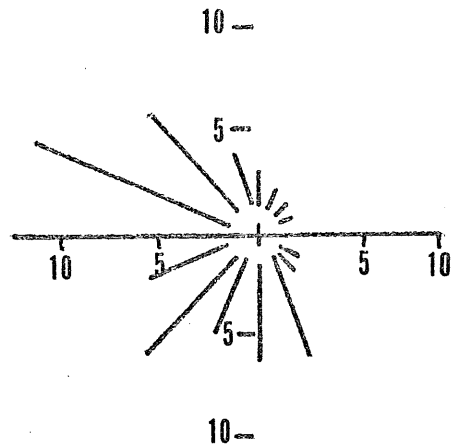
THUNDER BAY



DULUTH



HIBBING



INTERNATIONAL
FALLS

WATSON²⁷⁶

3.3.1. Temperature.

Temperatures can vary from -40°C during the long winter to as high as 40°C during the summer in the study region.²⁷⁹ Table 2 presents monthly mean temperatures along with long term averages for the four weather stations. When the data are averaged for the year used in the modeling runs (November, 1976 to October, 1977) annual average temperatures of 2.2°C , 3.5°C , 3.2°C , and 3.2°C are calculated for Thunder Bay, Duluth, Hibbing, and International Falls, respectively. Thunder Bay and Duluth had temperatures slightly below normal; Hibbing had an annual temperature that was about two and one-half times below normal; and International Falls had an annual average temperature slightly above normal.

3.3.2. Wind direction and wind speed.

Table 3 presents monthly and annual wind speed for 1976-1977 at the regional meteorological stations; normals are also included in the table.

Figure 4 shows annual wind roses base on long term data. The annual wind roses demonstrate strong westerly (Thunder Bay and International Falls) and northwesterly (Hibbing and Duluth) components.

Thunder Bay is located along the north shore of Lake Superior, and the weather station is located on flat ground west of the City. Duluth is also located along the north shore of Lake Superior; the weather station is located over the bluff at an elevation of 435 meters. Both of these stations are influenced by the lake. The weather station at Hibbing is located in the Mesabi Range on flat meadowland at an elevation of 411 meters. International Falls is influenced somewhat by the prairie wind regime, and the weather station is located at an elevation of 343 meters.

Table 1. Receptor coordinates for the modified gaussian model

Site No.	Comp. Code	Site Name	Longitude	Latitude
1	301-	Little Johnson Lake	92.7172	48.3714
2	106-	Little Vermillion Lake	92.4478	48.2904
3	104-	Birch Lake Dam	91.4410	48.0566
4	103-	Saganaga Lake	90.8894	48.2544
5	105-	Vermillion Lake	92.3789	47.9127
6	102-	Shagawa River Watershed	92.0309	47.9487
7	214-	Ely High School	91.8615	47.8979
8	224-	Fernberg Road	91.5045	47.9505
9	219-	Tower-Sudan	92.2715	47.7870
10	206-	Bear Island River W.	91.9237	47.8048
11	201-	Kawishiwi Lab Watershed	91.7438	47.8147
12	202-	Keeley Creek Watershed	91.6964	47.7868
13	107-	August Creek	91.5760	47.7868
14	101-	Isabella Watershed	91.3217	47.8228
15	212-	NW of Virginia	92.5779	47.6159
16	207-	Embarrass River W.	92.1241	47.6789
17	215-	Babbitt	91.9439	47.7111
18	204-	Unnamed Creek-Bob Bay W.	91.8302	47.7148
19	223-	Env. Learning Center (ELC)	91.5150	47.6690
20	225-	Parkville	92.5853	47.5170
21	221-	Erie Office	92.1513	47.5849
22	208-	Dunka Road	91.9771	47.6069
23	205-	Dunka River Watershed	91.8302	47.6429
24	203-	Stony River Watershed	91.5633	47.5889
25	217-	NW of Eveleth	92.6167	47.4270
26	218-	NE of Eveleth	92.3768	47.4270
27	213-	Hoyt Lakes G.C.	92.1104	47.5170
28	209-	St. Louis River W.	91.8970	47.4720
29	210-	Waterhen Creek W.	92.1502	47.3821
30	211-	Whiteface River W.	91.9503	47.3911
31	222-	Toimi	91.8038	47.3911
32	220-	Whiteface	92.2111	47.2701
33	226-	Tower	91.8705	47.1932

Table 8. Point sources in the air quality study region included in the emissions inventory.

STATE	COUNTY	CITY	FACILITY
Minnesota	Carlton	Cloquet	Potlatch Northwest Conwed
		Wrenshall	Continental Oil
	Cook	Taconite Harbor	Erie Mining Company
	Itasca	Cohasset	MP&L Clay Boswell Generating Station
		Keewatin Nashwauk	National Steel Pellet Butler Taconite
	Koochiching	Intl. Falls	Boise Cascade
	Lake	Silver Bay	Reserve Mining
	St. Louis	Aurora	MP&L Sy Laskin Generating Station
			Reserve Mining
		Babbitt Duluth	Arrowhead Blacktop
			Cargill Elevator B
			Cargill Elevator C
			Duluth Steam
			General Mills A
			International Multifoods
			MP&L Hibbard Generating Station
			Superwood Corp.
Eveleth Floodwood or Brookston Gilbert Hibbing	U.S. Steel-Duluth Coke		
	U.S. Steel-shipping		
	Eveleth Taconite		
	MP&L Generating Station		
	Jones & Laughlin		
	Public Utility		
	Hibbing Taconite		
	Hanna Mining Company		
	Erie Mining Company		
	Minutac		
Hoyt Lakes Mt. Iron Virginia	Public Utilities Dept.		
	Inland Steel		
	Pickands Mather		
Wisconsin	Ashland	Ashland	Lake Superior Power Dist. Roffler's Construction
	Douglas	Superior	Murphy Oil Corp. Farmer's Union Grain Globe Elevator Superior WL&P Orba Corp. Burlington Northern Univ. of Wisconsin CLM Corp.
<u>CANADA</u>			
Ontario		Atikokan	Ontario Hydro Generating Station
		Ft. Frances	Caland Ore Company Steep Rock Mines Minn. Pulp & Paper

Emissions data were taken directly from inventories which are compiled by Minnesota and Wisconsin from questionnaires sent to major emitters of air pollutants. Baseline emissions were also estimated directly from stack tests when the data were available.

Projected emissions were based on proposed source changes in the study area including expansions in the power generation and taconite industries, additions to pollution control systems, fuel conversions such as the change from gas to coal in the taconite industry, and the closing of some sources.

Sources for baseline and projected emissions data include the Minnesota Pollution Control Agency, Minnesota Energy Agency, Wisconsin Department of Natural Resources, and the Ontario Ministry of the Environment.

The data in the emissions inventory are not absolute numbers; that is, emissions data are continually being refined. The inventory that is compiled for SO₂ (section 7.1) and TSP (section 7.2) reflects the best available data at the time of the compilation.

3.4.1. Stack Parameters.

In order to estimate the air quality impact of a point source certain characteristics must be known. In addition to pollutant emission rates, the following information is required: source location, stack height, inside top diameter, exhaust gas temperature, flow rate, and heat emissions. Sources emitting the same pollutant from several stacks that are within approximately 100 meters of each other can be analyzed by treating all emissions as coming from a single representative stack.²⁶⁴

This technique involves calculating an arbitrary parameter, k, which accounts for the relative influence of stack height, plume rise, and emission rate.²⁸

The parameter k , which is an arbitrary parameter, is give by the equation: $k = hT_s V/Q$, where h is the stack height (m), T_s is the stack gas exit temperature ($^{\circ}\text{K}$), V is the stack gas flow rate (m^3/sec), and Q is the stack pollutant emission rate (g/sec).

The k value was then used to select representative stack parameters for a facility with several stacks as follows:

- 1) A k value was calculated for each stack with the facility,
- 2) The stack with the lowest k value was selected as the representative stack.
- 3) If the difference between stack height or flow rate was greater than 25%, the sum of emissions from all stacks was then assumed to be emitted from the representative stack.

If the difference between stack height or flow rate were greater than 25%, then the stack parameters of the largest emitter were used as representative parameters. The representative stack procedure may result in concentration estimates which are high if the stacks are located more than 100 meters apart, or if the stack heights or volume flow rates differ by more than 25%.

The sources in each community or city were then combined using the largest emitter as the representative stack.

Facilities which are located along and below Lake Superior were uniformly assigned a stack height of 10 meters because of the elevated terrain and probable plume interception by terrain.

Heat emissions were calculated according to the formula: $Q_H = \rho C_p V T_g$, where Q_H is the heat emission rate (cal/sec), T_g is the exhaust gas temperature ($^{\circ}\text{K}$), C_p is the specific heat of air ($\text{cal g}^{-1} \text{ } ^{\circ}\text{K}^{-1}$),

V is the exhaust gas flow rate (m^3/sec), and ρ is the density of air (kg/m^3).

In those instances where stack parameter data were not available for a particular facility, data from a similar facility were used. Specifically, stack data for the planned MP & L generating station at Floodwood were based on MP & L Clay Boswell unit No. 3, and stack data for the proposed operations of Jones and Laughlin at Gilbert and Pickands Mather at Biwabik were both taken from Hanna Mining Company.

Table 9 summarizes the representative stack data for the regional emissions inventory.

3.5. EXISTING LEGAL FRAMEWORK

The air quality regulations relevant to the development of a copper-nickel industry in Minnesota include emissions standards and ambient air standards.

Ambient air quality standards which exist for sulfur dioxide and particulates are summarized in Table 16 (Chapter 4). Trace elements and other pollutants such as copper, nickel, zinc, cadmium, mercury, silica, and asbestos-like fibers may pose environmental health risks, but the ambient air quality standards at present do not encompass these pollutants.

In addition to the ambient air quality standards, the entire nation is subject to the prevention of significant deterioration provisions of the 1977 amendments to the Clean Air Act of 1970.²⁷¹ The PSD amendments (40 CFR 52.21) require the establishment of a baseline of pollutants present in the atmosphere in 1977 due to existing major sources. The amendments allow incremental increases above these levels due to new or expanded sources in the area. Additionally, three classes of areas are established

Table 9. Representative¹ stack data for regional emissions inventory point sources

	<u>Coordinates</u>		<u>Stack dimension, meters</u>		<u>Temp., °K</u>	<u>Exhaust Gas</u>		
	<u>longitude</u>	<u>latitude</u>	<u>height</u>	<u>diameter</u>		<u>flowrate, m³/sec</u>	<u>heat emissiion, x 10⁶ cal/sec</u>	
MINNESOTA								
Cloquet	92.4399	46.7147	68.0	4.4	470	35.1	3.70	
Wrenshall	92.3746	46.6077	41.0	0.8	923	5.1	1.05	
Taconite Harbor	90.9765	47.5350	10.0	3.1	413	116.8	10.81	
Cohasset	93.6587	47.2571	122	5.3	386	565.0	48.86	
Keewatin	93.0656	47.4081	42.0	3.9	393	194.0	17.08	
Nashwauk	93.8638	47.3515	38.0	3.7	797	177.1	31.63	
Silver Bay	91.2449	47.3011	10.0	8.9	423	88.3	8.37	
Aurora	92.1625	47.5260	91.0	3.2	331	233.7	17.33	
Babbitt	91.8836	47.6708	10.0	0.4	260	4.7	0.27	
Duluth	92.1488	46.7345	66.4	3.3	449	76.9	7.74	
Eveleth	92.5735	47.3479	46.3	3.0	326	139.2	10.17	
Floodwood	92.8648	46.8607	120	1.6	386	565.0	48.86	
Gilbert	92.3998	47.5116	41.7	4.0	387	129.0	11.18	
Hibbing	92.9417	47.4162	41.7	4.0	387	129.0	11.18	
Hoyt Lakes	92.1359	47.5970	40.0	1.1	533	19.3	2.30	
Mountain Iron	92.6468	47.5476	31.7	4.6	324	262.2	19.03	
Virginia	92.5426	47.5188	40.0	2.2	453	38.7	3.93	
Biwabik	92.3506	47.5350	41.7	4.0	387	129.0	11.18	
International Falls								
Ft. Francis	93.4063	48.5962	30.0	2.5	433	35.4	33.43	
WISCONSIN								
Ashland	90.8645	46.6023	43.0	2.1	423	28.0	2.65	
Superior	92.1024	46.7210	10.0	2.0	923	23.6	4.88	
CANADA								
Atikokan	91.6198	48.8210	198	7.6	676	398.8	60.41	

¹ Since each city or community may have more than one stack a representative stack has been selected for modeling purposes.

-50-

with different allowed increments for each class. All of Minnesota falls into the Class II designation except areas within the borders of the BWCA and Voyageurs National Park. These areas are federally mandated Class I areas (40 CFR 52.21 (e)). Table 10 gives the allowable PSD increments for Class I and Class II areas. For any period other than an annual average, the applicable increment may be exceeded during one such period per year at any location (40 CFR 52.21 (c)).

The amendments provide that a Class I variance may be granted for a Federal Class I area if it is demonstrated to the Federal Land Manager that a new source or a source modification would have no adverse impact on the air quality related values of the Class I lands. If a Class I variance is granted, maximum allowable increases over baseline concentrations are limited to the Class II increments, except for the 3-hour SO₂ increment which is reduced to 325 ug/m³ (40 CFR 52.21 (q)(4)). Further, a variance of the 24-hour and 3-hour increments may be granted for federal mandatory Class I areas if approved by the Governor with the concurrence of the Federal Land Manager or the President (40 CFR 52.21 (q)(5) and (6)). In such cases it must be shown that the variance would not adversely affect the air quality related values of the area.

In order to determine whether or not a new or expanded source of pollutants in an area would cause the allowable PSD increments to be exceeded, a PSD review is required for new or modified sources which fall within certain major stationary source categories that could potentially emit 100 tons per year of pollutant regulated by the Clean Air Act. Primary copper smelters are included among the source categories subject to this review (40 CFR 52.21 (b)(1) and 52.21 (i)). In addition, any

source which is not included in the selected categories, but which emits or has the potential to emit 250 tons per year of pollutants regulated under the Act, is also required to undergo PSD review (40 CFR 52.21 (b)(1)(ii)).

When a new or modified source is identified as being subject to PSD review, the source must have the best available control technology (as defined in 40 CFR 52.21 (b)(10)) for each applicable pollutant, unless the increase in allowable emissions of that pollutant would be less than 50 tons per year, 1000 pounds per day, or 100 pounds per hour, whichever is most restrictive (40 CFR 52.21 (j)(2)).

The regulations require that a baseline concentration be established against which incremental increases can be evaluated. The baseline concentration is defined as the ambient concentration level reflecting actual air quality as of August 7, 1977 minus any contribution from major stationary sources and major modifications on which construction started on or after January 6, 1975. The regulations further define the baseline to include the allowable emissions of major stationary sources and major modification which started construction before January 6, 1975 but were not in operation by August 7, 1977 (40 CFR 52.21 (b)(11)). In the air quality study region, this clause has the effect of raising the PSD baseline above the actual concentration present on August 7, 1977 for both SO₂ and particulates. The principal reason for this is the taconite expansion currently taking place on the Iron Range.

Table 10. Maximum allowable PSD increments in Class I and Class II areas.

Pollutant	ALLOWABLE INCREMENT ^a ($\mu\text{g}/\text{m}^3$)	
	Class I Areas	Class II Areas
Particulate Matter:		
Annual geometric mean	5	19
24-hour maximum	10	37
Sulfur Dioxide		
Annual arithmetic mean	2	20
24-hour maximum	5	91
3-hour maximum	25	512

^aFor any period other than an annual period, the applicable maximum allowable increase may be exceeded during one such period per year at any one location.

In addition to the increments listed earlier, the PSD regulations also require that pollutant concentrations not exceed the national secondary ambient standard or the national primary ambient standard, whichever concentration is lowest for the pollutant for a given period of exposure (40 CFR 52.21 (d)).

Three steps are involved in the PSD review. The first step is to identify all sources that are to be used in determining the PSD baseline as defined by the act. Next, new sources in the area which are not part of the baseline contributors must be identified since they will consume all or part of the allowed increments. Third, the new proposed source under review must be characterized in terms of its location and emissions. Appropriate air quality modeling for the various periods specified in the regulations (3-hour, 24-hour, annual) can then be used to determine whether or not the new source, in conjunction with other new sources in the area, will result in the increments being exceeded. The modified gaussian model was used for 24-hour and annual PSD review. The 3-hour increment has been evaluated using the standard gaussian model.⁶¹

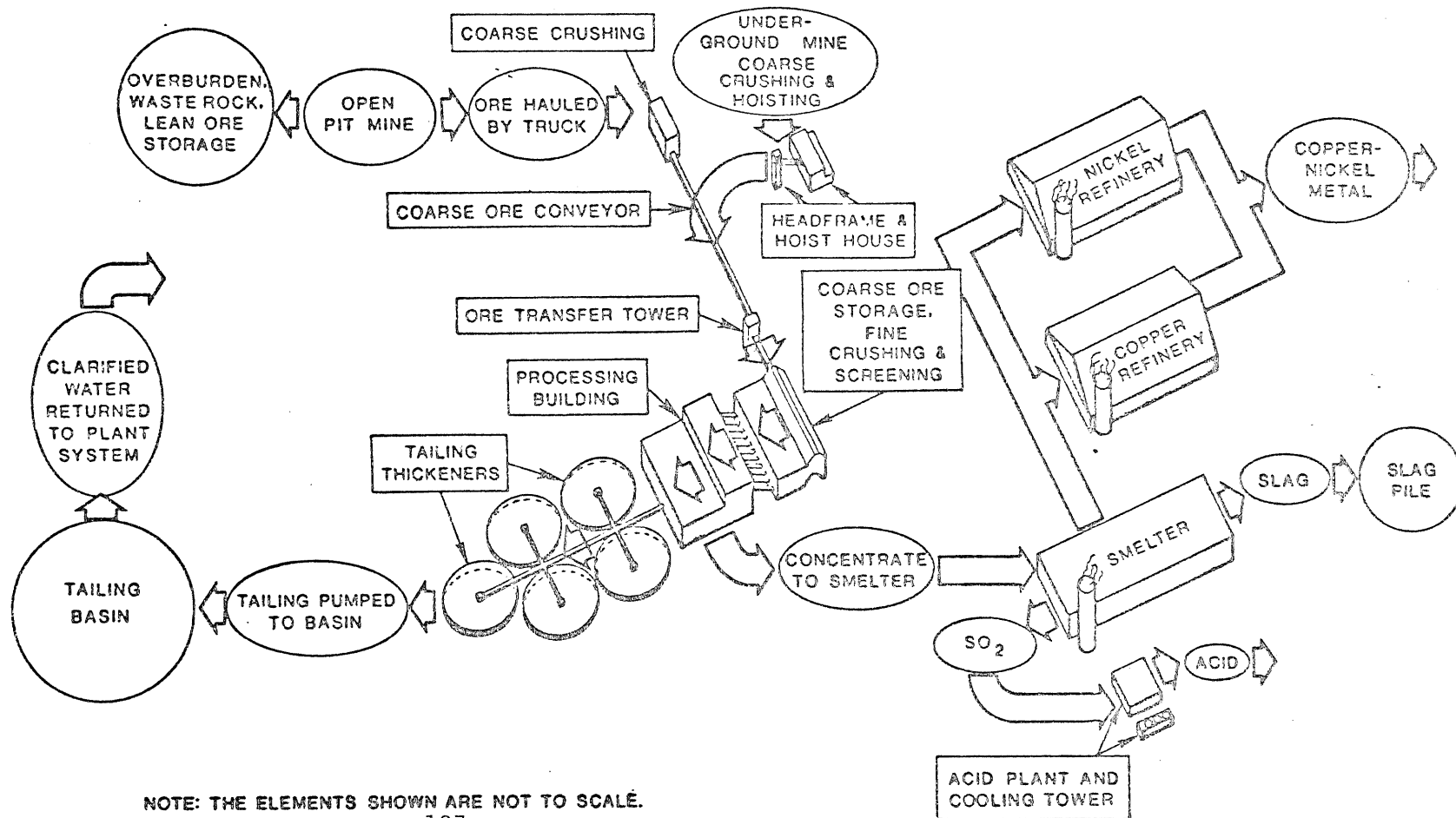
For purposes of studying potential copper-nickel development impacts, a target date of 1985 was selected for PSD review analysis. This is the earliest date that a major copper-nickel source such as a smelter might reasonably be expected to begin operations. Also, 1985 was the latest year for which emissions projections could be based on expansion plans for industrialization in the region, or on possible enforcement actions by the Minnesota Pollution Control Agency.

In terms of the sources located in Canada, it must be noted that their status in the PSD review is not certain. The regulations provide that upon the request of the Governor the increase in pollutant concentrations attributable to new sources outside the United States may be excluded in determining compliance with maximum allowable increases (40 CFR 52.21 (f)(1)(iv)). The major source of relevance here is the proposed coal-fired power plant at Atikokan, Ontario which is being constructed by Ontario Hydro.

In addition to ambient standards, copper-nickel development would also be subject to a variety of emissions standards. The federal new source performance standards (NSPS) are applicable to primary copper smelters.²⁶⁷ There is a technical legal question whether or not a copper-nickel smelter of the type envisioned to treat concentrates from a Minnesota mining operation is a primary copper smelter as the term is used in the existing NSPS as well as in the PSD regulations. A ruling by the appropriate legal authorities may be needed to clarify this matter. However, for the purposes of assessing impacts, it is assumed that the regulations apply.

Emissions of particulate matter in the gases discharged to the atmosphere from dryers are limited to 50 mg/m³ (dry) and an opacity of 20%

FIGURE 6
 PRINCIPAL MINING COMPONENT RELATIONSHIPS
 IN THE PRODUCTION OF COPPER AND NICKEL METAL



NOTE: THE ELEMENTS SHOWN ARE NOT TO SCALE.

Ritchie and Kreisman¹⁹⁷

55-

(40 CFR 60.162 and 60.164, respectively). Also, emissions of SO₂ from roasters, smelting furnaces, and copper converters are limited to 650 ppm (by volume) averaged over a 6-hour period (40 CFR 60.164). The standards also require the continuous monitoring of the opacity of dryer emissions and SO₂ content of emissions from roasters, smelting furnaces, and copper converters (40 CFR 60.165).

3.6. SMELTER MODELS

This section discusses sources air emissions from a smelter along with control equipment, emissions estimates, and stack input parameters.

Sulfur and metal particulates are the primary emissions of concern in terms of health and environmental effects of a sulfide mining development.

Figure 6 shows the various operations involved in copper-nickel mining, smelting and refining. Figure 7 shows a flowscheme for a copper-nickel smelter using a flash smelter furnace.

The wet concentrated smelter feed (635,260 mtpy; 14.3% Cu, 2.5% Ni, 33.3% Fe, 25.9% S) is processed using pyrometallurgical techniques which incorporate drying, smelting by a flash furnace, converting, and refining. All smelter models were scaled to represent a smelter/refinery complex producing 100,000 mtpy of refined copper plus nickel metal. 174, 186, 197, 274

3.6.1. Sulfur emissions.

Other point sources of sulfur dioxide which potentially could emit more than 100 mtpy include the copper refinery, nickel refinery, and supporting energy plants. The major source of sulfur dioxide emissions in a copper-nickel development complex is the smelter which processes the concentrated ore into unrefined metal. Mining and milling operations are

not significant sources of SO₂ emissions.

The refineries are potential sources of SO₂ because they consume fuel to provide heat for a variety of processes. SO₂ emissions from the refineries depend on the type of fuel used. Coal or high sulfur residual oil could result in major emissions, while a sulfur-free fuel such as natural gas would result in minimal emissions. If the refineries are located at the site of the smelter, then a significant part, if not all, of the thermal needs of the refineries could be met by the waste heat from the smelter.

Total energy requirements for an integrated copper-nickel development producing 100,000 mtpy of copper and nickel metal are estimated to be one billion kilowatt-hours of electrical energy per year, with a peak load of about 150 megawatts.¹⁹⁷

Although this could result in substantial SO₂ emissions, it is assumed the electrical energy needs of a copper-nickel development will be met by large central station power plants, and the added electrical demand will not require the construction of an additional coal-fired power plant in the study region.

Because there is no firm basis for modeling SO₂ emissions from the copper or nickel refineries or new power generating facilities specifically built for copper-nickel development, the major source of sulfur emissions is assumed to be the smelter.

A brief discussion of emission sources, mass balances, and control technology follows.

During the smelting operation, the bulk of the sulfur is removed by literally burning it to form sulfur dioxide. The fate of the input sulfur

depends on the types of control technologies used.

Point sources of SO_2 result from the control of the strong and weak gas stream as shown in Figure 7. Based on a review of the literature and communications with mining companies, it is likely that the major control devices for SO_2 emissions could be either a double contact acid plant and/or a wet calcium-based scrubber (turbulent contact absorber, TCA). Both of these control devices produce products which may require disposal; for example, sulfuric acid from the acid plant if there is no market, and sludge from the scrubber. Double contact acid plants can achieve efficiencies of 99.5% to as high as 99.9% with exit SO_2 concentrations ranging from about 500 ppm to as low as 100 ppm.^{228,265} A survey of domestic smelter installations using double contact acid plants showed that actual operating efficiencies of 97% to 99.7% have been achieved.^{139,165,282-284,289}

Calcium-based scrubbers have been installed in several domestic fossil-fuel fired power plants, a molybdenum ore roaster, a secondary lead smelter, and an ore sintering plant. Various pilot studies have also tested calcium-based scrubbers. The turbulent contact absorber, which would control low SO_2 concentration gas streams from the smelter and the acid plant, is a wet calcium-based scrubbing system. It has been used successfully in the electric utility industry where SO_2 gas stream concentrations are low, a few tenths of one percent.²⁹

Fugitive or uncontrolled sulfur dioxide emissions sources include leaks in ducts, converters, and the refining furnace.²⁸²⁻²⁹⁰ These emissions can be minimized by careful design of the furnace, gas handling equipment, ducts, and good housekeeping practices. It is difficult to quantify the magnitude of fugitive emissions and exact methods have not

been developed.²⁶⁵ Estimates of SO₂ fugitive emissions have been reported to be in the range of 0 to 15% of total sulfur input at domestic smelters.^{97, 165, 282-289}

Smelter mass balances were based on data from bench-scale processing analyses of Minnesota ore, on-site investigations of existing smelters, and consultations with mining/smelting engineers.^{38, 186} The literature reports that actual resolution of sulfur mass balances may be only 20% to 40% of input sulfur,³⁶⁵ and the mass balance does not consider time variations of input sulfur content.

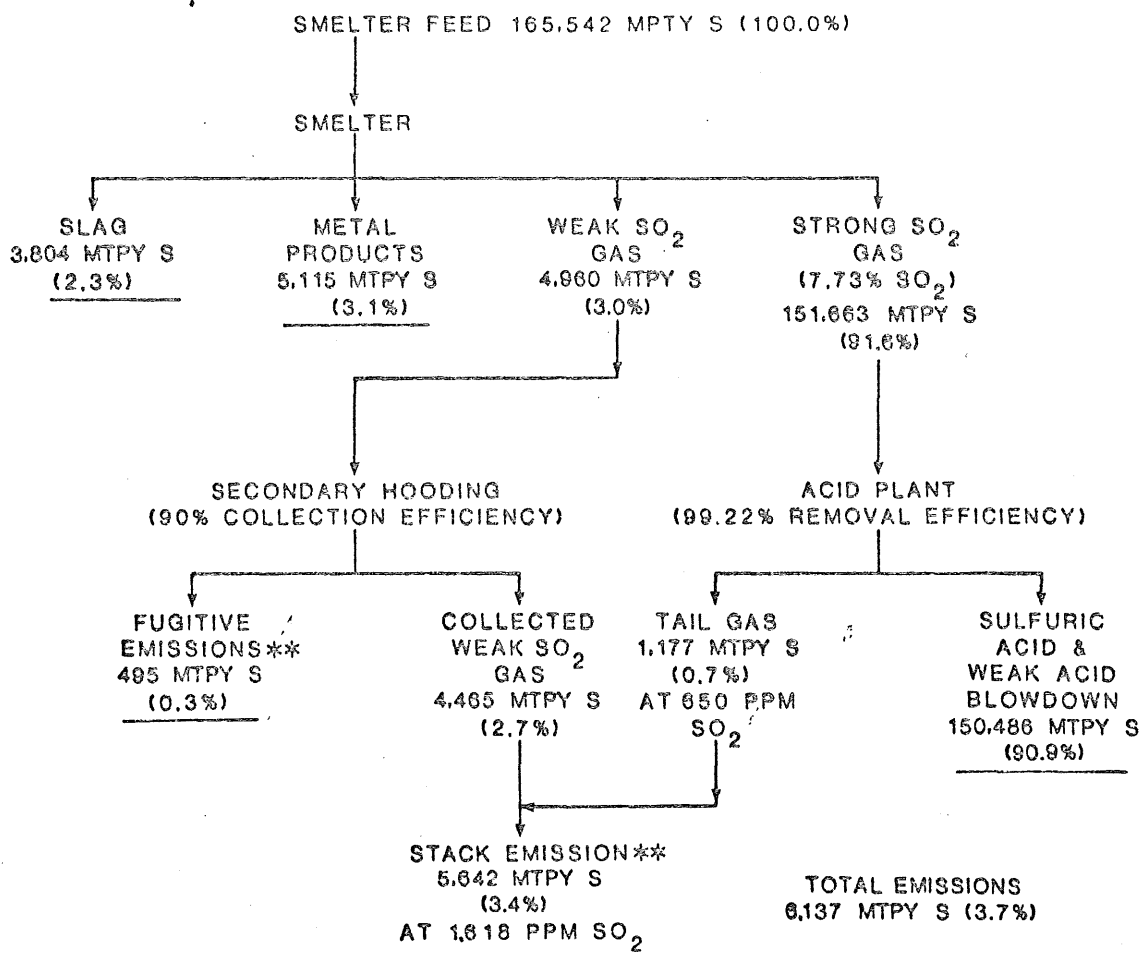
The federal new source performance standards (NSPS) provided a framework for smelter pollution control equipment configuration. In order to meet the NSPS limit of 0.065% SO₂, by volume, a smelter must have the equivalent of double contact acid plant control (99.5% removal by volume) for all process gases from roasters, smelting furnaces, and converters.²⁶⁷ One problem with NSPS is that removals are specified by volume, allowing the possibility for dilution in order to achieve the standard. The author feels that a standard based on mass would make a better standard.

Three pollution control configurations were selected to provide a range of emissions for modeling purposes; mass balances for each of the three smelter models are shown in Figures 8, 9, 10. The base case smelter which would not meet NSPS is the least likely to be built; it is included in the analysis to provide a worst case comparison. The smelter mass balances are shown in metric tons of sulfur per year; flows labeled stack and fugitive emissions actually leave the facility primarily as sulfur dioxide with some sulfuric acid.

All models have a sulfur input of 165,542 mtpy which comes from both

FIGURE 8

BASE CASE MODEL SULFUR BALANCE FOR FLASH FURNACE WITH ACID PLANT CONTROL OF STRONG SO₂ GAS TO 650 PPM SO₂, SECONDARY HOODING COLLECTION OF WEAK SO₂ GAS TO REDIRECT IT TO THE STACK DISCHARGE*

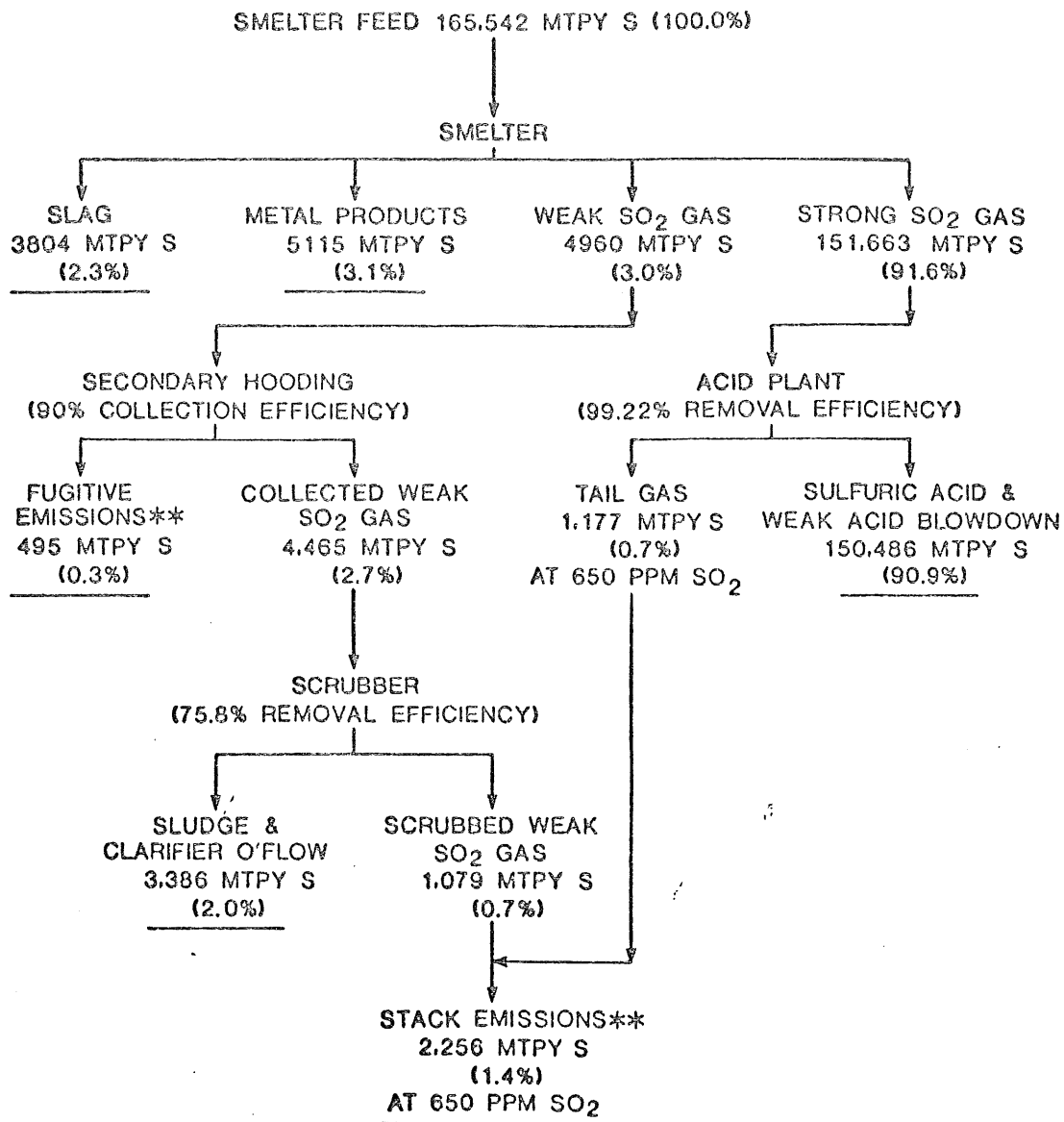


* NORMAL OPERATING CONDITIONS ARE ASSUMED.

** EMITTED TO THE ATMOSPHERE AS SO₂, WITH EACH METRIC TON OF SULFUR CONSTITUTING 2 METRIC TONS OF SO₂

FIGURE 9

OPTION 1 MODEL SULFUR BALANCE FOR FLASH FURNACE WITH ACID PLANT CONTROL OF STRONG SO₂ GAS TO 650 PPM SO₂, SECONDARY HOODING COLLECTION OF WEAK SO₂ GAS FOLLOWED BY SCRUBBING TO 650 PPM SO₂*



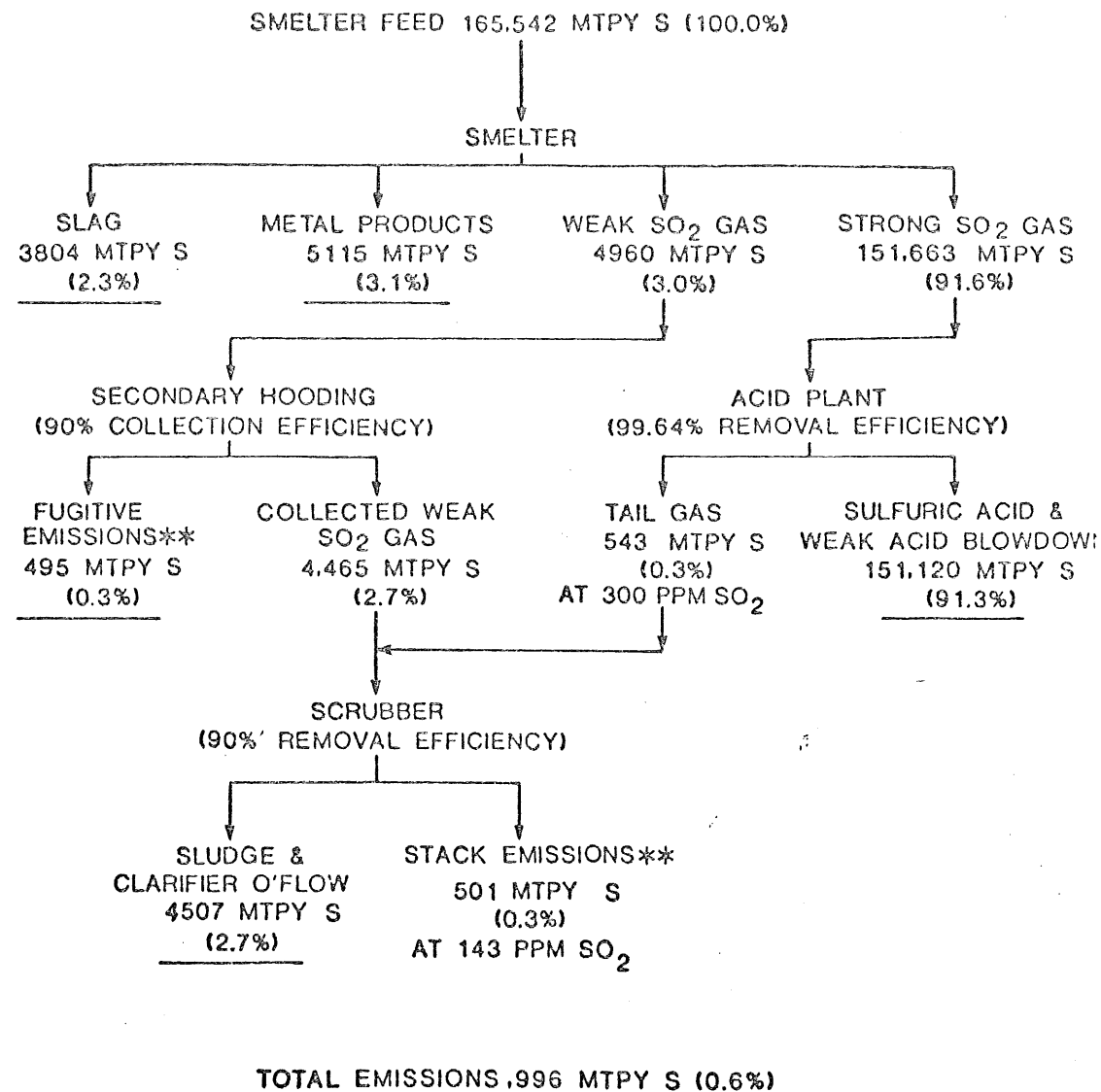
TOTAL EMISSIONS 2,751 MTPY S (1.7%)

* NORMAL OPERATING CONDITIONS ARE ASSUMED

** EMITTED TO THE ATMOSPHERE AS SO₂, WITH EACH METRIC TON OF SULFUR CONSTITUTING 2 METRIC TONS OF SO₂

FIGURE 10

OPTION 2 MODEL SULFUR BALANCE FOR FLASH FURNACE WITH ACID PLANT CONTROL OF STRONG SO₂ GAS TO 300 PPM SO₂, SECONDARY HOODING COLLECTION OF WEAK SO₂ GAS, AND SCRUBBING OF ACID PLANT TAIL GAS PLUS COLLECTED WEAK SO₂ GAS TO 143 PPM SO₂*



* NORMAL OPERATING CONDITIONS ARE ASSUMED

** EMITTED TO THE ATMOSPHERE AS SO₂, WITH EACH METRIC TON OF SULFUR CONSTITUTING 2 METRIC TONS OF SO₂

the concentrate (over 99%) and from the coal used as a fuel in the smelter. The three models are summarized below.

Base case model: The base case model assumes that SO_2 from the strong gas stream is treated by a double contact acid plant with a removal efficiency of 99.22%. The tail gas from the acid plant contains 650 ppm SO_2 (1177 mtpy S). The weak SO_2 gas stream is treated by secondary hoods with a 90% collection efficiency. About 4465 mtpy S are collected, and about 495 mtpy are estimated to escape secondary hooding and be released as fugitive emissions. The collected gases from secondary hooding combine with the acid plant tail gases and are emitted to the atmosphere. Total stack emissions from the weak and strong SO_2 gas streams are estimated to be 5642 mtpy S.

Option 1 model: The option 1 smelter assumes that both the weak and strong gas streams are treated to meet the new source performance SO_2 standard of 650 ppm, by volume. The strong gas stream treatment is the same as for the base case smelter. The collected weak gas stream (after secondary hooding) is further treated by a scrubber with 75.8% removal efficiency. The scrubbed weak gas stream (1079 mtpy S) is then combined with the acid plant tail gas to yield total sulfur stack emissions of 2256 mtpy S. Fugitive emissions from secondary hooding are the same as for the base case smelter.

Option 2 model: The option 2 smelter model assumes best available control technology removal for both the strong and weak gas streams. The acid plant removal efficiency is increased to 99.64% to yield a gas stream of 0.3% (543 mtpy S). Secondary hooding efficiency remains at 90%. The collected weak gases and the acid plant tail gas are then combined and

sent through a wet scrubber of 90% removal efficiency. The resulting gas stream from the stack is 0.3% S(501 mtpy S). Fugitive emissions resulting from secondary hooding are the same as for the base case smelter.

Table 11 summarizes the SO₂ emissions from the three smelter models for a smelter complex producing 100,000 mtpy of copper plus nickel metal.

The sulfur dioxide emissions from these hypothetical models can be placed into perspective by comparing them to other sources (Figure 11). The models have emissions ranging from 2 to 3 orders of magnitude below the emission rate from the Copper Cliff smelter at Sudbury as of 1975. Emissions from the Clay Boswell plant at Cohasset with the addition of Unit 4 are expected to be about four times the emission rate of the base case smelter and about eight times the emission rate for the smelter which meets NSPS.

Table 11. Summary of SO₂ emissions from three smelter configurations each producing 100,000 mtpy of copper plus nickel metal.

Smelter Models	Fugitive Emissions		Stack Emissions		Total Emissions	
	mtpy	(gm/sec)	mtpy	(gm/sec)	mtpy	(gm/sec)
Base	990	(31)	11284	(357)	12274	(388)
Option 1	990	(31)	4512	(143)	5502	(174)
Option 2	990	(31)	1002	(32)	1992	(63)

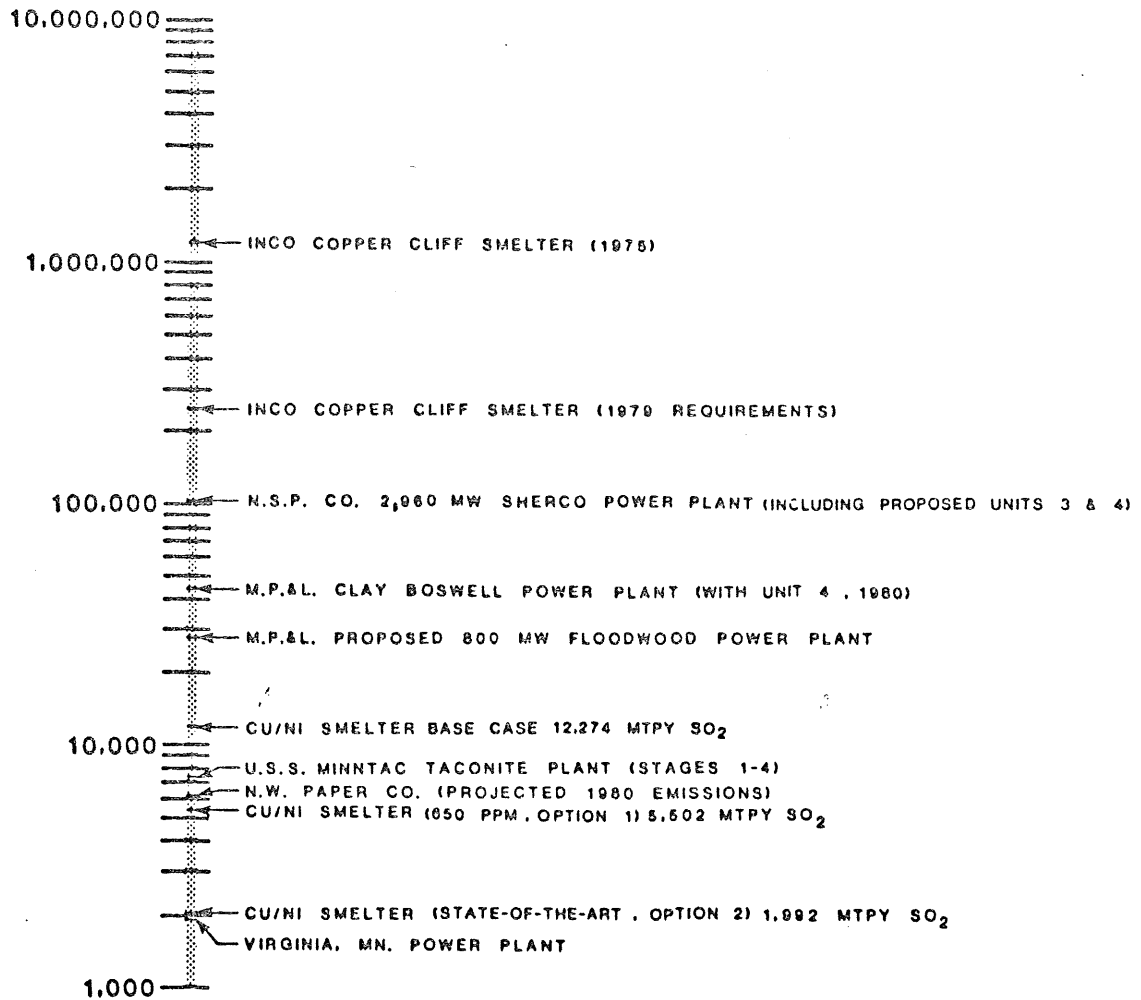
There is, of course, a possibility that extremely high concentrations of pollutants can be released during short periods of time as a result of an accident or other upset at the smelter. Failure of a major piece of equipment such as the acid plant could result in high emissions for up to a few hours before repairs could be made or the smelter operation stopped.

FIGURE 11

SUMMARY OF MODELED FLASH SMELTER SO₂ EMISSIONS* AND EMISSIONS FROM OTHER LARGE SO₂ SOURCES

(SOURCE: RITCHIE, 1978)

SULFUR DIOXIDE**
EMISSIONS
(MTPY)



*VALUES INCLUDE STACK PLUS FUGITIVE EMISSIONS

**VALUES SHOWN ARE MTPY OF SO₂ WHICH IS TWICE THE AMOUNT OF SULFUR

High emissions will also result from shut-downs due to routine maintenance. It is estimated that the smelter operations could be shut-down in 3 to 6 hours either as a result of accidental release or maintenance.

The modified gaussian model is not appropriate for simulating periods less than 24 hours so these upset situations were not modeled. However, two upset cases, low level fugitive release and stack release were modeled for 3-hour periods by Endersen⁶¹ using a fugitive emissions model.

Table 12 provides a comparison of the average sulfur balances for the three modeled smelter cases and other domestic copper smelters. All of the domestic smelters with the exception of the Phelps Dodge smelter at Hidalgo, New Mexico are older reverberatory type smelters. The Phelps Dodge smelter is a flash smelter with advanced pollution control equipment resulting in lower SO₂ emissions.

3.6.2. Particulate emissions.

Particulate emissions can result from nearly all phases of copper-nickel development including construction areas, mines, haul roads, mills, tailings basins, smelters, and stock piles of either lean ore or waste rock. Secondary development such as new road construction can also produce particulate emissions. Although the smelter is not the only source of particulates, there is more concern about these emissions than from other mining sources because of the high levels of metals in the concentrate.

Particulate control is accomplished primarily by cyclones, high efficiency electrostatic precipitators (ESP), hooding, and ventilation systems. The major potential source of stack particulates likely to be present within the smelter appears to be the dryer. Up to 10% of the concentrate is estimated to be carried out of the dryer as particulates

Table 12. Comparison of sulfur mass balances for the base case, option 1 and option 2 smelters to other domestic smelters

Installation	Sulfur Input	Sulfur Capture		Fugitive Emissions		Stack Emissions		Reference
	TPD-S	TPD-S (% of input)						
White Pine	113	3.4	3.1	2.2	1.9	108	95	282
Kennecott, Hayden	361	328	90.8	18	5.0	15	4.2	283
Kennecott, Hurley	351	215	61.1	--	--	137	38.9	284
Magma, San Manuel	660	472	71.5	16.5	2.5	172	26	285
Phelps Dodge, Ajo	203	183	90	10	5.0	10	5.0	286
Phelps Dodge, Morenci	981	668	68.2	17	1.7	296	30.1	287
Asarco, El Paso	185	141	76.5	--	15% estimated	44	23.5	97, 289
Asarco, Hayden	609	161	26.4	21	3.4	427	70.1	290
Phelps Dodge, Hidalgo	275	254	92.4	--	--	21	7.6	165
Phelps Dodge, Douglas	771	22	3.0	53	7.0	696	90	288
Base Case Smelter	499	465	93.2	3	0.6	31.0	6.2	
Option 1 Smelter	499	484	97	3	0.6	12.4	2.5	
Option 2 Smelter	499	493	98.8	3	0.6	2.8	0.6	

entrained in the exit gases.¹⁸⁶

Dryer gases, along with gas streams from secondary hooding devices, would be passed through one or more particulate removal devices such as an electrostatic precipitator. Removal efficiencies of 96% to 99% can be expected from electrostatic precipitators.²³⁹ Efficiencies ranging from 90% to over 99% have been reported at domestic smelters where electrostatic precipitators are used on all roaster, reverberatory furnaces, and converters.^{238, 283, 284, 286-291}

Gases from the smelting furnaces (a flash furnace is assumed in the smelter models) will also contain high particulate loads. After passing through an electrostatic precipitator, these gases will flow to a sulfuric acid plant. A high degree of removal of solid or gaseous contaminants is required before the gas stream can enter the acid plant to prevent damage to the catalyst beds and contamination of the product. Overall particulate removal efficiencies of 99.5% to 99.9% of the smelter off-gas contaminants are attainable.²⁶⁵

Cyclones are used as precleaners to remove large particulates (greater than 10 microns) from the gas stream. Efficiencies in the range of 50% to 90% are easily attained depending on flow and design characteristics.²⁰⁴ Removal efficiencies of 96.9% have been reported at a domestic smelter using cyclones for particulate control.

If wet scrubbers are used to remove SO_2 from the secondary hooding gases and possibly the acid plant tail gases, further particulate control will result. Again, removal efficiency depends on the gas stream and design characteristics. Removal efficiencies greater than 90% have been reported at two power plants using 3-stage turbulent contact absorbers.⁹²

A removal efficiency of 85% was selected for modeling purposes.

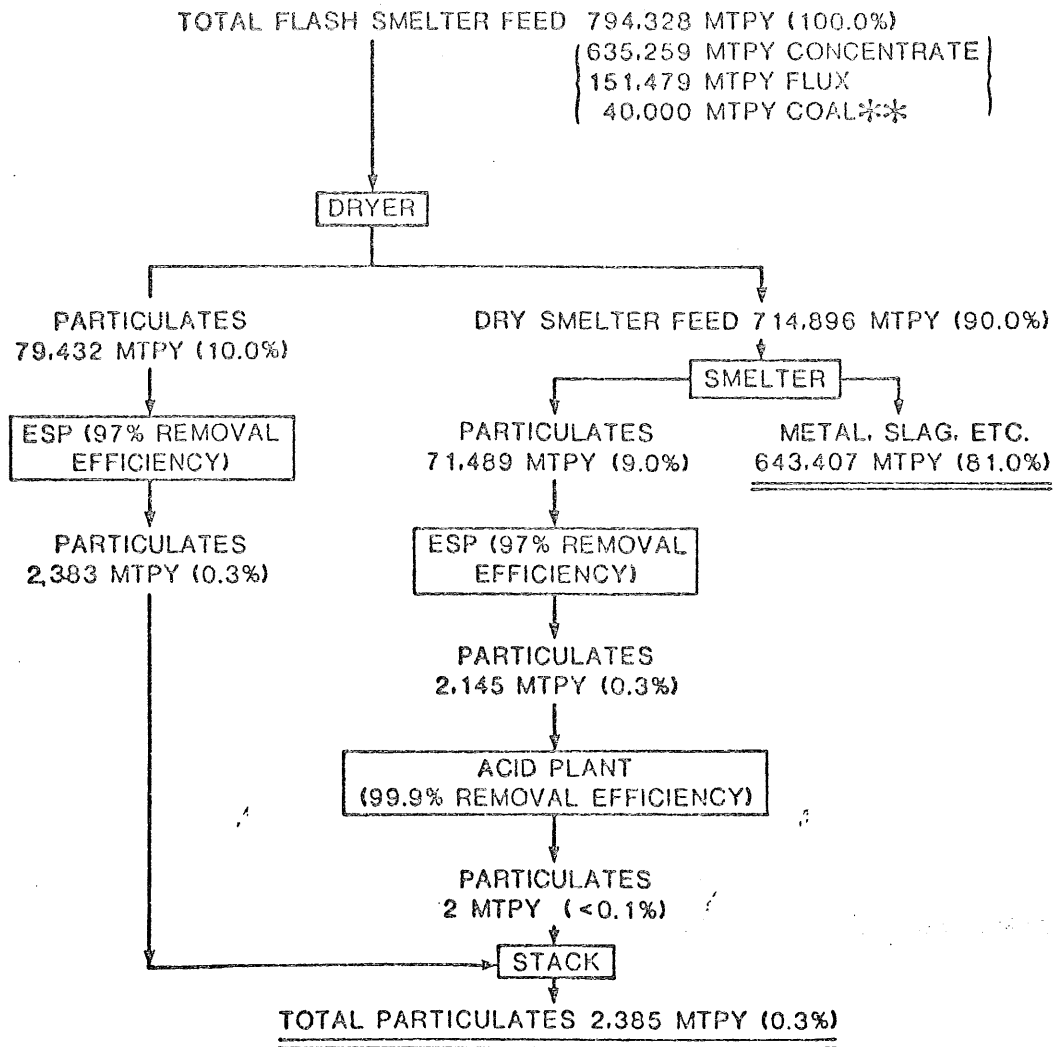
Sources of particulate fugitive emissions include leaks in ducts, converters, material handling during crushing and screening operations, drying, and the refining furnace.²⁸²⁻²⁸⁹ Particulate fugitive emissions may be effectively controlled in critical areas such as converters by collecting and routing gases to control equipment before final discharge.²⁶⁵

Based on the following considerations, two stack particulate mass balances¹⁸⁶ were generated based on a flash smelting facility with a spray dryer. As before, the facility is sized to produce 100,000 mtpy of copper plus nickel metal. The two models (shown in Figures 12 and 13) reflect emissions with and without the use of scrubbing units to treat the weak SO₂ gas streams. The modeled stack particulate emissions are 2385 mtpy without a scrubber and 358 mtpy with a scrubber. It is clear from the figures that the gases coming from the furnaces contribute a negligible part of these emissions as a result of the high particulate removal prior to the acid plant. Particulate fugitive emissions are estimated to be 1500 mtpy for both of the smelter models based on the middle of the range of estimated fugitive emissions from domestic smelters (7 to 3700 mtpy).^{166, 269} Figure 14 places the smelter particulate emissions in perspective with emissions from other point sources in the regional particulate emissions inventory.

Unlike the SO₂ emissions models the particulate models were not developed within the framework of emissions regulations, but rather, in terms of available control equipment performance.

FIGURE 12

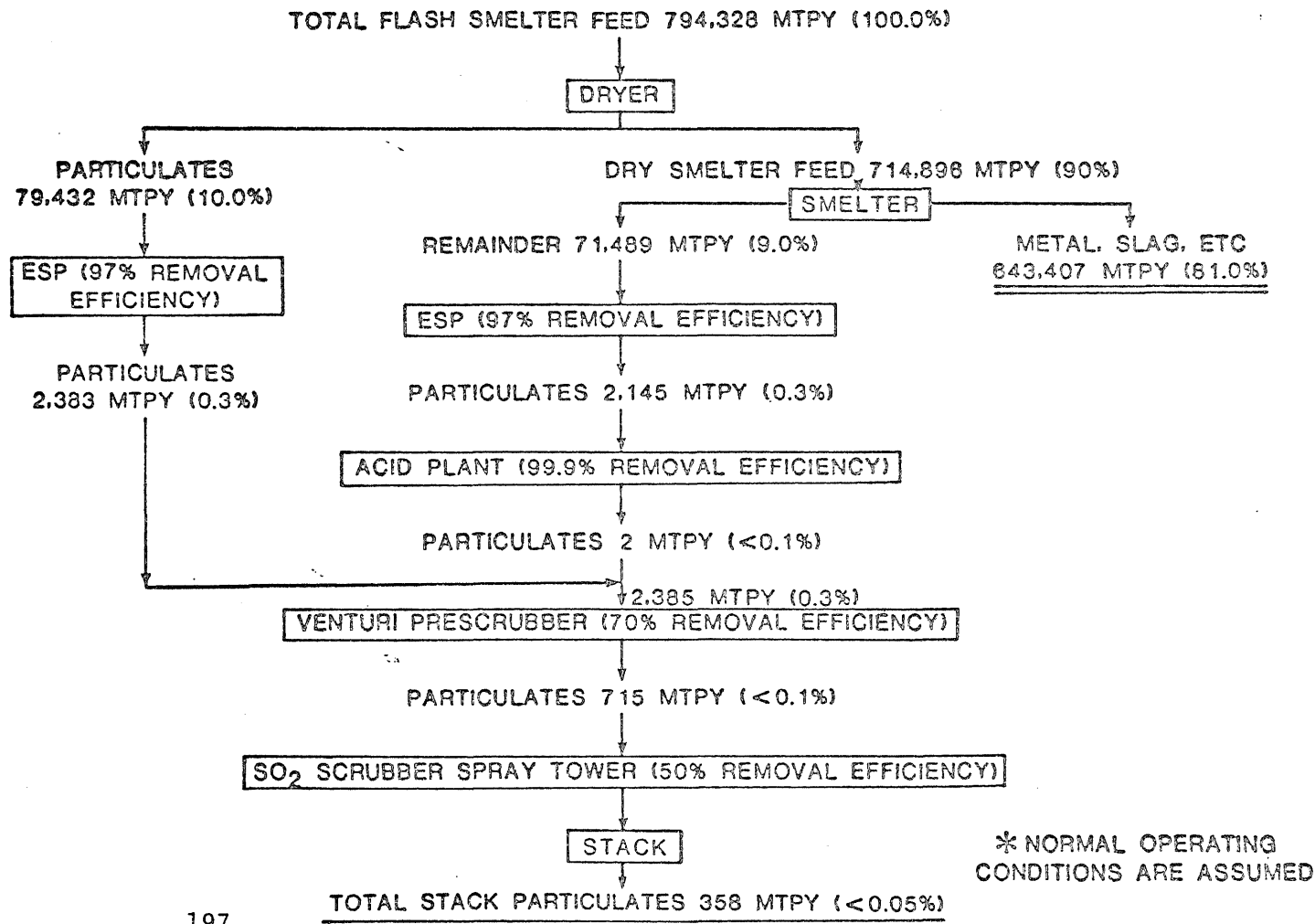
MODEL FOR STACK EMISSIONS PARTICULATE BALANCE
 FOR BASE CASE SMELTER/ REFINERY COMPLEX*



*NORMAL OPERATING CONDITIONS ARE ASSUMED, IGNORING FUGITIVES WHICH ARE UNKNOWN

**ONLY 7.590 MTPY OF THE 40,000 MTPY COAL ASSUMED TO REPORT AS PARTICULATE MATTER (SEE VOLUME 2, CHAPTER 4)

FIGURE 13. MODEL FOR STACK EMISSIONS
PARTICULATE BALANCE FOR OPTIONS 1 AND 2*



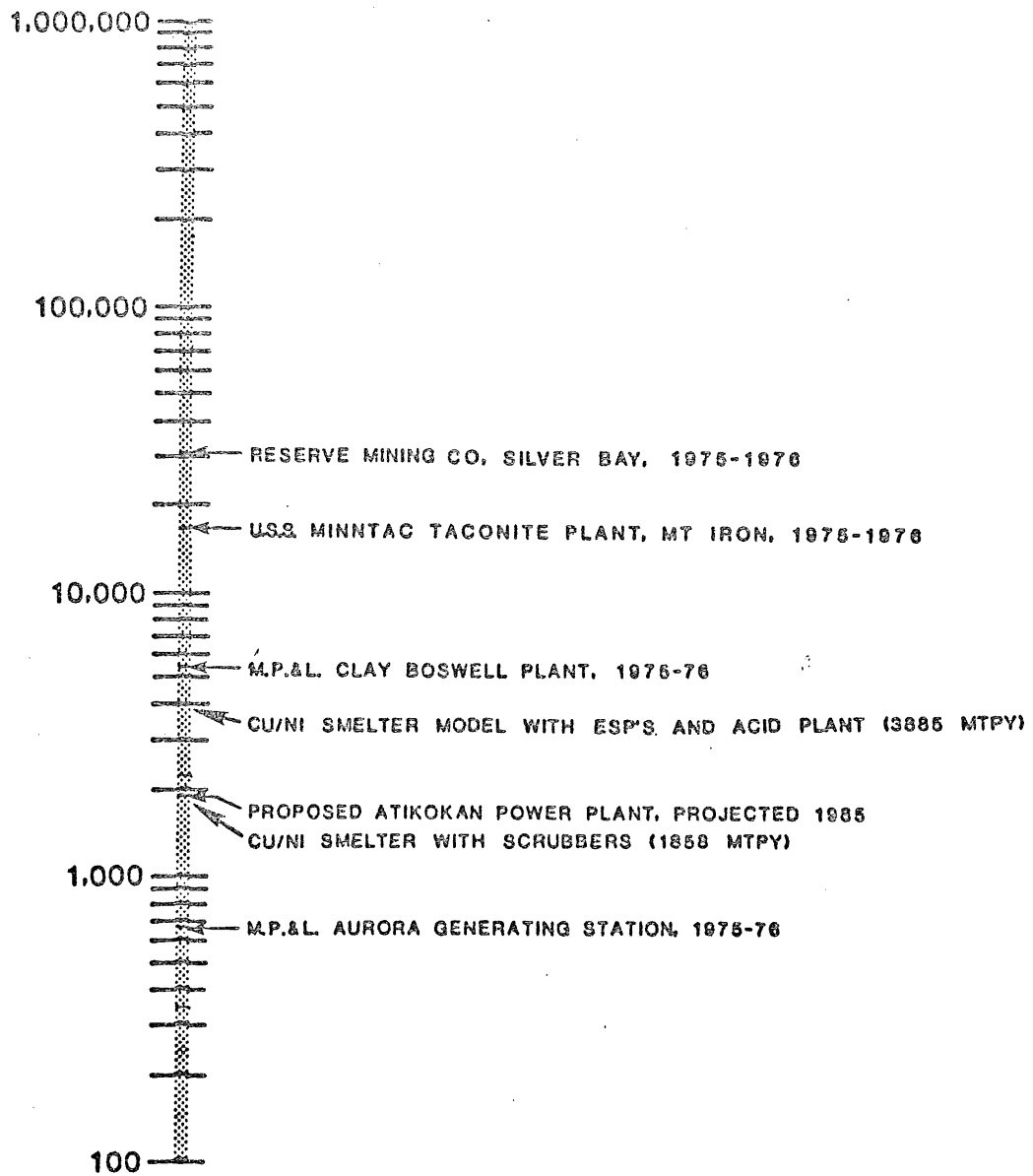
-72-

FIGURE 14

SUMMARY OF MODELED FLASH SMELTER TOTAL PARTICULATE EMISSIONS AND EMISSIONS FROM OTHER LARGE PARTICULATE SOURCES

PARTICULATE
EMISSIONS
(MTPY)

(SOURCE: RITCHIE, 1978)



3.6.3. Elemental constituents.

The distribution of elemental constituents and mass balances were estimated based on a combination of bench tests of the copper-nickel ore and operating data from existing smelters.^{38, 186} Uncertainties in the mass balances are estimated to range from +20% to an order of magnitude.³⁸ Table 13 summarizes the elemental particulate emissions expected from a smelter producing 100,000 mtpy of copper plus nickel metal.

Coleman³⁸ prioritized those elements in the Duluth Gabbro ore body which might pose operational and environmental pollution problems if they are processed in a primary copper-nickel smelter. The prioritization is based on the quantity of element present in the concentrate, toxicity to either human health or the environment, and the likelihood of release into the environment. Relative toxicity was based on the American Conference of Governmental Industrial Hygienists (ACGIH) TLV's and the National Institute of Health (NIH) LD 50's. Priority 1 elements are those that are present in significant concentration in the bench-scale concentrate, have a high toxicity relative to other elements present in the ore, or are likely to be released into the environment. Priority 2A elements present potential environmental hazards but are present in very small quantities, are expected to be relatively inert, or are not very toxic relative to priority 1 elements. Priority 2B elements are present in low concentrations, have low toxicity, or are unlikely to be released into the environment. Priority 2C elements present potential environmental problems, but bench-scale data were not available for further characterization. Table 14 prioritizes the elements associated with copper-nickel smelting.

Table 13. Stack and fugitive particulate emissions from a smelter complex producing 100,000 mtpy of Cu plus Ni metal.

Constituent	STACK EMISSIONS		FUGITIVE EMISSIONS
	Base Model ^b mtpy	option 1-option 2 model ^c mtpy	all smelters
total particulate	2383	358	1510
SO ₄	1490	223.6	0
Cu	263.5	39.53	281
Ni	50.45	7.57	61.9
As	17.44	0.01	0.12
Cd	1.84	0.01	0.07
Co	2.53	0.38	1.81
Be	0.02	0.00007	0
Pb	9.8	0.02	0.13
Hg	0.07	0.00006	0
Zn	23.82	0.33	3.23
Fe	581.67	87.26	83.0
Sb	0.003	0.0005	0
Bi			
Cl	0.39	0.06	0
F	0.02	0.003	0
Se	0	0	no data
Te	0	0	no data
Si (SiO ₂)	638.51	95.79	704
Al (Al ₂ O ₃)	101.83	15.28	116
Mg (MgO)	57.48	8.62	68
Ca (CaO)	100.18	15.03	119
Coleman ³⁸			

Table 14. Prioritization of elements in the Duluth-Gabbro ore.

Priority 1: arsenic, cadmium, cobalt, copper, nickel
selenium, sulfur, tellurium

Priority 2A: beryllium, lead, mercury, zinc

Priority 2B: aluminum, barium, boron, calcium, carbon,
chromium, iron, magnesium, manganese,
molybdenum, phosphorous, potassium, silicon,
silver, sodium, titanium, thorium, vanadium,
zirconium

Priority 2C: chlorine, fluorine, antimony, bismuth

Coleman³⁸

Six elements were selected for the modeling simulations based on their toxicity and expected emissions: copper, nickel, arsenic, cadmium, lead, and mercury.

Elements of particular interest are arsenic and mercury (and to a lesser extent lead, cadmium, and zinc) because these elements may be carried out of the smelting furnace with the exhaust gases either as vapor or particulate depending on gas stream characteristics. Although the available information is limited, indications are that these elements are present in low concentrations and a high degree of removal will occur as these elements pass through the electrostatic precipitators, acid plant, and possibly wet scrubber. These elements (with the exception of zinc which was not modeled) are treated as particulates rather than vapors in the modeling simulations. This approach should be re-evaluated for any specific proposal depending on the composition of material to be processed and the technology to be employed.

3.6.4. Smelter stack parameters.

In addition to smelter source emissions data, the modified gaussian model requires the following additional source information: stack height, heat emissions, and flow rate.

The selection of stack parameters (stack height, exit gas velocity, exit gas temperature, and inside top stack diameter) for the hypothetical smelter was based on data from the Phelps Dodge flash smelter at Hidalgo, New Mexico.¹⁶⁵ The same stack parameters were used for each of the three smelter cases, and gases from both the weak and strong gas streams were assumed to be combined for release through a single stack. Fugitive emissions were assumed to be released through the top of the smelter

building and were handled as exiting from a low level stack for modeling purposes.

Unlike the very tall stacks ranging from 180 to 360 meters²⁸³⁻²⁸⁹ found in many conventional smelters with poor SO₂ removal, the main stack for a smelter in northeastern Minnesota is expected to be relatively short.

A stack height of 60 meters and an exit gas temperature of 82°C were selected for modeling the main stack. A fugitive stack of 50 meters was selected based on the furnace building height of a new flash furnace smelter facility being planned in Louisiana.¹⁶⁶ An exit gas temperature of 4°C was used for the fugitive stack based on the annual average temperature of the region.²⁷⁷ An inside top diameter of 2.2 meters was used for both stacks.

The choice of an appropriate exit gas velocity for modeling purposes was based on an analysis of wind data for the study area. A value was selected to avoid stack downwash by using 1.5 times the 95th percentile of wind speed measured at Hibbing and adjusted to 50 meters under neutral stability.⁶¹ Neutral stability was used because it is the usual stability under strong winds. The resulting value, 21 m/sec, is high compared to gas exit velocities of 10.3 m/sec and 9.15 m/sec for the two Hidalgo stacks. Nevertheless, it seems reasonable, considering the wind conditions of the area, and was used in the modeling simulations.

Table 15 summarizes the primary and fugitive stack input parameters.

A hypothetical smelter site was selected at a location 4.8 km south of Babbitt in order to provide a spacial reference point in the study area. This location does not imply that a smelter has been proposed or

is being considered for this location; however, the site is adjacent to the most active mining exploration in the study area. The smelter coordinates are 91.8970° longitude and 47.6429° latitude.

Table 15. Smelter stack input data

<u>input parameter</u>	<u>primary stack</u>	<u>fugitive stack</u>
height (meters)	60	50
exit gas temp ($^{\circ}$ K)	355	277
exit gas flow (m^3 /sec)	80.4	1.0
heat emissions (cal/sec)	6.4×10^6	8.45×10^4

CHAPTER 4. HEALTH LITERATURE REVIEW

A major consideration to copper-nickel development in northeastern Minnesota are the health consequences of smelting. Sulfur dioxide, sulfate, total particulates, copper, nickel, arsenic, cadmium, lead, and mercury were selected for modeling based on toxicity, quantity of emissions, and availability of the required input parameters.

This chapter summarizes the relevant occupational and non-occupational health data of these pollutants, existing standards, and measured ambient air concentrations.

This information, particularly the existing standards, will provide a framework for assessing the environmental health impacts of copper-nickel smelting from an air quality perspective.

4.1. TOTAL SUSPENDED PARTICULATES AND SULFUR OXIDES

An excellent review of the epidemiologic literature relating to sulfur oxides and particulates is presented by Schuman et al.²¹⁵ This paper reviews experimental studies, both animal and human, for sulfuric acid, sulfur dioxide, sulfates, sulfites, and particulates along with epidemiologic studies. Because of the wealth of health data relating to sulfur oxides and particulates, the reader is referred to the Schuman et al.²¹⁵ review for a comprehensive summary of the literature.

Sulfur oxides refer to a large group of compounds including sulfur dioxide, sulfur trioxide, sulfuric acid, and sulfur salts or sulfates. Sulfur dioxide (SO_2) is emitted by industrial plants in larger quantities than the other oxides, and can undergo chemical conversion in the atmosphere to form sulfate aerosols (referred to as SO_4 in the remainder of the paper).

The effects of sulfur dioxide alone first appear as irritation to the mucous membranes of the eyes and respiratory tract.

Concentrations of sulfur dioxide in the range of 0.8-2.6 milligrams per cubic meter of air (mg/m^3) can be detected by taste and $7.9 \text{ mg}/\text{m}^3$ can be detected by smell.²⁰⁹ Toxic effects in the form of a reversible bronchiolar constriction can result in healthy individuals during several minutes exposure to $3.9 \text{ mg}/\text{m}^3 \text{ SO}_2$, and eye irritation is experienced above $26 \text{ mg}/\text{m}^3$.²⁹⁷

Stokinger and Coffin²⁴¹ concluded that concentrations greater than $2.6 \text{ mg}/\text{m}^3 \text{ SO}_2$ were required before serious or even significant effects could be expected in healthy individuals.

When SO_2 acts synergistically with particulates, its action is potentiated, and the threshold for health effects is reduced. Studies indicate that SO_2 aerosols potentiate health effects by a factor of 3 or 4 over the same SO_2 gaseous exposure.²⁹⁷

Health effects studies of sulfuric acid exposure in man are limited. Occupational exposures have shown that inhalation of sulfuric acid mist at concentrations of $0.5 \text{ mg}/\text{m}^3$ to $2.0 \text{ mg}/\text{m}^3$ is mildly annoying; concentrations in the range 6.0 to $10 \text{ mg}/\text{m}^3$ are unpleasant; and concentrations in the range 40 to $60 \text{ mg}/\text{m}^3$ result in severe coughing and irritation to the mucous membranes.²⁰⁹

Particulate matter is broadly defined as any material except uncombined water which exists as dispersed solid or liquid at standard temperature and pressure. Sulfates, metal salts, pollen, sand, and dust all fall under this definition. The individual particles are generally smaller than 500 microns, and can remain suspended in the

air from a few seconds to several months.

The most important characteristic of particles is their size; particle size determines deposition and retention in the respiratory system. Most particles larger than 10 microns (μm) are removed from inhaled air in the nasal region. For particles less than 10 μm the percentage deposited in the lung increases with decreasing particle size down to about 0.5 μm , and maximum deposition occurs in the range 1 to 2 μm .^{192, 261}

An important health aspect is the inhalation of respirable particles which can penetrate deeply into the lung alveoli. Respirable range particles are generally agreed to be those less than 10 μm diameter. Removal mechanisms may involve transfer to the blood, lymph, or intestinal tract resulting in damage elsewhere in the body.

The problem of relating health effects to particulate exposure is a difficult one. In order to define health effects the chemical nature of the particles, size, and distribution must be related to mechanisms of retention in and removal from the body.

Acute episodes of high sulfur oxide and particulate levels have been associated with a larger number of deaths than normally expected. The very young, very old, and those individuals with chronic pulmonary or cardiac disorders are the groups most severely affected. Two of the classic episodes occurred in Donora, Pennsylvania in 1948²¹⁰ and in London, England in 1952.¹³¹

Forty-three percent of the population in Donora became ill and twenty people died.²¹⁰ Sulfur dioxide, its oxidation products, and particulate matter were implicated.

In the London episode a sulfur dioxide concentration of 654 micrograms per cubic meter of air ($\mu\text{g}/\text{m}^3$) in the presence of $750 \mu\text{g}/\text{m}^3$ particulates caused a rise in the daily death rate.¹³¹ A 20% increase over the expected death rate was associated with SO_2 levels in excess of $1361 \mu\text{g}/\text{m}^3$ for one day along with particulate levels greater than $2000 \mu\text{g}/\text{m}^3$.²⁶¹

Epidemiologic studies demonstrate that exposure to high levels of contaminants of sulfurous smog causes excess morbidity and mortality in persons with chronic lung disease. Conditions like asthma may be aggravated by prolonged exposure to moderately high concentrations of pollution.

One of these projects, the Community Health and Environmental Surveillance System (CHESS), sought to determine the adequacy of the national primary air pollution standards, and provided a wealth of information on the relationship of air pollution to disease. Two of the CHESS studies were conducted in four communities in the Salt Lake Basin and in five communities of the Rocky Mountain Area.^{66,167}

In the Salt Lake Basin study the primary SO_2 source was a large copper smelter located 8 km from the high exposure group and 61 km from the low exposure group. This study of school aged children showed that the frequency of single or repeated episodes of acute lower respiratory illness, bronchitis, and croup increased 40 to 50% after exposure to elevated levels of SO_2 ($91 \mu\text{g}/\text{m}^3$) and suspended sulfates ($15 \mu\text{g}/\text{m}^3$) for over three years. Pollutant levels were also correlated with excess asthma attacks.

Sulfur dioxide sources in the Rocky Mountain area included a lead

smelter and a copper smelter. This study found significantly greater incidences of acute lower respiratory disease among asthmatic children and non-asthmatic children who were exposed to estimated annual SO₂ levels of 177 µg/m³, suspended sulfates of 7.2 µg/m³, and particulates of 65 µg/m³ for three or more years.

The present ambient air quality standards for SO₂ and particulates were established on the basis of these and other studies to protect the public health and welfare (Table 16).

At the present time, national standards have not been established for suspended sulfates; however, it is possible that standards based on total water soluble sulfates may be established by 1985.²⁰⁵ A potential 24-hour standard of 10 to 25 µg/m³ and a potential annual standard of 5 to 15 µg/m³ have been developed by the Brookhaven National Laboratory Office of Environmental Policy.²⁰⁵

4.2 COPPER

Copper is an essential element in plants, animals, and man. Dietary sources may range from 2 to 10 mg copper (Cu) per day, and about one-third to one-half of this is absorbed in the body.^{132, 161}

Average copper concentrations of 134 µg/l have been measured in 969 water systems in nine geographic areas of the U.S.¹⁴²

Atmospheric concentrations of copper have been measured in the range of 0.01 to 0.57 µg/m³ in urban areas and 0.01 to 0.25 µg/m³ in non-urban areas.²¹³ Concentrations averaging less than 1 µg/m³ have been measured over a 10 year period around copper smelters in the U.S.¹³²

Schroeder²¹³ estimates a total maximum daily intake of 11.4 µg from air and 1325 µg from food and water. The intake by air is only 0.86% of the total intake.

Table 16. National ambient air quality standards for sulfur oxides and total suspended particulates.

<u>Pollutant</u>	<u>Wording of Standard</u>	<u>Primary^a</u>	<u>Secondary^b</u>
Suspended Particulate Matter	annual geometric mean concentration	75 $\mu\text{g}/\text{m}^3$	60 $\mu\text{g}/\text{m}^3$
	max 24-hr concentration not to be exceeded more than once/year	260 $\mu\text{g}/\text{m}^3$	150 $\mu\text{g}/\text{m}^3$
Sulfur Oxides	annual arithmetic average concentration	80 $\mu\text{g}/\text{m}^3$	
	max 24-hr concentration not to be exceeded more than once/year	365 $\mu\text{g}/\text{m}^3$	
	max 3-hr concentration not to be exceeded more than once/year		1300 $\mu\text{g}/\text{m}^3$

^a primary standard: protects public health

^b secondary standard: protects against all other adverse effects of air pollution

An extensive review of the effects of copper on plants, animals, and man has been compiled by the National Research Council¹⁶¹ and Schuman *et al.*²¹⁶

Symptoms of copper poisoning by ingestion are similar to other forms of food poisoning and include a metallic taste in the mouth and vomiting.

Gleason⁸⁹ reported metal fume fever in three men who were exposed to dust during the polishing of copper plates. Concentrations of 0.12 mg/m^3 were found in the polisher's breathing zone.

Silicosis was studied in Rhodesian copper miners by Paul¹⁸¹ and in Russian workers by Yakshina and Makarov.³⁰¹

Blot and Fraumeni²⁰ studied cancer mortality in 36 counties with primary copper, lead, or zinc smelting and refining of non-ferrous metallic ores (18 of the counties had copper smelters). Lung cancer mortality was found to be significantly higher among males (17% higher) and females (15% higher) than the rest of the U.S. population.

The National Research Council¹⁶¹ concludes that because of the absence of reports on significant environmental effects from airborne copper, copper and its compounds as dusts or fumes dispersed into the atmosphere have not been considered to be hazardous.

At the present time there is no ambient air quality standard for copper. The adopted threshold limit value-time weighted average (TLV-TWA) is 0.2 mg/m^3 for copper fume and 1.0 mg/m^3 for dusts and mists. The tentative short-term exposure limit (STEL) for dusts and mists is 2.0 mg/m^3 as Cu.²

4.3. CADMIUM

The cadmium intake in man has been estimated to be about $160 \text{ } \mu\text{g/day}$ from food and water, and $7.4 \text{ } \mu\text{g/day}$ from air (about 4.6% of total intake).²¹³ Cadmium in air has been reported to range from $0.002 \text{ } \mu\text{g/m}^3$ to $0.37 \text{ } \mu\text{g/m}^3$ in urban air and from 0.0004 to $0.026 \text{ } \mu\text{g/m}^3$ in nonurban areas.²¹³ Schroeder²¹³ concluded, "There is little question that cadmium in air is a real and present hazard to human health."

Toxic effects of cadmium include acute effects at concentrations of several milligrams/ m^3 which result in pneumonitis, pulmonary edema, and sometimes death.^{15, 132}

Chronic effects of low level cadmium exposure are more difficult to diagnose. Some of these effects include shortness of breath due to

emphysema, total or partial loss of smell, coughing, weight loss, depressed appetite, and generalized irritability.⁶⁹ Proteinuria has also been reported as an important effect of cadmium poisoning.¹⁹⁰ A relationship between cadmium exposure and cancer has been suggested.^{128, 190} Schroeder²¹⁵ concluded there is a suggestive relationship between renal cadmium and hypertension.

Non-occupational acute poisoning generally results from inadvertent ingestion of a food or drink containing high concentrations of cadmium. Itai-itai disease in Toyama, Japan is probably the classic example of non-occupational chronic cadmium poisoning.²⁵³ Cadmium contamination resulted from a mining operation located by a river upstream from the community. Contaminated river water was used for irrigation resulting in accumulation of cadmium in the rice crop.

Baker et al.⁸ studied cadmium absorption in children (1 to 5 years old) living within 6.8 km of 11 U. S. copper smelters. In nine of the eleven smelter towns, the mean hair cadmium levels in the children were significantly higher than those of the controls.

At the present time there is no ambient air quality standard for cadmium. The adopted TLV-TWA is 0.05 mg/m^3 for cadmium dust and salts (as Cd), and the tentative STEL is 0.2 mg/m^3 .²

4.4. LEAD

The average daily intake of lead in the U.S. has been estimated to be about $300 \mu\text{g}$.²¹³ Only 5 to 10% of this amount ($30 \mu\text{g/day}$) is absorbed into the body.¹⁵⁷ Dietary sources are probably the most important, and the lead content of food varies from 10 to 2500 parts per billion (ppb) with an average of about 200 ppb; the average daily intake of

lead through water is about 20 $\mu\text{g}/\text{l}$.¹⁵⁷ Schroeder²¹³ estimates that about 15% of the total daily intake is from air.

Urban concentrations range from 0.1 to 2.3 $\mu\text{g}/\text{m}^3$, and nonurban concentrations range from 0.002 to 0.15 $\mu\text{g}/\text{m}^3$.²¹³

Ambient concentrations greater than 2 to 3 $\mu\text{g}/\text{m}^3$ result in increased blood levels.¹⁵⁷ Normal blood lead levels are below 40 $\mu\text{g}/100 \text{ ml}$.¹⁹

The effects of lead poisoning vary depending on whether the lead is organic or inorganic. Mild symptoms of inorganic lead poisoning include tiredness, irritability, anorexia, altered sleep patterns, anemia, and slight abdominal pain or discomfort; severe symptoms include muscle tenderness, colic, reduction of muscle power, and other symptoms of neuropathy or encephalopathy.¹²⁷ Inorganic lead poisoning inhibits several steps in the synthesis of heme.⁹⁹ Neurological and gastrointestinal effects have been reported at blood lead concentrations of 70 to 80 $\mu\text{g}/100 \text{ g}$ whole blood.¹⁵⁷

Organic lead poisoning is exhibited as a psychotic state, and symptoms include nervous irritability, agitation, and ultimately an irrational, delusional, and hallucinated state.²⁰⁷

Baker et al.⁸ studied children from 1 to 5 years old living within 6.5 km of 11 copper smelters in the U.S. Mean hair lead levels were higher than controls in all 11 copper smelter towns and 8 were significantly higher. Systematic absorption, however, occurred only in sporadic cases, and blood lead levels were rarely high enough to be associated with hematological or neurological toxicity.

Baker et al.⁷ studied 91 children and 12 wives of current and recently terminated workers of a secondary lead smelter. The concentra-

tion of lead in the dust of workers' homes averaged four times that of controls, and blood lead levels in the children correlated with the lead concentration in the dust.

Roberts et al.¹⁹⁹ found elevated blood lead levels (about 30% over 40 $\mu\text{g}/100$ ml blood) in children aged 0 to 14 years living near two secondary lead smelters in Toronto. Although distinct symptoms of lead poisoning were not observed, metabolic and subtle neurological changes did occur.

Landigran et al.¹²⁶ investigated blood lead levels in adults and children around a smelter in El Paso, Texas where 1012 metric tons of lead were emitted over a three year period. Blood lead levels over 40 $\mu\text{g}/100$ ml were found in 43% of those living within 1.6 km, in 8% of those living within 1.6 to 3.2 km, and in 1% of those living more than 3.2 km from the smelter. Soil levels of 3457 parts per million (ppm) lead were measured within 200 meters of the smelter; soil lead levels remained above the background level of less than 50 ppm as far as 10 km from the smelter.

Roels et al.²⁰³ found that blood lead levels in children living less than 1 km from a smelter averaged about 30 $\mu\text{g}/100$ ml; at 2.5 km the concentration was about 20 $\mu\text{g}/100$ ml; and in rural areas the concentration was 9.4 $\mu\text{g}/100$ ml blood.

Children and women are thought to be more susceptible to lead poisoning than men, and the National Safety Council¹⁵⁹ concluded that children in the 1 to 5 age group should not have exposures resulting in blood lead levels greater than 30 $\mu\text{g}/100$ ml.

The national ambient air quality standard for lead is 1.5 $\mu\text{g}/\text{m}^3$ per calendar quarter year average.²⁷²

The adopted TLV-TWA for inorganic lead is 0.15 mg/m^3 , and the tentative STEL is 0.45 mg/m^3 .²

4.5. MERCURY

Mercury compounds have no known normal metabolic function, and the National Research Council¹⁶² concludes that in view of the toxicity of mercury and the inability of researchers to specify the threshold levels of toxic effects on the basis of present knowledge, all mercury contamination must be regarded as undesirable and potentially hazardous.

Mercury may be present in an organic form (alkylated mercurials) or in an inorganic form (metallic mercury and mercury sulfide). Organic mercury compounds, particularly, methyl mercury, are most important because of their toxicity and bioaccumulation.¹⁶²

Ambient concentrations of mercury range from 0.7 nanograms per cubic meter (ng/m^3) in remote ocean areas (nearly all present as a vapor), to 4.0 ng/m^3 (less than 5% as particulate) in rural areas, to concentrations less than 10 ng/m^3 (variable particulate concentration) in urban areas.¹⁶²

Mercury contributions from drinking water have been estimated at less than $0.2 \text{ } \mu\text{g/person/day}$; the contribution from food can vary widely, but has been reported to range from $9 \text{ } \mu\text{g/person/day}$ in Brazil to $109 \text{ } \mu\text{g/person/day}$ in Japan.¹⁶² Schroeder²¹³ calculates a daily mercury intake of $10 \text{ } \mu\text{g}$ from food and water, and a maximum of $760 \text{ } \mu\text{g}$ from air.

Existing evidence indicates that methyl mercury poisoning first results in central nervous system damage. Toxic dosages in man result in neurological disturbances weeks to months after acute exposure; symptoms include blurred vision, blindness, deafness, and ultimately death.¹⁶²

The best known examples of methyl mercury poisoning occurred in Minamata Bay and in Niigata. Poisoning occurred as a result of industrial release of methyl mercury and other mercury compounds into Minamata Bay and the Agano River followed by accumulation of methyl mercury in edible fish and shellfish. The median total mercury level in fish caught in Minamata Bay during the epidemic is estimated to be 11 $\mu\text{g}/\text{gm}$ fresh weight.¹⁶² More than 700 cases of methyl mercury poisoning were identified in Minamata, and more than 500 in Niigata by 1974.²⁴⁹

The largest significant outbreak of methyl mercury poisoning occurred in Iraq during the winter of 1971-72 as a result of consumption of home-made bread prepared from seed treated with a methyl mercury fungicide. More than 6000 poisoned children and adults were admitted to hospitals throughout Iraq and nearly 500 deaths were reported.⁹

At the present time there is no ambient air quality standard for mercury. The adopted TLV-TWA is 0.01 mg/m^3 for alkyl mercury compounds and 0.05 mg/m^3 for all other forms (as Hg). The tentative STEL values are 0.03 mg/m^3 for alkyl compounds and 0.15 mg/m^3 for all other forms.²

4.6. ARSENIC

The health and environmental literature relating to arsenic and its compounds has been reviewed by the U.S. Dept. Health, Education, and Welfare,²⁶² the National Research Council,¹⁶⁰ and Ashbrook.⁴

Arsenic is most commonly present in the trivalent (arsenic trioxide, arsenous acid, arsenite) and pentavalent (arsenic pentoxide, arsenic acid, arsenate) forms.

Inorganic arsenic compounds can have a direct effect on the skin, or can be absorbed into the body through the skin, from the lungs, from

the tracheobronchiol tree, or from the gastrointestinal tract. Arsenic is distributed throughout the body.²¹⁴

Schroeder²¹³ calculates a daily intake of 1000 μg arsenic (As) from food and water, and a maximum of 1.4 μg (0.14% of the total intake) from air.

Arsenic concentrations in air have been reported to be less than 0.02 $\mu\text{g}/\text{m}^3$ in remote areas, and range from 0.01 to 0.16 $\mu\text{g}/\text{m}^3$ in urban areas.¹⁶⁰ During 1961-62 an air pollution survey in Montana reported an atmospheric arsenic concentration in Anaconda, where a large smelter is located, up to 2.5 $\mu\text{g}/\text{m}^3$ (0.45 $\mu\text{g As}/\text{m}^3$ average) compared to 0.0 to 0.55 $\mu\text{g}/\text{m}^3$ (0.07 $\mu\text{g}/\text{m}^3$ average) in Butte, where there are mines adjacent to the city. Annual average concentrations of 0.001 to 0.07 $\mu\text{g}/\text{m}^3$ were reported for five other Montana cities.¹⁵⁴

Arsenic has been strongly implicated as an occupational carcinogen.^{125, 146, 175} In 1979 the Environmental Protection Agency's Science Advisory Board concluded that the association between exposure to arsenic and the development of cancer was well established.²⁷³

Most nonferrous metal smelters produce arsenic in varying amounts depending on the ore concentrations and process, and there is some evidence that arsenic air pollution may have resulted in increased lung cancer mortality in the general population.

Fraumeni⁷⁴ reported that lung cancer mortality was increased in 26 of 38 U.S. counties that had nonferrous metal smelters. Heuper¹⁰⁰ reported excessive respiratory cancer mortality in three Montana counties in which the major industry was copper mining and/or smelting; Newman et al.¹⁶⁸ attributed the increased respiratory cancer mortality

in Anaconda, Montana to arsenic air pollution.

At the present time there is no ambient air quality standard for arsenic. The current TLY-TWA is 0.2 mg/m^3 for arsenic and compounds, 0.05 mg/m^3 for arsenic trioxide, and 0.2 mg/m^3 for arsine (all as As).²

4.7. NICKEL

Nickel (Ni) may enter the body through oral intake, inhalation, percutaneous absorption, and parenteral administration.

Schroeder²¹³ estimates that the total daily intake of nickel is $600 \text{ } \mu\text{g/day}$ from food and water, and $2.36 \text{ } \mu\text{g/day}$ (0.39% of total intake) is the maximum amount from air.

Ambient air concentrations may be as high as $0.118 \text{ } \mu\text{g/m}^3$ (New York City, 1966) and $0.69 \text{ } \mu\text{g/m}^3$ (East Chicago, Indiana, 1964).²¹³

Metallic nickel is relatively nontoxic. Nickel salts are highly toxic when administered intravenously or subcutaneously. Nickel carbonyl, an organonickel compound, is highly toxic and symptoms may occur immediately or be delayed. Major symptoms of acute nickel toxicity include hyperglycemia, gastrointestinal effects, and central nervous system effects.¹⁵⁸

Nickel is a common sensitizing agent for allergic dermatitis.⁶ Nickel carcinogenesis has been documented among nickel refinery workers in Wales,^{55, 104} Canada,²⁴⁵ and Norway.¹⁸²

Doll et al.⁵⁵ conducted an epidemiological survey of 845 men who had been employed by a nickel refinery in Wales for at least five years and who were first employed before May 1944. Men who worked at the refinery between 1900 and 1925 died of cancer of the nasal cavities at a rate of about 364 times the national average; no deaths were reported

from this cancer after 1925. Mortality from pulmonary cancer was 7.5 times the national average for those men who started working between 1900 and 1925; this dropped to only 1.3 times the national average for those starting after 1925.

Sutherland²⁴⁵ conducted an epidemiologic study of respiratory cancer at the Port Colborne nickel refinery in Canada; the study included 2355 workers with 5 or more years of service who were working in January, 1930 or later. Sutherland estimated that the nickel workers' risk of dying from cancer of the nasal cavities was 37 times the expected risk, and the risk of dying from pulmonary cancer was 2.2 times the expected risk during the period 1930-1957. A study of residents in the area during 1950-1957 did not show any increased risks of cancer of the nose or lungs.

Although the carcinogenic role of nickel has not conclusively been established on epidemiological grounds since workers were also exposed to other metals, authorities^{101, 118, 202} who have reviewed the problem have inferred that nickel compounds were the principal carcinogens in the epidemiologic studies.

Although nickel carbonyl may be present in some refineries, the more probable agents of concern are the dust of the nickel ore and its products.²¹⁶ Changes in the technology of nickel smelting and refining have probably diminished the risk of respiratory carcinogenesis.¹⁵⁸

At the present time there are no ambient air quality standards for nickel. The adopted TLV-TWA is 0.35 mg/m^3 for nickel carbonyl, 1.0 mg/m^3 for nickel metal, and 0.1 mg/m^3 for soluble nickel compounds; the tentative STEL for soluble nickel compounds is 0.3 mg/m^3 .²

4.8. POPULATION AT RISK

Table 17 provides a breakdown of the populations of Cook, Lake, and St. Louis counties by age (1975 data). People living in these counties are most likely to be impacted by a smelter operation in the Iron Range or in Duluth.

The most susceptible populations are, of course, the chronically ill, the young, the old, and those people in hospitals.

Approximately 8% of the total population in these counties is less than 5 years old, and about 12% is more than 65 years old. These numbers would be expected to increase along with the general population as a result of copper-nickel development.

Table 18 summarizes the number of beds in hospitals, nursing homes and convalescent centers in the three counties. A smelter sited in Duluth potentially could have the largest health impacts, particularly during breakdown conditions, because of the concentration of people.

Table 17. Population estimates for Cook, Lake, and St. Louis counties, July 1, 1975.

<u>County</u>	<u>Total</u>	<u><5</u>	<u>5-17</u>	<u>18-29</u>	<u>30-44</u>	<u>45-64</u>	<u>>65</u>
Cook	3700	230	880	560	680	890	470
Lake	13600	1010	3990	2100	2440	2920	1150
<u>St. Louis</u>	<u>216600</u>	<u>15150</u>	<u>50940</u>	<u>41360</u>	<u>32720</u>	<u>49350</u>	<u>27070</u>
Total	233900	18460	55810	44020	35840	53160	28690

Office of State Demographer¹⁷³

Table 18. Number of beds in licensed and certified health care facilities in Cook, Lake, and St. Louis counties, 1976.

<u>County</u>	<u>Town</u>	<u>hospital</u>		<u>nursing home and</u>
		<u>beds</u>	<u>bassinets</u>	<u>convalescent centers</u>
Cook	Grand			
	Marais	16	6	50
Lake	Two			
	Harbors	37	9	50
St. Louis	Aurora	16	4	74
	Buhl			31
	Chisholm	54	6	42
	Cook	14	8	41
	Duluth	1145	54	710
	Ely	45	11	100
	Eveleth	26		88
	Hibbing	176	20	316
	Noepming			211
Virginia	173	33	232	

Minnesota Dept. of Health¹⁴⁹

CHAPTER 5. MODIFIED GAUSSIAN MODEL

5.1. INTRODUCTION

The modified gaussian model can predict ambient concentrations and deposition rates for up to 23 pollutants including sulfur dioxide, sulfate, total particulates, and metals. The model can handle up to 25 sources, and requires source location, pollutant emission rate, stack height, and heat emission rate as input parameters.

Dry deposition rates, washout ratios, mixing height, and monthly temperature and pressure are also required as inputs. The model uses meteorological data from up to 5 stations to calculate the air quality impact of the various sources on a specified network or grid of up to 50 receptor sites.

The model provides ambient air concentrations (micrograms per cubic meter, $\mu\text{g}/\text{m}^3$, for SO_2 , SO_4 , and nanograms per cubic meter, ng/m^3 , for particulates and metals) and ground depositions (kilograms per hectare, kg/ha , for SO_4 and grams per hectare, g/ha , for particulates and metals) on a daily basis and various averaging time periods. The model has been verified in the range of 5 to 250 km from the source.

The model utilizes specific meteorological input data in the form of 24-hour inverse distance vector averages to compute the corresponding 24-hour air quality impacts of each source at each receptor. The effect of each source is summed to determine the total effect of all the regional sources at each receptor for each 24-hour period. The 24-hour results may then be averaged (or totaled) over a season or year to determine the average concentration (or total deposition).

Either geometric or arithmetic means can be calculated. Other distributions of the individual 24-hour results during the year can also be determined.

The major features of the model include:

1) Atmospheric dispersion: Horizontal plume spread is calculated using a gaussian equation. Vertical plume spread is calculated using a box model in which concentration is assumed to be uniform over the plume thickness limited by the surface and a specified mixing height.

2) Chemical conversion: The model provides for depletion of SO_2 by conversion to sulfate at a specified rate as the plume is transported downwind.

3) Dry deposition: Pollutants are removed from the air by interaction with the surface (vegetation, water, buildings, and so forth). This removal process is termed dry deposition, and is a function of the ambient concentration and a specified deposition velocity.

4) Precipitation scavenging: In addition to dry deposition pollutants are depleted as a result of scavenging during precipitation events. The frequency and duration of precipitation are among the input data required by the model. The effectiveness of precipitation scavenging for the removal of a particular pollutant is specified in the form of a scavenging rate coefficient.

A copy of the program for the modified gaussian model is presented in Appendix 1. This chapter describes the flow of the model and discusses the theory underlying the major program segments.

5.2. MODIFIED GAUSSIAN MODEL FLOWCHART

A flowchart for the model is given in Figure 15, and it should be referred to in the following discussion (the appropriate sections of the flowchart are tagged in the text by letters in parentheses).

Input data. (A) Index data include the number of sources (25, maximum), number of receptors (50, maximum), number of weather stations (5, maximum), and number of metals (20, maximum).

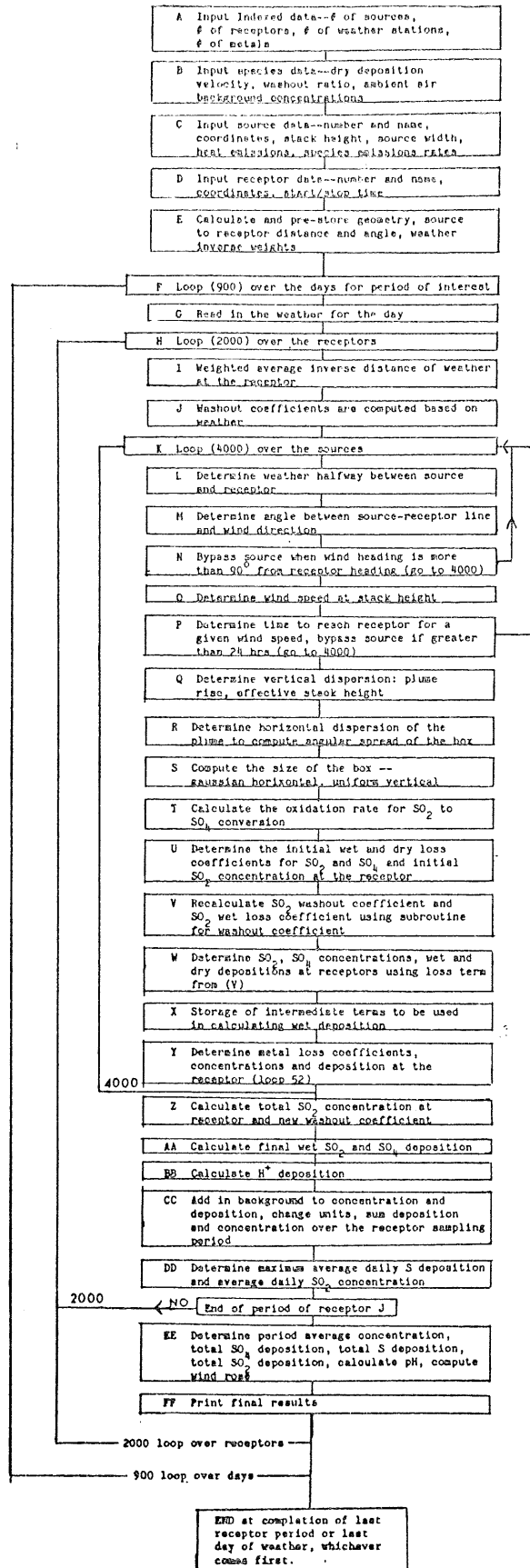
(B) All species require inputs for dry deposition velocity (cm/sec), washout ratio, and ambient air background concentration ($\mu\text{g}/\text{m}^3$). There are two sets of dry deposition velocities for sulfur dioxide and sulfate: one for the summer season (rain) and one for the winter season (snow). The dry deposition velocity and the washout ratios are used to calculate the dry and wet losses.

(C) Source data include the source number and name, the source coordinates in degrees longitude and latitude, the stack height (m), the source width (km), the source heat emission rate (cal/sec) which is used to calculate plume rise, and finally, the source pollutant emission rate (gm/sec).

(D) Receptor data include the number and name, coordinates in degrees longitude and latitude, and start/stop times for computing results. All receptors may be set to the same start/stop time or individual start/stop times may be used for each receptor. The weather data must span all periods.

(E) This section calculates the required positional geometry given the location of the sources, the receptors, and the weather stations. Since all positions are set, the various distances and weights are

FIGURE 1 FLOWCHART OF MODIFIED GAUSSIAN MODEL



calculated once and stored. The source to receptor distance (XSR) and the wind angle from east (AHW) are computed for each pair. The weather is calculated at one-half the distance between the source and receptor and weighted by the inverse distance between the receptor and the weather stations. Other weightings were considered and inverse distance was selected as the best.

(F) At this point the program progresses through a nested series of loops to calculate the desired deposition and air concentration. A loop is a section of the program that is repeated a given number of times. The outermost loop (900) is over the days of the weather period, starting with the first day of weather and progressing to the last. Then for each day of weather, the program loops (2000) over the receptors. Finally, the program loops (4000) over the sources.

(G) The weather at the five stations is read in for the day. Since there is so much weather data, it is not practical to read it in all at once, rather it is done on a day by day basis.

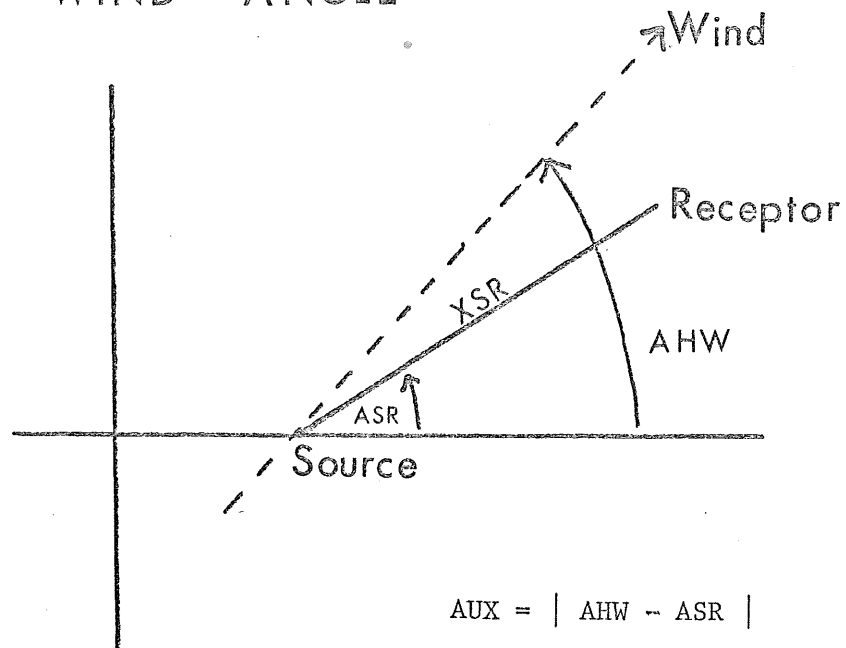
(H) The loop (2000) over the receptors begins. Within this loop days not in the measured time period are eliminated, an inverse distance average of the weather (I) at the receptor is calculated (total inches of rain are summed, data for the 16 point wind rose are collected, monthly mixing heights are calculated), scavenging coefficients (J) are computed for SO_2 , SO_4 , and the metals. The washout coefficients for SO_2 and SO_4 are first approximations and are recalculated later in the program.

(K) Next, the innermost loop (4000) over the sources is made. The actual ambient air concentration and deposition calculations are made within this loop.

(L) The weather half-way between the source and the receptor is determined.

(M) The angle (AUX) between the source-receptor line and the wind direction is found. If AUX is greater than 90° , the source is by-passed (Figure 16).

FIGURE 16. WIND ANGLE



(O) Wind speed, which increase with height, is calculated by the power law equation modified for stability. The wind speed at stack height is also used to approximate the average wind speed which is used to calculate both plume rise and dilution.

(P) The wind speed calculated in (O) determines the time required to reach the receptor. The source is by-passed if the time is greater than 24 hours.

(Q) Next, the program calculates the plume rise, the effective stack height, and the vertical dispersion angle. The effective stack height and the vertical dispersion angle are then used to calculate the vertical spread of the box.

The height of the box is less than the mixing height within a few kilometers of the source, and is bounded by the mixing height at farther distances.

At this point, a brief explanation of the "box" is in order. The stack plume is emitted continuously at an average rate and is transported downwind. The plume diffuses in the vertical direction to the mixing height a few kilometers from the source, and mixing (therefore, pollutant concentration) is considered to be uniform from the ground to the mixing height.

While traveling downwind, the plume also disperses horizontally, normal to the line of travel. The horizontal angular spread is primarily controlled by the wandering of the wind direction which is measured by the standard deviation of the wind angle.

In its simplest form the box model is a pie-shaped wedge spreading downwind with uniform concentration throughout the box.

In the modified gaussian model horizontal diffusion is approximated by the gaussian distribution which has the feature of being completely described by its standard deviation. Thus, instead of uniform concentration across the entire box, the standard deviation of the angular spread in the wind direction now becomes the standard deviation of the normal distribution. So, as the plume is transported downwind it diffuses horizontally so that the crosswind crosswind concentration

assumes a gaussian profile with the maximum concentration along the wind axis, falling off to either side. As the plume travels downwind, the bell-shaped profile lowers and broadens (R,S).

As the plume travels along, SO_2 is oxidized to sulfate (T), and an oxidation rate is computed as a function of plume travel time.

Losses which are due to dry deposition and wet scavenging are calculated using exponential functions. Clearly, oxidation and losses are taking place concurrently, and the equations describing the concentration and deposition at the receptors are coupled, simultaneous differential equations incorporating the modified box, oxidation, wet and dry losses. The equations for concentration and deposition as applied to the modified gaussian model have been solved by Bowman²¹ after Wendell, Powell and Drake.²⁹²

Losses for SO_2 and SO_4 are calculated in a boot strap manner. (U) The program initially determines loss coefficients (wet and dry) for SO_2 and SO_4 using the best guess input parameters. (V) The SO_2 wet and dry loss coefficients are then used to calculate an initial SO_2 concentration which in turn is used in a subroutine to recalculate the SO_2 washout coefficient, providing a refined wet loss term for SO_2 . (W) The recalculated wet loss term is then used along with the dry loss term from (U) to determine the concentration of SO_2 and SO_4 at the receptor after losses.

Losses at the receptor are approximated by the fraction of time it is raining per day, and it is assumed that dry deposition does not continue throughout the whole day. Losses are calculated along with concentration on a source by source basis rather than in a more integrated way.

(X) Next, the program stores intermediate terms for use in calculating wet deposition.

(Y) Metal loss coefficients, metal concentrations, and metal depositions are determined at the receptor in loop 52. These calculations are straightforward, and do not present the complications that SO_2 does.

(Z) Total SO_2 concentration at the receptor, which is the sum of the concentration from (W) and the background concentration, is used to calculate a new washout coefficient. At this point the SO_2 washout coefficient and SO_2 concentration at the receptor have been refined.

(AA) Next, the final wet SO_2 and SO_4 depositions are calculated with the final SO_2 washout coefficient in a loop (4002) over the sources.

(BB) The deposition of hydrogen ion is calculated.

(CC) The background concentration is added to the predicted concentrations and depositions; units are changed; and the depositions and concentrations are summed over the receptor sampling period.

(DD) Maximum average daily sulfur deposition and average daily SO_2 concentration are calculated. (EE) If the end of period for the receptor has been reached, the program then computes the period average concentration, total SO_4 deposition, pH and the wind rose.

(FF) Final results are printed.

The results are printed for each day, summed, or averaged as needed for the respective period of the receptor, and the complete period results are also printed. This is done for all periods until the end of the last receptor period or the end of the input weather is encountered at which point the program ends.

5.3. THEORY

5.3.1. Wind speed at stack height.

Plume transport and diffusion are determined by the motion of the atmospheric boundary layer. Air motion at a given point is described in terms of a turbulent component and a time mean value, the wind velocity. Wind velocity increases with elevation while turbulence is usually more intense at lower elevations. The scale of turbulence, however, increases with elevation.²⁴²

Due to the complexity of atmospheric interactions, it is impossible to accurately represent velocity profiles with a single analytical expression. Several simple empirical expressions have, however, been developed and successfully used to represent plume velocity profiles in diffusion studies. The most frequently used are the logarithmic, log-linear, and power law expressions.

The logarithmic velocity profile expression is based on the assumption of constant wind shear stress with elevation. Although this assumption is true for only distances of tens of meters above the surface, the equation has been used to cover larger distances. This equation applies to neutral stability conditions.²⁴²

The log-linear equation is a modification of the logarithmic equation that handles non-neutral stability conditions with the addition of a linear term for elevation. Both of these equations are limited in use because of the difficulty in evaluating some of the parameters.

The power law velocity profile equation is given by:

$$u = u_1 (z/z_1)^P \quad (1)$$

where u_1 and z_1 are the reference velocity and elevation, respectively,

p is an exponent dependent on surface configuration and stability, and z is the height at which u is determined.

This equation²⁴² is used in many plume studies and has been shown to be effective in covering a wide range of conditions when the parameters are properly evaluated.

The reference values u_1 and z_1 are selected from available meteorological and stack data. The exponent p may vary at a given site because of variation in stability or surface configuration. Values of p in smooth open country range from 0.11 in unstable conditions to 0.33 in very stable conditions. Under neutral conditions values of 0.16, 0.28, and 0.40 have been reported for flat open country, forest, and urban areas, respectively.²⁴²

The power law velocity equation modified to include five stability categories and the percentage of time each existed was used in the modified gaussian model as follows:

$$u = u_1 \left[0.003 (z/8)^{0.1} + 0.034 (z/8)^{0.15} + 0.091 (z/8)^{0.2} + 0.597 (z/8)^{0.25} + 0.275 (z/8)^{0.3} \right] \quad (2)$$

The reference height was taken as 8 meters and velocity u was calculated at stack height z. The frequency distribution of the stability classes were based on meteorological data from International Falls,⁶⁰ and stability class exponents were taken from DeMarrais.⁴⁹ when the model was applied to Minnesota.

Turner²⁵⁰ states that although the power law increase is reasonably correct over a long period of record, individual hours may be in error.

5.3.2. Plume rise.

Plume rise is defined as the elevation of the plume centerline above the stack outlet as a function of the downwind distance from the stack.²⁴² Plume rise is determined by characteristics of the exit gas and the ambient atmosphere. Two broad categories of forces affecting plume rise are those of momentum and buoyancy.

The turbulence of gases as they leave the stack causes mixing or entrainment with the atmosphere which dilutes both the upward momentum of the plume and its buoyancy. Rise induced by momentum is initially high and rapidly decreases with distance. A plume that is less dense than air, either because it is hot or has a lower mean molecular weight, experiences upward force or buoyancy. Rise due to buoyancy is not high initially, but continues with distance.

Plumes may be classified as buoyant or nonbuoyant. In buoyant plumes rise is dominated by buoyancy; equations for buoyant plumes either neglect momentum forces or include them indirectly through parameter selection. In nonbuoyant plumes or jets rise is dominated by initial momentum. An example of a jet plume occurs in the venting of air close to ambient temperature.

Total buoyant force in a given segment of the plume remains constant if heat is not lost and the atmosphere is well mixed. In this instance the plume's vertical momentum will increase at a constant rate although its vertical velocity may decrease because of dilution through entrainment. Somewhere downwind of the stack, atmospheric turbulence and vertical temperature begin to affect plume rise.

In stable air as the plume rises it entrains air from below, and

carries it upward into regions of warmer ambient air resulting in decay of plume buoyancy. Atmospheric turbulence is suppressed and has little effect on plume rise.

In neutral atmospheres the buoyancy of the plume remains constant in a given segment of the plume, provided that the plume does not radiate or absorb heat significantly or lose heavy particles. Since neutral stabilities are turbulent, the rate of entrainment is increased and plume buoyancy and vertical momentum are diluted.

If the atmosphere is unstable, the buoyancy of the plume grows as it rises.

Plume rise equations are both empirical and theoretical, and many equations exist in the literature. The rises predicted by the various formulas may differ by more than a factor of 10 largely because of the type of analysis and selection and weighting of data.²³

Reviews of plume rise equations are given in Briggs,^{23,24} Strom,²⁴² and Moses and Strom.¹⁵⁶

Recent buoyant plume rise equations are simple one-term power law expressions²⁴² with exponential variables of the form:

$$\Delta h(X) = K_1 Q_h^a X^b U^c \quad (3)$$

where Δh is the plume rise above the top of the stack, X is the downwind distance, U is the wind velocity, Q_h is the heat emission rate, K_1 is a constant dependent on other variables, and $a, b,$ and c are exponents evaluated from theoretical or experimental considerations.

The evaluation of the heat emission rate, Q_h , depends on available stack effluent data. Q_h for a heated effluent is the equivalent heat

emission relative to ambient air which would produce the same buoyancy. When the effluent gas has the same molecular weight and specific heat as air, Q_h is given by:

$$Q_h = Q_m c_p (T_s - T) \quad (4)$$

where c_p is the specific heat of air at constant pressure, T is the absolute temperature of the ambient air, T_s is the absolute temperature of the exit gas at the stack outlet, and Q_m is the effluent mass emission rate. Q_h may also be expressed in terms of the mass density differences between the ambient air and the stack gases.

The effluent mass emission rate, Q_m , is given by:

$$Q_m = \rho_s A_s V_s \quad (5)$$

where ρ_s is the mass density of effluent at the stack outlet, A_s is the stack outlet area, and V_s is the effluent emission velocity at the stack outlet.

Briggs,²³ Bringfelt,²⁶ Fay et al.,⁶⁴ and others have shown that good values of a , b , and c are $1/3$, $2/3$, and -1 , respectively. Other values have been found for a and b , but -1 is generally agreed to be the value of c .

The buoyant plumerise formula of Briggs²³ for neutral or unstable conditions was used in the modified gaussian model; stable conditions occurred only 24% of the time at Hibbing, therefore, formulas for rise in stable conditions were not used. Briggs found that buoyant plumes follow the "2/3 law" for transitional rise for considerable distances downwind when there is a wind, regardless of stratification. The "2/3 law" states that plume rise is proportional to the 2/3 power of distance downwind:

$$\Delta h = 1.6 F^{1/3} U^{-1} X^{2/3}. \quad (6)$$

This equation provides a conservative approximation for plume rise under neutral or unstable conditions up to a distance of $3.5X^*$. At this distance atmospheric turbulence begins to dominate plume growth and the following equation applies:

$$\Delta h = 1.6 F^{1/3} U^{-1} (3.5X^*)^{2/3}. \quad (7)$$

The buoyancy flux parameter, F , in m^4/sec^3 is given by:

$$F = g Q_h / \pi c_p \rho T, \quad (8)$$

where g is the acceleration due to gravity, Q_h is the heat emission rate, ρ is the mass density of ambient air, c_p is the specific heat of air at constant pressure, and T is the absolute temperature of ambient air.

If the effluent has the same molecular weight and specific heat as air the following form is used:

$$F = g V_s r_s^2 (T_s - T) / T_s, \quad (9)$$

where r_s is the stack radius.

Equation 9 was evaluated for use in the model giving:

$$F = 3.75 \times 10^{-5} Q_h. \quad (10)$$

The distance X^* at which atmospheric turbulence begins to dominate plume growth in unstable or neutral conditions is evaluated by:

$$X^* = 14 F^{0.625} \quad \text{for } F < 55, \text{ and} \quad (11)$$

$$X^* = 34 F^{0.4} \quad \text{for } F \geq 55. \quad \text{Briggs}^{23,24} \quad (12)$$

The distance of final plume rise is $3.5X^*$.

Briggs²³ concludes that X^* may vary by $\pm 20\%$ due to normal variation, and overall calculated plume rise may vary from measured values by $\pm 10\%$ for flat and uniform terrain, and $\pm 40\%$ for substantial

topographic variations and large water body influences.

For stable conditions Briggs²³ provides the following equations:

$$\Delta h = 2.4 (F/U S)^{1/3} \quad (\text{buoyant windy}) \quad (13)$$

$$\Delta h = 5 F^{0.25} / S^{3.75} \quad (\text{buoyant calm}) \quad (14)$$

where S is a stability factor.

5.3.3. Diffusion.

The first diffusion model was developed by Adolf Fick in 1855. This model was based on the idea that the time change in contaminant concentration at a point results from the existence of a gradient concentration at that point, and that the diffusive behaviour of the medium may be characterized by its diffusivity, K_d . The basic equation²³⁹ is given by:

$$dX/dt = K_d \nabla^2 X, \quad (15)$$

where X is the concentration of pollutant, and t is the time. For steady state conditions, mean wind along the x-axis, no change of wind with height, and limited anisotropy, an approximate solution is given by:

$$X_{(x,y,z)} = \{Q/4 \pi r (K_y, K_z)^{1/2}\} \exp\{(-U/4x) [(y^2/K_y) + (z^2/K_z)]\}, \quad (16)$$

where $r = (x^2 + y^2 + z^2)^{1/2}$, U is the wind speed, Q is the emission rate, y is the crosswind direction, and z is the vertical direction.

Fick's model was developed for predicting molecular diffusion processes. A major problem is that the model says that the downwind decay of concentration along the plume centerline is independent of wind speed, U, and is linearly inverse to distance, x. Observation,

however, has shown that X is inversely proportional to the wind speed and a power of x (Ux^a).²³⁹

The most used approach to modeling a continuous point source is the gaussian plume method. It is assumed that each particle of contaminant moves in a random fashion through continuous time and space, independently of the presence of any other particle. The result is that when a particle from a source of strength Q has been carried downwind for travel time, $t = x/U$, its probable departure from the x -axis must be accounted for along with all other particles. The general form of the relationship is given by:

$$X(x,y,z) = Q/U F_y G_z, \quad (17)$$

where U is the mean wind speed, and F and G are the horizontal and vertical diffusion functions, respectively.²³⁹

When the plume is not constrained horizontally and vertically, the diffusive functions are usually adaptations of the double normal probability (gaussian) surface described by:

$$P_r(x,y) = (2\pi\sigma_x\sigma_y)^{-1} \exp(-1/2) \{ [(x-\bar{x})^2/\sigma_x^2] + [(y-\bar{y})^2/\sigma_y^2] \}. \quad (18)$$

If it is assumed that surface absorption does not occur and pollutants are reflected from the surface, the model assumes final form by mirror imaging a second source and plume at distance h below the surface. The two resulting equations are added to give the gaussian plume model:

$$X(x,y,z) = (Q/2\pi\sigma_y\sigma_z U) \exp(-y^2/2\sigma_y^2) \exp[-(z-H)^2/2\sigma_z^2] + \exp[-(z+H)^2/2\sigma_z^2], \quad (19)$$

where H is the effective source height, and σ_y and σ_z are the horizontal and vertical diffusion coefficients, respectively.

Applications and modifications of the gaussian plume model are discussed in Turner,²⁵⁰ Slade,²³² and Pasquill.¹⁷⁸

The modified gaussian model assumes a gaussian distribution horizontally, and a vertical distribution that is uniform and limited by the mixing height:

$$X_{(x,y,z)} = (Q/\sqrt{2\pi} U \sigma_y L) \exp [-1/2 (y/\sigma_y)^2] \quad (20)$$

where L is the height of the mixing layer, and σ_y is the horizontal diffusion coefficient.

The standard deviations (σ_x , σ_y , σ_z) of the gaussian equation describe the rate of dispersion. It is assumed that diffusion in the x direction is negligible in comparison to transport by the wind. The horizontal and vertical diffusion coefficients are calculated theoretically or determined empirically from experimental data.

Sutton²⁴⁶ developed a diffusion equation in terms of diffusion coefficients, C_y and C_z , and a turbulence index, n, which depends on a wind velocity profile in the power law form. Sutton's parameters were redefined to abandon dependence on the velocity profile data:

$$\sigma_y = 2^{-1/2} C_y x^{(2-n_y)/2} \quad (21)$$

$$\sigma_z = 2^{-1/2} C_z x^{(2-n_z)/2}, \quad (22)$$

where n_y and n_z are two values of n associated with C_y and C_z .²⁴²

Extensive field programs on plume diffusion have resulted in many expressions for σ_y and σ_z ; a summary of these field studies is given in Strom.²⁴² These data cover a range of stabilities and surface

configurations for which the assumption of uniformity in atmospheric conditions is generally valid. The values of σ_y and σ_z vary with turbulence, height above the surface, surface roughness, wind speed, sampling time over which the concentration is to be estimated, and distance from the source. The parameters increase with distance, turbulence, and thermal instability; surface roughness also results in increases due to its effect on turbulence.

Curves of σ_y and σ_z with distance have been developed by Turner^{232, 250} based on the data of Pasquill.¹⁷⁷ Values of σ_y and σ_z are estimated from the stability of the atmosphere which is in turn estimated from the wind speed at a height of about 10 meters, and during the day, incoming solar radiation, or at night, cloud cover. These data apply to sampling times of about 10 minutes and relatively open country. Turner²⁵⁰ estimates that σ_y values are generally more accurate than σ_z , and that the more accurate σ_z values are within a factor of 2 accuracy.

Plume dispersion for large coal-fired power plants has been investigated at Tennessee Valley Authority power plants for many years.

Carpenter et al.³¹ identify the standard deviations σ_y and σ_z for six stability categories by potential temperature gradients. Montgomery et al.¹⁵⁵ developed simplified equations for neutral conditions and stable conditions prior to breakup. Urban diffusion experiments in St. Louis are reported by McElroy.¹⁴³ Hinds¹⁰⁵ reported on diffusion in the complex terrain in southern California.

Smith and Singer²³⁶ present the results of diffusion experiments at Brookhaven National Laboratory. Gustiness categories (B_2 , B_1 , C,

and D with C being closest to neutral) rather than stability categories were related to atmospheric turbulence based on wind direction data. Singer et al.²³¹ present a simplified method of estimating diffusion parameters based on various configurations of wind instruments that might be available at a site.

Table 19 gives the Smith-Singer diffusion parameters.

Table 19. Smith-Singer diffusion parameters--Brookhaven data.

Gustiness Category	meters	meters	z = 9 m	z = 108 m
B ₂	0.40 x ^{0.91}	0.41 x ^{0.91}	2.5	3.8
B ₁	0.36 x ^{0.86}	0.33 x ^{0.86}	3.4	7.0
C	0.32 x ^{0.78}	0.22 x ^{0.78}	4.7	10.4
D	0.31 x ^{0.71}	0.06 x ^{0.71}	1.9	6.4

²⁴²
Strom

Vertical diffusion in the modified gaussian model is gaussian out to the distance where reflection from the ground and from the mixing layer begin to produce vertical uniformity. Beyond that distance, concentrations are proportional to 1/L, where L is the height of the mixing layer.

Vertical dispersion is based on the Singer-Smith²³⁶ relationship:

$$\sigma_z = 0.33 x^{0.86}, \quad (23)$$

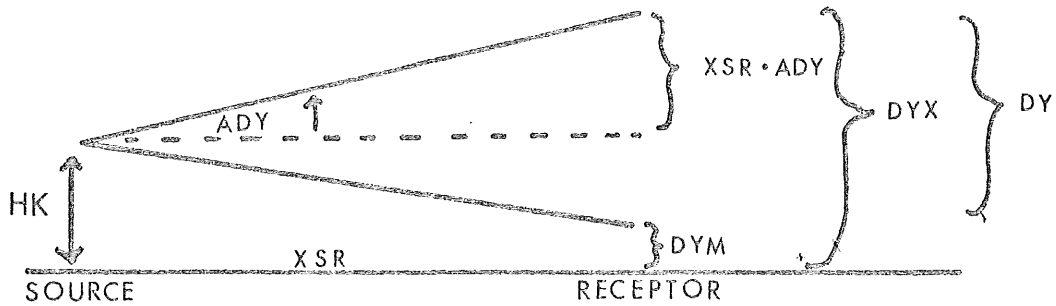
and is described in Figure 17.

Horizontal dispersion is based on Sutton²⁴⁶ who relates the dispersion angle to wind turbulence and the wind velocity profile.

$$DX = \sigma_y = 0.3 (SDWH) x^{0.85} = 2^{-1/2} C_y x^{(2-n_y)/2}, \quad (24)$$

where C_y is the horizontal diffusion coefficient taken as 0.42, SDWH is the average standard deviation of the wind heading over a 24-hour period, and $n_y = 0.86$ (Figure 18).

FIGURE 17. VERTICAL DIFFUSION



$$ADY = 0.33 XSR^{0.86} = \sigma_z$$

$$DYX = HK + |XSR \cdot ADY| \quad \text{IF } (DYX > HMAX) \quad DYX = HMAX$$

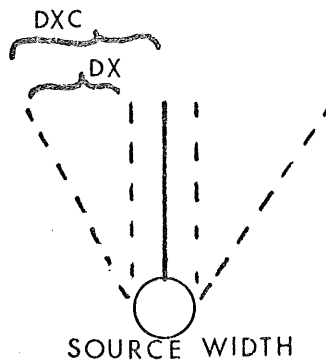
$$DYM = HK - |XSR \cdot ADY| \quad \text{IF } (DYM < 0) \quad DYM = 0$$

$$DY = DYX - DYM$$

$$DY = L, \text{ the box height}$$

HK is the effective stack height

FIGURE 18. HORIZONTAL DIFFUSION



$$DX = 0.30 \cdot SDWH \cdot XSR^{0.86} = \sigma_y$$

$$DXC = DX + \text{source width}$$

It is important to know the distance at which the plume touches down or intercepts the ground in order to determine when the assumption of uniform vertical mixing becomes valid. Plume touchdown distances were determined for several stack heights, heat emission rates, and wind speed configurations. The sources that were used include Copper Cliff, Falconbridge, and the hypothetical copper-nickel smelter main and fugitive stacks.

Table 20 summarizes the touchdown distance variation for each of the cases at varying wind speeds. The plume touchdown distance is largest for the Copper Cliff superstack; at wind speeds of greater than about 27 km/hr the plume touchdown distance becomes less than 5 km. The touchdown distances of the two smelter stacks are less than 0.5 km with the exception of the main stack at 10 km/hr when a touchdown distance of 1.4 km is computed.

5.3.4. Oxidation rate.

Ritchie¹⁹⁶ reviewed the literature relating to sulfur dioxide to sulfate conversion; a summary of the laboratory and field studies follow.

5.3.4.1. Laboratory studies: Four mechanisms have been identified for the oxidation of SO_2 to sulfate. These mechanisms, summarized in Table 21, are direct photo-oxidation, indirect photo-oxidation, uncatalyzed and catalyzed liquid phase oxidation, and catalyzed oxidation on dry surfaces. Reported oxidation rates are summarized in Table 22.

Direct photo-oxidation--Direct photo-oxidation is the oxidation of SO_2 by atmospheric oxygen in the presence of sunlight; this mechanism is not considered significant. The maximum theoretical rates correspond

Table 20. Plume touchdown distances.

Source	heat emissions m ⁴ /sec	stack height, m	wind speed, km/hr	touchdown distance, m
Copper Cliff	6142	380	10	5860
			20	5860
			30	4710
			40	3670
			50	2830
Falconbridge	1350	91	10	4240
			20	1990
			30	810
			40	550
			50	450
Smelter, main stack	236.8	60	10	1360
			20	440
			30	280
			40	230
			50	210
smelter, fugitive stack	3.1	50	10	160
			20	140
			30	130
			40	120
			50	120

to less than 0.02%/hr.³⁰ Laboratory studies have reported rates up to 24%/hr, but these rates are not applicable to direct photo-oxidation observed in the atmosphere because of experimental difficulties.³⁰

Indirect photo-oxidation--Indirect photo-oxidation of SO₂ involves the chemical reaction of SO₂ in a mixture of air containing oxides of nitrogen (NO_x), hydrocarbons (HC), hydroxyl radical (HO), hydroperoxyl radical (HO₂), and other species.

Rates calculated in laboratory studies are affected by many experimental factors including concentration of SO₂ and reacting species, irradiation sources, reaction vessels, water vapor, and gaseous impurities.

Table 21. Mechanisms that convert sulfur dioxide to sulfate.

MECHANISM	OVERALL REACTION	FACTORS ON WHICH SULFATE FORMATION PRIMARILY DEPENDS
1. Direct photo-oxidation	$\text{SO}_2 \xrightarrow[\text{water}]{\text{light, oxygen}} \text{H}_2\text{SO}_4$	SO ₂ concentration, sunlight intensity
2. Indirect photo-oxidation	$\text{SO}_2 \xrightarrow[\text{HO}]{\text{smog, water, NO, organic oxidants}} \text{H}_2\text{SO}_4$	SO ₂ concentration, sunlight intensity, concentration of NO _x , HO, and organics
3. Liquid phase oxidation		
a. uncatalyzed oxidation by O ₂ with and without NH ₃	$\text{SO}_2 \xrightarrow{\text{water}} \text{H}_2\text{SO}_3$ $\text{NH}_3 + \text{H}_2\text{SO}_3 \xrightarrow{\text{oxygen}} \text{NH}_4^+ + \text{SO}_4^{=}$	NH ₃ concentration, pH, temperature
b. catalyzed oxidation by O ₂	$\text{SO}_2 \xrightarrow[\text{metal ions}]{\text{water, oxygen}} \text{SO}_4^{=}$	concentration of metal ions, temperature, pH
c. oxidation by ozone and strong oxidizing agents	$\text{SO}_2 \xrightarrow[\text{agents}]{\text{water, ozone, oxidizing}} \text{H}_2\text{SO}_4$	concentration of ozone or oxidizing agent, pH
4. Catalyzed oxidation on dry surfaces	$\text{SO}_2 \xrightarrow[\text{water, carbon}]{\text{oxygen, particulate}} \text{H}_2\text{SO}_4$	carbon particle concentration, surface area

Table 22. Reported SO₂ oxidation rates.

LABORATORY STUDIES

	RATE (%/hr)
1) direct photo-oxidation	0.02
2) indirect photo-oxidation	average: 0-2.7 range: 0-100
3) liquid phase oxidation	6-150
4) catalyzed oxidation on dry surfaces	none reported

FIELD STUDIES

0-200
most values in the
range: 0-10

Indirect oxidation of SO₂ by singlet oxygen, ozone, NO_x, and CH₂O is not significant in the ambient environment.^{30, 46, 48, 129} The gas phase oxidation of SO₂ by HO may be the most important homogeneous sulfate formation mechanism. Reaction rates of 0.4%/hr in clean atmospheres to 2.7%/hr in polluted atmospheres have been calculated.³⁰ More information is needed, however, to quantify HO concentrations in the ambient atmosphere and in industrial plumes.²⁷⁵ HO₂ and CH₃O₂ are thought to be important in the gas phase oxidation of SO₂; however, experimental studies are limited. Reaction rates of up to 2%/hr have been postulated for polluted atmospheres.³⁰ Oxidation rates of up to 3%/hr in polluted atmospheres have been calculated for the ozone-olefin system.⁴²

Experimental results of SO₂ oxidation in smog are conflicting and encompass a variety of reactants and concentrations, irradiation sources, and reaction vessels. Reaction rates of 0-100%/hr have been reported for SO₂-smog systems.^{41, 43, 147, 191, 198, 237, 299, 300}

Uncatalyzed and catalyzed liquid phase oxidation---The liquid phase oxidation of SO_2 involves the diffusion of molecular SO_2 and other gases into a water droplet where the gases may encounter nucleating aerosol particles. Oxidation then proceeds through the process of hydration, and subsequent dissociation of the dissolved gases and oxidation of sulfite or bisulfite ion.

The results reported in the literature for the oxidation of SO_2 in the liquid phase vary. Many studies were conducted using higher concentrations of catalyst than normally found in the ambient atmosphere,^{37, 183} requiring extrapolation to ambient levels.

Oxidation in the aqueous phase has been found to be sensitive to pH, temperature, relative humidity, catalyst type, catalyst concentration, NH_3 concentration, and SO_2 concentration.^{12, 25, 79, 117, 184, 219}

Oxidation rates ranging from 0 to 15%/hr have been reported for the uncatalyzed oxidation of SO_2 by O_2 (with and without ammonia).^{17, 148, 219} Ammonia, although not a true catalyst, is important in the oxidation reaction because it maintains a high pH, and forms sulfate salts which lower solution vapor pressure.⁷⁵

Metal catalyzed oxidation rates for SO_2 ranging from 0-90%/hr have been reported.^{12, 25, 36} Dissolved manganese and iron are the most efficient catalysts; vanadium has been shown to be an inefficient catalyst.^{32, 72, 117, 140} A synergistic effect has been observed between iron and manganese, suggesting that plume oxidation rates may be accelerated in the presence of several catalysts.¹² Oxidation has been observed to stop at a pH of 2.2.^{12, 117}

Oxidation of SO_2 by ozone at a rate of 12.6%/r has been reported.¹⁸³ Plume oxidation by this mechanism is potentially important, particularly at distances farther from the source, where ozone concentrations have not been depleted by reaction with NO .^{16, 184}

Overall, aqueous phase oxidation rates ranging from 0 to 150%/hr have been reported.⁷²

Catalyzed oxidation on dry surfaces--The heterogeneous solid catalyzed gas phase oxidation studies reported in the literature lack reaction rate and/or mechanism studies relating dry heterogeneously catalyzed SO_2 oxidation systems to atmospheric processes.¹⁷² These reactions do not appear significant when compared to aqueous phase oxidation systems.⁴⁷ Manganese, iron, lead, and other suspended particulates in urban air have been reported as efficient catalysts; vanadium, however, appears to be a poor catalyst.^{29, 260}

5.3.4.2. Field studies: Levy et al.¹²⁹ reviewed the field studies of SO_2 oxidation in plumes. Oxidation has been widely investigated for power plant plumes, urban plumes, and smelter plumes. These studies encompass a variety of sampling, analytical, and modeling techniques. Some rate controlling factors believed to be important for both laboratory and field studies include: temperature, humidity, solar radiation, catalytic particles, hydrocarbons, and free radicals such as HO . No single factor is dominant under all conditions.

Most investigators believe that either indirect photo-oxidation or liquid phase oxidation of SO_2 in plumes and the atmosphere are the most important mechanisms.^{46, 133, 169, 170, 295} The nature of the plume and existing meteorological conditions are also important.⁵²

For example, gas phase oxidation by HO radical may be important during the summer months when UV fluxes, temperature, and relative humidity are greater because these conditions favor HO production. Conversely, liquid phase oxidation likely predominates in the winter when conditions do not favor indirect gas phase oxidation.

The relative importance of catalyzed and uncatalyzed liquid phase processes depends on the presence of active transition metal species. Catalytic processes may predominate in power plant plumes where particulate metals are abundant. A pollution control-equipped smelter plume contains fewer catalytic surfaces, and consequently catalytic reactions may be insignificant.

The type of mechanism which predominates in a single plume over the course of a year may experience both seasonal and diurnal variations. On a diurnal basis, high UV fluxes occur during daylight hours, which favor indirect gas phase oxidation; conversely, these mechanisms become slower or less important at night. The relative importance of the individual mechanisms in a plume may also vary with distance from the source. Oxidation by HO or ozone may predominate farther downwind while catalyzed-uncatalyzed liquid phase oxidation may be more important close to the source.⁴⁶

In summary, investigators have not elucidated the complex chemical reactions of SO₂ oxidation. Field investigations have shown that humidity, sunlight, temperature, catalyst concentration, and catalyst type are important factors in the oxidation process.^{85, 169, 170, 281} Neither the importance of the individual mechanisms nor the variation of the oxidation rate with distance have been determined. Some studies show that the oxidation rate remains constant throughout plume travel,

while others show increasing or decreasing trends in oxidation rates.^{134, 295} Problems in plume field study methodology (instrumentation, sample collection, rate calculation, and laboratory analysis) have not been resolved.^{114, 134, 169, 170, 295, 298}

SO₂ oxidation rates in the range 0 to 300%/hr have been measured for power plant, urban, and smelter plumes; most values are in the range of 0 to 10%/hr, and average values in this group are about two percent per hour.^{45, 52, 70, 71, 85, 133, 169, 170}

5.3.4.3. Plume chemistry modeling: Because of the lack of a well-defined experimental data base which describes the complex SO₂ chemical system, a single inclusive chemical reaction dispersion model has not been developed and verified. However, until more sophisticated mechanisms are elucidated, the incorporation of a first or second order expression into diffusion models appears to be a reasonable approximation for most purposes.

The sulfur dioxide to sulfate conversion rate is built into the model as an exponential expression based on the data of Lusic et al.¹³⁵ Reaction rates vary from about 5%/hr close to the source to about 0.6%/hr after 2 hours of plume travel. After 2 hours plume travel the reaction rate becomes negligible at 0.006%/hr. The rate after 2 hours is probably too low, and should be adjusted to about 0.6%/hr.

$$\begin{aligned} \text{OXR} &= 0.025 \times 10^{-4} \quad \text{IF } (T \text{ less than } 2), \text{ then} \\ \text{OXR} &= 0.625 \times 10^{-4} + 1.25 \times 10 \exp (-1.45 - 0.45 T) \end{aligned}$$

where OXR is the oxidation rate in parts/hr, and T is the plume travel time in hours.

Fatough et al.,³⁰² reported that inorganic sulfite species are present as complexes with Fe(III), Cu(II), Zn(II), and possibly Pb(II). The authors also reported that 10% to 30% of the sulfate concentration in primary aerosols produced by smelters is composed of these inorganic sulfite species, and that the sulfite species were found to be evenly distributed over various particle size ranges. The importance of stable sulfite from smelters and the formation mechanism have not been clearly elucidated; therefore, these species were not considered in the oxidation analysis.

5.3.5. Removal processes.

Trace constituents in the atmosphere may be removed by three main processes: 1) chemical transformation into new substances, 2) dry removal processes such as gravitational deposition and sorption at the atmosphere-earth interface, and 3) wet removal or precipitation scavenging.²⁹⁴

This section focuses on the wet and dry removal mechanisms.

5.3.5.1. Dry deposition: Particles transported through the atmosphere may be deposited directly onto vegetation, soil, water or other surfaces, and gases may be adsorbed onto these surfaces.

The mechanism of particle deposition is a complex function of all possible forces acting on a particle including Brownian motion, diffusio-phoresis, eddy diffusion, gravity, impaction, interception, and electrical charge effects.²²¹

Investigators differ on the mechanism of particle transport in the region close to the surface.^{76, 220, 234} Three basic theories have been proposed to describe the deposition of particles from turbulent air flow. Friedlander and Johnstone⁷⁶ proposed that the deposition process could be described by eddy diffusion up to a point near the surface followed by free flight due to particle momentum to reach the surface. Sehmel²²⁰ proposed that the turbulent deposition process could be described solely by effective eddy diffusion. Slinn²³⁴ presents a theory for dry deposition in which the collection of particles by a surface depends on a collection efficiency similar to the collection efficiency for particles in a viscous jet impactor.

The dry deposition flux is commonly calculated from an expression

developed by Chamberlain:^{33, 34}

$$N \text{ (mass deposited/area/time) = } V_d \text{ (length/time) } \cdot X \text{ (mass/volume) } \quad (26)$$

where V_d is the deposition velocity, and X is the atmospheric concentration of pollutant above the surface.

In field experiments the concentration, X , has been measured at different heights above the deposition surface. The deposition velocity is usually reported in cm/sec. Deposition velocities from field data are based on a wide particle size distribution, but deposition velocities have also been evaluated for single-sized particles in laboratory studies.²²¹ The deposition velocity depends strongly on particle size, wind speed, and deposition surface. Chamberlain³⁵ found that V_d increased by 50 to 100% when ground level wind speed increased from 2 to 4 m/sec.

For particles with a large diameter (1 to 100 microns), deposition occurs primarily by sedimentation; for submicron particles, molecular diffusion dominates. Neither of these processes is efficient for particles in the size range of 0.1 to 1.0 microns (sulfate aerosol and fly ash). Complicated diffusion processes are apparently involved in order to explain their transport to the surface.²³⁴ These processes are slow but dominate the deposition process more than the chemical nature of the particles or the nature of the deposition surface. Therefore, the dry deposition velocity can be estimated for any particle using the particle size distribution.²³⁴

A major exception is the deposition of particles in a forest where the canopy enhances the collection of aerosols. Slinn²³⁴ estimates

that a deep dense forest canopy will remove all sizes of particulates at the same rate.

In practice the particle size distribution may not be known, as in the case of metal bearing particulates emitted from a hypothetical smelter equipped with the latest pollution control devices.

In order to circumvent the problem of particle size distributions, available field measurement data of dry deposition velocities were used in the modeling simulations. Table 8 provides a summary of mass median particle diameters and deposition velocities for selected particulates. The primary source of field data was an excellent study of deposition at remote sites in Great Britain by Cawse.³²

Cawse³² determined the deposition velocity of individual elements at seven sites in Great Britain for two years. The deposition surface was a Whatman 541 filter which may not behave exactly as a natural surface such as water, soil, grass, or other vegetation. The data from only two of the sites, Chilton and Trebanos, are presents because these sites most closely approximate conditons in northeastern Minnesota. The deposition velocities at these sites are considered to be typical of industrially generated and transported particulates.

Deposition velocities were also estimated using the data of Sehmel,²²¹ Sehmel et al.,²²⁴ and Sehmel and Sutter.²²³ Deposition velocities in these studies were measured as a function of particle size over various surfaces in wind tunnel experiments using monodisperse particles. A minimum deposition velocity of about 0.01 cm/sec has been shown for particles of about 0.1 to 0.3 microns in diameter. For total particulates a mass median diameter was taken from Statnick's²³⁸ data

Table 23. Mass median size and dry deposition velocity data.

species	mass median diameter, microns	dry deposition velocity, cm/sec
SO ₄	0.65 Cawse(1974)	0.1 grass Sehmel & Sutter(1974)
	0.7 Dovland & Eliassen(1976)	0.02 water Sehmel & Sutter(1974)
		0.1 snow Dovland & Eliassen(1976)
	1 to 1.2 Kramer(1976)	0.025 to 0.1 Garland(1977) 0.3 to 3.0 Slinn(1977)
Cu	1.5 Cawse(1974)	<0.4 to 2.0 Cawse(1974)
	1 to 3 Kramer(1976)	0.02 to 0.40 water Sehmel & Sutter(1974)
		0.1 to 0.25 grass Sehmel & Sutter(1974)
Ni	1.8 to 5.9 Kramer(1976)	0.03 to 7.0 water Sehmel & Sutter(1974)
		0.18 to 0.5 grass Sutter(1974)
		1.0 to 3.0 Pierson <i>et al.</i> (1974)
		1.0 to 4.8 Cawse(1974)
Pb	0.6 Chamberlain(1976)	0.2 Chamberlain(1976)
	0.56 Cawse(1974)	0.17 to 1.4 Cawse(1974)
		0.16 snow Dovland & Eliassen (1976)
Fe	2.5 Cawse(1974)	0.36 to 4.1 Cawse(1974)
	4.0 Chamberlain(1976)	1.2 Chamberlain(1976)
		1 to 3 Pierson <i>et al.</i> (1974)
		0.04 to 7.0 water Sehmel & Sutter(1974)
TSP	2.8 Statnick(1974)	0.15 to 0.9 grass Sehmel & Sutter(1974)
As	0.55 to 0.68 Cawse(1974)	0.05 to 0.44 Cawse(1974)
		0.02 to 0.065 grass Sehmel & Sutter(1974)
Cd	0.9 by analogy to Zn Cawse(1974)	0.18 Cawse(1974)
		0.02 to 0.065 grass Sehmel & Sutter(1974)
Hg	_____	0.1 National Research Council(1978)

on trace metals from a copper smelter and reverberatory gas streams.

Garland⁸¹ reviewed the literature and suggested a mean SO₂ deposition velocity of about 0.8 cm/sec for large areas of Europe. Experimental measurements ranged from as high as 2.2 cm/sec over Lake Ontario²⁹⁴ to 0.1 cm/sec over pine forest.⁸³ Limited data are available for the snow season; Whelpdale and Shaw²⁹⁴ report a deposition velocity of 0.05 to 1.6 cm/sec, and Dovland and Eliassen⁵⁶ report a mean value of 0.1 cm/sec.

The dry deposition of gases from the atmosphere to soil, vegetation, or water is governed both by transfer in the gas phase and by sorption at the surface. Slinn²³⁴ shows that for most gases the dry deposition rate is limited by interaction with the surface. For simplicity, sorption at the surface is usually assumed to be irreversible. Table 24 presents a summary of some SO₂ dry deposition velocities reported in the literature.

The modified gaussian model is a source depletion model; that is, the deposition of pollutant is accounted for by reducing the source strength through the vertical extent of the plume. In reality, deposition is a surface phenomenon, and should be modeled by a surface depletion model in which the plume is selectively depleted in the vicinity of the surface. This type of model had been used in the numerical diffusion model of Ragland,¹⁹³ but it was not used in the modified gaussian model because of the additional complexity and cost.

The source depletion model has been shown to consistently overpredict the surface air concentration and the deposition at downwind locations close to the source, and underpredict at locations farther

Table 24. SO₂ dry deposition velocity data.

dry deposition velocity, cm/sec		reference
0.5 to 2.6	grass	Whelpdale & Shaw(1974)
0.5 to 1.6	snow	
0.16 to 4.0	water	
0.36	wheat	Fowler & Unsworth(1974)
0.3 autumn	grass	Shepherd(1977)
0.8 summer		
0.8		Owens & Powell(1974)
0.55	short grass	Garland <u>et al.</u> (1974)
0.85	grass	Garland <u>et al.</u> (1973)
0.8		Garland(1977)
0.1	snow	Dovland & Eliassen(1976)

from the source.¹⁰⁷ At all distances (up to 100 km) modeled by Horst¹⁰⁷ the source depletion model overestimated total deposition between source and receptor and underestimated ambient air concentrations. Draxler and Elliot⁵⁷ adapted a finite difference model to simulate the effect of diurnal stability variation and dry deposition on plume depletion.

They found that differences between source and surface depletion models were directly proportional to deposition velocity and travel time, and indirectly proportional to vertical mixing. Atmospheric residence times of the surface depletion model were about a factor of two greater than the source depletion model. The differences between the two models were greatest for large deposition velocities and low mixing rates. The stability at time of release was one of the major factors that determined airborne concentrations even after several days travel time. At low level releases the effect of a diurnal stability cycle changed the residence time from 1/5 (at night) to 3 times (day)

that obtained for constant neutral stability.

5.3.5.2. Wet removal: In many cases pollutants may be deposited in nearly equal amounts by wet and dry deposition processes. Estimates of the total mass of atmospheric particles removed by dry deposition range from 50%⁶³ to 33%¹⁸ to 20%.²⁰¹ However, the wet deposition process is usually the most efficient, and more likely to result in acute levels of pollutants which can cause ecological damage in surface waters.

Predicting the amount of wet deposition is not at all clear-cut or simple. The scavenging process within a storm is the subject of much debate, and research efforts continue to produce new models. The lack of detailed meteorological information is also a problem. Since an intense storm can deposit a large proportion of its soluble pollutants within minutes, it is important to accurately predict the time and place of the storm's onset.

Most models of pollutant scavenging are logarithmic:²¹⁸

$$dX/dt = -\lambda X + S, \quad (27)$$

where dX/dt is the removal rate, λ is the washout coefficient, X is the mass concentration of pollutant, and S denotes all other pollutant sources and sinks.

Considering only wet removal and neglecting S ,

$$X = X_0 e^{-\lambda t}, \quad (28)$$

where X_0 is the pollutant concentration before scavenging, and X is the concentration at time t .

The value of the washout coefficient (λ), which results from integrating over all sizes of pollutant containing hydrometers, is difficult to evaluate. The removal expression is generally applied to

a surface layer of air. This provides a crude approximation unless the surface layer encompasses the entire vertical extent of the region being scavenged.

Scott and Dana²¹⁸ provide an alternate method for computing wet removal which relies on a direct calculation of an average wet removal rate for the layer being scavenged. Their work provides the basis of predicting the precipitation scavenging of sulfate, sulfur dioxide, and particulate metals in the modified gaussian model.

Basically, the removal of pollutant is accomplished by large collector particles such as snowflakes or raindrops which sweep downward through the cloud, and capture cloud droplets containing high concentrations of the pollutant.

Three basic precipitation systems; the Bergeron cloud, the warm cloud, and the convective cloud; are considered by Scott and Dana.²¹⁸

In the Bergeron or cold cloud ice growth is responsible for precipitation development. Ice crystals in the upper part of the cloud nucleate, aggregate, and grow rapidly to precipitation sized particles. Pollutant is advected through the base of the cloud, and is picked up by the cloud water in the lower parts of the cloud. Surface precipitation from this cloud may be in the form of rain or snow.

In the warm or maritime cloud the ice growth process is assumed to be ineffective in initiating precipitation. Rain develops through warm phase mechanisms with gentle uplift and long times available for condensation and coalescence to precipitation sized drops. Pollutant transport is assumed to take place through the sides of the storm.

In the convective cloud strong updrafts produce large supersatura-

tions and liquid water concentrations which enable combined condensation and coalescence to produce precipitation sized drops faster than can be removed by hydrometeors falling from above. Pollutant transport is assumed to be through the base of the cloud.

The Bergeron or cold cloud is felt to be responsible for most of the precipitation from layer type clouds over the continents.¹³⁸ This cloud type is thought to produce most of the continuous rain or snow storms over northeastern Minnesota, and was used as the model for pollutant removal.²¹⁷ The warm cloud mechanism is rare in northeastern Minnesota, but the convective storm is responsible for showers during the summer.

Scott and Dana²¹⁸ derive an expression for wet removal based on the conservation of mass:

$$d\bar{X}_i/dt = (jC)_z - (jC)_{z_0} / (z-z_0) , \quad (29)$$

where j is the precipitation flux (mass of H_2O /area/time), C_i is the pollutant concentration of the precipitation water (pollutant mass/mass of H_2O), \bar{X}_i is the average pollutant concentration in a volume of air, and $z-z_0$ is a column of air extending from height z_0 to z .

Because detailed vertical profiles of precipitation and pollutant concentrations are not available, the use of wet removal expressions is restricted to a layer of air that extends from the surface to a height where the wet, downward flux of pollutant is near zero.²¹⁸

The concentration of pollutant in precipitation, C_i , is also related to the concentration in the air by the washout ratio:

$$W_i = C_i \rho_{air} / X_i(z=0) , \quad (30)$$

where W_i is the mass concentration of pollutant in precipitation/mass

concentration of pollutant in air, C_i is the mass of pollutant in water, X_i is the mass of pollutant in air, and ρ_{air} is the density of air (gm/m^3).

Substituting,

$$d\bar{X}_i/dt = -j W X_{i(z=0)} / (\rho_{\text{air}} (z-z_0)). \quad (31)$$

The problem at this point is to relate the average pollutant concentration, \bar{X}_i , in a volume of air to the ground level concentration, $X_{i(z=0)}$. Assuming that $\bar{X}_i = \alpha X_{i(z=0)}$, then:

$$dX_{i(z=0)}/dt = -j W_{i(z=0)} / \rho_{\text{air}} \alpha (z-z_0), \quad (32)$$

$$\text{and} \quad = \lambda_i X_{i(z=0)}$$

$$\text{where} \quad \lambda_i = j W_i / (\alpha \rho_{\text{air}} (z-z_0)).$$

The loss of pollutant in the air is now expressed as a first order rate equation with an exponential solution:

$$X_i = X_{i(t=0)} e^{-\lambda_i(t-t_0)} \quad (33)$$

In modeling the scavenging losses, the rainfall flux, j , is determined from meteorological data and the relationship:

$$j = \rho_{\text{H}_2\text{O}} J \quad (34)$$

where the rainfall flux, j , has the units $\text{gm/m}^2/\text{hr}$; the density of water, $\rho_{\text{H}_2\text{O}}$, has the units 10^{-3} gm/m^3 ; and the rainfall rate, J , has the units mm/hr .

Substituting, the basic expression for the washout coefficient, λ_i , now becomes:

$$\lambda_i = \rho_{H_2O} J W_i / (\alpha \rho_{air} (z-z_o)). \quad (35)$$

The parameters α and $z-z_o$ are determined from Scott and Dana.²¹⁸ The washout ratio, W_i , of particulates depends on aerosol diameter, but since particle size distributions were not available washout ratios determined by Cawse³² in field studies were used for particulate metals. For sulfate, theoretical values of the washout ratio which depend on the rainfall rate and type of storm were used.²¹⁷ The washout ratio of SO_2 was based on equilibrium concentrations of SO_2 in water.^{94, 95}

The expressions for the washout coefficient which were used in the model are developed in the following sections.

Wet removal of sulfate--The concentration of sulfate in precipitation is the result of several processes (Brownian motion, phoretic attachment, inertial impaction, and nucleation) occurring within and beneath the cloud.

The solubility of sulfate particles and their small size (<1 micron) indicates they should be effective as cloud condensation nuclei. In addition to being drawn into the cloud from below, sulfate may be generated within the cloud and precipitation water through the oxidation of SO_2 . However, observations by Scott²¹⁷ suggest that in-cloud conversion is negligible, and that sulfate deposited on the ground results mainly from the scavenging of sulfate in the air flowing into the storm system.

Scott's model for wet removal of sulfate neglects below cloud and in-cloud capture of "dry" sulfate. The model which is based on the Bergeron cloud assumes that in the portion of Figure 19 above the cloud base, the rimming zone, cloud droplets are nucleated on sulfate condensation nuclei. Large collector particles then enter the box from above. As they descend they grow larger by accretion of cloud droplets and may melt to form raindrops.

The scavenging height distance, $z-z_0$, is obtained by Scott and Dana²¹⁸ as follows. The rimming zone (Figure 19) is the region of the cloud where precipitation growth occurs primarily by accretion of cloud droplets. The wet downward flux of pollutant at the top of the rimming zone is zero because the collector particles are assumed to be pollutant free when they enter the box. The thickness of the rimming zone, Δz , is estimated from the fall speed of a typical collector particle and from the time required for the particles to grow to raindrop size:

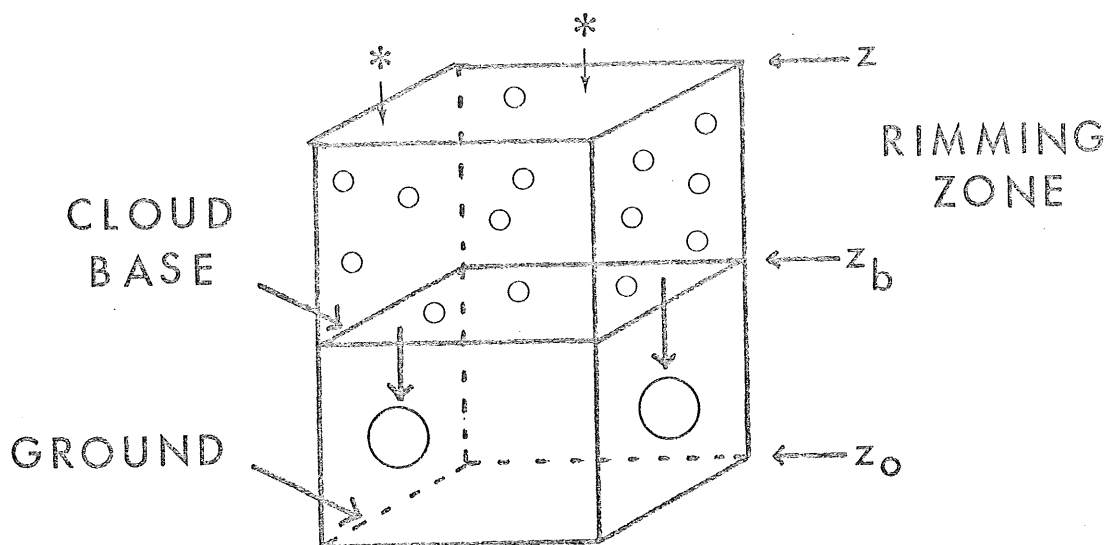
$$\Delta z = 744 J^{0.105} \text{ (meters) ,} \quad (36)$$

where J is the rainfall rate (mm/hr).

The rimming zone is generally 750 meters, and weakly depends on precipitation. The distance from the ground, z_0 , to the cloud base, z_b , in a precipitating cloud is comparable to the rimming zone thickness and is near 300 meters. The distance from the ground to the top of the cloud layer should then include the rimming zone thickness and the distance to the cloud base. Thus, the scavenging height distance is estimated by:

$$z-z_0 = 300 + 744 J^{0.105} \text{ (meters).} \quad (37)$$

FIGURE 19. SULFATE REMOVAL MODEL



SCOTT and DANA²¹⁸

Using this definition, the upper level wet pollutant flux would be zero, and the flux divergence over the entire column of air extending from the ground to the top of the rimming zone could then be evaluated by computing just the pollutant flux at the surface. Different layer thicknesses can be selected providing that the top of the rimming zone is below the upper boundary of the selected layer for all expected precipitation rates.

The convective storm, mentioned previously, could result in pollutant being carried to heights greater than 10 km within the cloud, creating the potential for scavenging height values dramatically different from the Bergeron cloud. The removal potential of the convective cloud exceeds that of either the warm or cold clouds and very high concentrations of sulfate can result. Although the convective cloud

does contribute to summertime precipitation in Minnesota, it's complexities are not well understood, and it is not considered further.

Scott and Dana²¹⁸ further simplify the expression for wet removal by parameterizing the sulfate concentration in the precipitation water reaching the surface in terms of the sulfate concentration being drawn into the base of the cloud. The final concentration of pollutant in a collector particle passing through the rimming zone is given by:

$$C = \bar{C} (1 - \exp(-2\bar{m})) , \quad (38)$$

where \bar{C} is the vertical average of the sulfate water concentration in the rimming zone, and \bar{m} is the vertical average of the cloud liquid water concentration. As the liquid cloud water concentration approaches zero, the wet removal of sulfate becomes negligible.

The liquid cloud water concentration is parameterized in terms of the precipitation rate:

$$\bar{m} = 1.56 + 0.44 \ln J \quad (39)$$

Using theoretical values of the washout ratio derived by Scott²¹⁷ for J less than 2.5 mm/hr and greater than 0.13 mm/hr, a surface water concentration of sulfate, C , in gms of sulfate per gm of water is determined:

$$C = 0.46 X_g(SO_4) J^{-0.27} \quad (40)$$

where $X_g(SO_4)$ is the ambient air concentration of sulfate ($\text{gm } SO_4/\text{m}^3$ air) being drawn into the cloud and cloud base. Assuming uniform mixing from the ground, which is the basic assumption of the modified gaussian model, $X_g \approx$ surface air concentration of sulfate and $\alpha = 1$.

The wet removal rate for sulfate is then given by:

$$d\bar{x}_{SO_4} / dt = - 460 X_g (SO_4) J^{0.73} / (z-z_o) , \quad (41)$$

$$\lambda_{SO_4} = 460 J^{0.73} / (300 + 744 J^{0.105}) . \quad (42)$$

The above result (equation 42) for the washout coefficient applies to both ground level rain and snow conditions in the modeling simulations.

Wet removal of particulates---Scavenging of particulates is usually treated as an irreversible process which is a function of the rate of encounter of particles by precipitation. If particles are wettable and small (< 1 micron) they can act as nuclei for the condensation of cloud water. Particulate drop evaporation is not considered in the modeling, and unwettable particulates could still be removed by impaction below the cloud.

Particles may be removed from the atmosphere by precipitation as nuclei being carried to the earth, or as particles collected by drops and crystals during collisions. The probability of scavenging is greater for particulates collected by droplets than for dry particulates because of drop size.

The washout coefficient used in the modeling for metals is obtained from the washout ratios of Cawse³² (Table 25) and equation 35:

$$\lambda_i = 2.86 \times 10^{-3} J T W_i / (P (300 + 744 J^{0.105})) , \quad (43)$$

where T is the temperature in °K, and P is the atmospheric pressures in atmospheres.

Because of a paucity of information on removal efficiencies in rain and snow, the scavenging of particulates during the two seasons is assumed to be the same.

Table 25. Washout ratios for particulates used in the modified gaussian model.

species	washout ratio
particulate	265 (by analogy to Fe) ^a
Cu	1150 ^a
Ni	625 ^a
As	410 ^a
Cd	325 (by analogy to Zn) ^a
Pb	315 ^a
Hg	50000 ^b

^aCawse³⁴

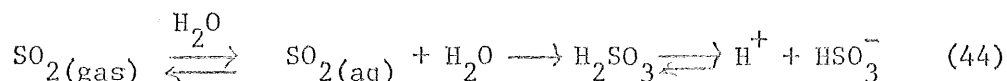
^bNational Research Council¹⁶²

Wet removal of SO₂ gas---Gas scavenging is more complex than particulate scavenging because capture of a gas molecule by a raindrop is to some extent reversible, a diffusional rather than a collisional phenomenon. Gas scavenging is a function of the concentration gradient of gas across the gas-liquid interface rather than the rate of encounter as in particulate scavenging. Because scavenging depends on a concentration gradient, the capture may be reversed either by increasing the pollutant concentration within the drop as a result of chemical transformation to another species or by drops falling into clean air.²³⁵ Because of the reversibility of the gradient the scavenging of gaseous pollutants is more strongly dependent upon the spatial distribution of the pollutant itself and of related species than is particulate scavenging.

Slinn,²³³ Garland,⁸¹ and Hales⁹⁴ agree that SO₂ gas dissolved in a raindrop will come to equilibrium with SO₂ in the air after falling as little as one meter through a plume. The rate of removal of SO₂ is dependent on the rainfall rate and the equilibrium concentration of

SO₂ in the rain water.

After SO₂ dissolves in water it forms sulfurous acid which partially dissociates:



If H⁺ are contributed by other sources such as dissolved sulfate in rain, the SO₂ solubility is reduced.

Removal of SO₂ by snow--In the case of SO₂ scavenging by snow it is assumed that frozen collector particles pick up the bulk of SO₂ as the particles capture cloud droplets in the rimming zone. The dissolved SO₂ in the cloud droplets is assumed to be in equilibrium with the environment. As the cloud droplets are collected, they freeze rapidly and have no opportunity to adjust to new equilibrium values as they are transported to lower levels in the cloud. Since the wet, downward flux of SO₂ through the upper boundary of the rimming zone is negligible, the SO₂ removal rate by snow is determined by evaluating the pollutant flux at the ground. The SO₂ removal rate may be expressed by:

$$d\bar{X}_{(\text{SO}_2)}/dt = -j C_{(\text{SO}_2)}/\Delta z, \quad (45)$$

where $\bar{X}_{(\text{SO}_2)}$ is the average atmospheric SO₂ concentration, $C_{(\text{SO}_2)}$ is the mass concentration of SO₂ in snow, j is the precipitation flux, and Δz is the fall distance for snowflakes.

From Scott and Dana,²¹⁸ $\Delta z = 300 + 744 J^{0.105}$ where J is the rainfall rate.

As in the case of sulfate, the final concentration of pollutant in a collector particle passing through the rimming zone is given by:

$$C = \bar{C} (1 - \exp(-2\bar{m})), \quad (46)$$

where \bar{C} is the vertical average of the SO_2 water concentration in the rimming zone, and \bar{m} is the vertical average of the cloud water concentration.

Letting \bar{C} equal the arithmetic average of the equilibrium concentration at the ground, $C_{(z=0)}$, and at the top of the rimming zone, then:

$$C = 0.5 [C_{\text{SO}_2(z=0)}] [1 - \exp(-2\bar{m})], \quad (47)$$

From the previous discussion:

$$C_i = W_i X_i / \rho_{\text{air}} \quad (48)$$

Substituting and collecting terms,

$$\left. \frac{dX_{\text{SO}_2}}{dt} \right|_{\text{snow}} = - \rho_{\text{H}_2\text{O}} J W_{\text{SO}_2} X_{\text{SO}_2} (1 - \exp(-2\bar{m})) / (2 \rho_{\text{air}} (z-z_o)), \quad (49)$$

and

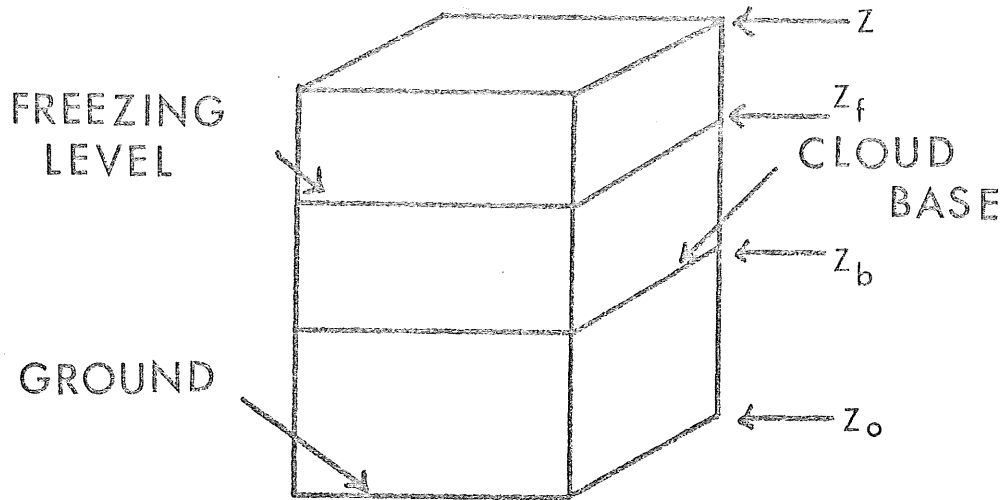
$$\lambda_{\text{SO}_2} \Big|_{\text{snow}} = 1.42 \times 10^{-3} W_{\text{SO}_2} J T (1 - \exp(-2(1.56 + J^{0.44}))) / (P (300 + 744 J^{0.105})). \quad (50)$$

Equation 50 was used in the model for the SO_2 snow washout coefficient.

Removal of SO_2 by rain--The model for SO_2 removal by rain assumes that snowflakes, as before, accrete cloud droplets containing dissolved SO_2 which melt to raindrops after falling through the freezing level. The model considers the vertical fluxes in and out of the boxes shown in Figure 20. The scavenging height is again represented by the distance, $z-z_o$, while the freezing height is given by $z_f - z_o$.

The only change in SO_2 concentration in the upper box results from a downward flux through the freezing level.

FIGURE 20. SO₂ RAIN REMOVAL MODEL



SCOTT and DANA²¹⁸

The amount removed is given by:

$$d\bar{x}_{SO_2}/dt|_{ice} = -j(z_f) C(z_f)/(z-z_f). \quad (51)$$

Both the precipitation rate and the SO₂ concentration in snow are evaluated at the freezing level.

Removal due to rain below the freezing level is given by:

$$d\bar{x}_{SO_2}/dt|_{liq} = [j(z_f) C(z_f) - j(z_o) C(z_o)]/(z-z_o), \quad (52)$$

where $j(z_o)$ and $C(z_o)$ are ground level values. Below the freezing level it is assumed that the SO₂ concentration in the drops is determined by establishing an equilibrium concentration between the dissolved and airborne SO₂.

The removal rate by rain is determined as a weighted average over both boxes:

$$\frac{d\bar{x}_{SO_2}}{dt} \Big|_{rain} = \left((z-z_f) \frac{d\bar{x}_{SO_2}}{dt} \Big|_{ice} + (z-z_f) \frac{d\bar{x}_{SO_2}}{dt} \Big|_{liq} \right) / (z-z_o) \quad (53)$$

Simplifying,

$$\frac{d\bar{x}_{SO_2}}{dt} \Big|_{rain} = - \rho_{H_2O} J W_{SO_2} x_{SO_2} / [\rho_{air} (z-z_o)] , \quad (54)$$

and

$$\lambda_{SO_2} \Big|_{rain} = 2.86 \times 10^{-3} J W_{SO_2} T / [(300 + 744J^{0.105}) P] . \quad (55)$$

Equation 55 was used in the model to calculate the SO₂ washout coefficient for rain removal.

Comparison of the expressions for wet removal by rain and snow shows that the rain removal can exceed snow removal by a factor of two or more at equivalent precipitation rates.

The washout ratio, W_i , in both the rain and snow expressions is calculated in a subroutine from the solubility of SO₂ in rainwater:^{44, 94}

$$C_{aq} = C_{gas} / H + 0.5 [- [H^+]_{ex} + ([H^+]_{ex} + 4 K_1 C_{gas}) / H]^{-1/2} \quad (56)$$

where $[H^+]_{ex}$ is the hydrogen ion concentration from background sources, C_{aq} and C_{gas} are the aqueous and gaseous concentrations, respectively, of SO₂, and K_1 is the first dissociation constant of SO₂ and H is Henry's constant.

5.3.6. Acidity of precipitation.

The acid-forming species responsible for acidic precipitation are generally considered to be sulfur dioxide and nitrogen dioxide which in the presence of rainwater form sulfuric and nitric acids.^{80,90,130,243} Hydrochloric and weak acids may also contribute to the acidity of precipitation.^{90, 124}

The deposition of H^+ is calculated in the model based on a background H^+ concentration in precipitation measured in the field, dissolved sulfate as calculated in the model, and the dissociation of dissolved SO_2 in rain.^{45, 95}

$$[H^+]_{total} = [H^+]_{bkg} + 1/2 [SO_2] + [HSO_3^-]_{dissolved} \quad (57)$$

Background hydrogen ion concentration is approximated by equating it to the total free hydrogen ion concentration; that is,

$$[H^+]_{bkg} \approx 10^{-pH}. \quad (58)$$

The background mean pH in northeastern Minnesota was reported to be 4.7 by Eisenreich *et al.*⁵⁹

Wet deposition of sulfate calculated by the model can be expressed as a concentration by:

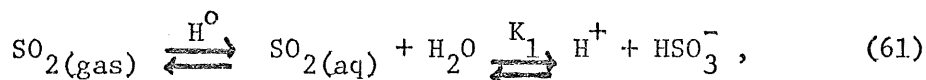
$$[SO_4^{=}] = [(4.1 \times 10^{-6}) (SO_{4dep})] / (R_T MW_{SO_4}), \quad (59)$$

where SO_{4dep} is the sulfate deposition in $\mu g/cm^2$, R_T is the rainfall amount in inches, MW_{SO_4} is the gram molecular weight of sulfate, $[SO_4^{=}]$ is the sulfate concentration in moles/liter, and 4.1×10^{-6} is a concentration conversion factor.

Assuming all of the sulfate contributes to acidity:

$$[H^+] = 1/2 [SO_4^{=}]. \quad (60)$$

The solubility of SO_2 in water varies as a function of concentration, temperature, and precipitation acidity.⁹⁴ The dissociation reactions are:



$$\text{and } H^O = [SO_2]_g / [SO_2]_{aq}$$

$$K_1 = [HSO_3^-] [H^+]_{total} / [SO_2]_{aq},$$

where H^0 and K_1 are the Henry's law and dissociation constants, respectively (Henry's constant is calculated in the subroutine). The second dissociation constant is assumed to be negligible.

The total acidity from the dissolution of aqueous SO_2 and outside sources may be derived as follows:

$$K_1 = [H^+]_{total} [HSO_3^-] / [SO_2]_{aq} = H^0 [H^+] [HSO_3^-] / [SO_2]_g, \quad (62)$$

$$\text{let } X = [HSO_3^-], \quad (63)$$

then,

$$[H^+]_{total} = [H^+]_{bkg} + 1/2[SO_4^{=}] + X. \quad (64)$$

Substituting equations 62 and 63 into 64, solving, and simplifying:

$$[H^+]_{total} = b/2 (1 + (1 + (4 K_1 [SO_2]_g) / (b^2 H^0))^{-1/2}),$$

where $b = [H^+]_{bkg} + 1/2[SO_4^{=}]$.

Total $[H^+]$ in moles/liter is then converted to deposition by:

$$H^+_{dep} = 2.54 \times 10^{-3} [H^+] R_T. \quad (66)$$

The hydrogen ion deposition, g/cm^2 , is then converted to pH by:

$$pH = - \log [H^+]. \quad (67)$$

5.3.7. Dynamics of dispersion.

All of the elements discussed previously (dispersion, chemical conversion, wet scavenging, and dry deposition) can be combined in a single dynamic model which was derived by Wendell, Powell, and Drake.²⁹²

The model is derived in the Lagrangian coordinate system in which wind velocity is defined to follow a single parcel of pollutant in its trajectory downwind from the source. The pollutant from a fixed source is emitted continuously at a rate Q_i , mass of i emitted per unit time. In this coordinate system a series of wind vectors $|\vec{u}|(\vec{r}, t)$ are defined

so that the x-axis is parallel to the wind vector, the y-axis is crosswind to the vector, and the z-axis is vertical to the vector (Figure 21).

The parcel's length, dx , is determined by the wind speed:

$$dx = |\vec{u}|(\vec{r}, t) dt \equiv u dt. \quad (68)$$

The mass of pollutant i remaining in the parcel at time t in its travel is known as the effective source term, $Q_i(t)$, and is related to the pollutant's concentration, $X_i(r, t)$, by a vertical and crosswind integration:

$$Q_i(t) = (\iint X_i dz dy) dx, \quad (69)$$

and

$$Q_i(t)/u dt = \int_0^\infty dz \int_{-\infty}^\infty dy X_i(r, t). \quad (70)$$

The effective source term, $Q_i(t)$, can be applied to all the conversion and deposition relationships which were determined for pollutant concentrations.

For nonreactive pollutants, such as total particulates and metals, the changes in $Q_i(t)$ are due to dry deposition and wet scavenging, and these losses can be approximated by first-order rate expressions. The time dependence of the effective source term for non-reactive pollutants is given by:

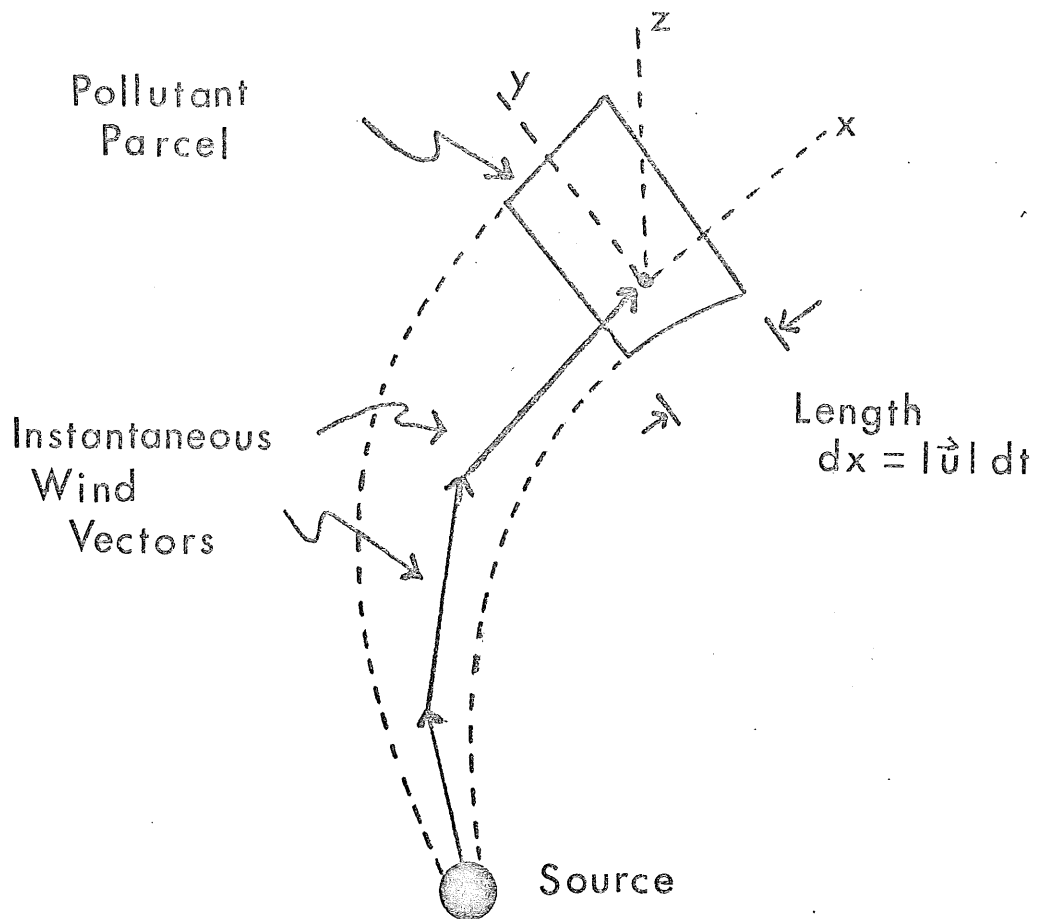
$$dQ_i/dt = -(V_i/\Delta z + \{\lambda\}) Q_i, \quad (71)$$

where V_i is the dry deposition velocity of pollutant i , Δz is the plume thickness, and $\{\lambda\}$ is the washout coefficient of pollutant i which equals λ_i during precipitation and 0 when there is no precipitation.

The solution to equation 71 is:

$$Q_i(t) = Q_i(t_0) \exp(-V_i/\Delta z + (\lambda_i)(t-t_0)). \quad (72)$$

FIGURE 21. LAGRANGIAN COORDINATE SYSTEM



It is assumed that dry deposition continues at the same rate whether or not it is raining. This assumption requires verification; opinions have ranged from no dry deposition during rain¹⁹³ to the same rate as under dry conditions.²⁹² In reality, it is likely that dry deposition continues during precipitation events at an altered rate.

For reactive species, like sulfur dioxide, chemical conversion must be considered along with wet scavenging and dry deposition. A first order

model with rate constant k is assumed for the oxidation reaction.

The coupled differential equations for sulfur dioxide and sulfate resulting from these processes are as follows:

$$dQ_2/dt = - (V_2/\Delta z + \{\lambda_{SO_2}\} + k) Q_2 \quad (73)$$

and

$$dQ_4/dt = k Q_2 - (V_4/\Delta z + \{\lambda_{SO_4}\}) Q_4, \quad (74)$$

where the subscripts 2 and 4 refer to SO_2 and SO_4 , respectively.

Solutions to these equations are:

$$Q_2(t) = Q_2(t_o) \exp [- (V_2/\Delta z + \{\lambda_2\} + k) (t-t_o)] \quad (75)$$

$$Q_4(t) = Q_4(t_o) \exp [- (V_4/\Delta z + \{\lambda_4\}) (t-t_o)] + Q_2(t_o) K \left[\exp [- (V_4/\Delta z + \{\lambda_4\}) (t-t_o)] - \exp [- (V_2/\Delta z + \{\lambda_2\} + k) (t-t_o)] \right], \quad (76)$$

$$\text{where } K = 3/2 k / ((V_2 - V_4)/\Delta z + \{\lambda_2\} - \{\lambda_4\} + k). \quad (77)$$

In order to determine the atmospheric concentrations, X_i , as a function of distance relative to the source, the occurrence of precipitation must also be modeled.

5.3.7.1. Storm model: The losses due to precipitation scavenging en route to the receptor is the segment of the model which required the broadest assumptions. Data on the geographical distribution of precipitation was limited. Hourly observations of precipitation events at four meteorological stations (International Falls, Thunder Bay, Duluth, and Hibbing) were available for northeastern Minnesota. It was assumed that one hour of precipitation occurred for each observation. These data were used to estimate the total daily time of precipitation, $T_p(W)$, for each weather station, W , for each day in the sampling period.

The daily duration of precipitation, $T_p(S-R)$, for each day's trajectory between the source and receptor is the average of $T_p(W)$ from the four weather stations using the inverse distance weights assumed for the wind.

The geometry of the storm is then assumed to be a band which follows the average wind for that trajectory as shown in Figure 22. This localized moving storm is one of three geometries which were visualized for the storm.²¹ The remaining models include a generalized storm which assume the storm occurs at all points from the source to the receptor, and the localized fixed storm which assumes the storm occurs over the receptor only. Compared to the other two models the localized moving storm maximizes the losses due to precipitation scavenging, and therefore minimizes the wet deposition at any given receptor.

The effective source term, $Q_i(t)$, can then be separated into wet and dry terms: $Q_{i\text{wet}}(t)$ for time $T_p(S-R)$ during precipitation and $Q_{i\text{dry}}(t)$ for the rest of the day. $Q_{i\text{wet}}(t)$ is calculated by setting $\{\lambda_i\} = \lambda$ for the entire time of travel from the moment of emission until the parcel reaches the distance $r = ut$ from the source. Likewise, $Q_{i\text{dry}}(t)$ is calculated by setting $\{\lambda_i\} = 0$ for the entire trajectory.

Table 26 gives the resulting expressions for the effective source terms for SO_2 , SO_4 , and metals.

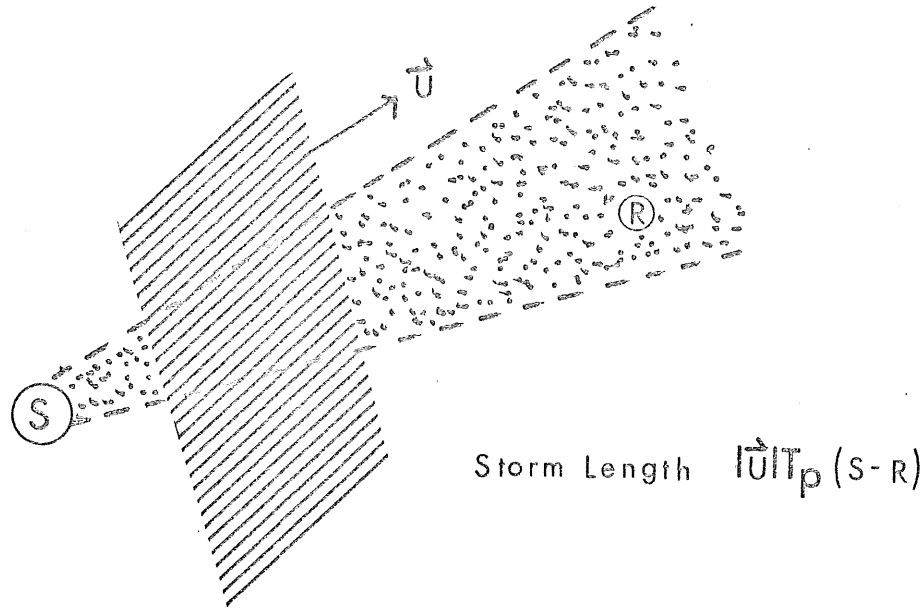
5.3.7.2. Losses: Losses en route are calculated as the average of the losses for each day's wet and dry periods using the length of each wet and dry period as the weighting factor. The daily average for the modified source term is expressed by:

$$Q_i(t) = 1/24(T_p(S-R) Q_{i\text{wet}}(t) + (24-T_p(S-R)) Q_{i\text{dry}}(t)). \quad (78)$$

Table 26. Effective source terms resulting from the localized moving storm model.

Species	Formula for $Q_{i,j}(t)$	$j = \text{dry}$	$j = \text{wet}$
	$Q_2(0) \exp(-K_{2j}t)$	$K_{2,\text{dry}} = V_2/\Delta z + k$	$K_{2,\text{wet}} = V_2/\Delta z + k + \lambda_2$
SO_4	$Q_4(0) \exp(-K_{4j}t) +$ $(3/2 Q_2(0) k/\Delta K_j) \times$ $(\exp(-K_{4j}t) - \exp(-K_{2j}t))$	$K_{4,\text{dry}} = V_4/\Delta z$	$K_{4,\text{wet}} = V_4/\Delta z + \lambda_4$
		$\Delta K_j \equiv K_{2j} - K_{4j}$	
metals	$Q_i(0) \exp(-K_{ij}t)$	$K_{i,\text{dry}} = V_i/\Delta z$	$K_{i,\text{wet}} = V_i/\Delta z + \lambda_i$

FIGURE 22. STORM MODEL



5.3.7.3. Receptor concentration: The total atmospheric concentration at a given receptor can be approximated by the sum of the partial concentrations contributed by each point source (weighted by one-half the inverse source to receptor distance) and the background concentration:

$$X_i(R) = \sum_{s=1}^n X_{iS}(R) + X_{ibkg} \quad (79)$$

where $X_{iS}(R) = Q(x/r) \phi(x,y)/u\Delta z$.

As discussed previously, the background concentration which should not be influenced by point sources is difficult to pinpoint. The background concentration, X_{ibkg} , can be ignored when evaluating the impact of point sources alone, but must be included when total concentrations are required or for model verification.

5.3.7.4. Receptor deposition: The deposition expressions can be derived from the wet and dry fluxes as follows:

$$\text{deposition} = (\text{flux}) (\Delta T) = (V_i + \{\lambda_i\} \Delta z) X_i \Delta T. \quad (80)$$

Table 29. Dry deposition velocity and ambient air background concentrations used as input parameters for the Sudbury Region modified gaussian model validation.

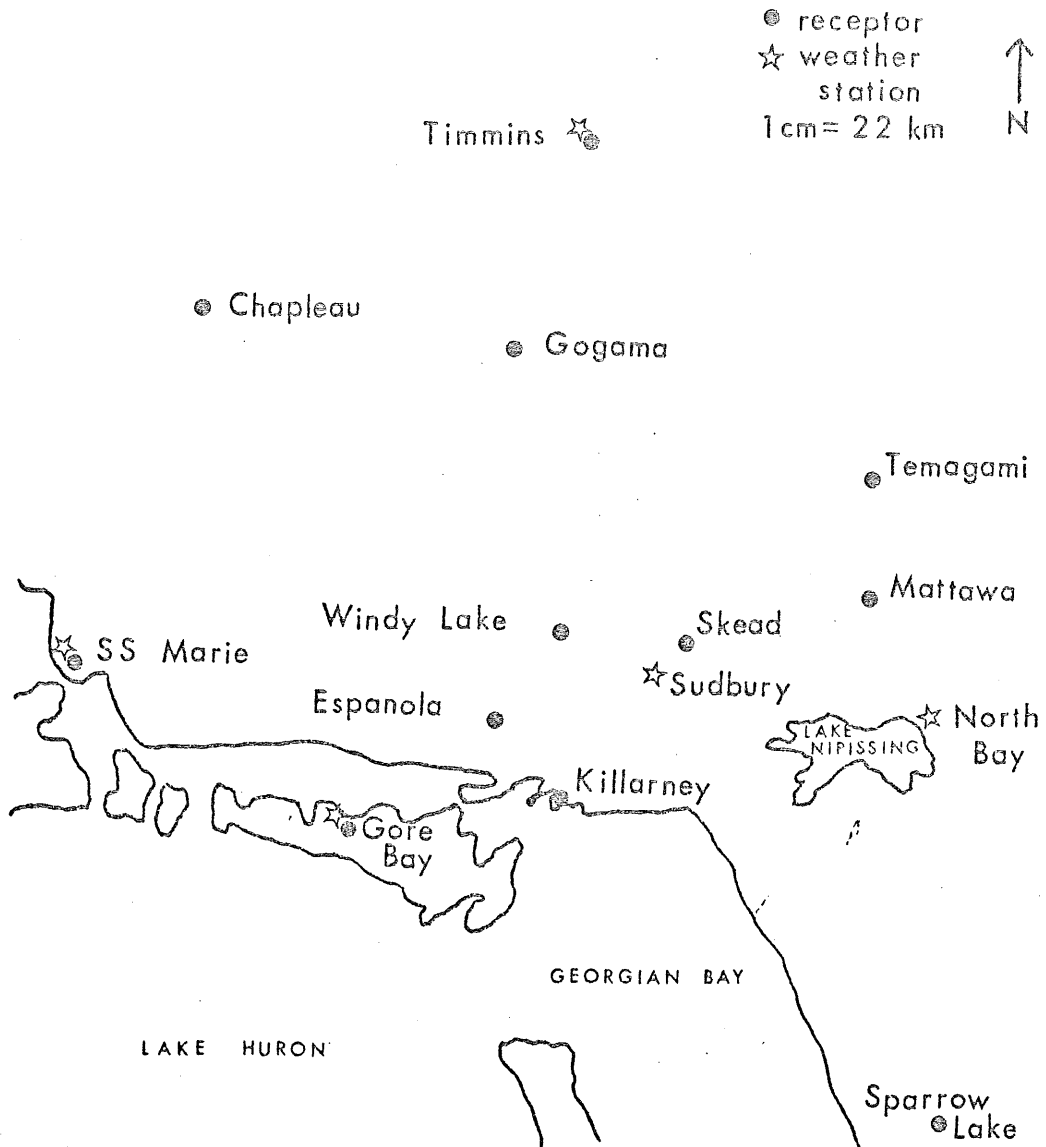
	<u>Dry Deposition Velocity</u> (cm/sec)	<u>Ambient Air Background</u> <u>Concentration ($\mu\text{g}/\text{m}^3$)</u>
SO ₂ rain	0.8 Garland (1977)	3.77×10^{-6} Huhn (1978)
snow	0.2 Whelpdale & Shaw (1974)	
SO ₄	0.1 Garland (1977)	2.00×10^{-6} Huhn (1978)
Cu - run 1	2.0 Cawse (1974)	6.23×10^{-9} Huhn (1978)
Cu - run 2	1.0 ^a	3.00×10^{-9}
Ni	1.4 Cawse (1974)	2.13×10^{-9} Huhn (1978)
Pb	0.3 Cawse (1974)	2.00×10^{-8} Huhn (1978)
Fe	1.1 Cawse (1974)	2.60×10^{-7} (1978)

^aRerun of copper using one-half the original dry deposition velocity and ambient air background concentrations.

Table 30. Sudbury region meteorological stations and coordinates.

<u>Station</u>	<u>Coordinates</u>	
	<u>Longitude</u>	<u>Latitude</u>
SS Marie	84.3333	46.5333
Sudbury Airport	80.8000	46.6162
Timmons	81.3333	48.5000
North Bay Airport	79.4333	46.3333
Gore Bay	82.4667	45.9000

FIGURE 23. SUDBURY RECEPTORS



6.2.2.3. Receptors: During 1973-74 Kramer¹²¹ operated a bulk deposition sampler network of 33 stations. Eleven of the stations (Figure 23) were selected for the model validation based on completeness, representativeness, and location in relation to the sources. Receptor coordinates are given in Table 28.

Table 28. Sudbury Receptor Coordinates

	<u>Longitude</u>	<u>Latitude</u>
Skead	80.7520	46.5830
Killarney	81.4470	45.9990
Windy Lake	81.4660	46.6150
Gore Bay	82.5700	45.8810
Gogama	81.7270	47.6750
SS Marie	84.2500	46.5050
Espanola	81.7680	46.2550
Chapleau	83.4000	47.8333
Timmins	81.3640	48.4770
Sparrow Lake	79.3838	44.7980

Table 29 presents the dry deposition velocity and ambient air background concentrations which were selected as inputs to the model.

A meteorological data tape provided by F. Huhn at McMaster University was used to drive the model. Wind speed, wind direction and precipitation were obtained from five first order weather stations covering approximately 150,000 km² around Sudbury. Table 30 lists the five stations and their coordinates. The location of the meteorological stations in relation to the receptors is shown in Figure 23.

superstack (380 meters) at the Copper Cliff smelter; prior to October 1972, a shorter stack was in use. In addition to the two major sources at Copper Cliff and Falconbridge, a third smelter was operating at Espanola. This source was not included in the analysis because SO₂ and SO₄ emissions from this smelter were low when compared to the other two sources and metals emissions data were not available. Emissions data and other input parameters for the Copper Cliff and Falconbridge smelters are given in Table 27.

Table 27. Sudbury Point Source Emissions Data, 1973-74.

<u>Parameter</u>	<u>Copper Cliff</u>	<u>Falconbridge</u>
longitude	81.0667	80.8333
latitude	46.4667	46.5667
stack height (m)	380	91
heat rate (cal/sec)	1.66 x 10 ⁸	3.65 x 10 ⁷
exit gas flow rate (m ³ /sec)	2832	167.4
exit gas temp (°C)	149	154
SO ₂ (g/sec)	36460	7280
SO ₄ (g/sec)	333.2	-----
TSP (g/sec)	278.8	222.1
Cu (g/sec)	12.04	10.65
Ni (g/sec)	10.10	14.35
Pb (g/sec)	5.90	1.62
Fe (g/sec)	42.2	9.37
Stevens ²⁴⁰		

the Trans-Canada Highway.

The establishment of mines and smelters in the Sudbury Basin which contains one of the world's major deposits of nickel and copper dates back to the late 1880's.

During the 1940's the Sudbury mining and smelting complex contributed about 92% of the free world's nickel.²² Although Canada's production has declined to 43%, nickel mining and smelting operations still contribute \$2.5 billion annually to the Canadian economy.²²

Decades of smelter emissions from the Sudbury complex, Canada's largest single source of sulfur dioxide, have resulted in a landscape so barren that U.S. astronauts trained there for moon walks.²²

During the period 1973-75, the Sudbury smelter emitted about 3.4×10^6 metric tons of sulfur dioxide.²⁴⁰ This figure is about 3% of the total sulfur dioxide emissions in the United States during the same period.²⁶⁶

Emissions from the smelter complex impact the vegetation, soils, and surface waters of the area through precipitation scavenging and dry deposition of stack emissions, surface leaching of ore outcrops and acid runoffs. Some of the environmental effects which have been reported in the Sudbury area include: 1) sulfur dioxide vegetation damage,^{58, 144, 145} 2) elevated sulfate levels in soils,⁹¹ 3) elevated concentrations of metals, particularly copper and nickel, in soils,^{40, 109} 4) increased acidity of lakes,¹³ 5) decreased fish and algal populations in sensitive lakes.^{13, 296} Elevated nickel blood levels have also been observed in Sudbury residents.²⁴⁴

6.2.2.2. Sources: The major point sources in the Sudbury area during 1973-74 were the two large copper smelters at Copper Cliff and Falconbridge.²⁴⁰ This time period includes the operation of the

good results may be due to compensating errors in various sections of the model. Ideally, each of the model units would be verified independently; however, this is usually omitted because of time expense, and logistics.

This section discusses the verification of the modified gaussian model, compares the modified gaussian model to two other models, and presents the results of a sensitivity analysis.

6.2. MODIFIED GAUSSIAN MODEL VERIFICATION

6.2.1. Introduction.

Ideally, the modified gaussian model should be verified using field data collected in the copper-nickel study region making it a site specific model for the region. However, the ambient air quality and deposition data collected in the study region were designed to characterize the region, and were not suitable for model verification. For this reason the modified gaussian model was verified using deposition data for the period 1973-74 collected by Kramer^{121,122,123} in the area surrounding the Sudbury smelter complex. The data collected by Kramer were part of a coordinated air-water study initiated in order to establish the cause-effect relations of increased acidity, emissions and transport of pollutants in Ontario.

A major advantage of the Sudbury data is that materials deposited in the Sudbury region originate mainly from local emissions sources, and are not the result of long-range atmospheric transport from distant sources.¹²¹

6.2.2. Comparison to Sudbury Data.

6.2.2.1. Description of Sudbury Area: The town of Sudbury is located in northern Ontario about 50 miles north of the Georgian Bay, at the apex of a triangle approximately half-way between Toronto and Sault Saint Marie on

flows due to stacks, buildings, highway vehicles and terrain obstacles, 2) flows over surfaces different from those in the basic experiments including water, forests, cities and rough terrain, 3) dispersion in extremely stable and unstable conditions, 4) dispersion at great downwind distances, and 5) buoyant fluid flows including power plant plumes and accidental releases of heavy, toxic gases. The use of models in these situations can result in order of magnitude inaccuracies.

The accuracy of a dispersion model is difficult to determine, and depends on both the ability of the model to simulate the physics of the atmosphere and the accuracy of the input information. Turner²⁵² provides a critical review of atmospheric dispersion modeling and discusses model evaluations and comparisons.

Some specific sources of error and problems in modeling include: the use of a single stability condition to characterize dispersion, treatment of plumes near the mixing height, diurnal variation, wet scavenging, dry deposition, chemical reactions, and the use of ground level meteorological data which are designed primarily for aviation needs. Two significant sources of error in meteorological data are wind speed and direction. These data are taken at ground level and do not simulate conditions at stack height. Wind speed increases with height and wind direction changes with height.

Errors in input data include coding errors, emissions estimates errors, source coordinate errors, and errors in estimating key modeling inputs such as conversion or chemical reaction rates, background concentrations, and other parameters.

Model accuracy is difficult to assess because although a comparison between model predictions and actual measurements may verify a model, the

CHAPTER 6. MODEL VERIFICATION AND SENSITIVITY ANALYSIS

6.1. ACCURACY OF DISPERSION MODELS

Mathematical models are widely used to predict ambient air pollutant concentrations and deposition to the ground. These models which have levels of uncertainties attached to them are also used to determine whether or not air quality regulations will be achieved.

During the 1950's and 1960's experiments were conducted to calculate the dispersion of pollutants at distances less than 1 km from the source for short averaging times of minutes to hours under idealized conditions of uniform terrain and meteorology.^{11, 98, 178} The precision of dispersion models which use experimental data bases such as the Pasquill-Gifford dispersion curves in ideal circumstances (uniform terrain, steady meteorology, carefully measured source and ambient parameters) can be quite good. For example, the observed maximum downwind ground level concentration value should be expected to be within 10-20% of the calculated value for a surface-level source and within 20-40% for an elevated source, such as a tall stack.¹⁷⁸

When dispersion models are applied to "real world" problems an accuracy within a factor of two is frequently estimated for routine modeling applications.¹¹² The American Meteorological Society's Committee on Atmospheric Turbulence and Diffusion³ concluded that this estimate is probably realistic when good field data are available, and meteorological conditions and terrain features are reasonably uniform and homogeneous.

The factor of two estimate may not apply when field conditions are markedly different from the experimental conditions on which the model was based. Some of these exceptional situations include: 1) aerodynamic wake

The numerical model of Ragland¹⁹³ requires 28K for a single non-reacting pollutant and 40K for the SO_2/SO_4 reacting species; computing time was about 9.7 sec for the single species and 20.1 sec for the SO_2/SO_4 species. The computer was a UNIVAC 1110. These data are taken from the simulation of a single source, a single meteorological station using about 6.5% of one year's data, and a box that was 13 x 17 x 6 with $\Delta X, \Delta Y = 9655$ meters, $\Delta Z = 50$ meters for the lower 3 boxes, and $\Delta Z = (ZM-150)/3$ for the upper 3 boxes where ZM is the height of the inversion layer. The time step input is 10 minutes. Concentrations and depositions were calculated.

Data were also provided by the Minnesota Pollution Control Agency¹⁴ on an annual model (CDM) and an hourly model (RAM). CDM required 11,850 sec and 135K on the Cyber 74 in a simulation of one pollutant, 200 point sources, 700 area sources, and 1500 receptors. RAM required 9100 sec and about 50K core on the Cyber 74 in a simulation of 42 point sources, 25 area sources, and 143 receptors. Both models used meteorological data from one station, and both models calculated concentrations.

The deposition for a given period of time, ΔT , depends on the atmospheric concentration, the dry deposition velocity, the precipitation scavenging rate (if it is precipitating), and the thickness of the plume. The deposition at a given receptor can also be separated into the wet and dry contributions from the source:

$$D_i(R) = \sum_{s=1}^n [D_{iSwet}(R) + D_{iSdry}(R)] + D_{ibkg}. \quad (81)$$

Wet deposition at the receptor is calculated by reaveraging the daily time of precipitation, T_p , using the source to receptor distance.

Since the scavenging rate constant (washout coefficient) of SO_2 depends on the total SO_2 concentration, the deposition calculation is made after the SO_2 concentration has been summed over all the sources.

If deposition or concentration periods larger than 24 hr are desired, the program sums the daily results for total deposition and average air concentrations.

5.3.8. Cost.

Direct cost comparisons among various models are difficult because of system variations and internal differences in the models themselves. Because of these limitations several models are compared in terms of the computing time and core requirements.

The modified gaussian model required 365 sec CPU time and 60K core on the Cyber 74 for a regional run (annual and maximum concentrations; annual deposition) which handled 33 receptors, 3 pollutants, 4 meteorological stations, and 25 sources.

The results of the annual regional runs or individual smelter runs (9 pollutants) can be converted to monthly summaries using an average of 100 sec and 155K core.

The first order stations record wind direction (degrees) and wind speed (mph) on an hourly basis, while precipitation is recorded every six hours. Precipitation is also categorized by type as rain, thunderstorm rain, fog/mist, or snow. Rainfall less than 0.01 inches in a 6 hour period is reported as trace.

The hourly weather data were processed in terms of daily averages for the weather tape. Wind direction at due east rather than due north was taken as zero degrees, and wind direction increases counter-clockwise from due east. The vector average wind direction in degrees to the nearest 11.25° and wind velocity in meters per second were calculated. Standard deviations of the wind velocity and wind direction were also computed. Trace rainfall was set to 0.005 inches of rain per day if measureable precipitation did not fall during the remaining 18 hour period. Rainfall duration was reported in hours and did not include trace periods. Rainfall rate in millimeters per hour was computed by dividing daily precipitation in millimeters by rainfall duration in hours.

6.2.2.4. Inputs to the Model: In addition to the sources and receptors the modified gaussian model requires the following input parameters: dry deposition velocity, ambient air background concentrations, meteorological data, and mixing height.

The choice of dry deposition velocity and ambient air background concentrations can be disconcerting. In the case of Sudbury an ample deposition data base existed but ambient air data on a regional basis were scanty. Dry deposition velocities for the Sudbury area were not available. Kramer¹²³ collected a limited amount of median particle size data for iron, nickel, and copper using a 4-stage cascade impactor. Three locations, two in Sudbury and one in Lively, were sampled on three

occasions during January and February, 1975. Kramer estimated particle size ranges of 3.2-5.3 μm for Fe, 1.8-5.9 μm for Ni, 1-3 μm for Cu, and 1-1.2 μm for SO_4 . Kramer's ranges of particle sizes and the data of Cawse³² and other investigators^{81, 294, 223} were used to estimate dry deposition velocities.

Defining the ambient air background concentrations is difficult, particularly since this parameter dominates in those cases where stack emissions are low, or at long distances from the source. For the Sudbury case, the background values are regional background concentrations provided by F. Huhn¹⁰⁸ and D. Balsillie.¹⁰ Although the Ontario Ministry of the Environment does maintain a high volume network around Sudbury, Timmons, and Sault Saint Marie, these samplers are source oriented and are not suitable for the verification.

The meteorological parameters which drive the model are total daily rainfall and duration, rainfall rate, average daily wind velocity and direction, and standard deviation of the wind speed and direction.

The equation for mixing height for the Sudbury Region was derived from the seasonal data of Portelli¹⁸⁷ at Sault Saint Marie.

$$\text{HMIX} = 1,000 + 0.510 \sin ((\text{IM}-3) * 0.524) \quad (82)$$

where HMIX is the mixing height and IM is the month.

Although the superstack at Coppercliff is tall, 380 meters, it is assumed that stack height plus plume rise does not penetrate the monthly mixing heights; that is, the effective stack height (ESH) equals HMIX if $\text{ESH} > \text{HMIX}$. The lowest mixing height used in the Sudbury simulations is 490 meters (in December); the highest is 1510 meters (in June). Actual reported afternoon mixing heights are 423 meters in December and 1088 meters in June.¹⁸⁷

6.2.2.5. Measured deposition: Kramer ¹²¹ measured the deposition rates of sulfate, copper, nickel, lead, iron and other species in central Ontario for the period 1970 to 1976. Kramer determined that the deposition of sulfates, total iron, total nickel, and total copper were highest in the immediate Sudbury area and decreased with distance from the source. A material balance of emitted versus deposited material showed removals of 100% for iron and emitted sulfate, 0.63% for total sulfur, 69% for nickel, and 42% for copper within 3900 km² of Sudbury. The difference in accountability for the emitted materials was thought to reflect deposition rates from the plume in the order Fe>Ni>Cu>>SO₄. Deposition rate contours generally followed an elliptical pattern along the prevailing wind direction (southwest to northeast) during precipitation events.

Deposition data from 5/73 through 12/74 were used to verify the model. Kramer ¹²¹ collected deposition data at monthly intervals using bulk deposition samplers. The samplers were simply 1.2 x 0.3 meter tubes covered with a polyethylene bag for sample collection which had previously been washed with 2N HCl and distilled water. ¹²⁰ The samples were analyzed using an atomic absorption technique for Cu, Ni, Pb and Fe and photometric titration for SO₄. The analytical reproducibility and detection limits for these species are given in Table 31.

Table 31. Analytical reproducibility and detection limits for SO₄, Cu, Ni, Pb and Fe

<u>Element</u>	<u>Reproducibility</u>	<u>Detection Limit</u>
Total SO ₄	± 5 ppm	0.5 ppm
Total Cu	± 5%	1.0 ppb
Total Ni	± 5%	1.0 ppb
Total Pb	± 5%	1.0 ppb
Total Fe	± 5%	1.0 ppb

Kramer¹²⁰

Kramer¹²⁰ found that HNO₃ blanks for copper (15 µg/l) and lead (7 µg/l) were high, but iron (3 µg/l) and nickel (0.6 µg/l) blanks were almost equal to the detection limit. Because of the high blank values for copper and lead, an error of about 100% must be expected when total concentrations of metals fall within the range of the blanks.¹²⁰ High blanks pose a problem only for copper.

Other possible problems with the measured data include sample evaporation, algal growth in rain samples which depletes metals and nutrients, and adsorption of metals to container surfaces. Samples were screened for algal growth and gross contamination before allowing further analysis.

6.2.2.6. Predicted deposition: The modified gaussian model was used to predict the deposition of sulfate, copper, nickel, lead, and iron for the same sampling periods as the reported measured data (5/73 through 12/74).

Summary statistics were computed for the individual sites and for all the sites together for each of the metals and sulfate.

The data were then tested for differences between the measured and calculated values. Differences between the pairs of data ($H_0: U_D = 0$; $H_A: U_D \neq 0$) were tested using the "student's t-test" at the 0.05 level.

Table 32 summarizes the measured and predicted statistics for each element over all the sites. Rain was included in the analysis to determine how good the model estimates the meteorology at the receptors.

Table 32. Summary Statistics, Sudbury Verification.

Species	No obs.	mean		std dev		mean diff.	std error	T value	P value
		meas	pred	meas	pred				
SO ₄	161	3.15	2.89	2.86	1.68	.264	.251	1.05	.296
Cu	165	6.68	16.5	7.59	8.44	-9.80	.782	-12.5	0
Ni	150	4.13	4.56	3.34	3.07	-.434	.236	-1.84	.068
Pb	178	18.7	12.9	15.4	7.14	5.80	1.19	4.87	0
Fe	177	172	180	14.1	6.07	-7.95	14.0	-.57	.572
rain	180	5.21	5.99	2.35	2.13	-.779	.156	-5.00	0
Rerun of copper adjusting dry deposition velocity and background									
Cu	165	6.68	6.67	7.59	3.85	.011	.590	.020	.985

The overall summary shows that at the 0.05 level the null hypothesis is rejected for lead, (P=0), rain (P=0), and copper (P=0) and accepted for sulfate, (P=.296), nickel (P=.068), and iron (P=.572).

The disappointing results for copper are probably due to the high variability in the measured data which can be explained by the high blank values in the analysis; about 75% of the measured values were at the level of the blank. Copper was rerun to get a better fit by adjusting the input values as follows: Dry deposition velocity was reduced from 2cm/sec to 1 cm/sec, and the background was reduced from 6.23×10^{-9} to 3.00×10^{-9} $\mu\text{g}/\text{m}^3$.

These corrections resulted in a near perfect correlation, P=.985, showing that the model can be made to fit the data; however, since the

variability in the measured data is high, it is not meaningful to substitute the revised input parameters for the original "best guess" values.

Although lead blank values were also somewhat high, $7 \mu\text{g}/\text{l}$, the measured values were considerably higher so that high blank values are probably not responsible for all the error. A more likely reason for differences in the measured and calculated values is that lead is emitted by other sources in the area, primarily transportation related sources.

Although the null hypotheses is rejected for rain, the measured vs calculated values look good. About 16% of the pairs had rain volumes that differed by more than $\pm 50\%$. It is likely that if these values were removed from the data set the mean difference would be minimal. However, these pairs were not removed from the analysis because it is not known if the differences were due to spillage, evaporation, or poor collection of the measured data, or to problems in the model.

The model on the whole is underpredicting sulfate and lead and overpredicting iron copper, nickel, lead and rain. The sensitivity analysis shows that the adjustments in background or dry deposition velocity can provide a near perfect fit.

Next, each of the sites were evaluated using the "t-test" to determine if the overall mean differences were largely influenced by one or two sites, or if differences existed between near and far locations. Table 33 summarizes the student "t-test" for each of the receptor locations.

Some of the sampling site differences can be explained. For example, it was discovered that the site at Espanola is located about a block from the pulp and paper plant, and received the impact of local truck traffic which was not included in the emissions inventory. This, of course, could

TABLE 33. Student's T-test for receptor locations, Sudbury validation.

Location	SO ₄				Cu-1(original input data)				Cu-2(revised input data)			
	mean diff	std error	T value	P value	mean diff	std error	T value	P value	mean diff	std error	T value	P value
SS Marie	0.0856	0.405	0.21	0.836	-14.80	2.77	-5.34	0	-3.49	1.12	-3.10	0.008
Windy L.	-2.49	0.677	-3.68	0.003	-15.7	2.55	-6.17	0	-3.98	1.71	-2.32	0.034
Gogama	-1.72	0.433	-2.59	0.025	-12.3	2.89	-4.25	0.001	-1.11	1.37	-0.800	0.438
Chapleau	-0.515	0.540	-0.96	0.358	-8.06	3.70	-2.18	0.048	3.70	3.11	1.19	0.255
Killarney	-0.559	0.392	-1.43	0.174	-9.78	1.90	-5.14	0	-0.631	0.991	-0.640	0.534
Gore Bay	0.125	0.380	0.330	0.748	-6.77	2.28	-2.97	0.013	0.054	1.10	0.050	0.962
Sparrow L.	1.55	0.594	2.61	0.018	-9.38	1.58	-5.93	0	-1.36	0.717	-1.90	0.078
Temagami	0.0088	0.473	0.020	0.985	-6.85	3.69	-1.85	0.083	3.95	3.93	1.00	0.332
Mattawa	0.947	0.910	1.04	0.315	-10.5	1.19	-8.84	0	-1.22	0.620	-1.96	0.066
Espanola	4.54	1.60	2.85	0.013	-6.67	1.65	-4.04	0.001	1.61	0.891	1.60	0.091
Timmons	-0.727	0.430	-1.69	0.125	-5.90	2.79	-2.11	0.054	3.31	1.93	1.72	0.110
all sites	0.264	0.251	1.05	0.296	-9.80	0.782	-12.5	0	0.011	0.590	0.985	0.985

TABLE 33. (continued).

Location	Fe				RaIn				HI				Pb			
	mean diff	std error	T value	P value												
SS Marie	-28.2	28.1	-1.00	0.330	-0.822	0.434	-1.89	0.076	-1.05	0.636	-1.66	0.122	4.69	4.62	1.02	0.325
Windy I.	-89.9	17.1	-5.26	0	-0.995	0.320	-3.11	0.007	-2.03	1.38	-1.47	0.163	0.698	2.07	0.340	0.741
Gogama	-18.1	19.7	-0.920	0.373	-1.01	0.448	-2.26	0.041	-0.634	0.820	-0.770	0.455	1.73	3.13	0.550	0.590
Chapleau	30.9	40.0	0.770	0.454	-1.00	0.540	-1.86	0.086	-1.05	0.473	-2.22	0.049	10.1	5.87	1.73	0.108
Kiljarney	-67.6	19.8	-3.42	0.004	-0.682	0.486	-1.40	0.180	-0.312	0.741	-4.20	0.680	8.63	3.52	2.45	0.026
Gore Bay	-55.3	21.8	-2.54	0.023	-1.39	0.245	-5.67	0	-0.911	0.513	0.180	0.858	0.465	1.82	0.260	0.801
Sparrow I.	-54.2	18.4	-2.95	0.009	-0.0128	0.460	-0.030	0.978	-0.0517	0.534	-0.100	0.925	7.52	3.08	2.44	0.026
Temagami	-37.4	32.6	-1.15	0.270	-1.51	0.592	-0.255	0.021	-1.56	0.754	-2.07	0.057	1.23	1.88	0.650	0.525
Mattawa	-113	14.7	-7.65	0	-1.01	0.564	-1.79	0.091	-0.211	0.650	-0.330	0.750	1.86	2.87	0.650	0.525
Espanola	186	48.5	3.83	0.002	0.943	0.387	-2.44	0.028	2.05	0.569	3.61	0.003	16.3	3.17	5.13	0
Timmons	212	111	1.91	0.007	0.863	0.883	0.980	0.345	-0.051	0.435	-0.120	0.909	12.1	8.13	1.49	0.140
all sites	-7.95	14.0	-0.57	0.572	-0.779	0.156	-5.00	0	-4.34	0.236	-1.84	0.068	5.80	1.19	4.87	0

be a large source of SO₂ and particulates. The measured values are larger than the calculated values for each element except the first run for copper and the variation can probably be explained by the local source impact on the sampler.

The sampler at Windy L. may be subject to a canopy effect in which the vegetation effectively filters pollutants from the air. All measured metals except Pb were less than the calculated values supporting the idea of canopy filtration. Differences between close and distant sources were investigated, but no clear pattern of model performance with respect to distance could be identified.

After the mean differences were calculated by parameter and site, a quantile test was applied to the data to determine confidence bounds (Table 34). At the 95% confidence interval 90% of the calculated values of sulfate, nickel, lead and rain are within 200%, or a factor of two, of the measured values. Iron is slightly higher at 300%. The results for copper, 721% for run 1 with the best guess input parameters compared to 206% for the run with revised input values, shows that the model can be made to fit the data. Because of the high variability in the measured data, copper would not be a good choice, however, for establishing accuracy. The model does seem to handle rainfall with good precision. At the 80th percentile almost all the calculated values are within a factor of two of the measured values at the 95% confidence interval.

The results are not analyzed to separate random and systematic errors because, from the standpoint of model usage, the overall comparison to real data and resulting total error is important.

In summary, at the 95% confidence interval the modified gaussian model has predicted sulfate, nickel, lead, iron and rainfall to within a factor

of two at the 90th percentile. The results for copper stress the need for accurate measurement data for model verification.

Table 34. Summary of precision bounds, Quantile Test.

Statement: X% of the Calculated values will be within Y% of the measured values.

Confidence Interval: The figures given represent the 95% confidence interval on X.

	<u>X: 90th percentile</u>			<u>80th percentile</u>			<u>70th percentile</u>		
	<u>LB</u>	<u>Ave</u>	<u>UB</u>	<u>LB</u>	<u>Ave</u>	<u>UB</u>	<u>LB</u>	<u>Ave</u>	<u>UB</u>
SO ₄	112	156	233	79	93	122	69	73	89
Cu ¹	580	721	1100	393	447	464	252	343	448
Cu ²	153	206	387	88	115	155	66	82	104
Ni	124	168	320	75	99	146	56	68	91
Pb	87	118	201	76	81	89	66	72	77
Fe	224	303	421	127	178	237	88	110	151
Rain	77	93	126	49	61	79	35	44	52

¹Original input parameters, "best guess"

²Revised input parameters

6.2.2.7. Measured ambient air quality: After verifying the model with deposition data, the next step was to use ambient air data. This task was difficult because of the lack of a suitable sampling network. Although the Ontario Ministry of the Environment does maintain high-volume and SO₂ sampling networks in the major cities, the samplers are source-oriented which makes them unsuitable for the analysis outside the Sudbury area.

For this reason the ambient air quality validation is limited to SO₂ data for five sampling stations in the Sudbury airshed. Data for Rayside, Burwash, Penage, Morgan and St. Charles were obtained from the Ontario

Ministry of the Environment for the period January-December 1974.¹⁸⁹

Figure 24 shows the receptors in relation to the sources, and Table 35 gives the source to receptor distances and angular directions of the receptors from east.

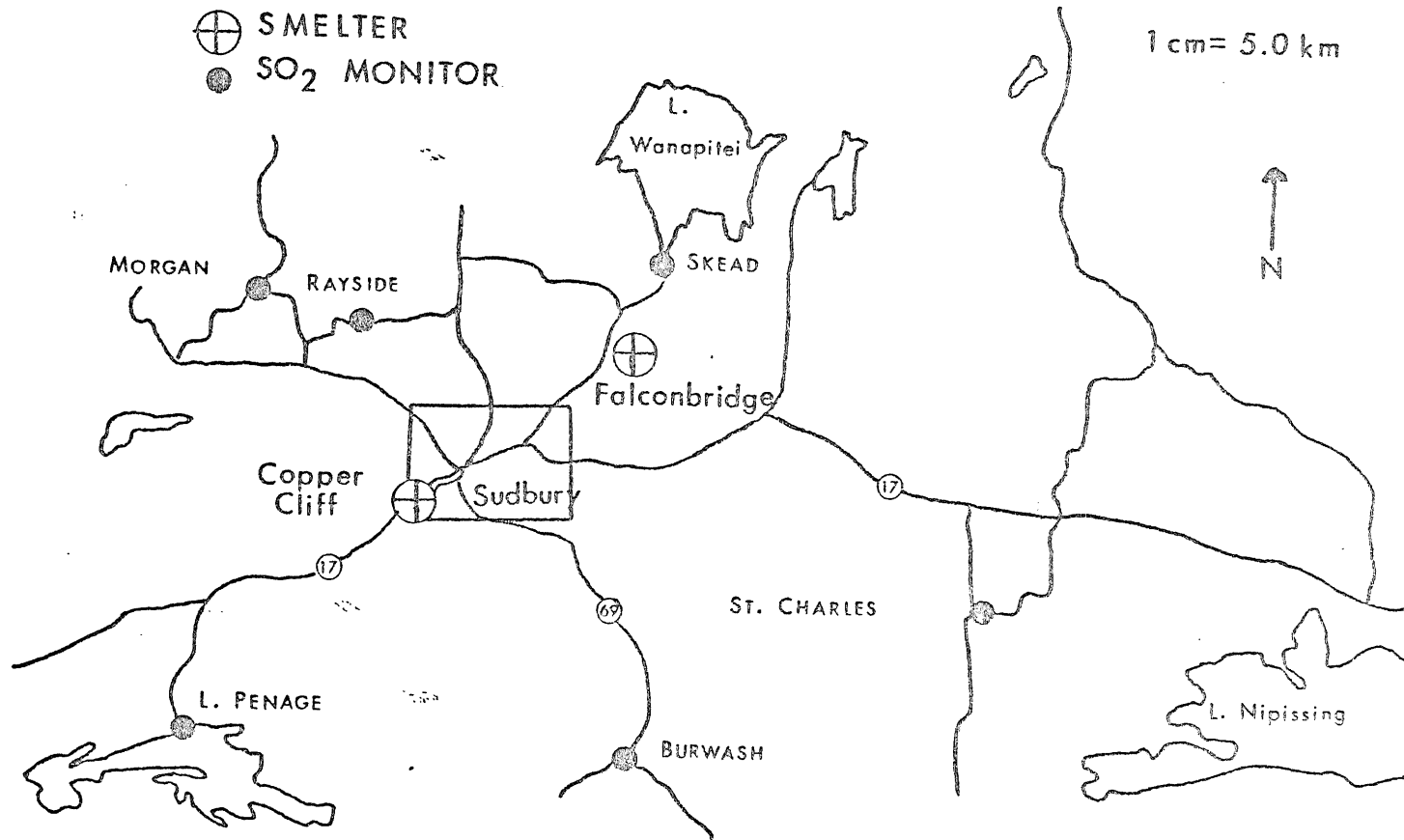
The measured data were collected using Davis conductivity instruments. The monitors were located to avoid interferences in the measuring cell which responds to any species that ionizes in water.¹⁸⁸ The lower detectable limits of SO₂ conductivity instruments (Scientific Industries Model 67) has been reported at 0.01 ppm (26.2 µg/m³) with an overall accuracy of ±5%.²²⁶ One-half the lower detectable limit, 13.1 µg/m³, was substituted for reported zero values.

6.2.2.8. Predicted ambient air quality: The modified gaussian model was used to predict ambient SO₂ concentrations at the five receptors for January-December, 1974.

Table 35. SO₂ receptor-source distances and angular direction of receptors from east

	Distance from Copper Cliff, km	Degrees from east	Distance from Falconbridge, km	Degrees from east
St. Charles	50.4	- 12	38.1	- 34
Rayside	14.4	97	19.9	171
Penage	30.2	-136	50.9	-141
Morgan	22.2	127	31.8	168
Burwash	30.8	- 56	36.7	- 91

FIGURE 24. SUDBURY AREA SO₂ MONITORS AND SMELTERS



Measured and predicted monthly mean and maximum 24 hour SO₂ concentrations along with measured to predicted concentration ratios are given in Table 36. Ratios for the monthly averages range from 0.28 to 3.4 at Penage, 0.30 to 1.1 at St. Charles, 0.31 to 3.1 at Burwash, 0.34 to 2.7 at Morgan, and 0.09 to 1.1 at Rayside. When the monthly concentrations are averaged for the year the ratios are 0.49 at Penage, 0.70 at St. Charles, 0.84 at Burwash, 0.64 at Morgan, and 0.27 at Rayside. The maximum 24 hour concentrations show greater variability with ratios of 0.12 to 5.9 at Penage, 0.06 to 0.64 at St. Charles, 0.12 to 2.6 at Burwash, 0.028 to 0.90 at Morgan, and 0.03 to 0.85 at Rayside. Eighty percent of the highest predicted 24-hour averages are within a factor of 10 of the measured values and about 65% are within a factor of 5 of the measured values. About 95% of the predicted monthly means were within a factor of five of the measured values; about 80% are within a factor of 3, and about 60% are within a factor of 2%.

The greater variability of the 24 hour values is probably due to problems with wind accuracy on individual days. Wind direction data were read only once during each hour at the weather stations rather than being recorded continuously. When these data were transferred to the weather tape the data were recorded as one of 32 compass points (increments of 11.25^o) rather than to the nearest degree. The wind direction data were also measured at ground level rather than at stack height; direction changes with height and could be an important source of error for the Copper Cliff superstack.²⁵² Another important source of error could be the input background concentrations. The overall error in the 24-hour values would be reduced when background concentrations are not included as in the case of evaluating the impact of the sources themselves. Other problems

Table 36. Measured and predicted monthly mean and maximum 24 hr SO₂ concentrations in Sudbury Airshed, µg/m³

Penaze	monthly mean concentration			maximum 24 hr concentration		
	measured	predicted	ratio (M/P)	measured	predicted	ratio (M/P)
Jan	23.6	83.9	0.28	183	836	0.22
Feb	34.1	100	0.34	210	1685	0.12
Mar	13.1*	9.0	1.5	78.6	132	0.60
Apr	28.8	61.4	0.47	262	521	0.50
May	13.1*	16.5	0.79	131	322	0.41
Jun	13.1*	4.27	3.1	78.6	13.2	5.9
Jul	13.1*	3.98	3.3	52.4	10.1	5.2
Aug	13.1*	5.52	2.4	157	277	0.57
Sept	13.1*	3.85	3.4	13.1	6.13	2.1
Oct	13.1*	5.03	2.6	26.2	37.0	0.71
Nov	21.2	72.3	0.29	314	835	0.38
Dec	26.2	95.4	0.27	157	673	0.23
Annual	18.8	38.4	0.49	139	446	0.31

* for monthly mean measured concentration and maximum 24 hr concentration less than LDL; one-half of LDL for SO₂ conductivity instruments substituted for zero values.

St. Charles	monthly mean concentration			maximum 24 hr concentration		
	measured	predicted	ratio (M/P)	measured	predicted	ratio (M/P)
Jan	13.1*	27.5	0.48	78.6	326	0.24
Feb	26.2	35.9	0.73	78.6	420	0.19
Mar	13.1*	15.6	0.84	52.4	203	0.26
Apr	13.1*	43.5	0.30	52.4	871	0.06
May	13.1*	17.4	0.75	52.4	101	0.52
Jun	13.3*	7.22	1.8	26.2	95	0.28
Jul	13.3*	18.3	0.72	52.4	176	0.30
Aug	13.1*	11.4	1.1	78.6	123	0.64
Sept	13.1*	17.5	0.75	78.6	270	0.29
Oct	13.1*	20.8	0.63	52.4	126	0.42
Nov	26.2	29.9	0.88	131	452	0.29
Dec	26.2	34.2	0.77	52.4	397	0.13
Annual	16.4	23.3	0.780	65.5	297	0.22

* for monthly mean concentration and maximum 24 hr concentration less than LDL; one-half LDL for SO₂ conductivity instruments substituted for zero values.

Table 36. (continued)

Rurwash

<u>Month</u>	<u>monthly mean concentration</u>			<u>maximum 24 hr concentration</u>		
	<u>measured</u>	<u>predicted</u>	<u>ratio (M/P)</u>	<u>measured</u>	<u>predicted</u>	<u>ratio (M/P)</u>
Jan						
Feb	131	130	1.0	943	1737	0.54
Mar	26.2	35.9	0.73	157	230	0.68
Apr	26.2	33.4	0.78	78.6	409	0.19
May	26.2	42.8	0.61	78.6	661	0.12
Jun	13.1 ^a	7.61	1.7	26.2	44.6	0.59
Jul	26.2	8.51	3.1	157	60.2	2.6
Aug	26.2	25.1	1.0	78.6	232	0.34
Sept	26.2	84.4	0.31	105	535	0.20
Oct	26.2	26.9	0.97	105	158	0.66
Nov	26.2	15.7	1.7	105	178	0.59
Dec	26.2	41.8	0.63	78.6	411	0.19
Annual	31.7	37.7	0.84	159	388	0.41

^a for monthly mean concentration and maximum 24 hr concentration less than LDL; one-half for LDL for SO₂ conductivity instruments substituted for zero values.

Morgan

<u>Month</u>	<u>monthly mean concentration</u>			<u>maximum 24 hr concentration</u>		
	<u>measured</u>	<u>predicted</u>	<u>ratio (M/P)</u>	<u>measured</u>	<u>predicted</u>	<u>ratio (M/P)</u>
Jan	26.2	40.1	0.65	105	625	0.17
Feb	13.1 ^a	23.3	0.56	52.4	353	0.15
Mar	26.2	12.3	2.1	157	175	0.90
Apr	13.1 ^a	4.86	2.7	26.2	34.2	0.77
May	13.1 ^a	19.1	0.69	210	233	0.90
Jun	13.1 ^a	23.1	0.57	13.1 ^a	298	0.044
Jul	13.1 ^a	7.37	1.8	52.4	115	0.46
Aug	13.1 ^a	15.5	0.85	131	277	0.47
Sept	13.1 ^a	21.9	0.60	26.2	457	0.057
Oct	13.1 ^a	25.0	0.52	13.1 ^a	463	0.028
Nov	26.2	60.4	0.43	78.6	940	0.084
Dec	26.2	73.0	0.34	78.6	1706	0.046
Annual	17.5	27.2	0.64	78.7	468	0.17

^a for monthly mean concentration and maximum 24 hr concentration less than LDL; one-half of LDL for SO₂ conductivity instruments substituted for zero values.

Table 36. (continued)

Month	monthly mean concentration			maximum 24 hr concentration		
	measured	predicted	ratio (M/P)	measured	predicted	ratio (M/P)
Jan	36.7	35.5	1.0	262	310	0.85
Feb	18.3	54.1	0.34	105	509	0.21
Mar	21.0	37.5	0.56	157	528	0.30
Apr	13.1 [#]	12.2	1.1	52.4	113	0.46
May	13.1 [#]	50.5	0.26	52.4	754	0.069
Jun	13.1	32.4	0.40	105	263	0.40
Jul	13.1 [#]	26.8	0.49	52.4	348	0.15
Aug	13.1	56.1	0.23	78.6	613	0.13
Sept	13.1	54.5	0.24	52.4	616	0.085
Oct	13.1	141	0.093	78.6	1087	0.072
Nov	13.1	132	0.10	78.6	2363	0.033
Dec	13.1 [#]	83.7	0.16	52.4	1041	0.050
Annual	16.2	59.7	0.27	93.9	712	0.13

* for monthly mean concentration and maximum 24 hr concentration less than LDL; one-half of LDL for SO₂ conductivity instruments substituted for zero values.

include the instrumentation used to collect the data and the practice of recording zero values for measured data instead of a less than value.

Although the ambient air validation is not conclusive because of the limited data base, it does appear that accuracy bounds on single 24-hour events are larger than for monthly or annual averages. Accuracy for 24-hour events may range from a factor of two to a factor of ten. The model is over-predicting the monthly mean and maximum 24 hour ambient SO₂ concentrations at distances less than 50 km from the sources.

6.2.3. Comparison to other models.

6.2.3.1. Comparison between the Standard Gaussian Model and the Modified Gaussian Model: The model verification was extended to include a comparison to the standard gaussian model which is generally accepted to have accuracies of a factor of two in routine applications.³ The comparison was made using the hypothetical smelter stack emissions and input parameters for the copper-nickel study region. Ambient air background concentrations were not included in the analysis.

Predicted SO₂ concentrations were obtained on 5 selected days at 5 and 10 km downwind from the smelter source using both the standard gaussian model⁶¹ and the modified gaussian model. The ratios of the predicted concentrations (standard gaussian results/modified gaussian results) are shown in Table 37 along with meteorology and the predicted concentrations.

Although the comparison is limited to five days, the results are encouraging. Predicted concentrations from the two models are within about 50% of each other.

6.2.3.2. Comparison between the numerical model and the modified gaussian model: The modified gaussian model was also compared to a model which numerically integrates the species continuity equation (referred to in the

Table 37. Comparison between the standard gaussian model and the modified gaussian model using stack emissions to predict SO_2 concentrations for selected single day runs, $\mu\text{g}/\text{m}^3$.

<u>Date</u>	Distance from source <u>km</u>	<u>Predicted Concentrations</u>		
		<u>Standard Gaussian</u>	<u>Modified Gaussian</u>	<u>Ratio[#]</u>
10/28/76	5	41	35	1.2
	10	22	19	1.2
12/20/76	5	45	56	0.8
	10	33	30	1.1
11/6/76	5	36	61	0.59
	10	22	34	0.65
1/15/77	5	49	57	0.86
	10	32	32	1.0
2/28/77	5	43	38	1.1
	10	34	21	1.6

Meteorology

<u>Date</u>	<u>wind direction</u>	<u>wind speed, km/hr</u>	<u>stability</u>	<u>mixing height, meters</u>
10/28/76	SSW	22.2	neutral	1100
12/20/76	NW	23.4	neutral	650
11/6/76	WNW	24.6	neutral	1100
1/15/77	WNW	19.6	neutral	650
2/28/77	NW	16.9	neutral	1150

remaining text as the numerical model). This complex model includes chemical reaction between two species, horizontal advection, vertical diffusion, and wet and dry removal processes. The numerical model differs from the standard gaussian model in that wind and eddy diffusivity profiles are varied with height, surface roughness, and net heat flux.^{193, 194} The model also assumes that dry deposition does not occur during precipitation events. The model requires the following input parameters: surface wind speed, surface wind direction, net heat flux, surface air temperature, inversion height, precipitation type and amount, chemical reaction rate, dry deposition surface resistance, wet deposition coefficient, and surface roughness. In addition cloud over and cloud ceiling height are required to calculate the net heat flux.

The numerical model was used to calculate the atmospheric impacts of emissions from the proposed 800 MW power plant (now reduced to 400 MW) at Atikokan, Ontario on the Boundary Waters Canoe Area and the Quetico Provincial Park.¹⁹³ A grid size of 6 mi² and a time increment of 10 minutes were used in the model. Sulfur dioxide to sulfate conversion rates of 2%/hour during the day and 0.5%/hour at night were used as input. Table 38 shows the emissions data used in both the modified gaussian model and the numerical model simulations. Meteorological data from International Falls during 1964 was used to drive the numerical model. Only those periods when the wind persisted from the NW to NE (90° sector) for at least six hours were included. These criteria were met 10.3% of the time in 1964 for a total of 49 different periods covering 901 hours. The modified gaussian model used meteorological data for the period 1976-77 from four stations and was run continuously for a one year period.

Although the numerical model was not verified directly in the field, a simplified version of the model which does not include deposition or chemical transformation was used in a seven county region in southeastern Wisconsin. A correlation coefficient of 0.87 was obtained when computer annual average particulate concentrations were compared with data from 25 high-volume samplers. A correlation coefficient of 0.78 was obtained when computed annual SO₂ concentrations were compared with data from 6 monitoring stations. A sensitivity analysis of the numerical model for Atikokan on a single day showed that doubling the eddy diffusivity decreased the SO₂ concentration by 10-15%; doubling the chemical reaction rate, the surface resistance, and the surface roughness resulted in less than a 10% change in concentrations.

Modeling data from the numerical model were available for comparison to the modified gaussian model at 35 km and 80 km due south of the Atikokan plant and are summarized in Table 39.

The comparison between the two models is good and lends support to the modified gaussian model.

Table 38. Atikokan 800 MW power plant emissions used for both the modified gaussian model and numerical model simulations.

Heating value (BTU/lb)	7500
Sulfur content (% weight)	0.8
Ash content (% weight)	12.0
Mercury content (% weight)	2×10^{-5}
Sulfur dioxide emissions (g/sec)	2230
Sulfate emissions (g/sec)	67
Particulate emissions (g/sec)	75
Mercury emissions (g/sec)	0.029
stack height (meters)	198
Heat emissions (cal/sec)	6.04×10^7
Ragland ¹⁹³	

6.2.4. Summary.

The verification of the modified gaussian model against the Sudbury data shows that the model underestimates the deposition of sulfate and lead and overestimates the deposition of copper, nickel, iron, rainfall amount, and ambient air concentrations. Accuracies of a factor of two were calculated for the deposition of sulfate, nickel, lead and iron. The results for copper are not conclusive because of high blank values in the measured data. The verification against ambient SO₂ concentrations indicates the model is not as accurate for single 24 hour events as for monthly or annual averages. When background concentrations were included in the simulation accuracies for 24 hour concentrations ranged from a factor of two to a factor of 10; about 80% of the predicted maximum 24 hour concentrations were within a factor of 10 of the measured values and

Table 39. Comparison between the numerical model and the modified gaussian model for the proposed 800 MW Atikokan power plant.

<u>35 km south of Atikokan</u>			
	<u>numerical model</u>	<u>modified gaussian model</u>	<u>ratio</u>
SO ₄ deposition kg/ha/yr	3.4	2.2	1.5
fly ash deposition g/ha/yr	88	89	~1.0
Hg deposition mg/ha/yr	4	3	1.3
<u>80 km south of Atikokan</u>			
annual SO ₂ conc ug/m ³	0.25	0.30	0.83
annual SO ₄ conc ug/m ³	0.025	0.01	2.5
annual fly ash conc ug/m ³	0.01	.009	1.1
annual Hg conc ug/m ³	4x10 ⁻⁶	4x10 ⁻⁶	1.0
SO ₄ deposition kg/ha/ya	0.90	0.86	~1.0
fly ash deposition g/ha/yr	18	31	0.58
Hg deposition mg/ha/yr	1.6	1.0	1.6

about 65% were within a factor of five. About 95% of the predicted monthly means were within a factor of three and 60% were within a factor of two.

Although the comparison to the standard gaussian model and the numerical model are based on limited data the comparisons are good (generally, $\pm 50\%$) and the results support the modified gaussian model.

6.3. SENSITIVITY ANALYSIS

Sensitivity testing refers to determining the changes in predicted model estimates as a result of changes in the values of input parameters. Sensitivity testing tells the model user which input parameters are the most important in terms of potential modeling errors (assuming the model theory accurately describes the atmospheric processes) and what range of uncertainty is acceptable in the input parameters.

A sensitivity analysis was performed on the primary input and meteorological parameters. The meteorological parameters which were tested are rainfall rate, rainfall duration, wind speed, wind direction, and standard deviation of the wind direction. Other input parameters which were tested are the oxidation rate, dry deposition velocity, washout coefficient and ambient air background concentrations.

Rainfall rate and rainfall duration were varied by $\pm 15\%$ based on a comparison of measured to predicted rainfall. Wind speed, wind direction, and standard deviation of the wind direction were varied by $\pm 20\%$ based on meteorological equipment performance.⁶⁰ Washout coefficients were also varied by $\pm 20\%$. Oxidation rate was varied over two orders of magnitude from 0.02%/hr to 2.0%/hr based on values found in the literature.

Dry deposition velocity was varied over the range reported in the literature. Ambient air background concentrations were also varied over the range of values reported in the literature except in those cases where literature values varied by more than one order of magnitude from the best guess. In these cases the best guess value was varied by $\pm 50\%$.

The predicted values over the high and low ranges were compared to concentrations and depositions calculated at the best guess values.

The sensitivity analysis was performed for a one year period, July, 1973 - July, 1974, at Chapleau, Mattawa, Gore Bay, Timmons, and Skead for both concentrations and depositions.

The results are tabulated as percent variation (relative sensitivity) for rainfall rate, rainfall duration, wind speed, wind direction, standard deviation of the wind direction, and washout coefficient. The results for deposition velocity, ambient air background concentration and oxidation rate are expressed as ratios.

Relative sensitivities were calculated at each of the sites for each of the pollutant species that were varied by $\pm X\%$ from the best guess value.

The relative sensitivity of a parameter is expressed by:

$$S_R = \frac{C_{\text{high}} - C_{\text{low}}}{C}$$

where, S_p is the relative sensitivity of the parameter, C_{high} , C_{low} is the concentration or deposition calculated at the parameter values plus and minus a given percent, and C is the concentration at the median value

6.3.1. Rainfall rate.

Rainfall rates were varied by $\pm 15\%$ based on a comparison of measured to predicted rainfall in the Sudbury comparison. Relative sensitivities were calculated both with and without the best guess ambient background concentrations and are summarized in Table 40.

The ambient air concentrations are relatively insensitive to changes of $\pm 15\%$ in the rainfall rate, and concentrations are less sensitive when ambient air background concentrations are included in the modeling simulations. In general changes of $\pm 15\%$ in the rainfall rate result in ambient air concentration changes of less than $\pm 5\%$.

Not surprisingly, deposition is more sensitive than ambient air concentrations to changes in the rainfall rate. The deposition values are also more sensitive when ambient air background concentrations are included in the simulations.

A $\pm 15\%$ change in the rainfall rate results in an average change in the best guess value of less than $\pm 2\%$ in total sulfate, $\pm 4\%$ in wet sulfate, and $\pm 3\%$ in Cu, Ni, Pb and Fe when the ambient air background concentrations are not included in the simulations.

When the ambient air background concentrations are included in the simulations the average change in the best guess deposition value is less than $\pm 7\%$ for total sulfate, $\pm 10\%$ for wet sulfate, Ni, and Fe, and $\pm 13\%$ for Cu and Pb.

Dry sulfate is not affected by variations in the rainfall rate.

6.3.2. Rainfall duration.

Rainfall duration was also varied by $\pm 15\%$ (Table 41). Both concentration and deposition are more sensitive to changes in rainfall duration than rainfall rate.

Table 40. Sensitivity of ambient air concentrations and depositions to $\pm 15\%$ change in the rainfall rate.

% change in ambient air concentration for $\pm 15\%$ change in rainfall rate²

	SO ₂		SO ₄		Cu		Ni		Pb		Fe	
	no		no		no		no		no		no	
	bkg	bkg	bkg	bkg	bkg	bkg	bkg	bkg	bkg	bkg	bkg	bkg
Gore Bay	0	<1	0	2.4	1.4	3.6	1.7	3.7	0	3.4	0	3.1
Mattawa	<1	<1	0	2.8	1.3	3.2	1.8	3.1	0	2.0	0	1.7
Timmons	<1	1.5	0	0	<1	1.4	<1	1.8	0	2.3	0	2.2
Chapleau	<1	2.1	0	7.1	0	1.6	<1	2.3	<1	5.6	0	6.3
ave	<1	1.1	0	3.1	<1	2.5	1.1	2.7	<1	3.3	0	3.3

% change in deposition for $\pm 15\%$ change in rainfall rate²

	Total ¹ sulfate		Wet sulfate		Cu		Ni		Pb		Fe	
	no		no		no		no		no		no	
	bkg	bkg	bkg	bkg	bkg	bkg	bkg	bkg	bkg	bkg	bkg	bkg
Gore Bay	12	4.3	17	10	21	6.5	13	5.0	24	<1	18	<1
Mattawa	13	1.8	19	6.0	22	<1	17	<1	25	2.0	19	0
Timmons	15	1.8	20	5.0	25	2.6	23	2.7	26	3.7	23	2.6
Chapleau	16	5.3	20	9.4	25	7.4	23	9.5	26	17	21	11
ave	14	3.3	19	7.5	23	4.3	19	4.4	25	5.8	20	3.6

¹dry sulfate is not affected by variation in rainfall rate
²percents are rounded

Table 41. Sensitivity of ambient air concentrations and depositions to $\pm 15\%$ change in the rainfall duration.

% change in ambient air concentration to $\pm 15\%$ change in rainfall duration¹

	SO ₂		SO ₁₁		Cu		Ni		Pb		Fe	
	no bkg	bkg	no bkg	bkg	no bkg	bkg	no bkg	bkg	no bkg	bkg	no bkg	bkg
Gore Bay	0	<1	<1	12	5.0	12	5.3	12	<1	7.0	0	6.4
Mattawa	<1	<1	0	8.3	3.3	7.9	3.4	6.7	<1	4.0	0	3.6
Timmons	<1	1.5	0	12	2.2	10	2.3	9.3	<1	7.6	0	7.3
Chapleau	<1	2.1	<1	21	3.8	30	4.4	29	<1	20	0	20
ave	<1	1.2	<1	13	3.6	15	3.9	14	<1	9.7	0	9.3

% change in deposition to $\pm 15\%$ change in rainfall duration¹

	Total sulfate		wet sulfate		dry sulfate		Cu		Ni		Pb		Fe	
	no bkg	bkg	no bkg	bkg	no bkg	bkg	no bkg	bkg	no bkg	bkg	no bkg	bkg	no bkg	bkg
Gore Bay	17	14	33	60	15	20	24	7.5	15	5.6	27	35	15	
Mattawa	21	5.7	41	60	17	19	32	9.8	23	6.6	34	24	21	7.9
Timmons	18	9.5	30	60	18	15	24	1	20	1	26	24	18	7.7
Chapleau	33	25	34	60	25	25	27	18	22	14	49	34	19	15
ave	22	14	35	60	19	20	27	9.1	24	6.8	34	29	18	12

¹percents are rounded

Gaseous SO_2 is not sensitive to changes in rainfall duration with or without ambient air background concentrations in the simulations. SO_4 and metals concentrations change in on the average by less than $\pm 2\%$ from the best guess when the background is included in the simulations and less than $\pm(5-10)\%$ when the background is not included in the simulations.

The average variation in deposition about the best guess value is less than $\pm 7\%$ for total sulfate, $\pm 30\%$ for wet sulfate, $\pm 10\%$ for dry sulfate, $\pm 5\%$ for Cu, $\pm 4\%$ for Ni, $\pm 15\%$ for Pb and $\pm 6\%$ for Fe when the background is not included. When the background is included the average change in deposition is less than $\pm 12\%$ for total SO_4 , $\pm 18\%$ for wet sulfate, $\pm 10\%$ for dry sulfate, Ni, and Fe, $\pm 14\%$ for Cu, and $\pm 17\%$ for Pb.

6.3.3. Average wind velocity, wind direction and standard deviation of the wind heading.

Average wind velocity, wind direction and standard deviation of the wind heading were each varied by $\pm 20\%$ based on reported performance of meteorological equipment⁶⁰ (Tables 42, 43 and 44). Resulting changes in ambient air concentrations and depositions were generally less than $\pm 10\%$. Although the effect of a $\pm 20\%$ uncertainty in a signal input parameter is not large, the additive effect for all the meteorological parameters could range to $\pm 50\%$.

SO_2 concentration is the most sensitive species, and sensitivity to wind direction decreases with distance.

Deposition is slightly more sensitive than ambient air concentration, reflecting the effect of ambient air background concentration. Mattawa which is the only receptor located to the east of the sources appears to be the most sensitive receptor.

Table 42. Sensitivity of ambient air concentrations and depositions to $\pm 20\%$ changes in the average wind direction.

% change in ambient air concentration to $\pm 20\%$ change in wind direction¹

	SO ₂	SO ₄	Cu	Ni	Pb	Fe
Gore Bay	31	2.0	19	23	2.4	1.1
Mattawa	4.2	0	1.9	1.1	0	0
Timmons	8.5	<1	2.2	2.2	0	0
Chapleau	13	<1	5.5	5.6	<1	0
ave	14	<1	7.1	8.1	<1	<1

% change in deposition to $\pm 20\%$ change in wind direction¹

	Total sulfate	Wet sulfate	Dry sulfate	Cu	Ni	Pb	Fe
Gore Bay	2.7	5.9	21	6.1	1.8	13	7.9
Mattawa	13	11	14	4.9	4.2	6.0	4.2
Timmons	5.4	5.4	7.0	1.6	2.0	1.4	1.1
Chapleau	<1	6.1	3.1	1.8	1.6	1.6	1.2
ave	5.4	7.2	11	3.6	2.4	5.4	3.6

¹percents are rounded

Table 43. Sensitivity of ambient air concentrations and depositions to $\pm 20\%$ change in average wind velocity.

% change in ambient air concentration to $\pm 20\%$ change in wind velocity¹

	SO ₂	SO ₄	Cu	Ni	Pb	Fe
Gore Bay	19	0	6.3	6.0	<1	0
Mattawa	18	1.5	8.2	8.5	1.4	<1
Timmons	3.7	0	0	1.8	0	0
Chapleau	1.8	0	<1	<1	0	0
ave	11	<1	3.7	4.2	<1	<1

% change in deposition to $\pm 20\%$ change in wind velocity¹

	Total sulfate	Wet sulfate	Dry sulfate	Cu	Ni	Pb	Fe
Gore Bay	2.4	4.7	1.6	17	0	<1	0
Mattawa	5.0	4.4	6.0	49	3.2	1.5	1.0
Timmons	1.7	27	3.9	<1	1.2	<1	<1
Chapleau	<1	<1	4.3	6.2	42	<1	<1
ave	2.5	9.2	4.0	18	12	<1	<1

¹percents are rounded

Table 44. Sensitivity of ambient air quality concentrations and depositions to $\pm 20\%$ changes in the standard deviation of the wind direction.

% change in ambient air concentration to $\pm 20\%$ change in standard deviation of wind

	SO ₂	SO ₄	Cu	Ni	Pb	Fe
Gore Bay	<1	<1	12	<1	8.1	0
Mattawa	48	0	<1	1.1	0	0
Timmons	8.5	<1	3.8	4.7	<1	0
Chapleau	2.0	<1	1.5	<1	0	0
ave	15	<1	4.5	1.8	2.0	0

% change in deposition to $\pm 20\%$ change in standard deviation of the wind heading¹

	Total sulfate	Wet sulfate	Dry sulfate	Cu	Ni	Pb	Fe
Gore Bay	<1	<1	1.6	<1	<1	<1	0
Mattawa	3.4	3.2	3.0	0	<1	<1	0
Timmons	3.1	1.5	8.6	3.6	<1	0	0
Chapleau	<1	<1	1.8	<1	<1	0	0
ave	1.9	1.4	3.8	<1	<1	<1	0

¹percents are rounded

Resulting concentration may also be less sensitive to wind speed since it is used to calculate both plume rise and dilution which tend to work against each other. 252

6.3.4. Washout coefficient.

Washout coefficients which are calculated internally in the model were varied by $\pm 20\%$ (Table 45). Although it was not done, it would be informative to also vary the washout ratio input parameters for metals since they are used to calculate the washout coefficient and show variation in the literature.

Ambient air concentrations are relatively insensitive to $\pm 20\%$ changes in the washout ratio (less than $\pm 1\%$ when background is included and less than $\pm 5\%$ when background concentrations are not included). A $\pm 20\%$ change in the washout ratio results in an average change of about $\pm 15\%$ change in Ni, total SO_4 , and Fe, and $\pm 20\%$ change in wet SO_4 , Cu and Pb when the background is included in the simulations. When the background is not included in the simulations a $\pm 20\%$ change in the washout coefficient results in about a $\pm 3\%$ change in total sulfate, Cu, Ni and Fe, and about a $\pm 5\%$ change in wet SO_4 and Pb. Dry sulfate is not affected by changes in the washout ratio.

6.3.5. Deposition velocity.

The deposition velocity was varied over the range of values given in the literature (the range may extend over 1-2 orders of magnitude). Table 46 presents values used in the sensitivity analysis and Table 47 shows the ratio of the predicted values over the value resulting from the input deposition velocity.

Table 45. Sensitivity of ambient air concentrations and depositions to $\pm 20\%$ change in the washout coefficient.

% change in ambient air concentration to $\pm 20\%$ change in washout coefficient¹

	SO ₂		SO ₄		Cu		Ni		Pb		Fe	
	no bkg	bkg	no bkg	bkg	no bkg	bkg	no bkg	bkg	no bkg	bkg	no bkg	bkg
Gore Bay	0	<1	0	7.1	2.0	5.1	2.4	5.3	<1	4.9	0	4.5
Mattawa	<1	<1	0	3.8	1.9	4.6	0	4.0	0	2.9	0	2.8
Timmons	<1	1.5	0	0	<1	2.2	<1	2.6	<1	3.1	0	3.4
Chapleau	1.2	3.0	0	7.1	<1	2.4	<1	3.9	0	8.2	0	8.6
ave	<1	1.5	0	4.5	1.1	2.3	<1	4.0	<1	4.8	0	4.8

% change in deposition to $\pm 20\%$ change in washout coefficient¹

	Total sulfate		wet sulfate		dry sulfate		Cu		Ni		Pb		Fe	
	no bkg	bkg	no bkg	bkg	no bkg	bkg	no bkg	bkg	no bkg	bkg	no bkg	bkg	no bkg	bkg
Gore Bay	24	6.1	35	14	0	0	33	9.6	20	7.2	29	1.3	28	<1
Mattawa	30	2.6	46	8.5	0	0	42	<1	33	<1	47	1.9	36	0
Timmons	27	2.6	35	7.8	0	0	34	4.1	31	3.6	36	5.5	12	3.6
Chapleau	32	7.2	40	13	0	0	39	12	34	14	40	24	33	15
ave	28	4.6	39	11	0	0	37	6.5	30	6.4	38	8.2	27	4.9

¹percents are rounded

Large uncertainties in the deposition velocity do not appreciably affect ambient air concentrations; SO_2 is the most sensitive species. Increasing the deposition velocity from 0.3 cm/sec to 2.6 cm/sec (a factor of about 9) resulted in only a 6% decrease in the SO_2 concentration at Skead and about a 30% decrease at each of the remaining sites. Skead was included in the analysis to determine whether or not sensitivity differences with distance could be demonstrated (Skead is about 45 km from the sources).

Increasing the deposition velocity of Cu from 0.1 cm/sec to 2.0 cm/sec (a factor of 20) resulted in a 4% change at Skead, about 30% at Gore Bay and Mattawa and less than 15% at Timmons and Chapleau. Increasing the deposition velocity of Ni from 0.18 cm/sec to 4.8 cm/sec (a factor of 27) resulted in a 9% change at Skead, 62% at Gore Bay, 15% at Mattawa, 39% at Timmons and 30% at Chapleau. Deposition velocity changes of a factor of 40 for SO_4 , a factor of 8 for Pb, and a factor of 20 for Fe did not appreciably change concentrations.

Deposition is more sensitive than ambient air concentration, and sensitivity decreases with distance from the source. Dry SO_4 deposition is the most sensitive species with change in deposition ranging from a factor of 9 to a factor of 16. Total sulfate deposition changes ranged from a factor of 1 to a factor of 7, wet sulfate, Ni and Fe up to a factor of 3, and Cu and Pb up to a factor of 2.

Table 46. Dry deposition velocity values (cm/sec) for sensitivity analysis

		low	best guess	high
SO ₂	rain	0.3	0.8	2.6
	snow	0.001	0.2	1.6
SO ₄		0.025	0.1	3.0
Cu		0.1	1.0	2.0
Ni		0.18	1.4	4.8
Pb		0.17	0.3	1.4
Fe		0.2	1.1	4.1

6.3.6. Ambient Air Background Concentration.

Ambient air background concentrations used in the sensitivity analysis are given in Table 48 along with ranges of values from the literature. The upper limits in the simulations were set to two times the best guess value while the lower limits were set to the lower limit found in the literature.

Defining the ambient air background concentration can be a problem as seen by the broad ranges from the literature. Background concentrations can be used to calibrate the model, but this means the model is technically valid only for the particular site and data base. Calibration as a method of obtaining good fit is not recommended.²⁵²

Table 49 summarizes the % changes in ambient air concentrations and depositions when the background input concentrations are doubled. The most sensitive species are SO₂, Cu, Ni, total sulfate, wet sulfate, and dry sulfate. If the ambient air background concentration is included in

Table 47. Sensitivity of ambient air concentration and deposition to deposition velocity (V_d).

Ratio of predicted concentration at low deposition velocity to predicted concentration at high deposition velocity.

	SO ₂	SO ₄	Cu	Ni	Pb	Fe
$\frac{\text{low } V_d}{\text{high } V_d} =$	0.12 ^a	0.0083	0.05	0.038	0.12	0.049
Skead	1.07	1.04	1.04	1.09	0.93	1.02
Gore Bay	1.33	1.00	1.30	1.62	0.82	1.02
Mattawa	1.33	1.01	1.28	1.15	1.01	1.01
Timmons	1.31	1.00	1.11	1.39	1.00	1.00
Chapleau	1.31	1.00	1.14	1.30	1.01	1.00
ave	1.27	1.01	1.24	1.31	0.95	1.01

Ratio of predicted deposition at low deposition velocity to predicted concentration at high deposition velocity

	Total sulfate	wet sulfate	dry sulfate	Cu	Ni	Pb	Fe
Skead	6.96	3.19	9.58	1.85	3.39	1.54	2.69
Gore Bay	3.53	1.39	16.6	1.37	1.92	1.48	2.74
Mattawa	3.06	1.23	13.1	1.32	1.91	1.41	2.48
Timmons	1.87	1.06	8.39	1.15	1.42	1.21	1.78
Chapleau	2.10	1.10	13.3	1.16	1.15	1.27	1.99
ave	3.50	1.59	12.2	1.37	2.03	1.38	2.34

^a 0.12 rain; 6.3×10^{-4} snow

the modeling simulations it is an important variable. Uncertainties of $\pm 50\%$ result in variations of 50-100% in ambient air concentrations and depositions. Background concentration is not a factor in assessing the impact of copper-nickel smelting since it is not used in the simulations.

Concentrations and depositions at Skead are less sensitive to doubling the background concentrations than the remaining sites which are further from the sources. Doubling the background concentrations of SO_2 , SO_4 , Cu, Ni, Pb, and Fe results in concentration changes of less than 10% for SO_2 , Cu and Ni at Skead. The average change for the remaining sites is 58% for SO_2 , 95% for SO_4 , 68% for Cu and Ni, and about 100% for Pb and Fe.

Doubling the background concentrations results in changes of less than 15% for total SO_4 , dry SO_4 , and Ni at Skead. Average changes for the four remaining sites about 79% for total SO_4 , wet SO_4 and Ni, 61% for dry SO_4 , 93% for Cu, and about 100% for Pb and Fe.

Table 48. Background concentrations used in the sensitivity analysis compared to the range of values in the literature ($\mu\text{g}/\text{m}^3$)

	low	best guess	high	literature range
SO_2	7.5×10^{-6}	0.1×10^{-6}	3.77×10^{-6}	$(0.1-3.77) \times 10^{-6}$
SO_4	4.0×10^{-6}	1.0×10^{-6}	2.0×10^{-6}	$(1.0-3.62) \times 10^{-6}$
Cu	6.0×10^{-9}	0.625×10^{-9}	3.0×10^{-9}	$(6.25-4.4) \times 10^{-9}$
Ni	4.26×10^{-9}	0.413×10^{-9}	2.13×10^{-9}	$(0.413-5.0) \times 10^{-9}$
Pb	4.0×10^{-8}	1.0×10^{-8}	2.0×10^{-8}	$(0.1-10) \times 10^{-8}$
Fe	5.2×10^{-7}	0.26×10^{-7}	2.6×10^{-7}	$2.6 \times 10^{-8} - 1.33 \times 10^{-4}$

Table 49. Sensitivity of ambient air concentrations and depositions to doubling the ambient air background concentration input.

% change in ambient air concentration to +100% change in ambient air background concentration

	SO ₂	SO ₄	Cu	Ni	Pb	Fe
Skead	5.0	65	5.0	3.0	76	63
Gore Bay	37	99	59	51	95	98
Mattawa	41	98	57	48	96	98
Timmons	66	99	81	77	98	99
Chapleau	89	82	62	100	99	100

average of Gore Bay, Mattawa, Timmons and Chapleau:

58	95	68	69	97	99
----	----	----	----	----	----

% change in deposition to +100% change in ambient air background concentration

	Total sulfate	Wet sulfate	Dry sulfate	Cu	Ni	Pb	Fe
Skead	14	29	5.0	36	6.0	77	83
Gore Bay	69	42	60	85	45	97	99
Mattawa	76	89	56	90	78	99	100
Timmons	84	93	54	97	93	99	100
Chapleau	87	91	75	98	94	110	100

average of Gore Bay, Mattawa, Timmons and Chapleau:

79	79	61	93	78	101	100
----	----	----	----	----	-----	-----

¹ percents are rounded

6.3.7. Oxidation rate.

The oxidation rate was varied from 0.02%/hr to 2.0%/hr based on values reported in the literature. The oxidation rate expression used in the model is a function of plume travel time and results in rates of 2.6%/hr at 0.5 hrs, 1.6%/hr at 1 hr, and 0.006%/hr after 2 hours plume travel time. Table 50 presents the predicted concentrations and depositions at 0.02%/hr, 2.0%/hr and the best guess rate.

Uncertainties in the oxidation rate can be a significant source of error in the model and the sensitivity shows a strong dependence on distance.

When the oxidation rate is varied from 0.02%/hr to 2.0%/hr the ambient air SO₂ concentration decreases by factors of about 3 at Skead and Gore Bay, 2 at Mattawa, and 1.5 at Timmons and Chapleau. Ambient sulfate concentrations increase by factors of 14 at Skead, 3.5 at Gore Bay, 3.2 at Mattawa, 2.2 at Timmons, and 1.6 at Chapleau.

Sulfate deposition is less sensitive to oxidation rate than ambient air concentration, but also shows significant variation at Skead and Gore Bay which are 45 and 143 km, respectively, from the source.

Total SO₄ deposition rates increase by a factor of about 2 at Skead and do not vary by more than $\pm 10\%$ at the remaining sites. Wet SO₄ increases by a factor of about 4 at Skead, 1.3 at Gore Bay, and by less than $\pm 10\%$ at the remaining sites. Dry SO₄ decreases by a factor of 2 at Skead, about 1.5 at Gore Bay, Mattawa and Timmons, and 1.2 at Chapleau.

6.3.8. Summary

The most sensitive inputs to the model are oxidation rate, background concentration, and deposition velocity because of the large variation in these values reported in the literature.

Table 50. Ambient air concentrations and depositions at 2.0/hr and 0.02%/hr oxidation rates compared to the best guess values.

Concentration, $\mu\text{g}/\text{m}^3$

	SO_2			SO_4		
	2.0%/hr	best guess	0.02%/hr	2.0%/hr	best guess	0.02%/hr
Skead	27	73	82	65	3.5	4.7
Gore Bay	3.8	11	11	11	2.0	3.0
Mattawa	3.8	9.5	8.8	9.8	2.0	3.1
Timmons	3.8	5.7	6.0	6.2	2.0	2.8
Chapleau	3.8	6.1	5.7	4.1	2.0	2.5

Deposition, g/ha

	Total sulfate			Wet sulfate		
	2.0%/hr	best guess	0.02%/hr	2.0%/hr	best guess	0.02%/hr
Skead	490	210	320	320	78	81
Gore Bay	42	37	39	33	25	25
Mattawa	39	40	40	30	25	27
Timmons	52	52	58	43	39	45
Chapleau	43	45	46	35	36	37

dry sulfate

	2.0%/hr	best guess	0.02%/hr
Skead	66	130	130
Gore Bay	8.8	12	12
Mattawa	8.9	13	13
Timmons	8.8	13	13
Chapleau	7.6	9.3	8.9

Uncertainties in the oxidation rate (2 orders of magnitude) can result in significant changes in ambient air concentrations of SO_2 and SO_4 (factors of 2 to 4). Deposition is less sensitive but may vary up to a factor of 4 for wet sulfate. Sensitivity decreases with distance from the source.

Ambient air background concentration is difficult to define. Concentrations and depositions were less sensitive close to the source (45 km), and sensitivity increased with distance from the source. A factor of 2 uncertainty results in linear uncertainty in concentration and deposition at about 45-150 km from the source.

Ambient air concentration is relatively insensitive to deposition velocity. Deposition, however, is sensitive, and sensitivity decreased with distance from the sources. The factor of 2 to 3 uncertainty in the background concentration literature values is within and greater than the uncertainty of the model making ambient air background values important if they are used.

In general uncertainties of $\pm(15-20)$ % in the remaining parameters (rainfall rate, rainfall duration, wind speed, wind direction, standard deviation of the wind direction and the washout coefficient do not result in significant uncertainties in ambient air concentrations or depositions. The variation is less than $\pm 20\%$ as shown in Table 51.

Table 51. Sensitivity of ambient air concentrations and depositions to uncertainties in rainfall rate, rainfall duration, wind velocity, wind direction, standard deviation of the wind direction, and the washout coefficient

± % change in concentration due to uncertainty (± x %) in the input parameter

	SO ₂	SO ₄	Cu	Ni	Pb	Fe
rainfall rate(±15)%	<2	2	<2	2	2	2
rainfall duration(±15)%	<2	<10	<10	<10	5	5
wind vel (±20)%	<10	<2	2	2	<2	<2
wind dir (±20)%	<10	<2	<5	<5	<2	<2
SDWH (±20)%	<10	<2	<5	2	<2	0
washout coeff (+20)%	2	<5	<2	2	<5	<5

± % change in deposition due to uncertainty (± x %) in the input parameter

	total sulfate	wet sulfate	dry sulfate	Cu	Ni	Pb	Fe
rainfall rate(±15)%	<10	10	0	<15	10	<15	10
rainfall dur(±15)%	10	30	10	<15	10	15	10
wind vel (±20)%	<2	5	2	<10	<10	<2	<2
wind dir (±20)%	<5	<5	<10	2	<2	<5	2
SDWH (±20)%	<2	<2	<2	<2	<2	<2	0
washout coeff (±20)%	<15	20	0	20	15	20	15

¹ percents are rounded

CHAPTER 7. CHARACTERIZATION OF THE COPPER-NICKEL STUDY REGION

7.1. SULFUR OXIDES

This section characterizes the sulfur dioxide and sulfate ambient air quality of the study region in terms of local emissions sources, pollutant concentrations, and pollutant deposition for the baseline period, 1975-77, and for the projected year, 1985.

Measured ambient air concentrations and deposition data for the baseline period are compared to modeling results to allow general statements to be made about the contributions of local point sources and area sources to ambient air quality. Projections for 1985 are presented to simulate the effects of growth in the region. The data are also evaluated in terms of regulatory constraints to development.

7.1.1. Sources, present and 1985.

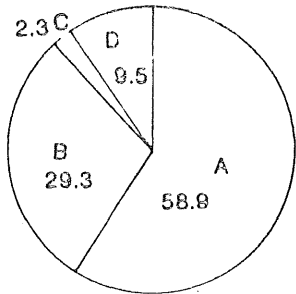
Present and future sources of SO_2 emissions in the air quality study region can be divided for simplicity into area and point sources. It is demonstrated later in this section that the regional ambient SO_2 concentrations can be adequately explained in terms of point sources emitting greater than 100 metric tons per year (mtpy) of SO_2 . Other sources such as small point sources and mobile sources will not be considered.

Table 52 lists the present and projected (1985) SO_2 emissions for the various SO_2 point sources included in the inventory. Figure 25 gives a breakdown of emissions by source categories (power generation, taconite processing, refineries, and commercial-industrial), and by geographic area (Minnesota, Wisconsin, and Canada).

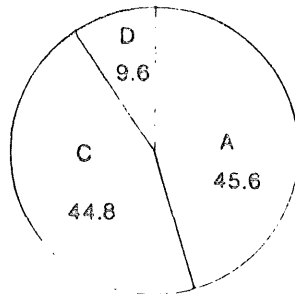
The projected emissions for 1985 are based on proposed source

FIGURE 25

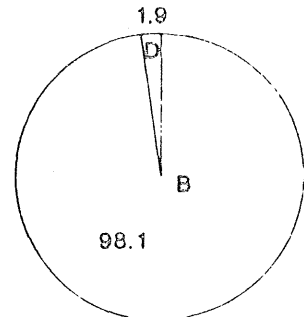
SOURCE CATEGORY CONTRIBUTIONS TO SULFUR DIOXIDE EMISSIONS BY LOCATION



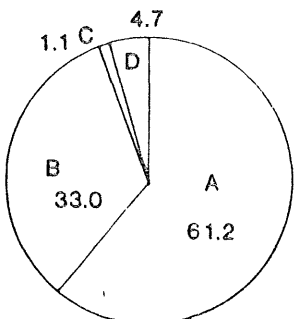
MINNESOTA BASELINE
TOTAL : 68880 MTPY



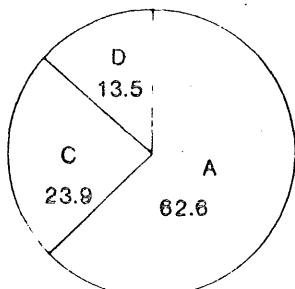
WISCONSIN BASELINE
TOTAL : 4068 MTPY



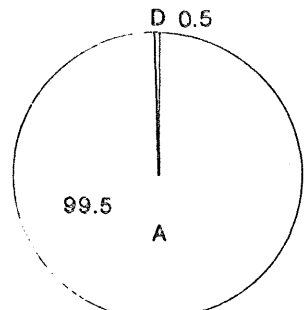
CANADA BASELINE
TOTAL 13880 MTPY



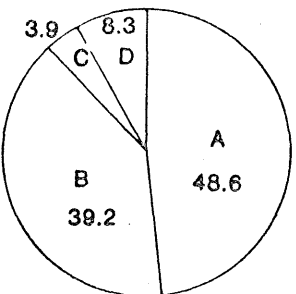
MINNESOTA PROJECTED
TOTAL : 135800 MTPY



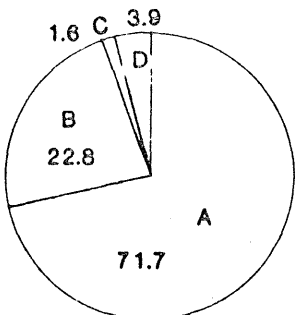
WISCONSIN PROJECTED
TOTAL : 7626 MTPY



CANADA PROJECTED
TOTAL : 53320 MTPY



REGION BASELINE
TOTAL : 84820 MTPY



REGION PROJECTED
TOTAL 196700 MTPY

LEGEND

- A - % POWER GENERATION
- B - % TACONITE PROCESSING
- C - % REFINERIES
- D - % COMMERCIAL / INDUSTRIAL

SOURCE : RITCHIE (1978)

Table 52. Regional SO₂ emissions inventory used for sources emitting more than 100 mtpy of SO₂.

SOURCE FACILITY(3)	BASELINE EMISSIONS 1975-76 (mtpy)	1977 BASELINE (if different from 1975-76 values)(mtpy)	PROJECTED EMISSIONS 1985 (mtpy)
Potlach Northwest	1522		5300
Conwed	104	"90"(1,2)	"90"
Continental Oil	1512		1512
Erie Mining (Taconite Harbor)	15310		15310
MP & L Clay Boswell	28400		45720
Butler Taconite	1		"1545"
National Steel	0		1364
Boise Cascade	838		"818"
Reserve Mining (Silver Bay)	3226		"3182"
MP&L (Sy Laskin)	6095		6095
Reserve Mining (Babbitt)	111		111
Duluth Steam	418		"327"
MP & L Hibbard Station	1555		--
Superwood Corp.	139		139
U.S.S.-Duluth Coke	3468		--
U.S.S.-Shipping	326		0
Eveleth Taconite	0	"2273"(1,2)	"3364"
MP&L (Floodwood or Brookston)	--		"28180"
Jones and Laughlin	--		"1455"
Hibbing Public Utility	1009		1009
Hibbing Taconite	0	1382 (1,2)	2073
Hanna Mining	0		1000
Erie Mining (Hoyt Lskes)	707		"5000"
Minntac	238	2036 (2)	"7364"
Virginia PUD	1896	"1818"(1)	"1818"
Inland Steel	0	636 (2)	"1272"
Pickands Mather	--		"1727"
Lake Superior Power District	1440		"4364"
Roffler's Construction	2		2
Murphy Oil Corp.	1824		1824
Superior WL & P	413		413
Univ. of Wisconsin	105		105
CLM Corp.	284		918
Ontario Hydro (Atikokan)	--		53060
Caland Ore Co.	254		--
Steep Rock Mines	13360		--
Minnesota Pulp & Paper	257		257

NOTE: A missing entry indicates the facility does not exist or will be phased out by the date shown. Tonnages shown in quotation marks indicate estimates by the staff of the Copper-Nickel Study based on available data.

(1) Used in 1977 regional baseline in place of value shown for 1975-76.

(2) Used in 1977 PSD baseline in place of value shown for 1975-76.

changes in the region including expansions in the power generation and taconite industries, additions to pollution control systems, fuel conversions such as the change from gas to coal in the taconite industry, and the closing of some sources.

The definition of baseline emissions changes with application. For example, a baseline of emissions that reflects the actual pollutants emitted in the region as of July 1977 (termed the regional 1977 baseline) is different from the baseline of emissions prescribed by the legal framework of the prevention of significant deterioration amendments to the Clean Air Act of 1970 (refer to section 3.5). Values different from the 1975-76 baseline emissions which have been used for either the regional 1977 or PSD 1977 baseline are also indicated in Table 52.

Point source sulfur dioxide emissions are expected to increase by 130% over the next ten years from 84,820 mtpy in 1975-76 to 196,700 mtpy by 1985. This dramatic rise can be traced directly to proposed growth in the power generation and taconite industries (Figure 25). The taconite companies are planning on a steady expansion which could result in an additional taconite pellet annual processing capacity of 36.3 million metric tons over the 1976-77 capacity of 56.6 million mtpy, requiring 1,300 megawatts of additional electrical power availability in northeastern Minnesota. In addition, taconite companies are converting their operations from natural gas to coal or synthetic gas made from coal. Coal can contain as much as 2,000 times more sulfur than natural gas to supply an equivalent amount of energy, creating increased SO₂ emission possibilities.

If the planned taconite expansions and fuel conversions are implemented in Minnesota, sulfur dioxide emissions from these sources could increase by 25,170 mtpy by 1985 (from 19,600 mtpy to 44,770 mtpy, nearly a 130% increase). This increase is partially offset, however, by the planned closing of two taconite mines near Atikokan, Ontario which will result in a sulfur dioxide emissions decrease of about 13,620 mtpy. On a regional basis sulfur dioxide emissions from the taconite industry are projected to increase 35% by 1985.

The 99,760 mtpy increase (about 240%) in SO₂ emissions from the electric power generation industry will be due primarily to 53,060 mtpy (53%) from the proposed Atikokan generating station (800 MW assumed), 28,180 mtpy (18%) from the proposed generating station at Floodwood, Minnesota, and an increase of 17,320 mtpy (17%) projected for the MP & L Clay Boswell plant at Cohasset, Minnesota. Development plans for the proposed Atikokan plant (800 MW) which will contribute about 27% of the total projected regional SO₂ emissions are being closely monitored because the plant will be located on the edge of the Quetico Provincial Park, a Canadian wilderness area adjacent to the Boundary Waters Canoe Area. If the size of the plant is reduced to 400 MW the emissions would be reduced accordingly.

Refineries and commercial-industrial sources have substantially smaller impacts on regional SO₂ emissions. These categories contribute less than 13% of the total baseline emissions and less than 6% of the total projected emissions (Figure 25).

The SO₂ point source emissions inventory does not include area sources such as residential space heating requirements or line sources

such as automobile traffic which could increase regional emissions. The significance of area source contributions to SO₂ concentrations is discussed in section 7.1.2.

SO₂ emissions in the region can be put into perspective by comparison to global, national, and local emissions. On a global scale natural sulfur emissions, expressed as SO₂, have been estimated to be 258 million mtpy.²⁹⁷ Sulfate aerosols produced by sea spray and hydrogen sulfide (H₂S) from volcanic activity and organic decomposition are the primary sources (66%) of natural sulfur compounds. Anthropogenic sources which may predominate on a local basis, have been estimated at 133 million mtpy, expressed as SO₂, and result primarily from the combustion of fossil fuels.²⁹⁷ About 70% of anthropogenic sulfur emissions are the result of coal combustion.²⁰⁰

On a national scale sulfur dioxide emissions decreased slightly from 1972 to 1975. Anthropogenic emissions in 1972 were estimated to be 33.4 million mtpy compared to 29.9 million mtpy in 1975, a 12% decrease.²⁶⁶ The National Air Quality and Emission Trend report for 1975 states that ambient SO₂ levels in urban areas declined markedly probably due to a combination of more stringent pollution control efforts, and a significant shift in the use of high sulfur fuels from urban to rural sources.²⁶⁶

In Minnesota available data indicate that sulfur dioxide point source emissions decreased slightly from 1970-71 to 1973-74. The 5% decrease (from 316,900 mtpy compared to 302,700 mtpy) is likely to be reversed in the future due to statewide growth in coal consumption.

In 1976 coal consumption by 71 facilities was reported to be

12.0 million mtpy. By 1985, it is projected that 75 facilities will consume 25.8 million mtpy, over a two-fold increase.¹⁵⁰ Most of this increase will occur in the power generation industry.

In 1976 the three largest coal consumption development areas in Minnesota were the seven-county metropolitan area (36% of State total), northeastern Minnesota (30.3% of State total), and central Minnesota (19% of State total). By 1985, these three areas will still be the largest users but their ranking will be shifted: central Minnesota (36% of total), northeastern Minnesota (35% of total), and the metropolitan area (17% of total).¹⁵⁰ The shift in coal usage from the metropolitan area is due primarily to the growth in the taconite and power industries anticipated in central and northeastern Minnesota.

A comparison between the seven-county metropolitan area and northeastern Minnesota's copper-nickel study region is given in Table 53 for point sources emitting more than 100 mtpy SO₂.

Table 53. 1976 point source SO₂ emissions inventory summary by source category for the Air Quality Study Region and the seven-county Metropolitan area.

REGION		POWER GENERATION	TACONITE	REFINERY	COMMERCIAL ^c INDUSTRIAL	TOTAL ^b
Seven- ^a county Metro	mtpy	136800	0	22620	23597	183000
	Percent of Total	74.8	0	12.4	12.9	100
Air Quality Study Region	mtpy	41230	33210	3336	7045	84820
	Percent of Total	48.6	39.2	3.9	8.3	100

^aMinnesota Pollution Control Agency¹⁵³
^bTotal is rounded off.
^cIncludes grain.

7.1.2. Ambient SO₂ concentrations.

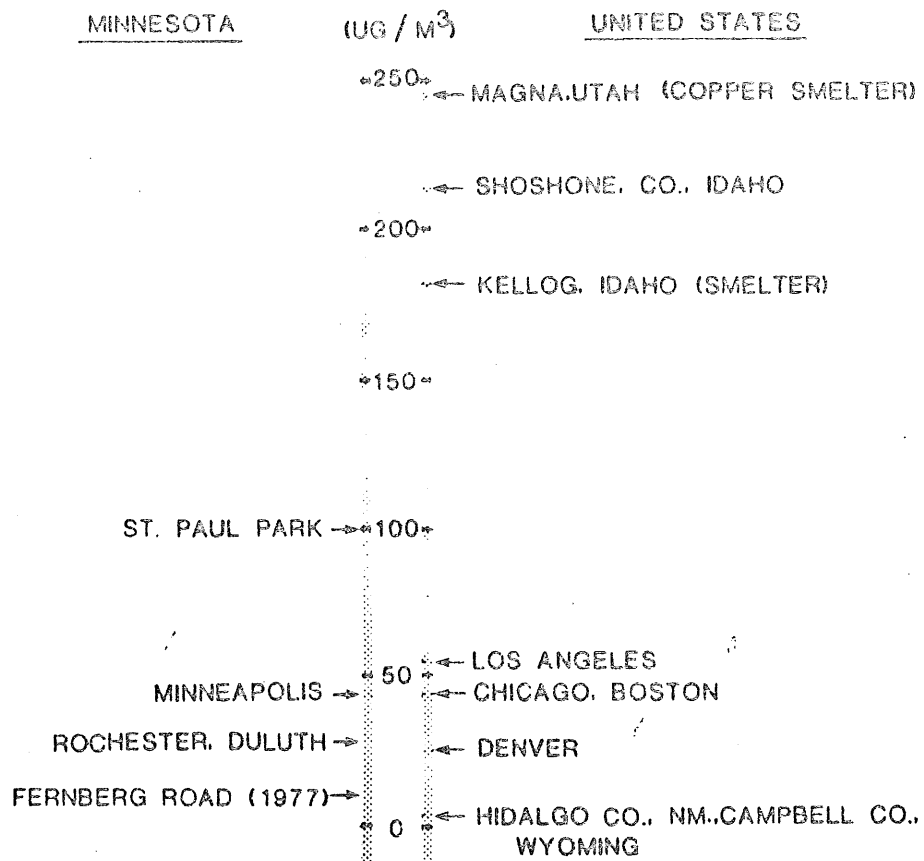
A regional annual average SO₂ background concentration of less than 5.2 µg/m³ (lower detectable limit of the analyzer) was measured at the Fernberg Road site during 1976-77. Since concentrations less than 5.2 µg/m³ could not be detected by the continuous recording monitor, the true value lies somewhere between 0 and 5.2 µg/m³. Although the recorder trace of this monitor remained on zero during the 1976-77 sampling period, a "less than" value is reported for data handling purposes rather than recording zero values. Figure 26 shows the measured ambient concentration at the Fernberg Road site in relation to other parts of Minnesota and the nation.

When the SO₂ concentrations predicted from the regional sources listed in the emissions inventory are calculated using the modified gaussian model and averaged, a regional annual mean of 1.1 µg/m³ (based on 33 receptors) is obtained. Although this number is consistent with a value of less than or equal to 5.2 µg/m³, the real annual average concentration may be underestimated because the modified gaussian model considers only major point sources (those with more than 100 mtpy pollutant emissions). Therefore, it is necessary to consider whether or not a significant part of the region's total emissions may be due to area sources. Area sources are defined as a collection of small unidentifiable stationary points of pollutant emissions, all emitting less than the minimum level of 100 mtpy prescribed for point sources.⁹⁶

The major area sources of SO₂ emissions in the study region would result from heating requirements during the colder months. An estimate of the contribution of area sources to SO₂ emissions was obtained from

FIGURE 26

1975 ANNUAL ARITHMETIC MEAN SO₂ CONCENTRATIONS FOR
SELECTED MEASURING STATIONS IN THE UNITED STATES



SOURCE : U.S.E.P.A. (1977C)

total reported fuel usage. Area fuel usage, as reported by the Minnesota Energy Agency,¹⁵¹ was separated by type of use (industrial, residential, commercial, institutional, and other uses) and type of fuel (natural gas, coal, fuel oil, and liquid propane gas) for the base year 1976. Total emissions by source category and fuel type were then calculated using EPA emission factors.²⁶⁸ Table 54 shows the resulting estimated SO₂ area source emissions based on fuel usage.

Table 54. Estimated SO₂ area source emissions for 1976, based on fuel usage (metric tons).

SECTOR	NATURAL GAS	COAL	FUEL OIL	LPG	TOTAL
Industry	12.7	4.03x10 ⁴	86.1	---	4.04x10 ⁴
Residential	0.778		63.3	0.165	84.2
Commercial/ Institutional/ Other	0.603		23.9		24.5
TOTAL	14.1	4.03x10 ⁴	173	0.165	4.05x10 ⁴

SOURCE: USEPA²⁶⁸ and Minnesota Energy Agency¹⁵¹

The fuel usage estimates indicate that residential, and commercial/institutional/other sectors contribute less than 0.3% of the total SO₂ emissions. The bulk of the emissions come from the industrial sector, and, in fact, from those industries including public and private utilities, which utilize coal as a fuel. About 99.5% of the SO₂ emissions estimated from fuel usage are attributed to industrial use of coal. This use occurs at facilities which are included in the point source emissions inventory. From this discussion it is concluded that area source contributions to regional SO₂ emissions are minimal and that emissions can be adequately characterized, for purposes of

evaluating ambient SO₂ concentrations, in terms of the sources listed in the inventory. Area sources, therefore, are not considered further.

7.1.2.1. Regulatory analysis--annual average SO₂ concentrations: In the regulatory analysis discussions, it should be remembered that the conclusions are based on predicted values at a finite set of receptors. These sections are intended to indicate the general pollutant levels expected, and in this context, to identify which of the legal standards may be in jeopardy.

The modified gaussian model predicts that the federal primary annual standard of 80 µg/m³ will not be exceeded at any of the 33 regional receptors for either the baseline year, 1977, or 1985 within the stated bounds on model accuracy of a factor of two. Figures 27 and 28 show the predicted 1977 baseline and 1985 annual average ambient SO₂ concentrations.

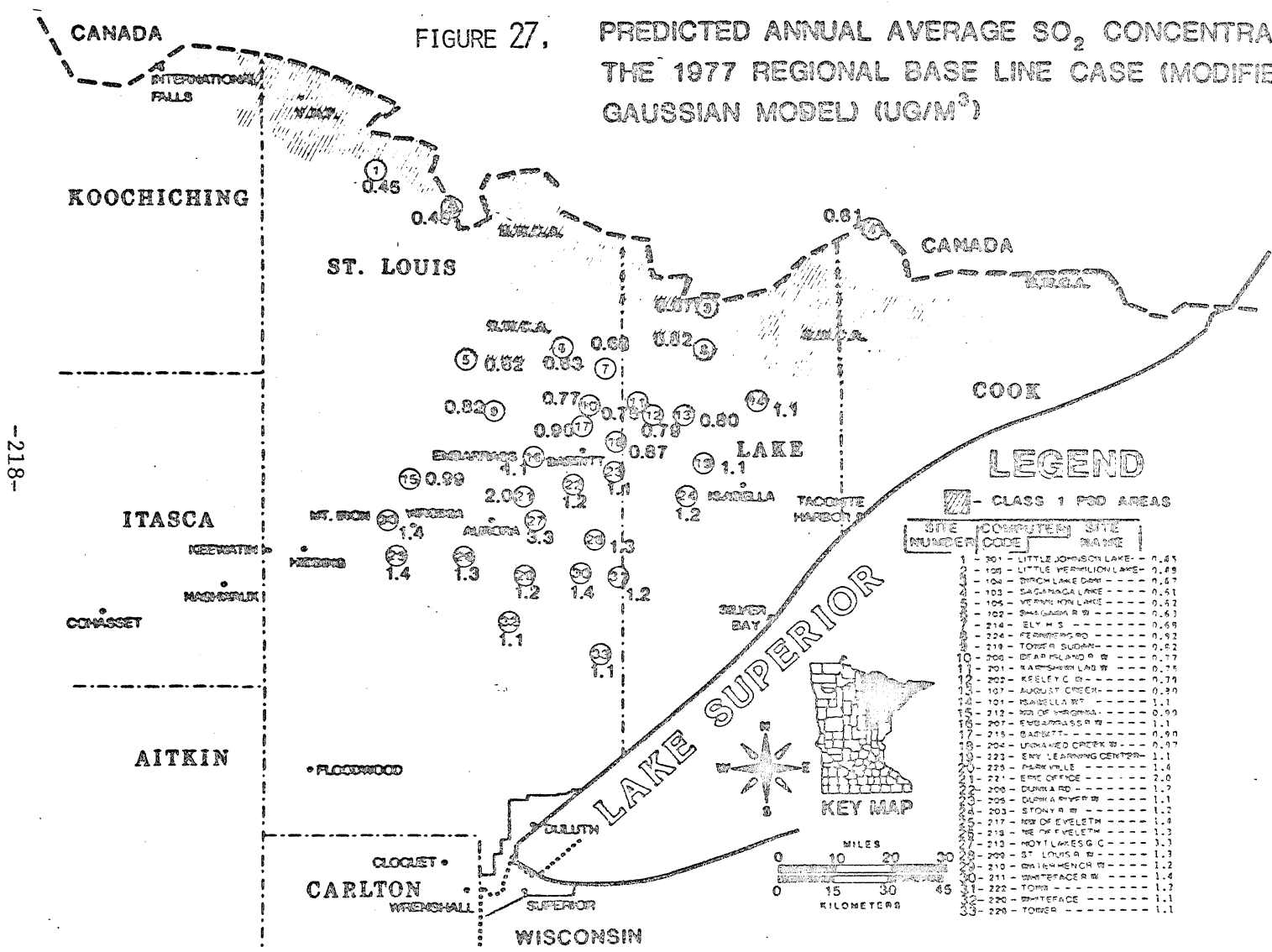
In 1977 a regional mean (defined as the arithmetic mean of the annual average concentrations at the 33 receptors in the region) of 1.1 µg/m³ was calculated. The highest predicted annual SO₂ concentration of 3.3 µg/m³ (4% of the primary standard) occurred at Hoyt Lakes Golf Course (Figure 27). This value primarily reflects SO₂ emissions from the Aurora power plant which is 4 km to the west-southwest.

In general, by 1985, annual SO₂ concentrations are expected to double over the region. Spatial differences are expected to occur, directly following the increases in SO₂ point source emissions.

The modified gaussian model predicts a 1985 regional SO₂ annual average concentration of 2.3 µg/m³, an increase of about 110% over the 1977 regional average. The highest annual average in the region,

ATBCKKAN •

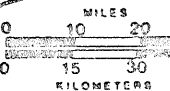
FIGURE 27, PREDICTED ANNUAL AVERAGE SO₂ CONCENTRATION FOR THE 1977 REGIONAL BASE LINE CASE (MODIFIED GAUSSIAN MODEL) (UG/M³)



LEGEND

▨ - CLASS 1 FOD AREAS

SITE NUMBER	COMPUTER CODE	SITE NAME	CONCENTRATION
1	301	LITTLE JOHNSON LAKE	0.45
2	125	LITTLE WERNHOLM LAKE	0.48
3	154	BIRCH LAKE DAM	0.57
4	103	SAGANAGA LAKE	0.51
5	105	VERMILION LAKE	0.52
6	102	DEAR LAKE R W	0.63
7	214	ELY H S	0.65
8	224	FERRELLING RD	0.92
9	219	TOUSE R SUON	0.82
10	206	DEAR ISLAND R W	0.77
11	201	KARTHSHORN LAB W	0.75
12	202	KESLEY C R	0.79
13	107	AUGUST CREEK	0.80
14	101	BLANDELL ST	0.87
15	212	RD OF WERNHOLM	0.90
16	207	ENGELHASS R W	1.1
17	215	SABRETT	1.1
18	204	UNIONED CREEK W	0.97
19	222	ENV LEARNING CENTER	1.1
20	225	PARKVILLE	1.4
21	21	ENV OFFICE	2.0
22	200	DUNKLA RD	1.7
23	205	DUNKLA RIVER W	1.1
24	203	STONY R W	1.2
25	217	RD OF EVELETH	1.4
26	218	RD OF EVELETH	1.3
27	213	HOYT LAKES G C	1.3
28	208	ST LOUIS R W	1.3
29	210	DARK HENCH W	1.2
30	211	WATERFACER W	1.4
31	222	TOWN	1.7
32	220	WHITEFACE	1.1
33	220	TOWER	1.1



-218-

Table 56. Summary of measured sulfur content of atmospheric particulates at eight study area sites, expressed as sulfate.^a

MONITORING SITE	SO ₄ CONCENTRATION (µg/m ³)	
	Average	Standard Deviation
Babbitt	2.1	1.8
Whiteface	2.3	1.7
Hoyt Lakes	1.9	1.7
Erie	1.0	1.4
Dunka Road	2.0	1.6
Fernberg	2.1	1.7
Isabella	2.0	1.8
Toimi	<u>1.4</u>	1.4
AVERAGE ^b	1.9	

SOURCE: Eisenreich, Hollod and Langevin⁵⁸

^aData represents sampling from Dec. 1977 through Oct. 1978. Values have been rounded.

^bArithmetic average of above eight values.

southwest) in the midwest and south, and is not due to local sources.

It is generally agreed that the average residence time of atmospheric sulfur is about 5 days and transport distances may average 1,000 km.⁷⁸

The measured values in Table 56 compare favorably to sulfate values which have been reported in remote midcontinental areas.⁵⁹ It is interesting to compare these concentrations to the values derived from the modified gaussian model using the SO₂ point sources from the regional emissions inventory. Data from studies of the Sudbury plume were used to estimate the rate of conversion of SO₂ to sulfate in the model.¹³⁴ The rate varied from nearly 0%/hr to about 5%/hr depending on the distances from the sources. The resulting regional arithmetic average modeled for 1977 was 5.4 ng/m³. This result, when compared to the

year (with the number of days shown at the top of each bar) each concentration level was predicted. For example, in 1977, a 24-hour SO₂ concentration of less than 5 µg/m³ is predicted 93% of the time (338 days) at Isabella compared to only 84% of the time (305 days) at Hoyt Lakes Golf Course. The frequency plots also demonstrate the predicted shift to higher concentration levels in 1985. Minimum, maximum, arithmetic mean, and standard deviation are also included in the plots.

7.1.3. Ambient sulfate concentrations.

Ambient sulfate concentrations in the study region were determined from membrane samples which were subsequently analyzed by x-ray fluorescence at EPA laboratories, Research Triangle Park, North Carolina.⁵⁹ Samples were analyzed for total sulfur and concentrations were expressed as sulfate. Since SO₂ concentrations were low in the study region it seems likely that most of the sulfur present was actually in the sulfate form. The mean sulfur content of air particulates, expressed as sulfate, at eight sites (both urban and non-urban) was not significantly different (Table 56). This uniformity in urban and non-urban areas is attributed to regional transport and dispersion of sub-micron sized particles into the study region, possibly from distant sources.⁵⁹

Weiss et al.²⁹³ investigated the geographical extent of sulfate aerosol in the midwestern and southern United States and concluded that haze-producing aerosol in the forested Ozark location was not predominately organic, but was dominated by sulfate particles [(NH₄)₂SO₄] which were similar in nature to those observed in the midwest. The authors also determined that sulfate aerosol is distributed over a large geographical region (1000 km from northeast to

ANNUAL FREQUENCY DISTRIBUTION OF PREDICTED 24-HOUR AMBIENT SO₂ CONCENTRATIONS
FOR 1977 AND 1985 AT SELECTED SITES (MODIFIED GAUSSIAN MODEL).

FIGURE 33.

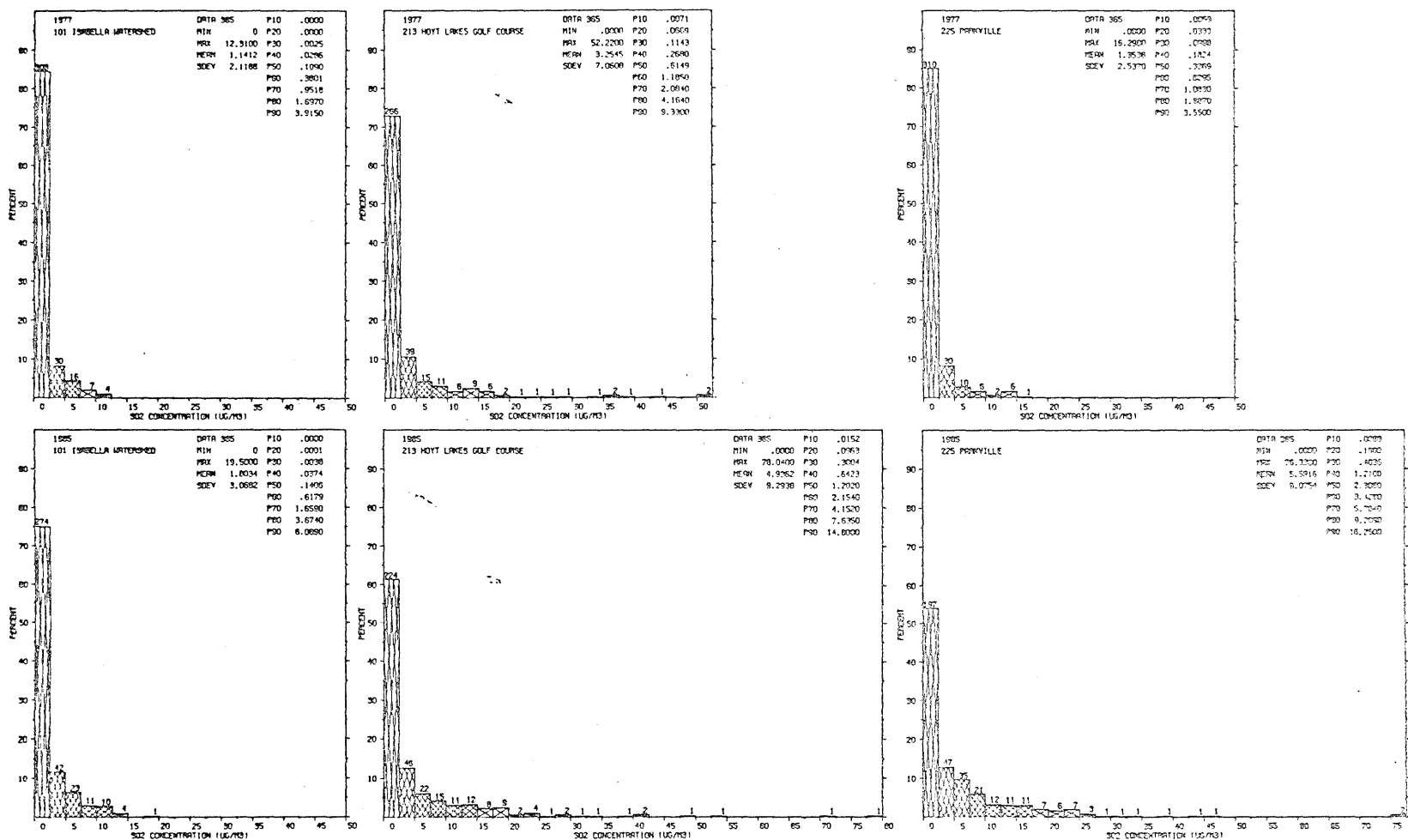
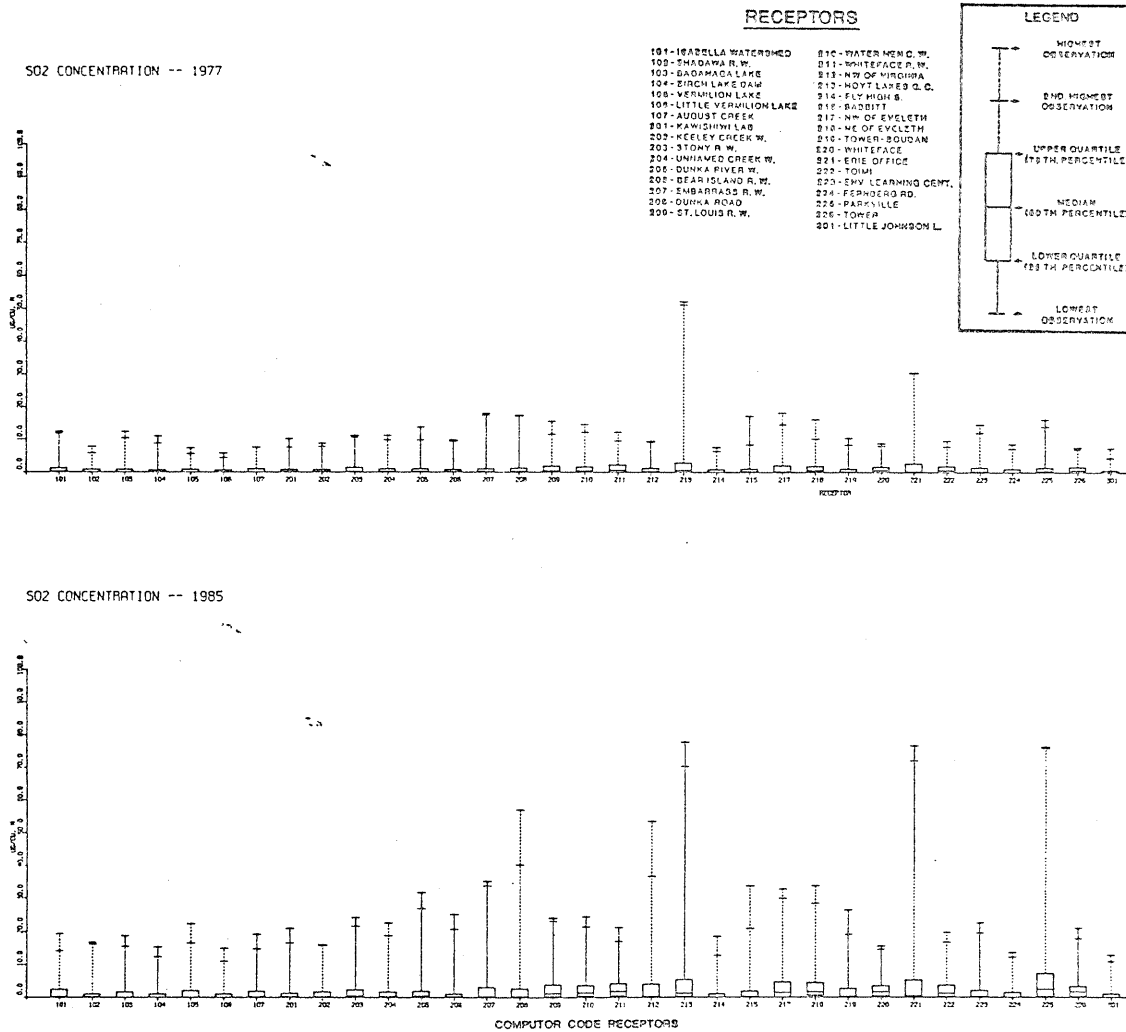


FIGURE 32. BOX PLOTS OF PREDICTED 24-HOUR AMBIENT SO₂ CONCENTRATIONS FOR 1977 AND 1985 FROM LOCAL SOURCES (MODIFIED GAUSSIAN MODEL).



the time. Concentrations in the Class II region would change very little because of the distance, and the low percentage of the time the wind is blowing from the N-NE.

In summary, neither the ambient air quality standards (annual and 24-hour) nor the annual PSD Class I and Class II increments are expected to be exceeded by regional growth in 1985. However, the 24-hour PSD Class I increment is expected to be exceeded in 1985, and there is a small chance that the Class II increment would also be exceeded. Removing the proposed Atikokan power plant (assumed to be 800 MW) from the 1985 simulations results in an annual ambient air concentration decrease of about 4% at Class II area receptors and 15% at the Class I receptors; larger decreases are predicted at individual Class I receptors. Maximum 24-hour concentrations remain the same except at two Class I receptors on the Canadian-Minnesota border.

The box plots in Figure 32 permit easy comparison of all the modeled receptors for SO₂ concentrations in 1977 and 1985. The box plot illustrates the median, quartile, minimum, maximum, and 2nd high values for one year of 24-hour concentrations.

Three sites were selected to show the spatial and temporal variation in concentration levels expected in the study region. The emphasis is on contrasting concentration frequency distributions among a remote site in the eastern corner of the region (Isabella Watershed, site No. 14), an urban site in the center of the region (Hoyt Lakes Golf Course, site No. 27), and an urban site in the western corner of the region (Parkville, site No. 20).

The frequency plots (Figure 33) show the percent of days in the

Table 55. Difference between the baseline concentration and the highest and 2nd highest 24-hour SO₂ concentration in a Class I area (ug/m³).

SITE NO.	COMPUTER CODE	BASELINE	1985		Difference: 1985-baseline	
			Highest	2nd Highest	Highest	2nd Highest
14	101	12	20	14	8	2
6	102	7.8	17	16	9.2	8.2
4	103	12	19	16	7	4
3	104	11	15	12	4	1
5	105	7.4	23	17	15.6	9.6
2	106	5.9	15	11	9.1	5.1
13	107	8.7	19	15	10.3	6.3
1	301	7.3	13	11	5.7	3.7

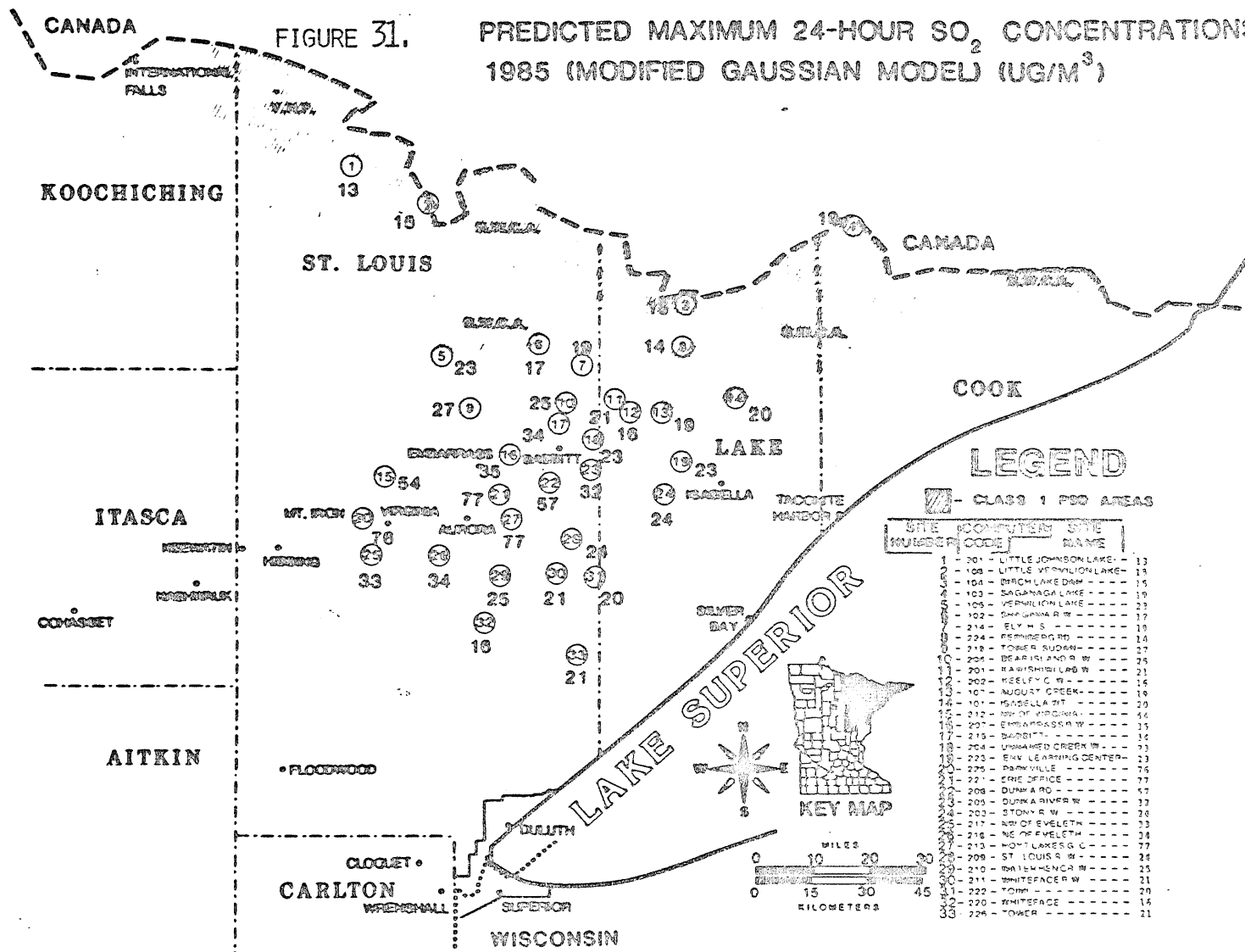
on the frequency and magnitude of the values greater than the increment. In the Class II area the largest 24-hour SO₂ difference was 55 µg/m³ at Parkville (60% of the 91 µg/m³ increment). The second largest difference was about 50% of the increment. Therefore, considering a modeling accuracy of a factor of two it is possible that the Class II increment could be exceeded.

When the proposed Atikokan power plant (800 MW) is removed from the 1985 modeling simulations the maximum 24-hour SO₂ concentration at each receptor is virtually the same throughout the region except at two sites. Predicted concentrations are 20% lower at the Birch Lake Dam site (13 µg/m³ compared to 15 µg/m³) and 32% lower at Saganaga Lake (13 µg/m³ compared to 19 µg/m³). In this case, the 24-hour PSD increment would be exceeded at 3 of 8 Class I receptors, using the second highest value at each receptor, compared to 4 of 8 receptors if Atikokan is included in the inventory. The wind can be expected to blow from Atikokan to the study area (from N-NE to S-SW) only 7.5% of

ATKINSON •

FIGURE 31.

PREDICTED MAXIMUM 24-HOUR SO₂ CONCENTRATIONS FOR 1985 (MODIFIED GAUSSIAN MODEL) (UG/M³)



LEGEND

▨ - CLASS 1 PSD AREAS

SITE NUMBER COMPUTER CODE SITE NAME

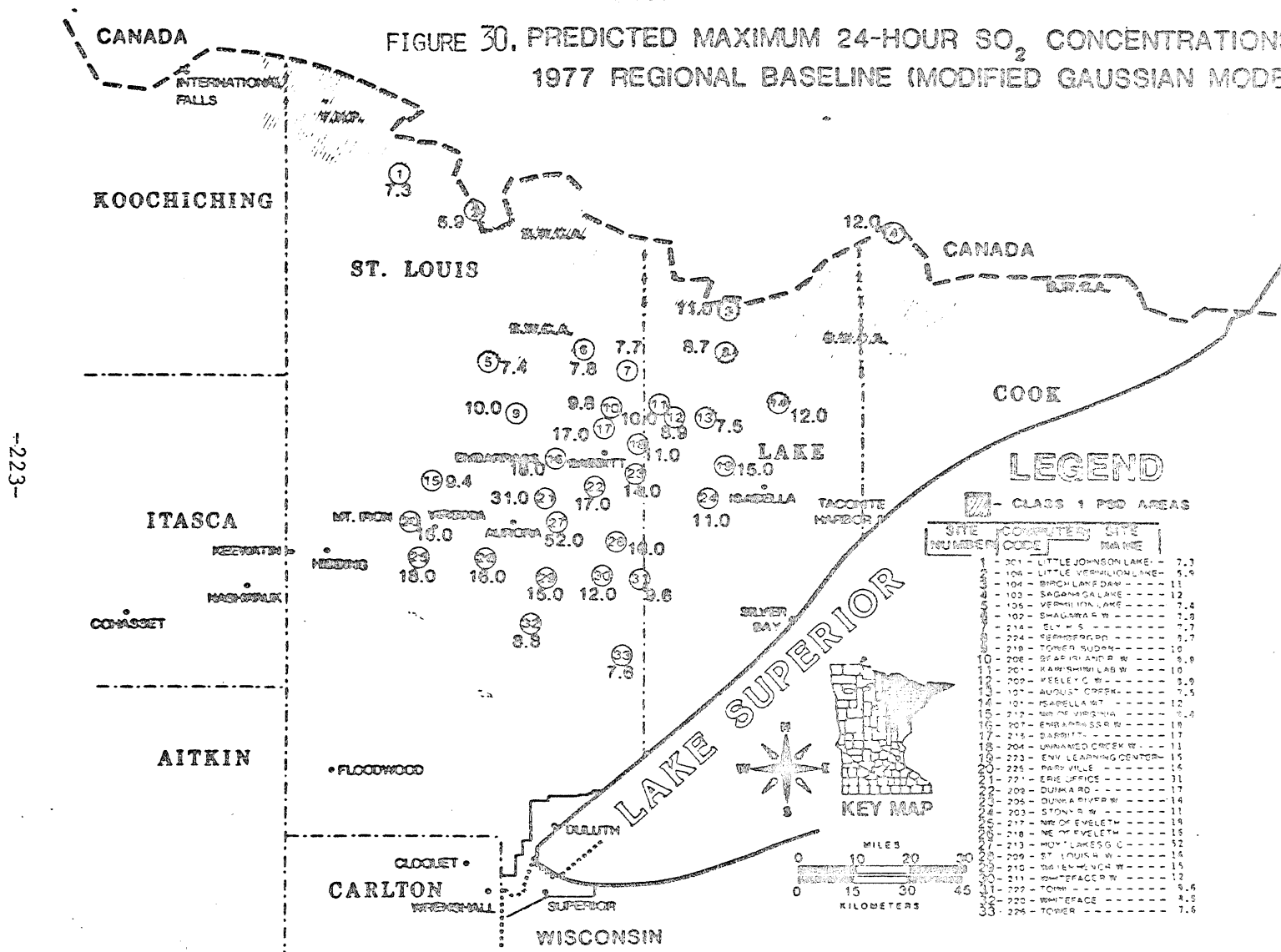
1	201	LITTLE JOHNSON LAKE	13
2	108	LITTLE VERMILION LAKE	18
3	104	BIRCH LAKE DAM	15
4	103	SAGANAWA LAKE	19
5	105	VERMILION LAKE	23
6	102	SHAWANNA R W	17
7	214	ELY H S	10
8	224	PERMISSION RD	14
9	218	FORER SUOMI	27
10	204	BEAR ISLAND W	25
11	201	KAWISHUMI LAKE W	21
12	202	KEELY C W	16
13	10	AUGUST CREEK	18
14	10	ISABELLA 217	20
15	212	TOP OF VERMILION	14
16	207	EMBARRASSA W	15
17	219	BAIDOTT	14
18	204	UNWAKED CREEK W	23
19	222	ENV LEARNING CENTER	23
20	225	PARVILLE	25
21	22	ERIC OFFICE	27
22	208	DUNKA RD	17
23	205	DUNKA RIVER W	17
24	202	STONY R W	26
25	217	RD OF EWELETH	13
26	216	NC OF EWELETH	14
27	213	HOMY LAKES G C	27
28	209	ST LOUIS R W	25
29	210	DALEWENOR W	25
30	211	WHITEFACE W	21
31	222	TOWP	20
32	220	WHITEFACE	14
33	224	TOWER	21



-224-

ATROCKAN •

FIGURE 30. PREDICTED MAXIMUM 24-HOUR SO₂ CONCENTRATIONS FOR 1977 REGIONAL BASELINE (MODIFIED GAUSSIAN MODEL) (UG/M³)



-223-

LEGEND

▣ - CLASS 1 PSD AREAS

SITE NUMBER	COUNTY	SITE NAME	CONCENTRATION (UG/M ³)
1	COOK	LITTLE JOHNSON LAKE	7.3
2	ST. LOUIS	LITTLE VERMILION LAKE	5.0
3	ST. LOUIS	BIRCH LAKE DAM	11
4	ST. LOUIS	SAGAMOGAN LAKE	12
5	ST. LOUIS	VERMILION LAKE	7.4
6	ST. LOUIS	SHAGBEE W	7.9
7	ST. LOUIS	ELM S	7.7
8	ST. LOUIS	REMPER RD	5.7
9	ST. LOUIS	TOWER SUDON	10
10	ST. LOUIS	BEAVER AND R W	5.8
11	ST. LOUIS	KARSHWILL LAB W	10
12	ST. LOUIS	WEELE C W	5.9
13	ST. LOUIS	AUGUST CREEK	7.5
14	ST. LOUIS	ISABELLA RT	12
15	ST. LOUIS	NE OF VIRGINIA	7.8
16	ST. LOUIS	EMERSON ST W	19
17	ST. LOUIS	SASBUTT	11
18	ST. LOUIS	UNWINDO CREEK W	11
19	ST. LOUIS	ENV LEARNING CENTER	15
20	ST. LOUIS	PARDYVILLE	14
21	ST. LOUIS	ERK OFFICE	31
22	ST. LOUIS	DUNBAR RD	17
23	ST. LOUIS	DUNBAR RD W	14
24	ST. LOUIS	STONER W	11
25	ST. LOUIS	NE OF EYELETH	19
26	ST. LOUIS	NE OF EYELETH	15
27	ST. LOUIS	HOYT LAKES S C	15
28	ST. LOUIS	ST LOUIS W	14
29	ST. LOUIS	WILHELM W	15
30	ST. LOUIS	WHITEFACE W	12
31	ST. LOUIS	TOWN	5.6
32	ST. LOUIS	WHITEFACE	4.9
33	ST. LOUIS	TOWER	7.6

to $0.6 \mu\text{g}/\text{m}^3$ for 1985 without the power plant.

7.1.2.2. Regulatory analysis--maximum 24-hour SO_2 concentrations: The modified gaussian model predicts that the federal primary 24-hour standard of $365 \mu\text{g}/\text{m}^3$ will not be exceeded at any of the 33 regional receptors for either the baseline year, 1977, or 1985. Figures 30 and 31 show the predicted 1977 baseline and 1985 maximum 24-hour concentrations at each receptor in the region.

In 1977 the predicted maximum 24-hour SO_2 concentration is $52 \mu\text{g}/\text{m}^3$ (14% of the standard) at the Hoyt Lakes Golf Course; the second highest 24-hour concentration is $31 \mu\text{g}/\text{m}^3$ (8.5% of the standard) at the Erie Mining Office. Both sites are impacted primarily by emissions from Hoyt Lakes and Aurora. By 1985, the maximum 24-hour SO_2 concentration is predicted to increase to $78 \mu\text{g}/\text{m}^3$ (21% of the standard) at the Hoyt Lakes Golf Course, followed by a second high of $77 \mu\text{g}/\text{m}^3$ at the Erie Mining Office.

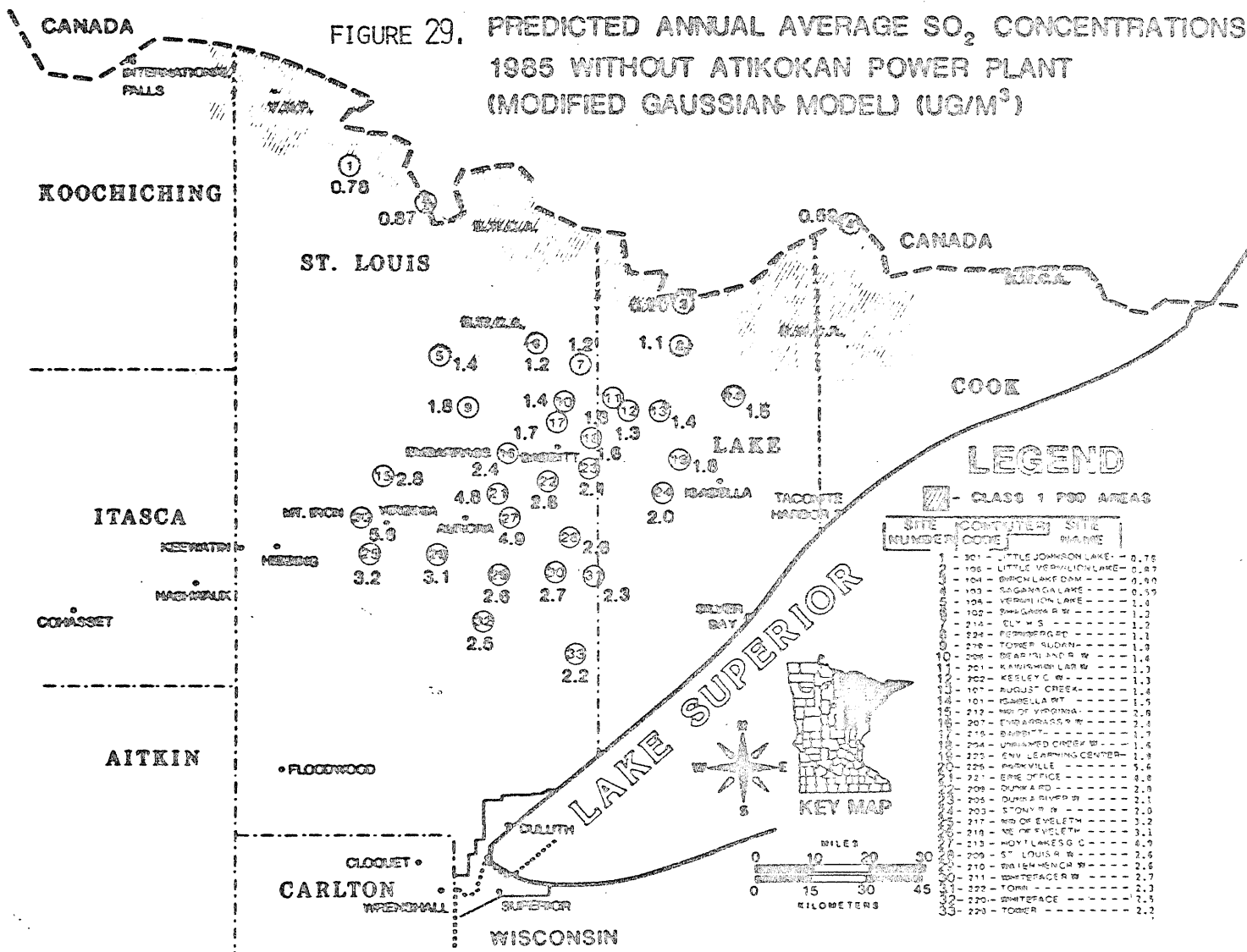
The maximum 24-hour SO_2 increment is expected to be exceeded at some Class I ($5 \mu\text{g}/\text{m}^3$) receptors, and perhaps at one Class II ($91 \mu\text{g}/\text{m}^3$) receptor. Table 55 shows the differences between the baseline and the highest and 2nd highest SO_2 concentrations predicted at Class I receptors.

When the highest value at each site is used for the evaluation, the PSD increment is exceeded at 7 of 8 receptors; when the 2nd highest value is used, this number drops to 4 of 8 receptors.

Although from a regulatory standpoint the increment is exceeded in a Class I or Class II area when the 2nd highest value is larger than the allowed increment at any receptor,²⁷¹ the results of using both the high and the second high values are included to provide a perspective

ATIKOKAN

FIGURE 29. PREDICTED ANNUAL AVERAGE SO₂ CONCENTRATIONS FOR 1985 WITHOUT ATIKOKAN POWER PLANT (MODIFIED GAUSSIAN MODEL) (UG/M³)



LEGEND

▨ - CLASS 1 FOOD AREAS

SITE NUMBER	COMPUTER CODE	SITE NAME
1	301	LITTLE JOHNSON LAKE - 0.75
2	100	LITTLE VERBONIA LAKE - 0.87
3	104	BIRCH LAKE DAM - 0.80
4	103	SAGANOG LAKE - 0.50
5	104	VERBONIA LAKE - 1.0
6	102	TRADITION W - 1.2
7	214	CLY W S - 1.2
8	224	RENNERBERG - 1.1
9	218	TORPEL SUDAN - 1.0
10	204	BEAR H AND R W - 1.4
11	201	KANAWHAW LAKE W - 1.3
12	202	KEELEY W - 1.3
13	101	AUGUST CREEK - 1.4
14	101	ISABELLA MT - 1.5
15	212	RD OF VIRGINIA - 2.6
16	207	ENDARRASS W - 2.1
17	216	BARRETT - 1.7
18	204	UNNAMED CREEK W - 1.4
19	223	ENV LEARNING CENTER - 1.8
20	224	PARKVILLE - 5.4
21	221	EMR OFFICE - 8.8
22	208	DUNN RD - 2.8
23	205	DUNKS RIVER W - 2.0
24	203	STONY R W - 2.0
25	217	RD OF EVELTH - 3.2
26	218	RD OF EVELTH - 3.1
27	213	HOYT LAKE S C - 4.9
28	209	ST LOUIS R W - 2.6
29	210	BLENHING R W - 2.6
30	211	WHITFACER W - 2.7
31	222	TOMR - 2.3
32	220	WHITFACE - 7.5
33	220	TOMR - 2.2

-221-

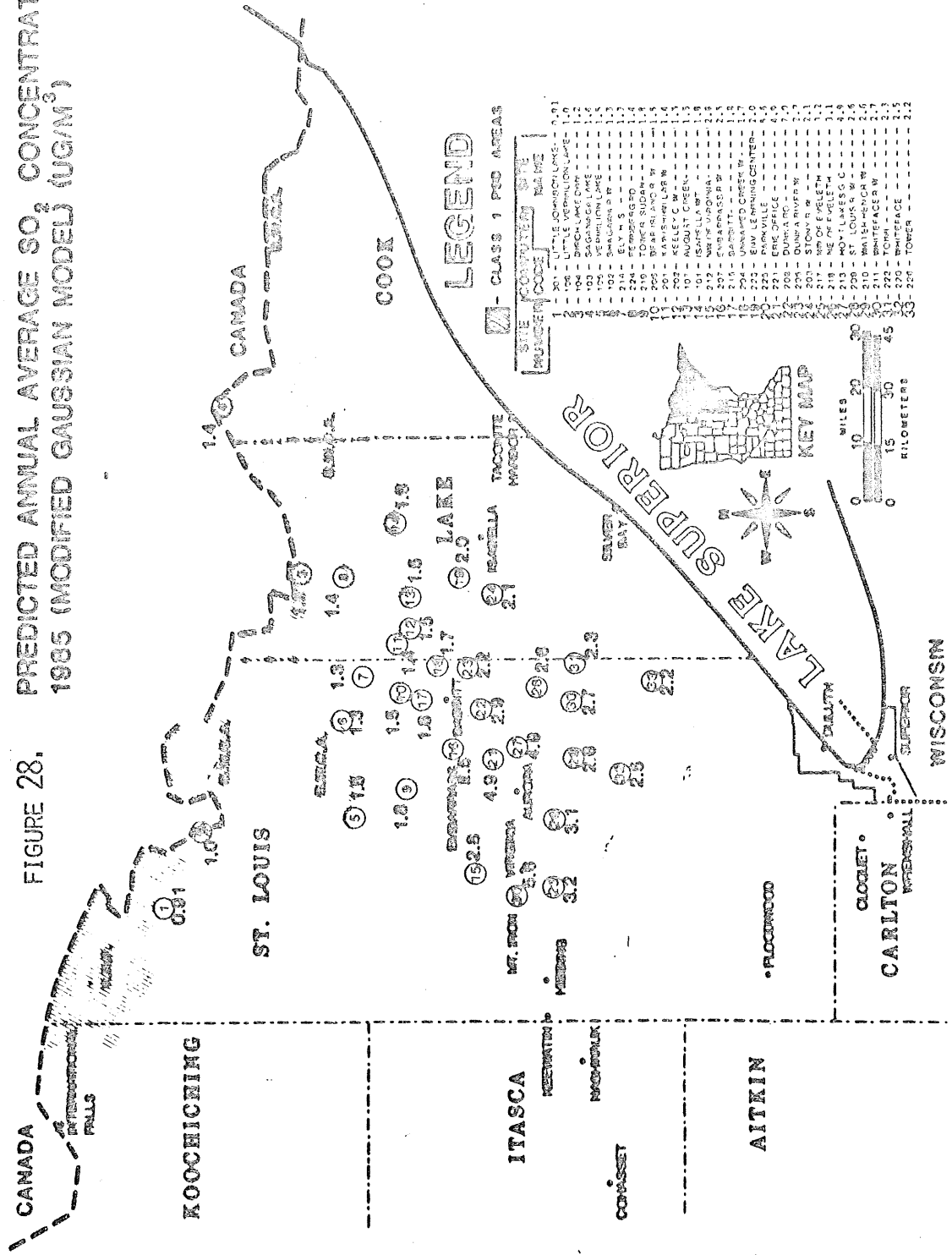
5.6 $\mu\text{g}/\text{m}^3$, which is 7% of the primary standard, is predicted at Parkville. This receptor is impacted primarily by the Duluth sources to the south, Mt. Iron, Eveleth, and the complex of towns to the southwest (Figure 28).

Neither the Class I ($2 \mu\text{g}/\text{m}^3$) nor the Class II ($20 \mu\text{g}/\text{m}^3$) annual PSD increments are expected to be exceeded in 1985 with the regional growth estimated in the emissions inventory. The largest annual SO_2 difference in a Class I area was $0.81 \mu\text{g}/\text{m}^3$ (41% of the increment) at Vermillion Lake. In the Class II area the largest difference was $3.4 \mu\text{g}/\text{m}^3$ (16% of the increment) at Parkville. The proposed Atikokan power plant is expected to contribute about 27% of the region's 1985 SO_2 emissions (assuming 800 MW capacity). This facility could be legally excluded from PSD review under a variance pertaining to sources located outside of the United States [USEPA;²⁷¹ 40 CFR 52.21 (f)(1)(iv)]. Therefore, an assessment of the effect of the proposed facility on the regional receptors, particularly the BWCA sites, is important.

Figure 29 shows the results of annual SO_2 concentration simulations excluding Atikokan from the 1985 emissions inventory. Removing the proposed Atikokan power plant from the modeling simulations results in about a 9% decrease in the 1985 mean regional mean annual SO_2 concentration, but larger reductions occur in the Class I area (about a 15% decrease). The decrease in the Class II area is only about 4%.

The largest predicted effect of the proposed power plant occurred at Saganaga Lake on the Minnesota-Canadian border. An increase in the annual ambient SO_2 concentration of about 2.5 times is expected from an 800 MW facility, $1.4 \mu\text{g}/\text{m}^3$ for 1985 with the power plant compared

ATTACHMENT •
FIGURE 28. PREDICTED ANNUAL AVERAGE SO₂ CONCENTRATIONS FOR 1985 (MODIFIED GAUSSIAN MODEL) (UG/M³)



average of the measured values shown in Table 56 ($1.9 \mu\text{g}/\text{m}^3$) clearly suggests that major point sources in the region are not primary contributors to ambient sulfate levels in the study region. This is in contrast to the situation with ambient SO_2 . It appears that nearly all of the measured ambient sulfate levels (estimated at more than 99%) are the result of transport from outside the study region.

The modified gaussian model predicts that by 1985 the ambient sulfate concentration due to point sources in the region will increase to $84 \text{ ng}/\text{m}^3$, an increase of roughly a factor of 15 over the modeled 1977 value. Maximum 24 hr concentrations of $1.2 \mu\text{g}/\text{m}^3$ are predicted at the Hoyt Lakes Golf Course for both 1977 and 1985. The question of possible increases in sulfate transport into the region from remote sources is discussed in the next section.

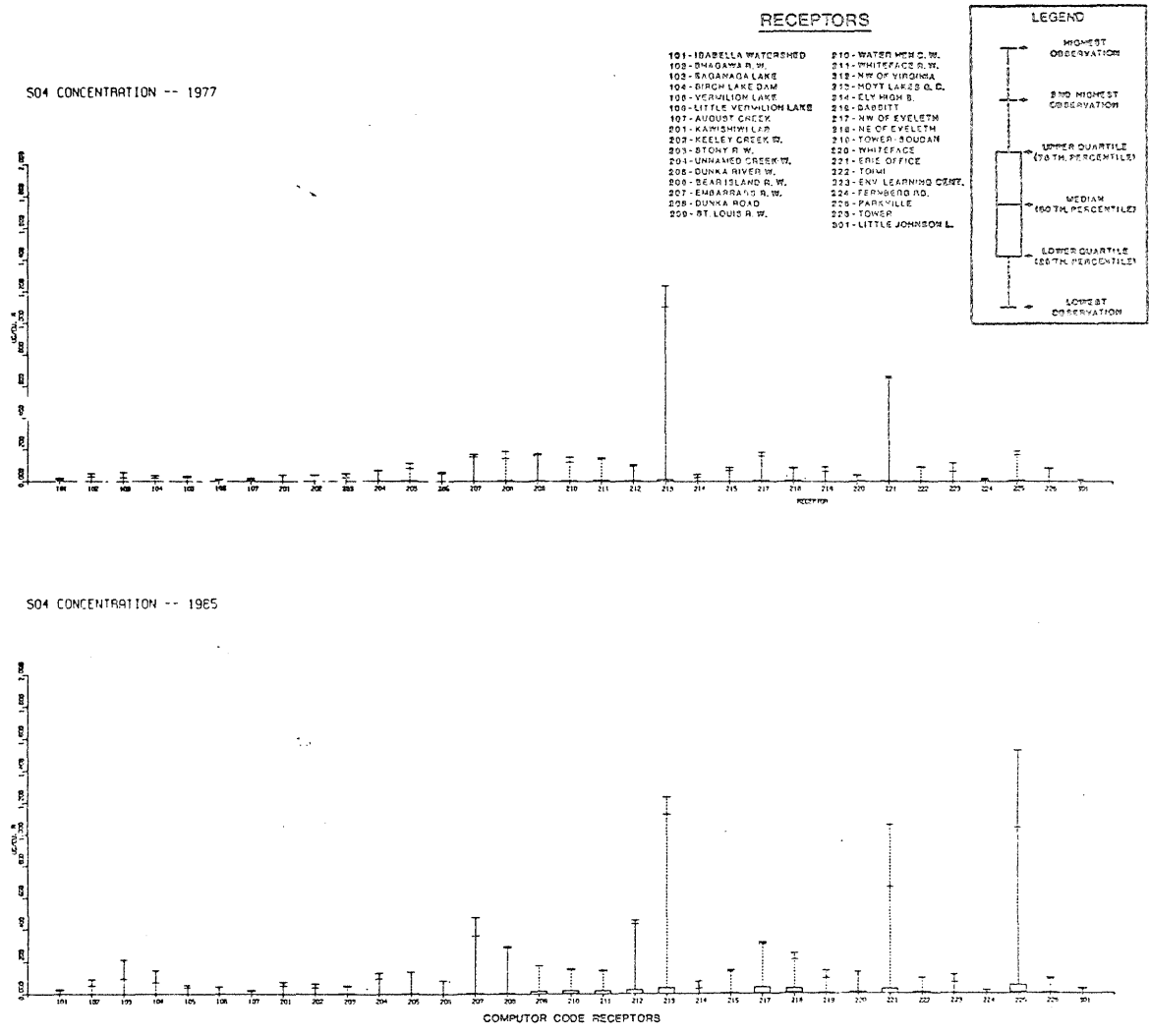
At the present time there is no ambient air quality standard for sulfates. It is possible that standards based on total water-soluble sulfates may be established by 1985. A potential 24 hr standard of $10\text{-}25 \mu\text{g}/\text{m}^3$ and a potential annual standard of $5\text{-}15 \mu\text{g}/\text{m}^3$ have been developed by the Brookhaven National Laboratory Office of Environmental Policy.²⁰⁵

Sulfate concentrations for all the modeled receptors are given in the box plots in Figure 34 for 1977 and 1985. Annual frequency distributions for sulfate concentrations are shown for Isabella Watershed, Hoyt Lakes Golf Course, and Parkville in Figure 35.

7.1.4. Sulfate deposition.

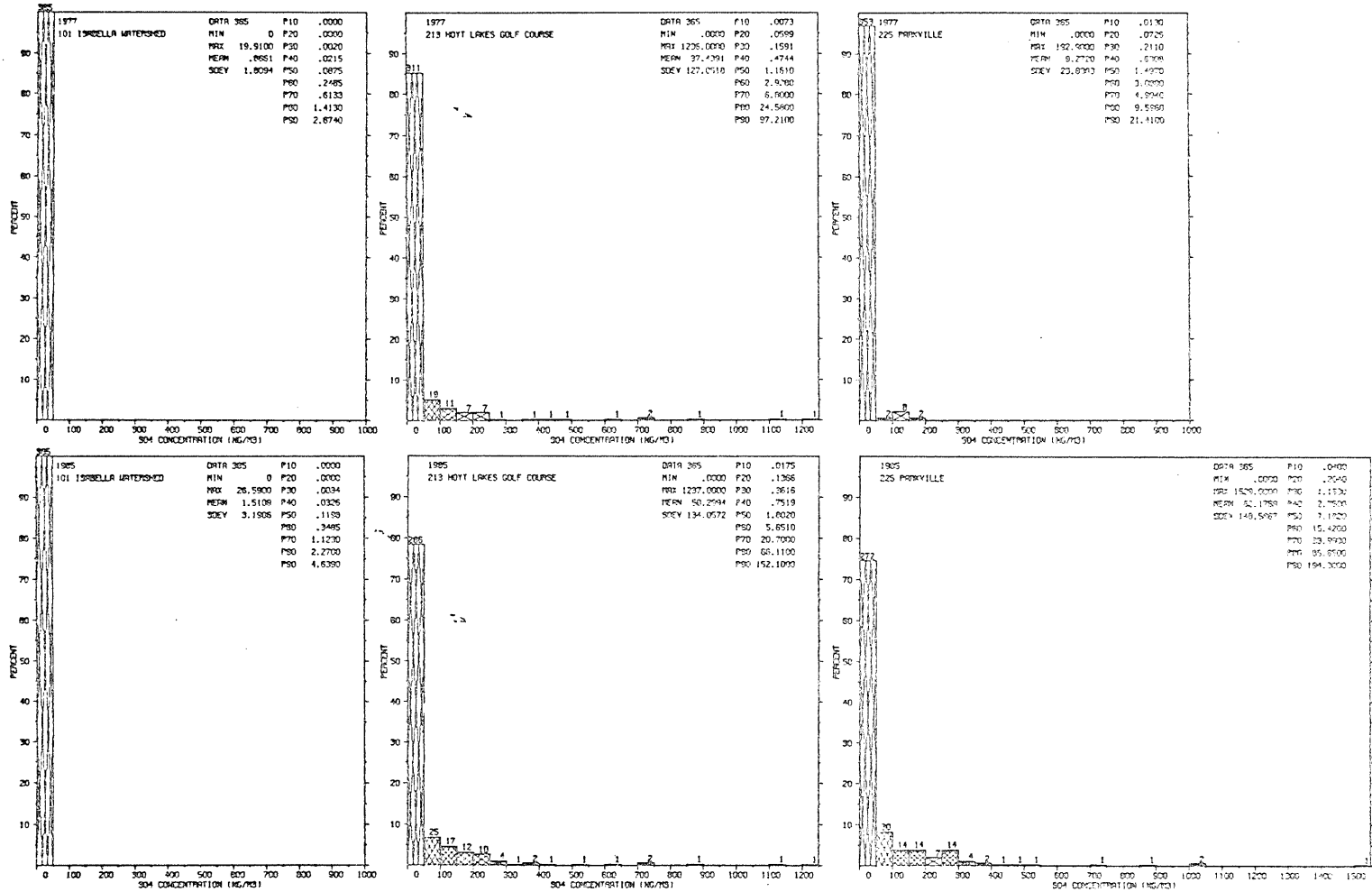
The surface deposition rates for sulfate are of special interest, particularly in the context of water quality impacts. In order to

FIGURE 34. BOX PLOTS OF 24-HOUR VALUES PREDICTED FOR AMBIENT SULFATE CONCENTRATIONS FROM LOCAL SOURCES, 1977 AND 1985 (MODIFIED GAUSSIAN MODEL).



ANNUAL FREQUENCY DISTRIBUTION OF PREDICTED 24-HOUR AVERAGE AMBIENT SULFATE CONCENTRATIONS, 1977 AND 1985, AT SELECTED SITES (MODIFIED GAUSSIAN MODEL)

FIGURE 35



properly understand the total deposition of sulfate, it is necessary to consider both wet and dry deposition. This in turn will facilitate an understanding of the importance of the roles played by local and long distance sources.

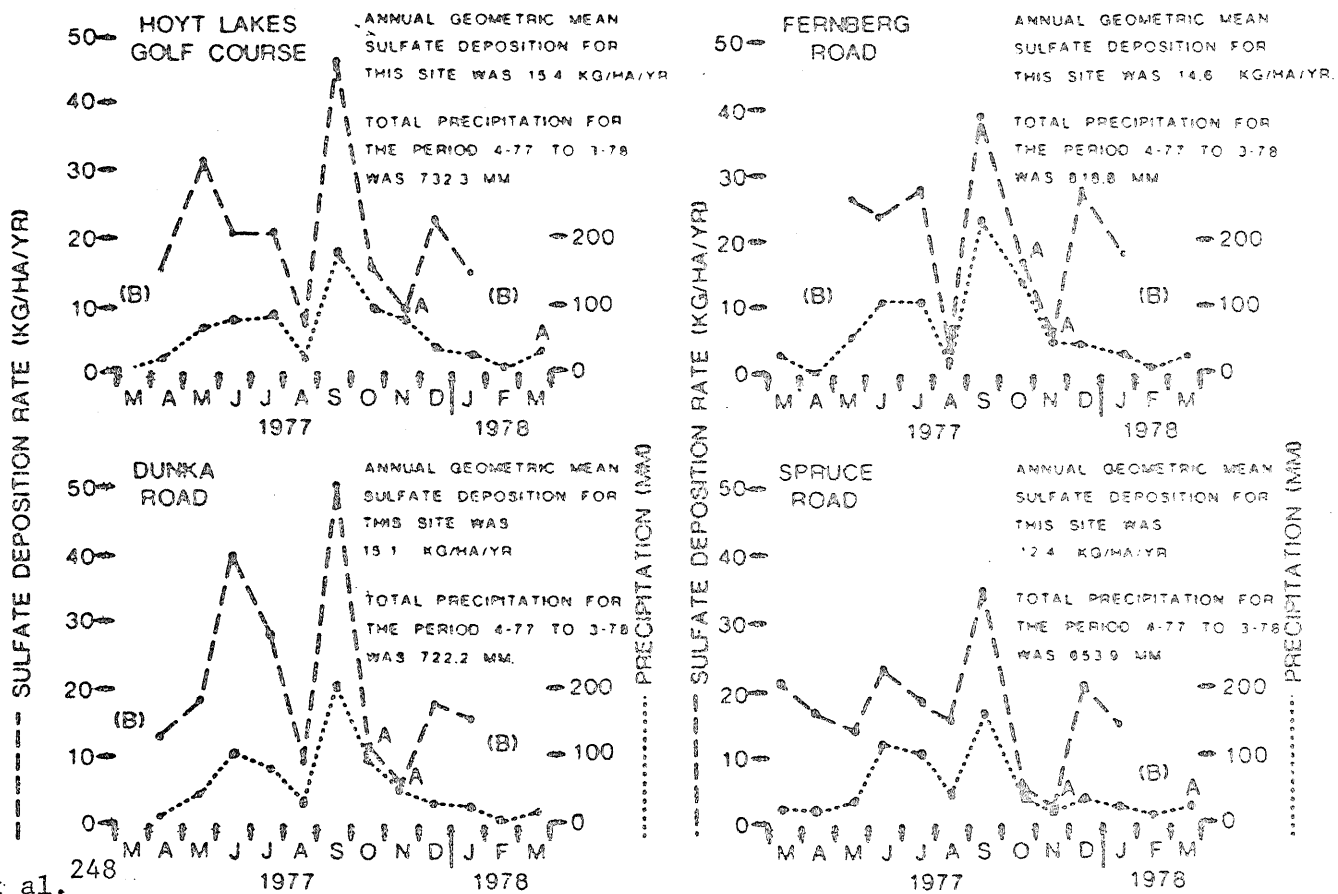
Sulfate deposition in the study area was measured using bulk samplers, rain event samplers, canopy through-fall samplers, and membrane samplers. The results of the through-fall samples and the rain-event samples are comparable to the bulk collected samples, and they are not included in this section to simplify data presentation. A complete discussion of the measured data can be found in Eisenreich, Hollod, and Langevin.⁵⁹

Bulk deposition measurements reflect the combined effects of wet and dry deposition; the collectors are open to the atmosphere for a 30-day sampling period. Bulk deposition samplers were located at four sites: Hoyt Lakes Golf Course, Fernberg Road, Spruce Road/Kawishiwi Laboratory, and Dunka Road. The samples were each collected for 30 days, and then analyzed for a variety of parameters, including sulfate, for the period February, 1977 through January, 1978. Table 57 shows the annual sulfate deposition data from the bulk samplers expressed as both geometric and arithmetic means. The concentration of sulfate in the region seems to be uniformly distributed, once again suggesting that locally generated sulfate deposition is minimal.

Figure 36 shows the monthly deposition values for each site on a line graph along with monthly precipitation. The highest sulfate loadings occurred around September and the second highest loadings occurred around June. These months were also months of highest precipitation which supports the idea that wet scavenging of sulfate is

FIGURE 36. MONTHLY BULK SULFATE DEPOSITION AND PRECIPITATION AT SAMPLING SITES

(A)- INDICATES VALUE WAS LESS THAN THE NUMBER SHOWN
 (B)- DATA NOT AVAILABLE



-235-

Table 57. Annual sulfate deposition based on bulk deposition data, kg/ha/yr.

Location	Geometric mean	Arithmetic mean
Fernberg Road	14.6	18.3
Spruce Road/Kawishiwi	12.4	15.7
Dunka Road Laboratory	15.1	19.3
Hoyt Lakes Golf Course	15.4	21.6
Average	14.4	18.7

Source: Thingvold et al.²⁴⁸

is probably more important than dry deposition.²⁴⁸

An estimate of dry deposition of sulfate for the region was also calculated using measured atmospheric concentration from membrane samplers and deposition velocity data from Chilton, England.³² It is assumed that the dry deposition value represents total sulfur, not sulfate.

On an annual basis, the measured regional dry sulfate deposition was calculated to be 1.78 kg/ha/yr (with a standard deviation of 1.78 kg/ha/yr).²⁴⁸ The average wet-dry rate from the bulk samplers is 14.4 kg/ha/yr. On this basis, from 0 to 24% of the total deposition is estimated to be dry (within 1 standard deviation). Because the dry deposition value is low and because very little ambient SO₂ was measured in the region, it is believed that most of the sulfate originates outside of the region, perhaps from St. Louis, the Ohio Valley and the east coast area.^{136, 137} Long-range transport of sulfate is quite feasible when large high-pressure systems are centered to the east and south of Minnesota. The large, clockwise vortex of winds can then move

sulfur compounds and other pollutants from the industrialized areas of the east to Minnesota. Under certain conditions, Canadian cold fronts can collide with this sulfur-laden, warm air mass over northeastern Minnesota causing high levels of sulfate in the precipitation. In this situation rain scavenging is an important mechanism for sulfate deposition.

Deposition values due to local sources were predicted using the modified gaussian model during each 30 day sampling period at selected receptors. This allows a direct comparison of measured sulfate deposition to predicted deposition expected from local sources. Table 58 summarizes the results of both the measured bulk data and the predicted data. The ratios of the measured to calculated data range from 0.63 (the only ratio less than 1) to 21. The typically large value of the ratio again supports the thesis that the bulk of the sulfate deposition in the region is due to sources outside the region.

In order to understand the role of local SO_2 sources in regional sulfate deposition, it is useful to consider the data on dry deposition. A comparison of the mean annual deposition rates (based on dry deposition velocity from Chilton, England and Minnesota measured ambient sulfate concentrations) and predicted total sulfate deposition rates from local sources alone is given in Table 59. It is important to emphasize that the predicted average sulfate deposition rates for the 8 sites shown in the table include both the wet and dry deposition values. The annual arithmetic rate of 2.85 kg/ha/yr (or 2.2 kg/ha/yr using all 33 receptor sites to calculate a regional average) includes both wet and dry deposition. This is in contrast to the values calculated

Table 58. Measured and predicted local sulfate deposition^a (kg/ha/yr).

	DUNKA RD.	SPRUCE RD/ KAWISHIWI	FERNBERG RD.	HOYT LAKE GOLF COURSE
March M ^b	1.1	1.4		1.3
P ^b	0.073	0.076		.11
April M	1.5	1.2	2.2	2.6
P	0.27	0.27	0.39	0.33
May M	3.3	1.9	2.0	1.7
P	0.28	0.33	0.36	0.21
June M	2.3	1.5	2.3	1.7
P	0.41	0.26	.34	0.83
July M	0.76	1.3	0.31	0.59
P	0.14	0.13	0.13	0.93
Aug M		2.9	3.2	3.9
P		0.14	0.21	0.75
Sept M		0.47		1.3
P		0.28		0.75

RATIO: MEASURED/PREDICTED

March	15	18		12
April	5.6	4.4	5.6	7.9
May	12	5.6	5.6	8.1
June	5.6	5.8	6.8	2.0
July	5.4	10	2.4	0.63
Aug		21	15	5.2
Sept		1.7		1.7

^aMeasured values are based on bulk deposition results, predicted values reflect the effects of local SO₂ sources only, using the modified gaussian model.

^bM=measured; P=predicted.

Table 59. Calculated^a dry deposition rates and predicted^b total sulfate deposition (kg/ha/yr).

Location	Calculated	Predicted
Fernberg	2.01	2.2
Isabella (ELC)	1.92	2.5
Dunka	1.86	2.5
Toimi	1.32	2.1
Erie	1.01	4.0
Hoyt Lakes	1.79	5.5
Whiteface	2.13	2.1
Babbitt	1.98	1.9
Region	1.78 ^c	2.85 ^c (2.2 ^d)

^a using Chilton, England dry deposition velocity and

Minnesota measured air concentrations

^b based on local (1977) sources

^c based on 8 sites shown in the table

^d based on all 33 receptors in the region

from ambient air concentrations which include only dry deposition to yield an average of 1.78 kg/ha/yr for the eight sites.

In order to compare these two results, it is first necessary to isolate that portion of the predicted deposition attributable to dry deposition. This value can then be compared to the calculated result based only on dry deposition data. Accordingly, the predicted wet and dry sulfate deposition components from local sources at four sites (Hoyt Lakes Golf Course, Dunka Road, Kawishiwi, and Fernberg Road) are shown in Table 60. The resulting dry deposition ranges from 91.4% to 95.9% of the total deposition.

If it is assumed on the basis of these data that at most 10% of the total predicted deposition from local sources is wet, a predicted dry deposition average of 2.56 kg/ha/yr is calculated for the eight sites.

Table 60. Predicted wet and dry sulfate deposition from local point sources (kg/ha/30 day).

	DUNKA RD.		HOYT LAKES GOLF COURSE		KAWISHIWI		FERNBERG RD.	
	wet	dry	wet	dry	wet	dry	wet	dry
March	0.003	0.070	0.004	0.103	0.004	0.073		
April	0.016	0.257	0.010	0.317	0.008	0.265	0.010	0.376
May	0.019	0.260	0.026	0.186	0.017	0.311	0.016	0.345
June	0.016	0.392	0.021	0.807	0.006	0.255	0.010	0.328
July	0.005	0.132	0.008	0.919	0.010	0.120	0.010	0.116
Aug	0.017	0.377	0.066	0.683	0.018	0.119	0.028	0.182
Sept	<u>0.098</u>	<u>0.355</u>	<u>0.121</u>	<u>0.626</u>	<u>0.030</u>	<u>0.253</u>		
Total	0.174	1.843	0.256	3.641	0.093	1.396	0.074	1.723
% of Total	8.6%	91.4%	6.6%	93.4%	6.2%	93.8%	4.1%	95.9%

A value of 1.98 kg/ha/yr is calculated for the region based on 33 receptors. These values compare favorably to the dry deposition rate of 1.78 kg/ha/yr which is based on regional measured data and a dry sulfate deposition velocity from Chilton, England.³²

Since the comparison between predicted local source and measured dry sulfate deposition is excellent, it is concluded that the bulk of the measured dry deposition in the region is due to local sources. However, about 85% of the measured total (wet and dry) sulfate deposition is not accounted for by the regional point sources.

The International Joint Commission¹¹¹ predicts that sulfate loadings in Minnesota could double from 16.4 kg/ha/yr in 1974 to 32.8 kg/ha/yr by the year 2000 with no full-scale SO₂ removal at the sources. However,

sulfate loadings could remain at about the 1974 level if additional SO₂ removal is applied to planned and existing sources. Since the specific origins of sulfate deposited in the region from remote sources are not known, it is impossible to predict sulfate deposition increases as a result of SO₂ emission increases at specific locations. However, it is known that sulfate deposition, for example, was high in the region during the months of May, June, and September when south and southeast winds constituted important components of the wind roses for these periods. Thus, it is reasonable to look at projections for increased SO₂ emissions to the south and east of the region for general validation of the IJC prediction concerning sulfate loading.

In a report to the Minnesota Legislature, the Minnesota Energy Agency¹⁵⁰ estimates that total stack emissions of SO₂ in the State were about 312,000 mtpy in 1976. Of this total, about 226,000 mtpy, or 72%, was due to the combustion of coal. Projections for coal use in the State show an estimated 59% increase in coal-related SO₂ emissions by 1985, with an increase of 104% by 1995. Although the Twin Cities area is forecasted to have a slight decline in coal-derived stack SO₂ emissions, the Duluth-Superior area is estimated to experience increases greater than the State as a whole, with 98% and 172% increases projected for 1985 and 1995, respectively. The Central Air Quality Control Region just south of Duluth is expected to show increases over 1976 levels of 305% and 455% in coal-related stack SO₂ emissions by 1985 and 1995, respectively.

Since these areas may serve as sources of sulfate transported into the study region, this information certainly supports the predictions

of significant increases in sulfate deposition over the next 20 to 25 years made by the LJC. The energy shortages related to gas and oil which will increase coal usage may constitute the determining factor in increasing sulfate deposition. Since this situation is not unique to Minnesota, but affects the entire nation, it is reasonable to expect that sulfate deposition in the region can be expected to increase due to the influence of outside sources.

The annual arithmetic mean sulfate deposition due to local point sources is predicted to more than double from 2.2 kg/ha/yr in 1977 to 4.5 kg/ha/yr in 1985. If it is assumed that background sulfate increases correspondingly, then by 1985 the total regional sulfate deposition would be about 29 kg/ha/yr.

Table 61 presents predicted annual sulfate deposition at the regional receptors for 1977 and 1985 due to point sources alone.

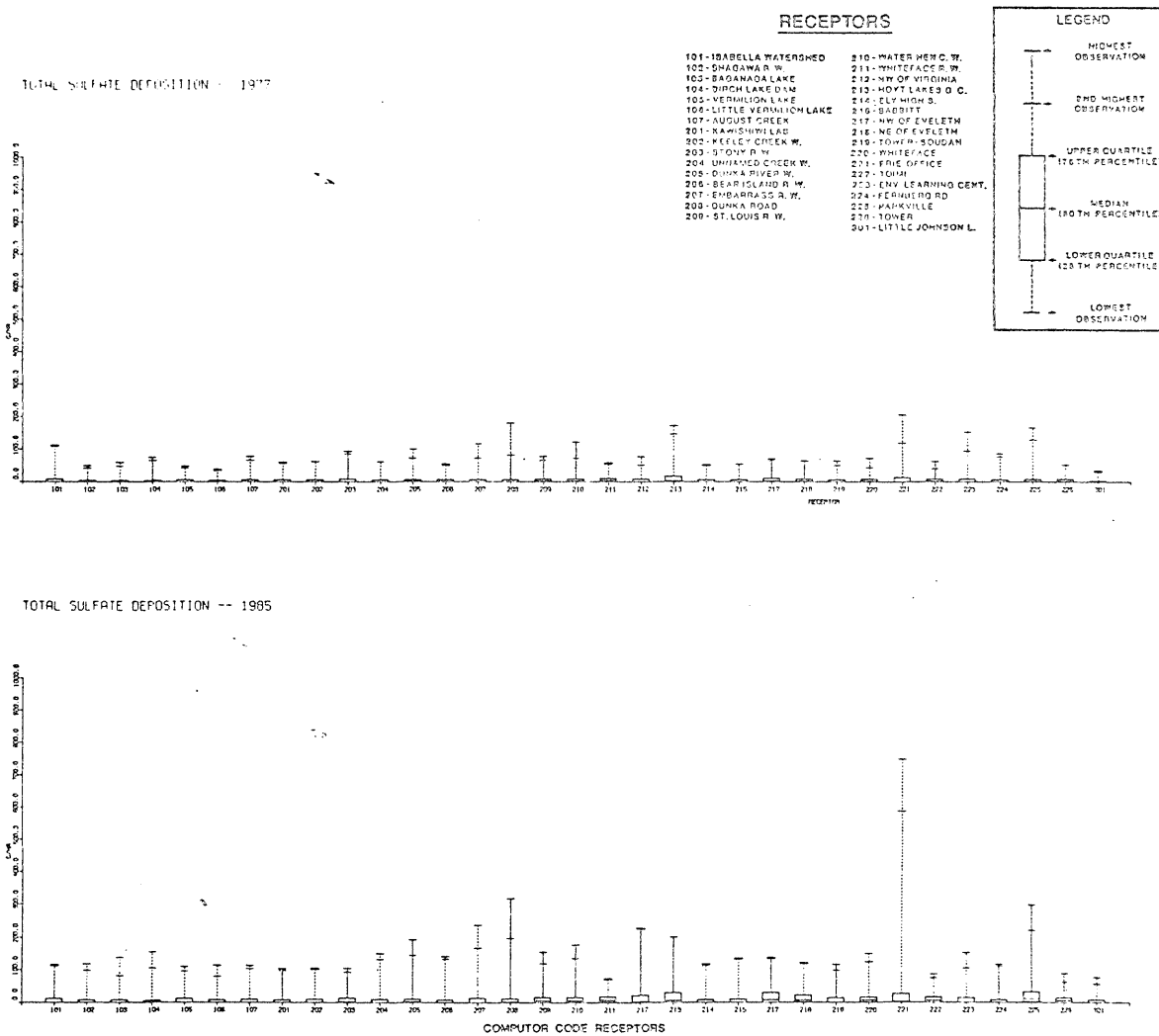
Box plots of predicted sulfate deposition from local sources for 1977 and 1985 are shown in Figure 37, and frequency distributions are given in Figure 38 for three sites (Isabella Watershed, Hoyt Lakes Golf Course, and Parkville).

7.2. PARTICULATES

The previous discussion focused on characterization of sulfur in the absence of copper-nickel development. This section presents a similar characterization of particulates (TSP) in the atmosphere. Major regional sources are enumerated, the resulting ambient particulate levels due to emissions from these sources are discussed, and changes in the future air quality due to regional development in 1985 without a copper-nickel industry are forecast.

FIGURE 37.

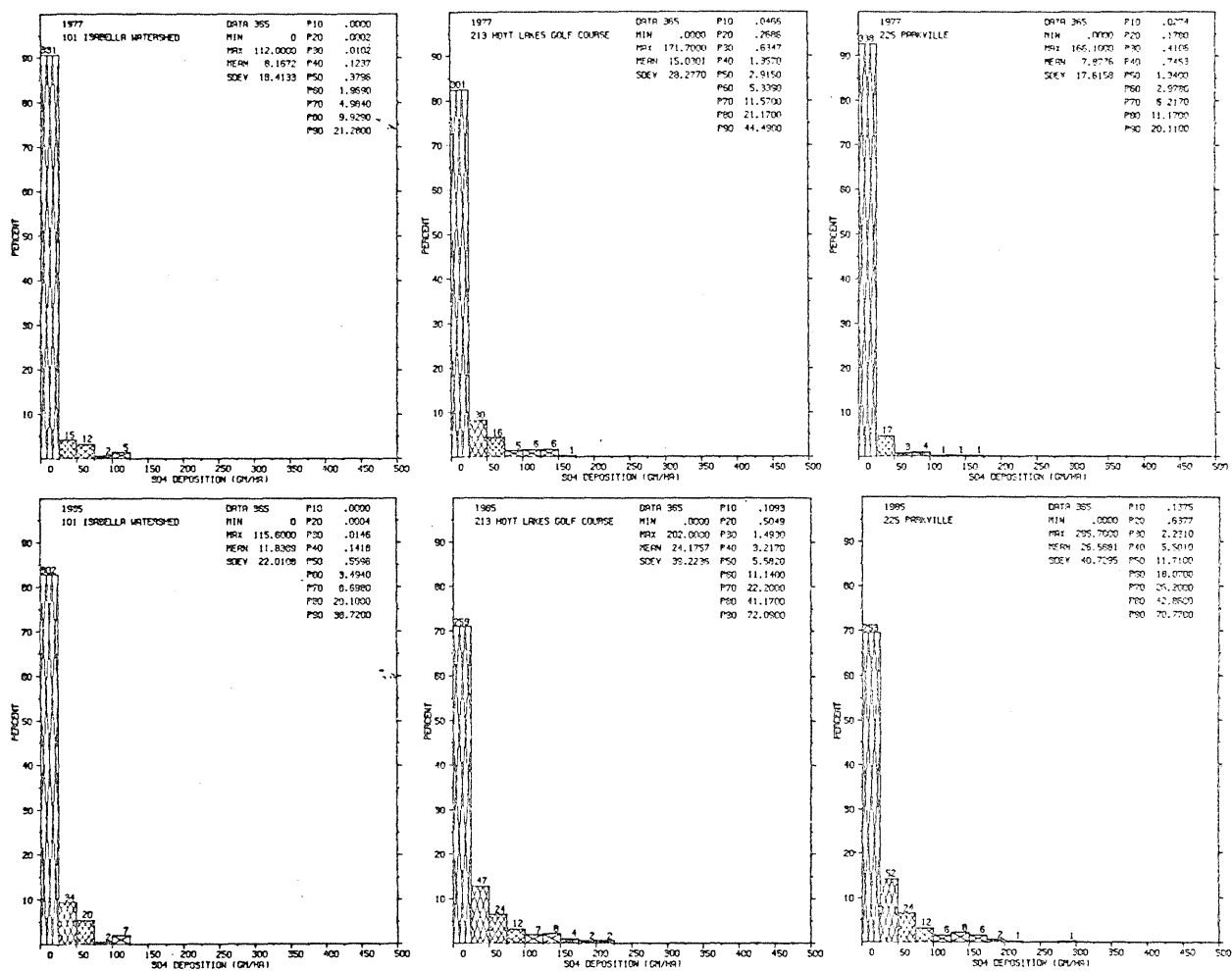
BOX PLOTS OF 24-HOUR VALUES FOR PREDICTED TOTAL SULFATE DEPOSITION FROM LOCAL SOURCES, 1977 AND 1985 (MODIFIED BOX MODEL)



243

ANNUAL FREQUENCY DISTRIBUTION OF PREDICTED 24-HOUR SULFATE DEPOSITION
FROM LOCAL SOURCES, 1977 AND 1985, FOR SELECTED SITES (MODIFIED GAUSSIAN MODEL)

FIGURE 38



244

Table 61. Predicted annual deposition of sulfate at various receptor sites due to point source emissions in the Region: (kg/ha/yr).

SITE NO.	COMPUTER CODE	NAME	1977	1985	PERCENT
			REGIONAL BASELINE	PROJECTION	CHANGE BY 1985
1	301	Little Johnson Lake	2.1	2.4	+14
2	106	Little Vermillion Lake	1.1	2.4	+118
3	104	Birch Lake Dam	1.6	3.0	+88
4	103	Saganaga Lake	1.1	2.5	+127
5	105	Vermillion Lake	1.4	3.2	+329
6	102	Shagawa R.W.	1.4	2.7	+93
7	214	Ely High School	1.5	2.9	+93
8	224	Fernberg Road	2.2	3.5	+59
9	219	Tower-Sudan	1.8	3.9	+117
10	206	Bear Island R.W.	1.7	3.2	+88
11	201	Kawishiwi Lab W.	1.7	3.1	+82
12	202	Keeley Creek W.	1.8	3.2	+78
13	107	August Creek	1.9	3.4	+79
14	101	Isabella Watershed	3.0	4.3	+43
15	212	NW of Virginia	2.2	6.2	+182
16	207	Embarrass R.W.	2.2	4.9	+123
17	215	Babbitt	1.9	3.8	+100
18	204	Unnamed Creek W.	1.9	3.7	+95
19	223	Environ. Learning C.	2.5	4.1	+64
20	225	Parkville	2.9	9.7	+234
21	221	Erie Office	4.0	11	+175
22	208	Dunka Road	2.5	5.5	+120
23	205	Dunka R.W.	2.2	4.3	+95
24	203	Stony River W.	2.6	4.2	+62
25	217	NW of Eveleth	2.9	7.0	+141
26	218	NE of Eveleth	2.5	5.9	+136
27	213	Hoyt Lakes Golf Course	5.5	8.8	+60
28	209	St. Louis River W.	2.4	4.7	+96
29	210	Waterhen Creek W.	2.4	4.9	+104
30	211	Whiteface River W.	2.3	4.6	+100
31	222	Toimi	2.1	4.1	+95
32	220	Whiteface	2.1	4.5	+114
33	226	Tower	1.8	3.9	+117

7.2.1. Sources, present and 1985.

As was the case for sulfur emissions, sources which emit at least 100 mtpy particulates were inventoried. Unlike the case for SO₂, however, smaller, more widely distributed area sources are very important. Their existence explains the general background particulate levels observed in the region. These sources will be discussed after consideration of the point sources.

The point source particulate inventory includes sources present during the baseline period (1975-76) as well as those projected to be in existence by 1985. Table 62 lists the various sources and the amounts of particulate emissions. As with the SO₂ inventory, it must be realized that these figures reflect the best estimates currently available, and the 1985 projections, in particular, will most certainly be refined as plans evolve and new information becomes available.

The 1975-76 baseline regional emissions (92,480 mtpy) are expected to decrease about 38% by 1985 (57,740 mtpy). Figure 39 gives a breakdown of emissions in terms of source categories (power generation, taconite processing, grain elevators, refineries, commercial-industrial), and geographic area (Minnesota, Wisconsin, and Canada).

The 38% decrease in regional particulate emissions by 1985 is due primarily to abatement efforts. Based on emissions data and estimates, these efforts will result in a 68% decrease for point sources in Duluth, a 48% decrease in Carlton County, and nearly a 97% decrease in particulate emissions at the Reserve Mining Company operations at Silver Bay, Minnesota. Particulate emissions in Atikokan, Ontario are expected to decrease by 85% due to the closing of the Steep Rock Iron Mines, Ltd.

Table 62. Regional particulate emissions inventory used for sources emitting more than 100 mtpy.

SOURCE FACILITY ³	BASELINE EMISSIONS 1975-76 (mtpy)	1977 BASELINE (if different from 1975-76 values)(mtpy)	PROJECTED EMISSIONS 1985 (mtpy)
Potlach Northwest	1312		691
Conwed	444	"227"(1,2)	"227"
Continental Oil	92		92
Erie Mining (Taconite Harbor)	813		813
MP & L Clay Boswell	5504		7649
National Steel Pellet	1766	"1392"(1,2)	2093
Butler Taconite	1575		3182
Boise Cascade	2335		"546"
Reserve Mining (Silver Bay)	31140		"1000"
MP&L Sy Laskin	662		662
Reserve Mining (Babbitt)	none reported		0
Arrowhead Blacktop	100		100
Cargill Elevator B	498		"91"
Cargill Elevator C	205		" 36"
Duluth Steam	150		"150"
General Mills A	306		" 64"
International Multifoods	496		"236"
MP & L Hibbard Station	19		---
Superwood Corp.	279		279
U.S.S.-Duluth Coke	1053		---
U.S.S.-Shipping	193		" 46"
Eveleth Taconite	857	"2545"(1,2)	"3909"
MP&L (Floodwood or Brookston)	---		"2364"
Jones and Laughlin	---		"1909"
Hibbing Public Utility	52		52
Hibbing Taconite	---	1218 (1,2)	1791
Hanna Mining	703		1273
Erie Mining (Hoyt Lakes)	7727		"10460"
Minntac	17440	19160 (2)	"7000"
Virginia PUD	612	"127" (1)	"127"
Inland Steel	---	1227 (2)	2455
Pickands Mather	---		"2273"
Lake Superior Power District	648		"1909"
Roffler's Construction	277		277
Murphy Oil Corp.	56		56
Farmers' Union Grain	354		13
Globe Elevator	321		2
Superior WL&P	5		5
Orba Corp.	---		318
Burlington Northern	---		146
Univ. of Wisconsin	76		76
CLM Corp.	2		8
Ontario Hydro (Atikokan)	---		1900
Caland Ore Co.	1356		---
Steep Rock Mines	11650		---
Minnesota Pulp & Paper	1405		1405

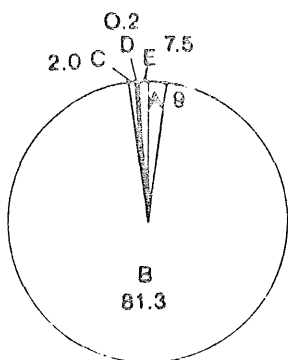
NOTE: A missing entry (--) indicates the facility does not exist or will be phased out by the date shown. Tonnages shown in quotation marks indicate estimates by the staff of the Copper-Nickel Study based on available data.

1) Used in 1977 regional baseline in place of value shown for 1975-76.

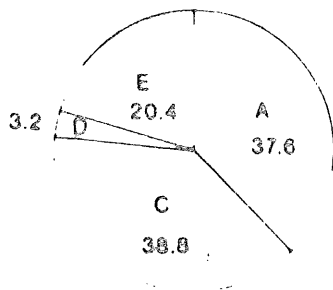
2) Used in 1977 PSD baseline in place of value shown for 1975-76.

FIGURE 39

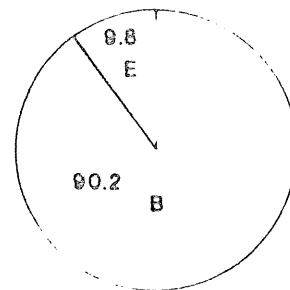
SOURCE CATEGORY CONTRIBUTIONS TO PARTICULATE EMISSIONS



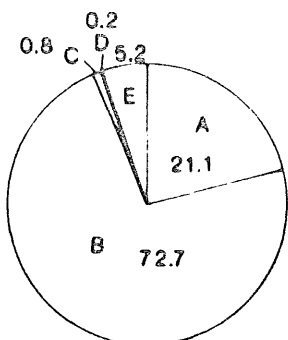
MINNESOTA BASELINE
TOTAL : 78340 MTPY



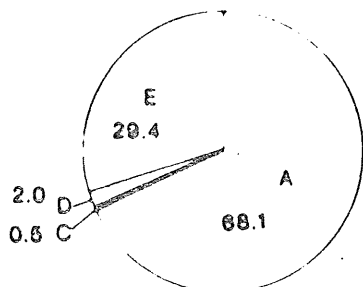
WISCONSIN BASELINE
TOTAL : 1739 MTPY



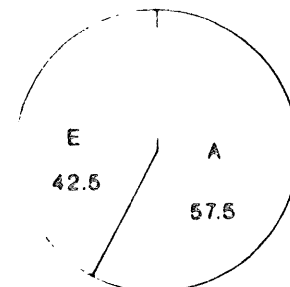
CANADA BASELINE
TOTAL : 14410 MTPY



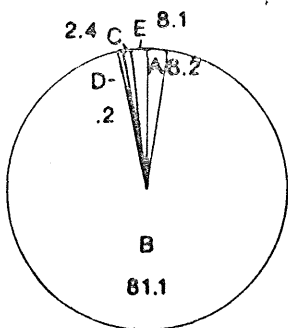
MINNESOTA PROJECTED
TOTAL : 51830 MTPY



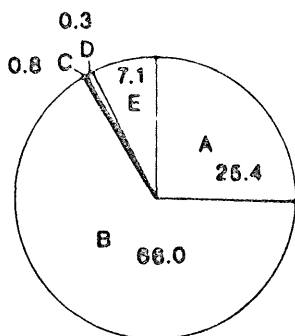
WISCONSIN PROJECTED
TOTAL : 2810 MTPY



CANADA PROJECTED
TOTAL : 3305 MTPY



REGION BASELINE
TOTAL : 92480 MTPY



REGION PROJECTED
TOTAL : 57740 MTPY

LEGEND

- A - % POWER GENERATION
- B - % TACONITE PROCESSING
- C - % GRAIN ELEVATORS
- D - % REFINERIES
- E - % COMMERCIAL/INDUSTRIAL

SOURCE : RITCHIE (1978)

and the Caland Ore Company, Ltd., two major taconite mining companies.

These decreases, however, are partially offset by projected growth in both the taconite processing industry in Minnesota and the power generating industry in Minnesota and Canada. Proposed generating stations near Floodwood, Minnesota and Atikokan, Ontario, and the planned expansion of the MP & L Clay Boswell power plant in Cohasset, Minnesota will increase regional particulate emissions by 2364, 1900, and 2145 mtpy, respectively. By 1985, taconite processing in Minnesota is expected to contribute an estimated additional 6,274 mtpy particulates over present emissions. The taconite industry is the largest contributor to regional point source particulate emissions for both the baseline (81% of the total baseline) and projected (66% of the total projected) emissions.

Although particulate point source emissions are expected to decrease, the decline may have little overall effect on the study region where fugitive emissions from area sources such as taconite mines and unpaved roads appear to be the major sources of particulates. The extent of the fugitive emissions problem is currently being assessed by the Minnesota Pollution Control Agency. The contribution of area source emissions to ambient particulate (TSP) concentrations is discussed in section 7.2.2.

Total suspended particulate point source emissions in the region may be placed into perspective by comparison to global, national and local emissions. The largest sources of atmospheric particulates are natural, contributing about 2,273 million mtpy.²⁰⁰ Natural sources of particulate matter include wind erosion of land and sea, forest fires,

volcanic eruptions, vegetation, and gas-to-particle reactions. Anthropogenic sources contribute approximately 295 million mtpy which arise from industrial processes, combustion of fossil fuels, and agricultural activities.²²⁰

Nationally, there has been a 23% decrease in particulate point source emissions from 1972 to 1975 (21.3 million mtpy compared to 16.4 million mtpy). This decrease has been attributed primarily to the installation of control equipment on industrial processes and utilities, a reduction in coal consumption by non-utility stationary sources, and a decrease in the burning of solid wastes.²⁶⁸

In Minnesota, point source particulates decreased by a substantial 43% from 1970-71 to 1973-74 (278,000 mtpy compared to 157,700 mtpy) primarily due to greater use of pollution control equipment. A comparison by source category of point source particulate emissions between the seven county metro area and the study region is given in Table 63 which clearly shows regional differences in industrial patterns.

Table 63. 1976 point source particulate emissions inventory summary by source category for the Air Quality Study Region and the seven-county metro area.

REGION	POWER GENERATION	TACONITE	GRAIN	REFINERY	COMMERCIAL- INDUSTRIAL	TOTAL ^a
<u>Seven-County Metro Area</u>						
mtpy	10230	0	6285	2882	21230	40630
% of total	25.2	0	15.5	7.1	52.2	100
<u>Air Quality Study Region</u>						
mtpy	7651	75020	2180	148	7476	92480
% of total	8.2	81.1	2.4	.2	8.1	100

^atotals are rounded.

7.2.2. Ambient particulate concentrations.

Total suspended particulates (TSP) were measured at 11 locations using high-volume samplers from October, 1976 to March, 1978.²²⁷ Sites were selected to represent rural, industrial, and community areas. A wide range of TSP concentrations were measured over this period. Twenty-four hour concentrations ranged from 1 $\mu\text{g}/\text{m}^3$ (the minimum detectable level) to 367 $\mu\text{g}/\text{m}^3$. Annual geometric mean concentrations ranged from 10 $\mu\text{g}/\text{m}^3$ at Kawishiwi Lab to 55 $\mu\text{g}/\text{m}^3$ at Virginia as shown in Table 64. All of the annual means are below both the federal primary (75 $\mu\text{g}/\text{m}^3$) and the secondary (60 $\mu\text{g}/\text{m}^3$) annual standards for TSP concentrations.

Table 64. Adjusted annual geometric means at TSP sample sites, 1977.^a

Site Number		Mean TSP ($\mu\text{g}/\text{m}^3$)	Site Characteristics
7001	Fernberg Road	10	Rural
7003	Kawishiwi Laboratory	10	Rural
7007	Toimi	12	Rural
7010	Hoyt Lakes Golf Course	15	Near town
7008	Erie Mining Office	19	Taconite mining
7006	Dunka Road	20	Taconite mining
7002	Ely High School	22	Community
7009	Hoyt Lakes Police Station	30	Community
7516	Hibbing	37	Community
7514	Mountain Iron	42	Community
1300	Virginia	54	Community

SOURCE: Endersen and Feeney⁶²

^a means have been adjusted for missing data⁶⁵

Feeney⁶⁵ concluded that both snow cover and mining activity can have substantial impacts on TSP concentrations. Table 65 shows mean TSP concentrations during different time intervals of snow cover and

Table 65. The effect of snow cover and mining activity on TSP levels in the study area.

Dates	Event	Adjusted ^a Mean TSP ($\mu\text{g}/\text{m}^3$)
11/26/76-3/7/77	Snow cover	18.97
3/14/77-7/24/77	Mining activity No snow cover	35.64
7/30/77-10/4/77	Mine Strike No snow cover	14.63 ^b
10/10/77	Snow event	7.23
10/16/77-11/9/77	Mining strike No snow cover	16.68
11/16/77-12/15/77	Mine strike Snow cover	13.02
12/21/77-3/27/77	Mining activity resumed Snow cover	

SOURCE: Endersen and Feeney⁶²

^aValues have been adjusted for missing data.⁶²

^bThe mining strike began officially on August 1, but the mines were effectively shut down as of July 30. Samples taken on July 30 were included in the strike period.

mining activity. Measured TSP concentrations in all parts of the study region decreased substantially during the taconite mining strike of August-December 1977. Concentrations on a regional basis decreased an average of 59% over the preceding spring and summer. Not surprisingly, the impact was greatest at locations on mining property, with the Erie Mining Office site showing a 76% decrease. Areas showing less effect were background sites and the communities. Kawishiwi Lab experienced a 46% decrease, and Virginia and Hibbing each experienced a decrease of

about 45% in particulate levels over the previous spring and summer.

Endersen and Feeney⁶² also conclude that long distant transport of TSP appears to be a major component of the regional background concentrations measured at the three remote sites in the region.

Because TSP concentrations are not homogeneous throughout the region, quantifying the background concentration becomes difficult. It appears that $10 \mu\text{g}/\text{m}^3$ is a reasonable estimate, and this value includes both long distance transport and region-wide dust generation.

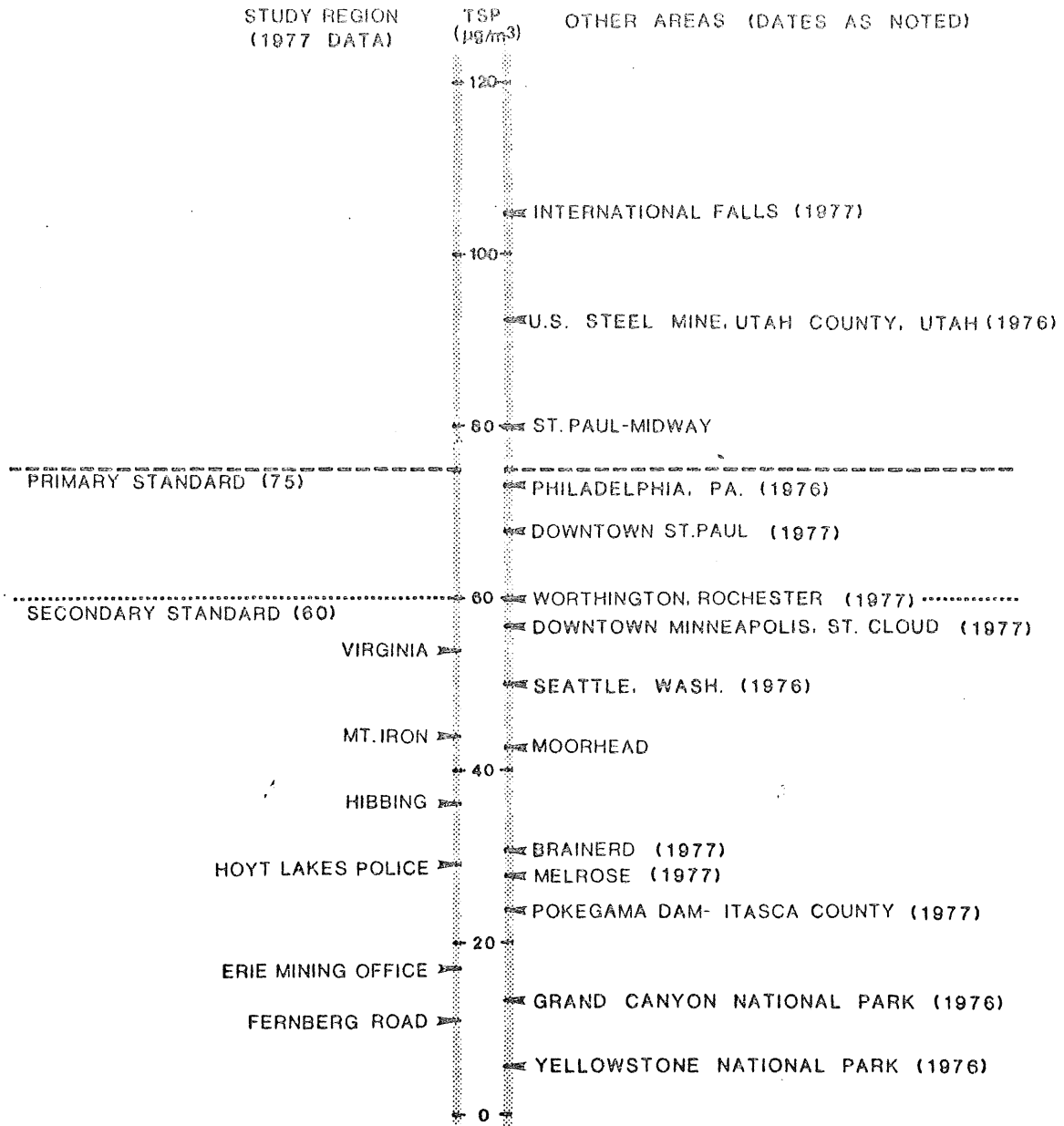
Figure 40 presents a comparison of measured particulates in the region and other areas of Minnesota and the nation.

7.2.2.1. Regulatory analysis--annual average TSP concentrations: The ambient TSP concentrations were modeled to estimate the relative contribution of particulate point sources to the overall TSP levels. This provided a basis for predicting TSP concentrations based on expected changes in point source emissions by 1985.

The modified gaussian model was run using the emissions sources existing during the period of measured concentrations. Figure 41 shows the resulting predicted annual geometric mean concentrations at each receptor site in the study region. Although the contribution of point sources to annual particulate levels would not be detected by the monitoring equipment, the predicted values are presented and discussed to provide perspective on regional source contributions.

When the predicted annual means (due to local point sources) at each receptor in the region are averaged for the baseline period, a regional TSP arithmetic mean of $0.1 \mu\text{g}/\text{m}^3$ is calculated. The predicted regional mean is negligible (less than 1%) by comparison to either the

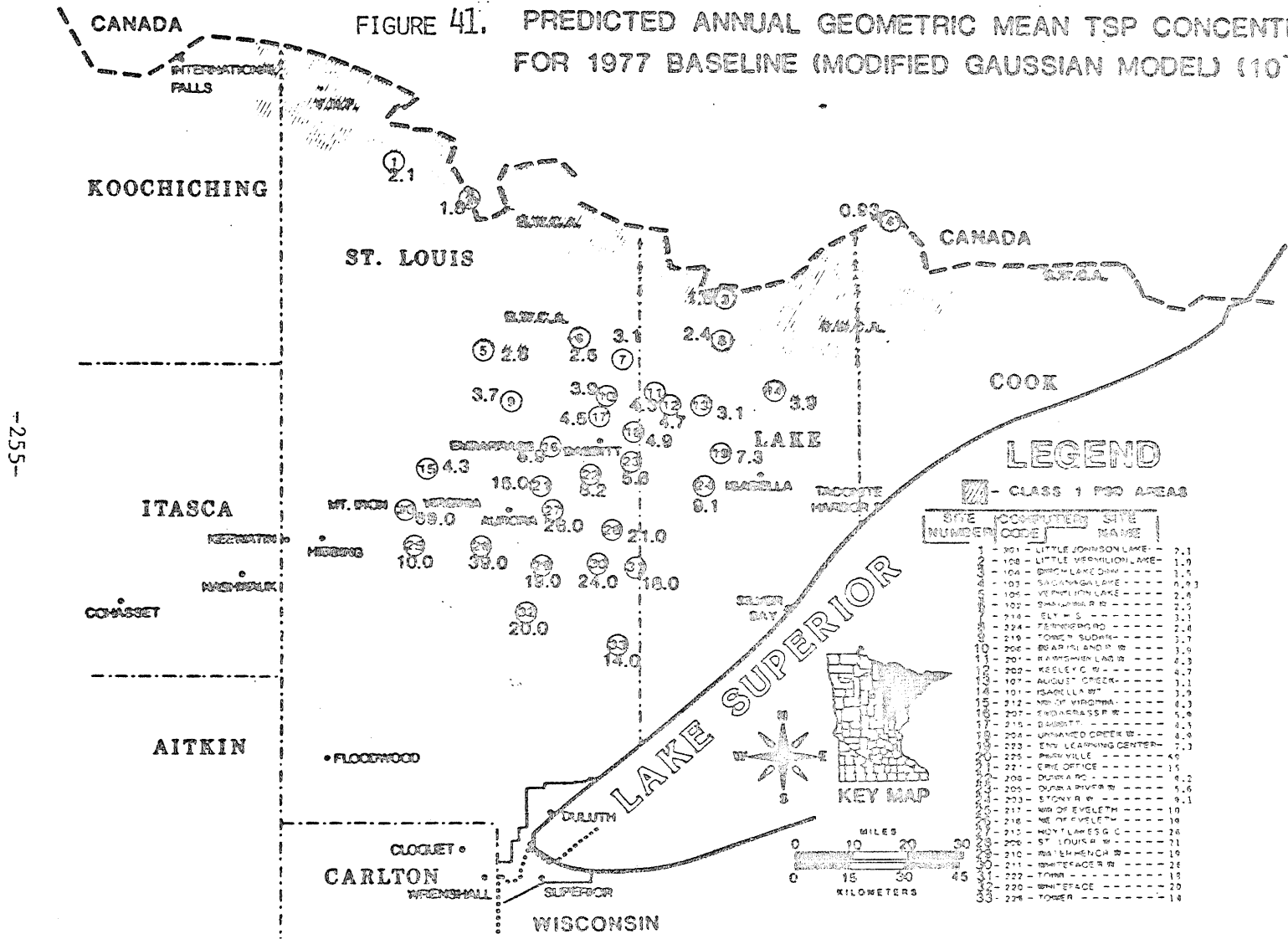
FIGURE 40. GEOMETRIC MEAN ANNUAL TSP CONCENTRATIONS



SOURCE: ENDERSON AND FEENEY (1978)

ATKINIAN

FIGURE 41. PREDICTED ANNUAL GEOMETRIC MEAN TSP CONCENTRATIONS FOR 1977 BASELINE (MODIFIED GAUSSIAN MODEL) (10^{-2} UG/M³)



LEGEND

CLASS 1 FOOD AREAS

SITE NUMBER	COMPUTED SITE CODE	SITE NAME	CONCENTRATION
1	301	LITTLE JOHNSON LAKE	2.1
2	108	LITTLE DENNISON LAKE	1.9
3	104	BIRCH LAKE DAM	3.5
4	103	SAGANAGA LAKE	2.3
5	105	VERMILION LAKE	2.8
6	102	SARASOTA R. W.	2.5
7	216	ELY W. C.	3.1
8	324	FERINGWOOD	2.8
9	219	TOWER SUDLEY	2.8
10	206	BEAR ISLAND R. W.	3.7
11	201	BARTISMAN LAKE W.	4.3
12	202	KEELEY C. W.	4.7
13	107	AUGUST CREEK	3.9
14	101	SHANILLA ST.	3.1
15	212	NE. OF VIRGINIA	4.3
16	207	WINDYBASS P. W.	5.0
17	215	BAUSSETT	4.3
18	204	UNWINDO CREEK W.	4.9
19	222	ST. LOUIS LEARNING CENTER	7.3
20	225	PRINCEVILLE	4.0
21	221	CRNE OFFICE	1.5
22	200	DUPRE RD.	6.2
23	205	DUPRE RD. W.	5.6
24	203	STONY R. W.	9.1
25	217	NE. OF EVELETH	10
26	218	NE. OF EVELETH	10
27	210	HOLY LAKE S. C.	26
28	208	ST. LOUIS W. W.	21
29	210	RAVEN HENCH W.	10
30	211	WHITEFACE R.	26
31	222	TOWN	18
32	220	WHITEFACE	20
33	226	TOWER	18



-255-

arithmetic mean of $25 \mu\text{g}/\text{m}^3$ for the measured values (average of 11 sites in Table 64), or to the regional background concentration of $10 \mu\text{g}/\text{m}^3$.

The low predicted TSP concentrations are to be expected since the modified gaussian model considers only particulate point source emissions, and the measured values, of course, include point and area source contributions. It appears from the model simulations that over 99% of the regional ambient particulate concentrations on an annual basis are due to regional area source emissions, or to long distant transport from sources outside the region.

This conclusion is supported by a dispersion modeling study of the Iron Range from Grand Rapids to Buhl²²⁹ which found that area source emissions had an impact relative to point sources of at least 10 to 1 in most grids inventoried. The emissions inventory in this report showed that unpaved and paved roads were the major contributors to TSP concentrations, followed by areas exposed by mining activities, and combustion sources. This finding also agrees with the previous discussion of variables affecting TSP levels observed in the region. The effects of the mine strike, snow cover, and community activity all indicate the importance of area sources. The uniformity of the concentrations observed at remote sites supports the conclusion that area sources and regional transport play a key role in regional TSP concentrations rather than specific point sources in the region.

Since TSP concentrations are not homogeneous, but are highly dependent on local factors, the modified gaussian model can be used to predict 24-hour TSP concentrations where point sources in the vicinity of a receptor are the primary contributors.

For example, at Hoyt Lakes Golf Course 27% of the predicted 24-hour TSP concentrations (based on point sources) were within a factor of 10 of the measured values, compared to only 9% at Fernberg Road, which is remote from the regional point sources. Table 66 provides a summary of these comparisons at seven sites.

Table 66. Percent of the predicted 24-hour concentrations that are within a factor of 10 of the measured concentrations.

Site	Percent	Possible Source Influences
Fernberg	9	No local sources
Ely	7	No local sources
Kawishiwi	17	Local dirt parking lot; dirt road
Dunka	18	Local dirt logging road
Toimi	41	Local gravel driveway
Erie Mining Office	35	Open pit mining operation
Hoyt Lakes Golf Course	27	Possibly Erie Mining, or auto traffic to golf course

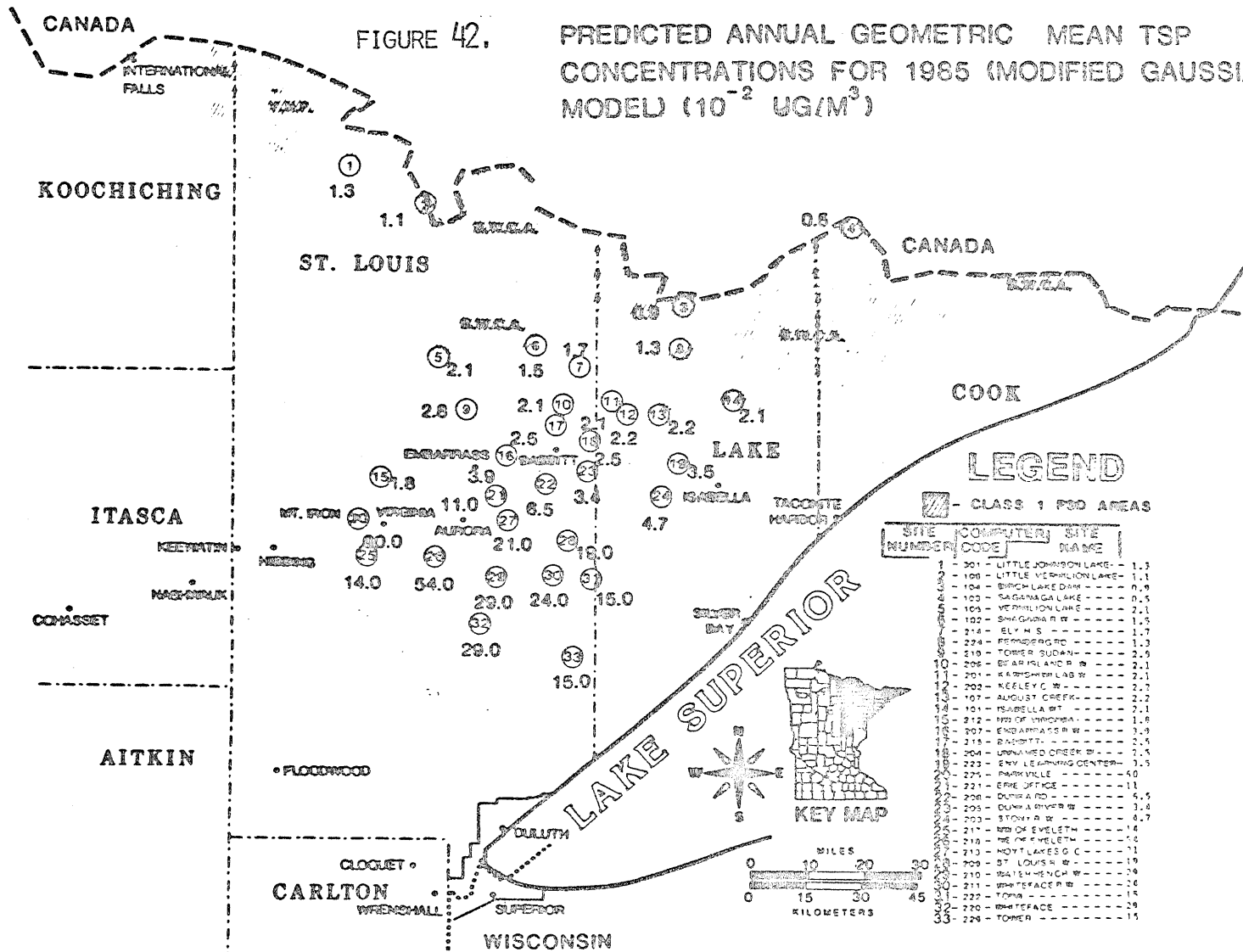
Although a regional TSP background concentration could be input into the model, and a better fit to the measured data could be obtained, the point source contribution would obviously be masked. The modeling results and subsequent discussions, therefore, are limited to the point sources listed in the emissions inventory.

In terms of TSP regulations it is not surprising that neither the federal primary ($75 \mu\text{g}/\text{m}^3$) nor secondary ($60 \mu\text{g}/\text{m}^3$) annual TSP standards are predicted to be exceeded in the region based on the point source modeling results for 1977 and 1985. The predicted 1985 annual TSP levels from expected point source emissions are shown in Figure 42.

ATKOVAN •

FIGURE 42.

PREDICTED ANNUAL GEOMETRIC MEAN TSP CONCENTRATIONS FOR 1985 (MODIFIED GAUSSIAN MODEL) (10^{-2} UG/M³)



-258-

When the predicted annual means at each site in the region are averaged, regional means of about $0.1 \mu\text{g}/\text{m}^3$ are calculated for both 1977 and 1985. Although point source particulate emissions in the region expected to decrease 38% from 1977 to 1985, the regional averages are about the same for the two years because of higher annual averages at a few sites that are impacted by sources which show substantial increases in emissions from 1977 to 1985. For example, the receptor northeast Eveleth shows nearly a doubling of ambient annual TSP concentrations from 1977 to 1985. This receptor is impacted primarily by Eveleth and Gilbert, and TSP emissions from these two locations are predicted to increase by about 130% from 2,545 mtpy in 1977 to 5,818 mtpy in 1985.

The highest predicted annual concentrations in the region occurred at Parkville for both 1977 ($0.7 \mu\text{g}/\text{m}^3$) and 1985 ($0.6 \mu\text{g}/\text{m}^3$). Both values are less than 1% of the annual primary ambient air quality standard, and are 5-7% of background concentrations of $10-12 \mu\text{g}/\text{m}^3$.

Neither the annual TSP Class I ($5 \mu\text{g}/\text{m}^3$) nor the Class II ($19 \mu\text{g}/\text{m}^3$) PSD increments are expected to be exceeded by point sources in the region. The largest modeled annual difference in a Class I area was $0.02 \mu\text{g}/\text{m}^3$ at Dunka River Watershed (less than 0.1% of the increment); the largest difference in the Class II area was $0.3 \mu\text{g}/\text{m}^3$ at the site northwest of Eveleth (1.5% of the increment). Although area source particulate contributions are important in determining whether or not ambient air quality standards will be exceeded, this contribution is less important in the PSD review because differences are determined rather than absolute values.

On a regional basis, the proposed Atikokan power plant (800 MW)

contributes about 3% of the emissions; however, the effect on regional TSP concentration is negligible. A regional mean annual concentration of about $0.1 \mu\text{g}/\text{m}^3$ is calculated both with and without the power plant. The effect of the proposed plant is most pronounced at the Class I receptor sites where a 30% decrease is calculated (based on 8 Class I receptor sites) if the power plant is removed from the 1985 inventory.

7.2.2.2. Regulatory analysis--maximum 24-hour TSP concentrations: The modified gaussian model predicts that the maximum 24-hour TSP federal primary standard ($260 \mu\text{g}/\text{m}^3$) will not be exceeded by modeled point sources in 1977 or in 1985, but that the secondary standard ($150 \mu\text{g}/\text{m}^3$) will be exceeded at one site during each year. If a factor of two modeling error is applied, the possibility is raised that the primary standard could be exceeded at one receptor site. Figures 43 and 44 show the predicted 1977 regional baseline and 1985 maximum 24-hour concentrations at each receptor in the region.

In 1977 the predicted maximum 24-hour concentration was $172 \mu\text{g}/\text{m}^3$ (66% of the primary standard) at Parkville followed by a second high of $162 \mu\text{g}/\text{m}^3$ (62% of the primary standard) at the same site. By 1985, the predicted maximum 24-hour concentration is expected to drop slightly to $160 \mu\text{g}/\text{m}^3$ at the Erie receptor followed by a second high of $150 \mu\text{g}/\text{m}^3$ at the same site. For comparison, Table 67 shows the air quality sampling sites where recorded TSP concentrations exceeded the 24-hour primary and secondary TSP standards during the 1976-77 sampling period.

The maximum 24-hour TSP increment is predicted to be exceeded in the Class II area ($37 \mu\text{g}/\text{m}^3$) but not in the Class I area ($10 \mu\text{g}/\text{m}^3$). The largest difference in the Class I area was $3 \mu\text{g}/\text{m}^3$ (30% of the

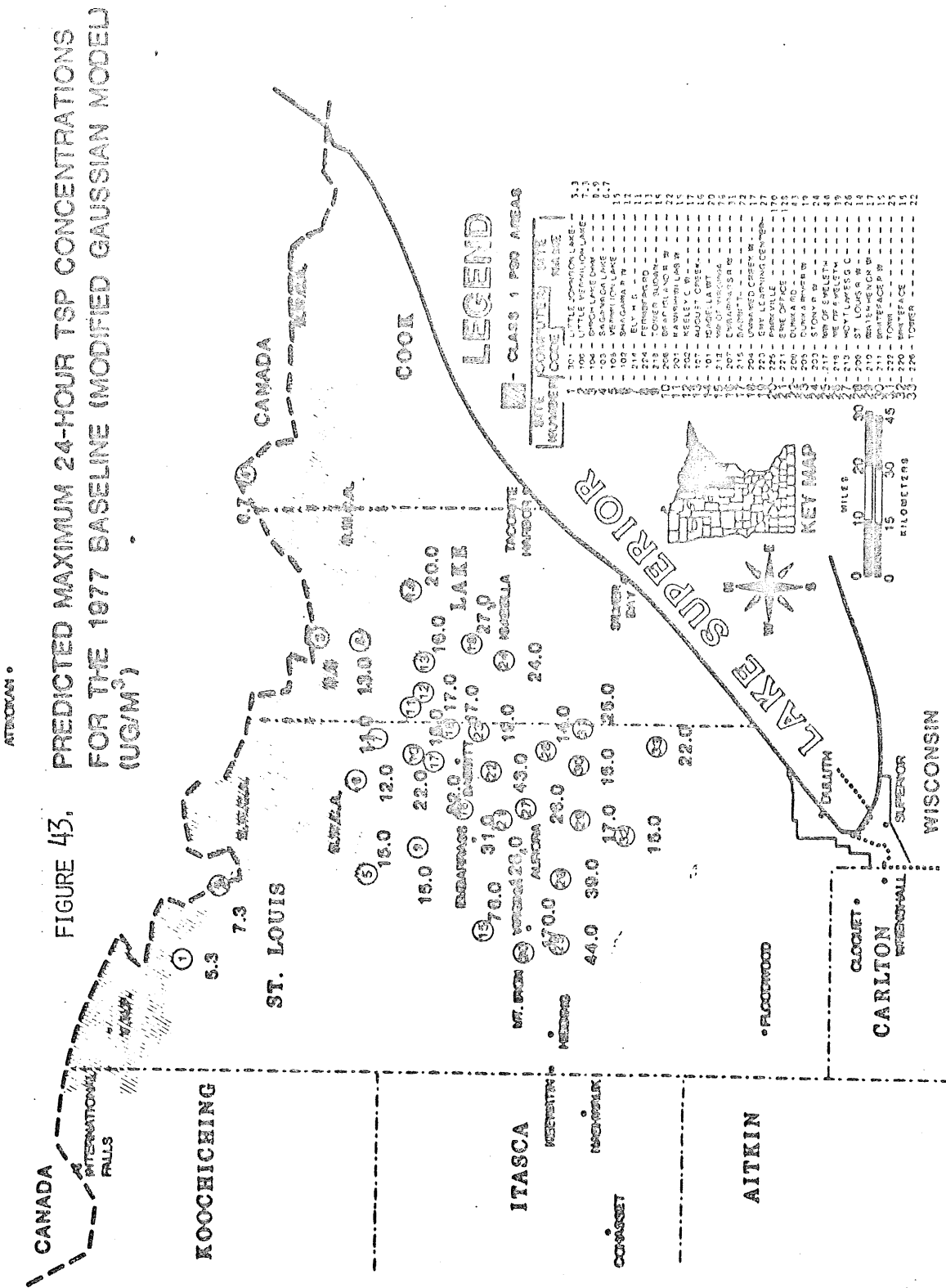
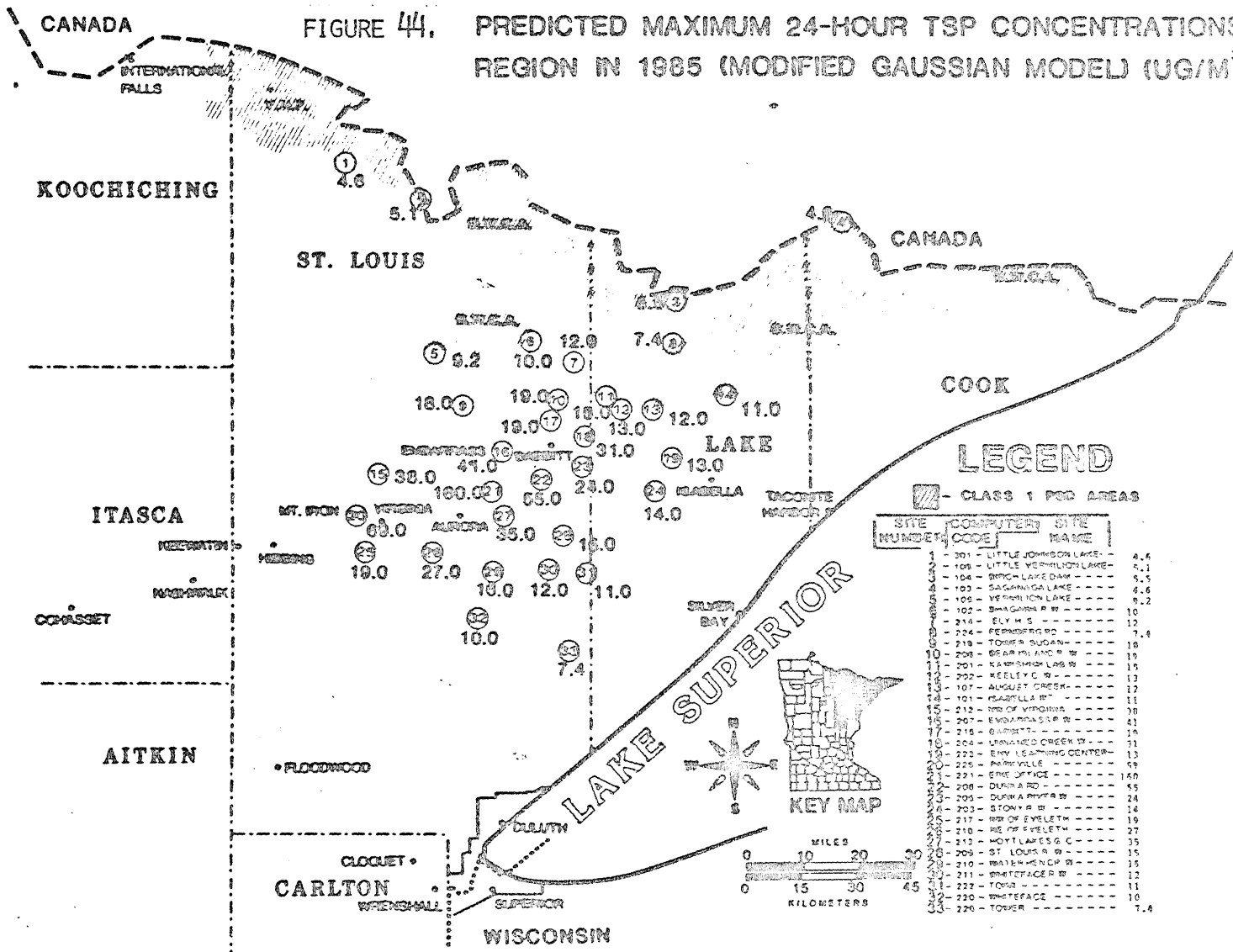


FIGURE 44. PREDICTED MAXIMUM 24-HOUR TSP CONCENTRATIONS IN THE REGION IN 1985 (MODIFIED GAUSSIAN MODEL) (UG/M³)

-262-



LEGEND

▨ - CLASS 1 POP AREAS

SITE NUMBER	COMPUTER CODE	SITE NAME	CONCENTRATION
1	201	LITTLE JOHNSON LAKE	4.6
2	108	LITTLE VERMILION LAKE	5.1
3	104	BIRCH LAKE DAM	5.5
4	103	SAGANAGA LAKE	4.6
5	105	VERMILION LAKE	5.2
6	102	SHAGODA R W	10
7	214	ELY W S	12
8	224	REIMSBERG RD	7.4
9	218	TOWER SUONA	11.0
10	208	BEAR H AND R W	19
11	201	KAWISHAW LAS W	15
12	202	KEELYE W	13
13	107	AUGUST CREEK	17
14	101	ISABELLA R	11
15	212	RD OF VERMION	10
16	207	EMERALD STAR W	41
17	215	QUINCY	19
18	204	LONGHED CREEK W	31
19	222	EVY LEARNING CENTER	13
20	225	PARROTTVILLE	58
21	221	ENE OFFICE	160
22	208	DUMBA RD	55
23	205	DUMBA RIVER W	24
24	203	STONY R W	16
25	217	RD OF EYELETH	19
26	210	RD OF EYELETH	27
27	212	MOYTLAKES G C	35
28	205	ST LOUIS R W	15
29	210	WATER HENR W	15
30	211	WHITEFACE R	22
31	223	TOWER	11
32	220	WHITEFACE	10
33	220	TOWER	7.4

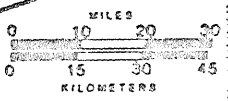


Table 67. Summary of 24-hour TSP measurements during the 1976-77 sampling period which exceeded the primary (260 ug/m³) and secondary (150 ug/m³) ambient TSP standards.

Site	24-hour TSP concentrations (ug/m ³)
Virginia	367, 310, 233, 214, 211, 193, 177, 177, 167, 151
Hibbing	279
Dunka Road	243, 174, 153
Mountain Iron	201, 179, 174, 165
Hoyt Lakes Police Station	191, 178

SOURCE: Endersen and Feeney⁶²

increment), which occurred at the receptor site in the Isabella watershed. Table 68 summarizes the predicted values exceeding the 24-hour TSP PSD increment in the Class II areas. Removing the proposed Atikokan power plant from the 1985 emissions inventory did not significantly affect the maximum 24-hour TSP concentrations at any receptor.

In summary, neither the annual TSP ambient air quality standards nor the TSP annual PSD Class I and Class II increments are predicted to be exceeded by point source regional growth in 1985. Annual TSP contributions from point sources in the region are low, less than 1% of the primary air quality standard. The maximum 24-hour TSP primary standard is not predicted to be exceeded in 1985, but the secondary standard is predicted to be exceeded.

The maximum 24-hour PSD increment is predicted to be exceeded in the Class II area but not in the Class I area. The proposed Atikokan power plant does not affect the regional mean annual concentration, but

Table 68. Predicted values exceeding the 24-hour TSP PSD₃ increment of 37 ug/m³ in Class II areas. Values in ug/m³.

Site	Baseling	1985		1985-Baseline ^a	
		High	2nd High	High	2nd High
Erie	118	160	152	42	34 ^b
Parkville	19	69	65	50	46

^bThis difference does not exceed the increment.

does have some impact on the Class I receptors. If it is assumed that the TSP sources shown in the emissions inventory will exist in 1985, further growth in the region could be precluded because both the 24-hour ambient air quality secondary standards and the allowable PSD Class II increments could be exceeded by point source emissions in the region.

Figure 45 presents box plots of predicted 24-hour TSP concentrations for 1977 and 1985 at regional receptors. Figure 46 shows the frequency distribution of these TSP concentrations for 3 sites in the region, permitting a comparison of a rural site, Isabella, with two community sites, Hoyt Lakes Golf Course and Parkville.

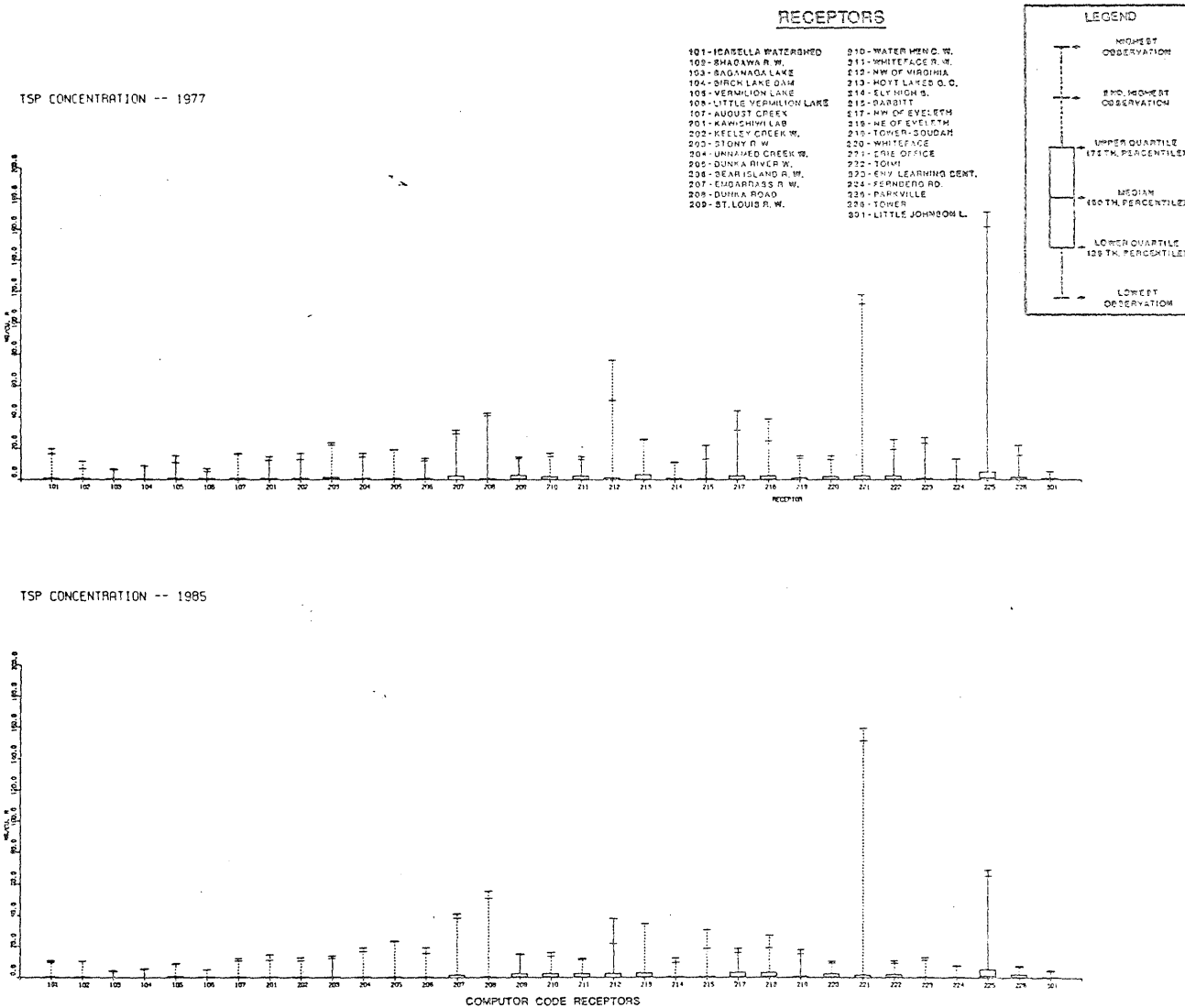
7.2.3. Particulate deposition.

Total particulate deposition was not measured in the region; however, deposition rates were measured for elemental constituents such as copper, nickel, and other metals, and these data are presented in Chapter 10.

Predictions of total particulate deposition in the region from local point sources were made using the modified gaussian model.

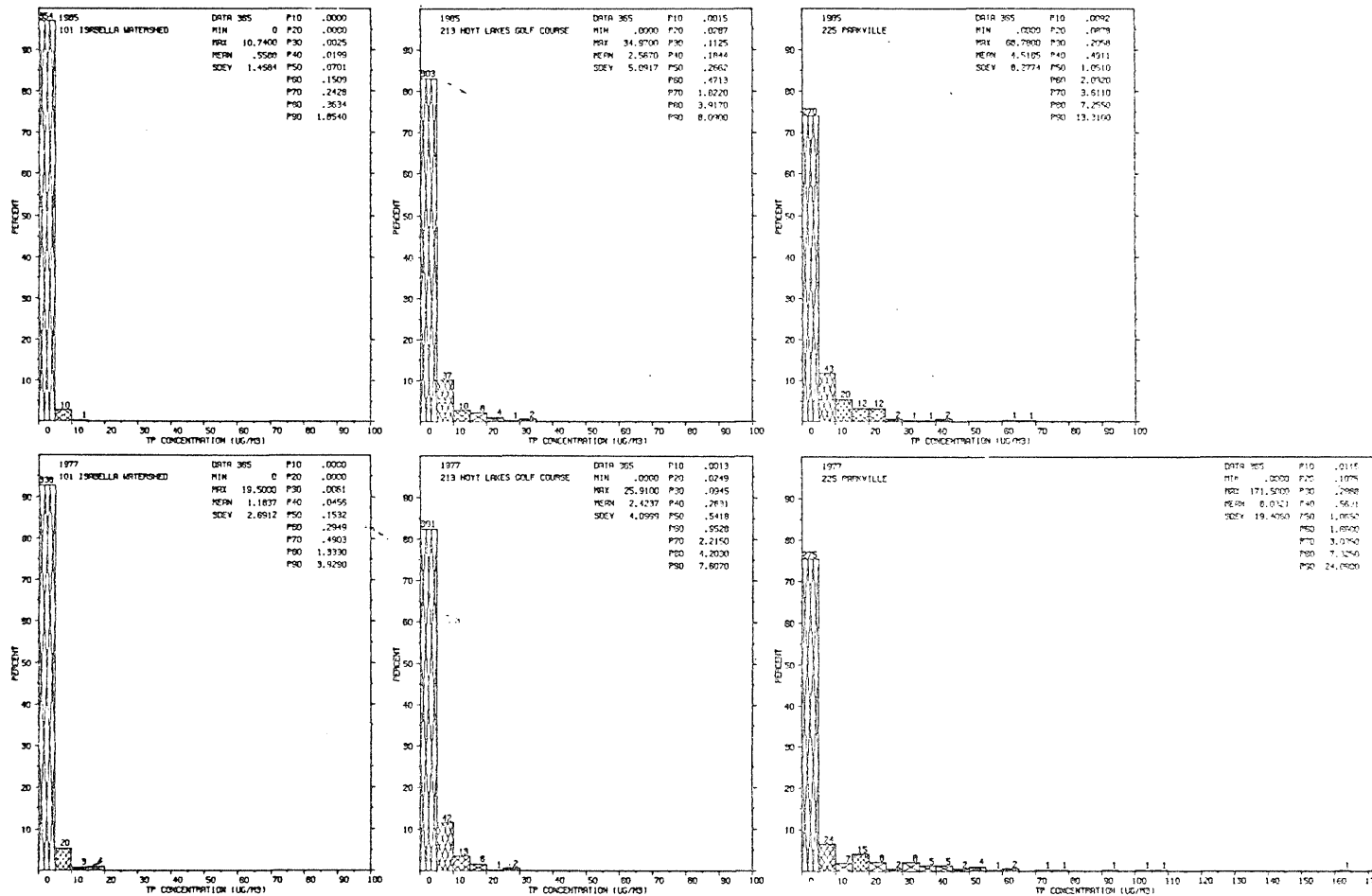
Figure 47 provides box plots of the predicted 1977 and 1985 24-hour

FIGURE 45. BOX PLOTS OF PREDICTED 24-HOUR TSP CONCENTRATIONS (MODIFIED GAUSSIAN MODEL).



ANNUAL FREQUENCY DISTRIBUTION OF PREDICTED 24-HOUR TSP CONCENTRATIONS,
1977 AND 1985, AT SELECTED SITES (MODIFIED GAUSSIAN MODEL).

FIGURE 46

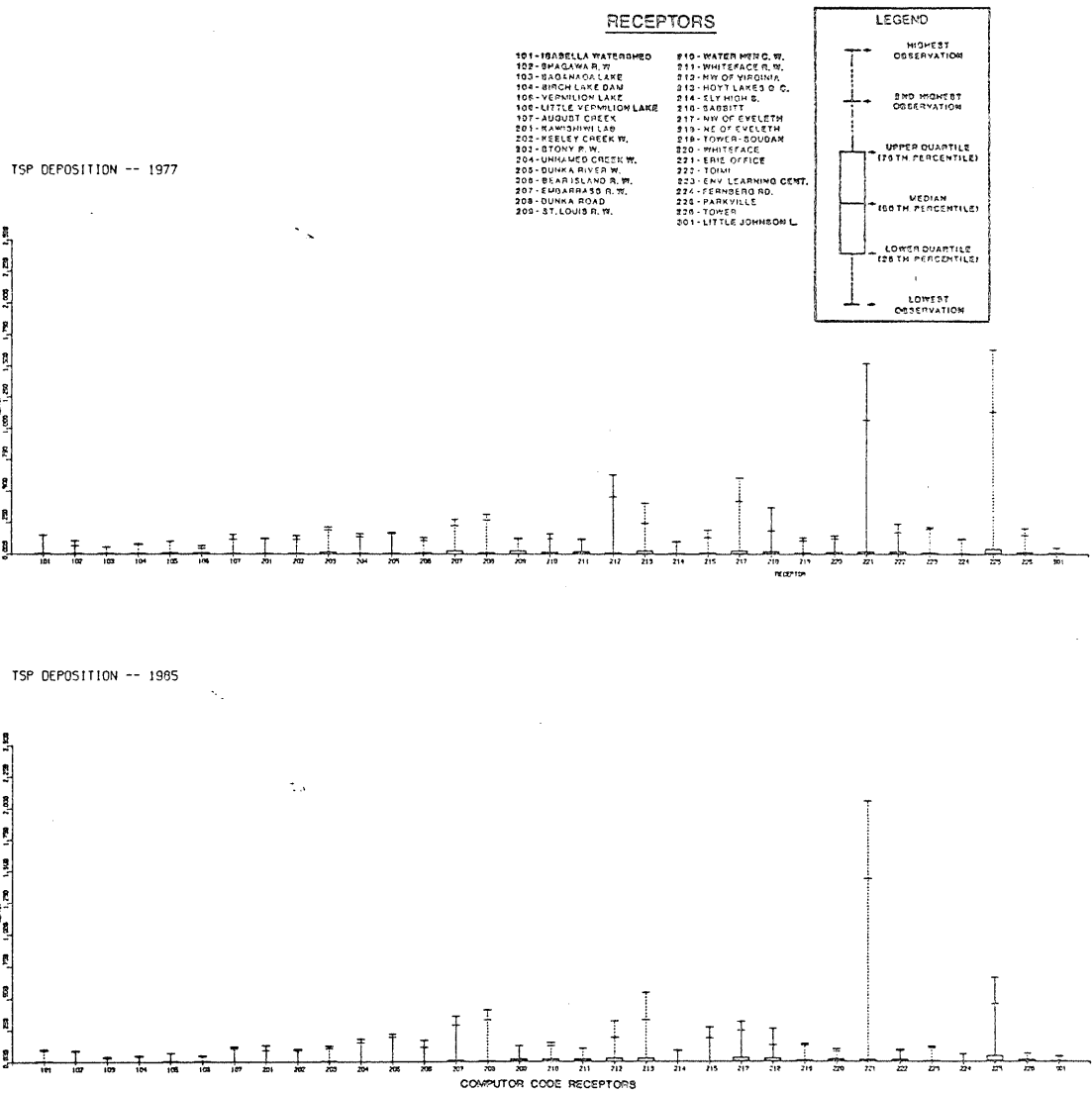


deposition values, and Figure 48 shows predicted annual frequency distributions of the 24-hour values at 3 sites in the region. These results are given to provide a reference for subsequent modeling of potential particulate deposition from a smelter operation. Modeled values of local point source contributions to TSP deposition are typically less than 50 gm/ha in a 24-hour period, but range up to 600 gm/ha or more in several cases.

Table 69 summarizes the predicted annual deposition of particulates at all receptor sites from local point source emissions for 1977 and 1985. Aside from elevated levels near population centers and industrial sources, values tend to range from 1 to 5 kg/ha/yr. Deposition rates near major sources are above 10 kg/ha/yr.

FIGURE 47.

BOX PLOTS OF PREDICTED 24-HOUR TSP DEPOSITION VALUES (MODIFIED GAUSSIAN MODEL).



-268-

ANNUAL FREQUENCY DISTRIBUTIONS OF PREDICTED 24-HOUR TSP DEPOSITION VALUES, 1977 AND 1985, AT SELECTED SITES (MODIFIED GAUSSIAN MODEL).

FIGURE 48

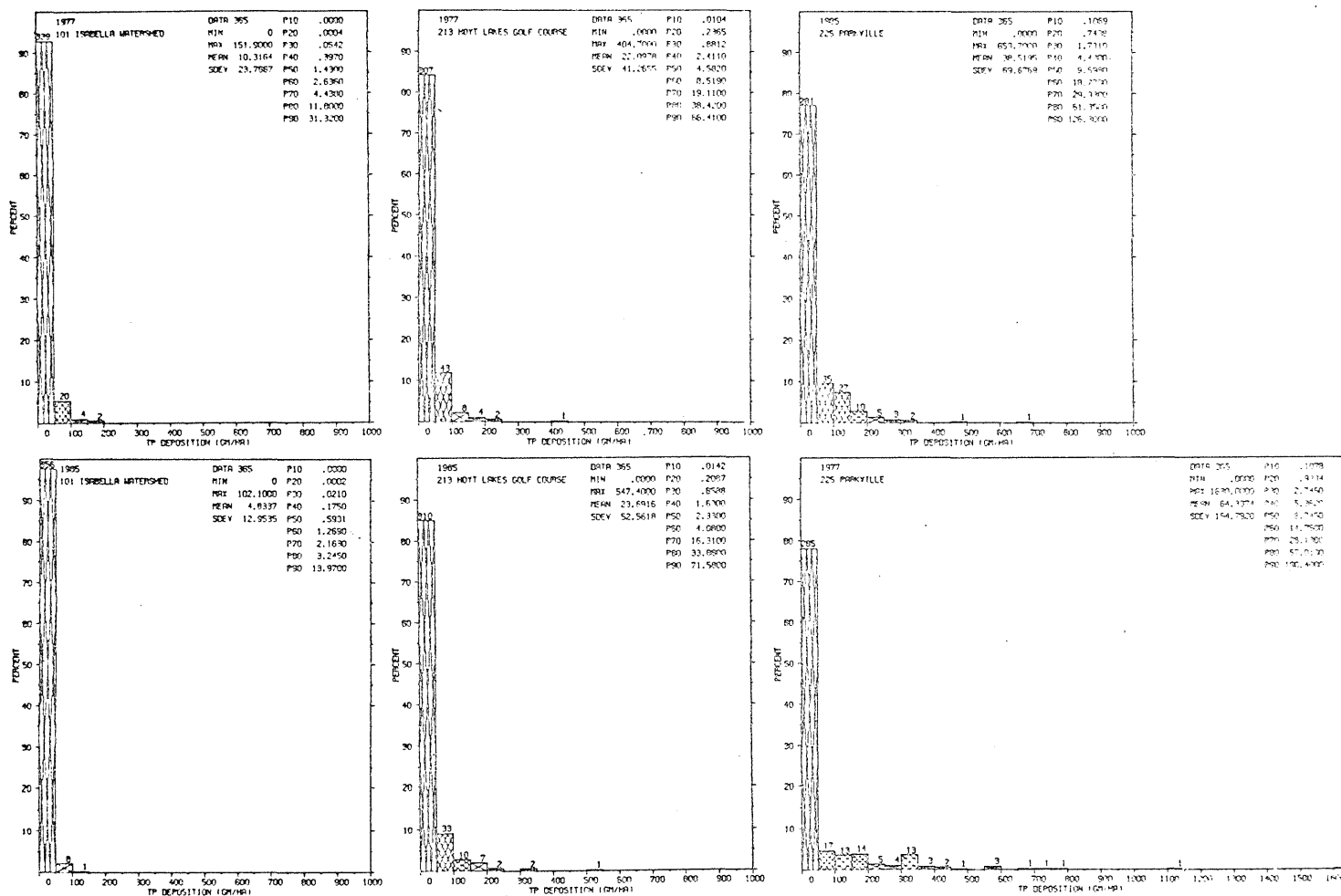


Table 69. Predicted annual deposition of particulates at various receptor sites due to point source emissions in the region (kg/ha/yr).

SITE NO.	COMPUTER CODE	NAME	1977	1985	PERCENT
			REGIONAL BASELINE	PROJECTION	CHANGE BY 1985
1	301	Little Johnson Lake	1.9	1.2	-37
2	106	Little Vermillion Lake	2.2	1.3	-41
3	104	Birch Lake Dam	2.0	1.0	-50
4	103	Saganaga Lake	1.6	0.6	-62
5	105	Vermillion Lake	3.3	2.8	-15
6	102	Shagawa R. W.	2.9	2.1	-28
7	214	Ely High School	3.2	2.0	-39
8	224	Fernberg Road	2.6	1.2	-54
9	219	Tower-Sudan	4.0	4.0	0
10	206	Bear Island R.W.	3.7	2.7	-27
11	201	Kawishiwi Lab W.	3.6	2.0	-44
12	202	Keeley Creek W.	3.9	2.1	-46
13	107	August Creek	4.0	2.1	-47
14	101	Isabella Watershed	3.8	1.8	-53
15	212	NW of Virginia	9.3	6.9	-26
16	207	Embarrass R.W.	6.7	6.6	-1
17	215	Babbitt	4.3	3.6	-16
18	204	Unnamed Creek W.	4.5	3.2	-29
19	223	Environ. Learning C.	5.3	2.8	-47
20	225	Parkville	23	7.9	-66
21	221	Erie Office	16	20	+25
22	208	Dunka Road	7.9	8.2	+4
23	205	Dunka River W.	5.3	4.7	-11
24	203	Stony River W.	6.2	3.1	-50
25	217	NW of Eveleth	8.9	7.6	-15
26	218	NE of Eveleth	7.1	7.0	-1
27	213	Hoyt Lakes Golf C.	8.1	8.6	+6
28	209	St. Louis R. W.	6.3	5.7	-10
29	210	Waterhen Creek W.	5.2	5.0	-4
30	211	Whiteface River W.	5.7	5.2	-9
31	222	Toimi	5.8	4.4	-24
32	220	Whiteface	4.9	4.4	-10
33	226	Tower	4.2	3.4	-19

CHAPTER 8. IMPACT ANALYSIS FOR SULFUR EMISSIONS

In previous chapters the major sources of atmospheric pollutants from potential smelting operations were identified, the region was characterized in terms of present sources and future development, and the atmospheric impacts of regional growth were discussed. This chapter and chapter 9 will assess the atmospheric impacts of a smelter alone and in terms of anticipated regional growth in order to highlight the regulatory, health, and environmental implications of copper-nickel development.

The purpose of the atmospheric modeling program was to estimate the spatial and temporal impacts of emissions from the various smelter cases, and to provide a consistent comparison of development alternatives.

Ideally, all possible smelter locations would have been considered by the modeling program. Since this was unrealistic, geographic areas of modeling similarity were identified on the basis of terrain features and wind regimes. The modeling effort was concentrated near the copper-nickel ore body where atmospheric dispersion patterns are considered to be fairly uniform.

The modified gaussian modeling results do not consider short-range effects within 5 km of the smelter. Although it was demonstrated that the modified gaussian model generally compares favorably to the standard short-range gaussian model, the long-range model may underestimate the extent of the area affected by elevated readings if receptors are not located on a preferred wind axis from the source. Since the short-range model is not reliable at distances more than 10-15 km from the source,

both types of models are needed to produce a complete picture. The results of the short-range modeling simulations are given in Enderesen.⁶¹

8.1. AMBIENT SO₂ CONCENTRATIONS

This section discusses the predicted ambient annual and 24-hour SO₂ concentrations resulting from point sources (smelter stack and fugitive emissions along with existing and projected regional point source emissions) in terms of ambient air quality standards and allowable PSD increments. The atmospheric impacts of the three smelter cases are presented and then discussed in combination with projected regional growth by 1985.

8.1.1. Annual concentrations.

It must be noted in the following discussion that when various ambient air quality standards are expected to be exceeded, this does not imply a violation of the standard. The distinction is noted for two reasons. First, the occurrence of a violation is a legal determination to be made only by a properly authorized body such as the Minnesota Pollution Control Agency. Second, one 24-hour value greater than the standard at a given site is not considered a violation, but much of the following discussion is in the context of a single maximum 24-hour value predicted at a given receptor site. Therefore, situations are highlighted where problems are most likely to arise in the context of present air quality regulations, but legal determinations are not made.

A hypothetical smelter site was selected at a location 4.8 km south of Babbitt. This reference location does not imply that a smelter has been proposed or is being recommended at this site. Neither of these is the case. The selected site does lie adjacent to the most active

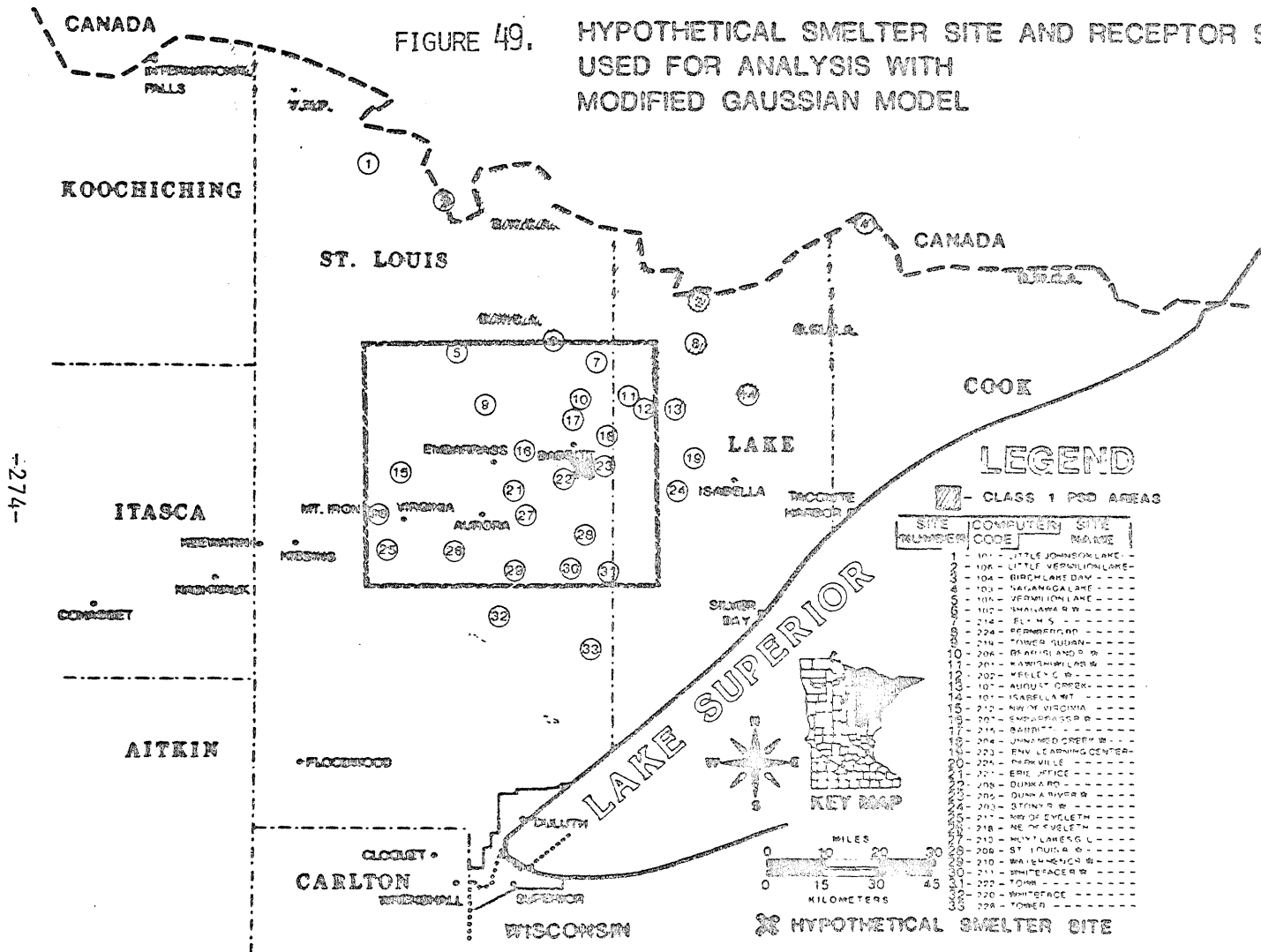
mining exploration in the area, so it is reasonable to consider the the implications of a smelter in the vicinity. Figure 49 shows the hypothetical smelter site in relation to the various receptor sites used in the modified gaussian model simulations.

With these locational caveats in mind, the modified gaussian model was used to predict annual SO₂ concentrations resulting from the three smelter cases at the various regional receptors. The results are shown in Figures 50, 51 and 52. The modified gaussian model predicts that the annual ambient air quality SO₂ standards would not be exceeded by any of the three smelter models. The closest receptor to the hypothetical smelter site is the Dunka River Watershed located about 5 km east of the source. The highest predicted annual average for the region is 4.7 µg/m³ which, of course, occurs for the base case smelter at the Dunka River Watershed receptor. This is only about 6% of the federal primary annual ambient air quality standard. The highest annual averages predicted for the option 1 and option 2 smelters are 2.1 µg/m³ and 0.79 µg/m³ which are about 3% and 1% of the primary standard, respectively.

The results also indicate that for this location in the region, none of the smelter models alone are predicted to exceed the Class I or Class II PSD annual increments (2 and 20 µg/m³, respectively) at any of the receptor sites. The highest concentrations (occurring for the base case smelter) in Class I and Class II areas are 0.47 µg/m⁴ and 4.7 µg/m³, respectively. These values are both about 25% of the allowed increments. Using the option 1 smelter in the simulations drops these highs by about 50% to 0.21 µg/m³ and 2.1 µg/m³, respectively. The option 2 smelter results in further decreases to 0.08 µg/m³ and 0.79 µg/m³,

ATKOKAN •

FIGURE 49. HYPOTHETICAL SMELTER SITE AND RECEPTOR SITES USED FOR ANALYSIS WITH MODIFIED GAUSSIAN MODEL

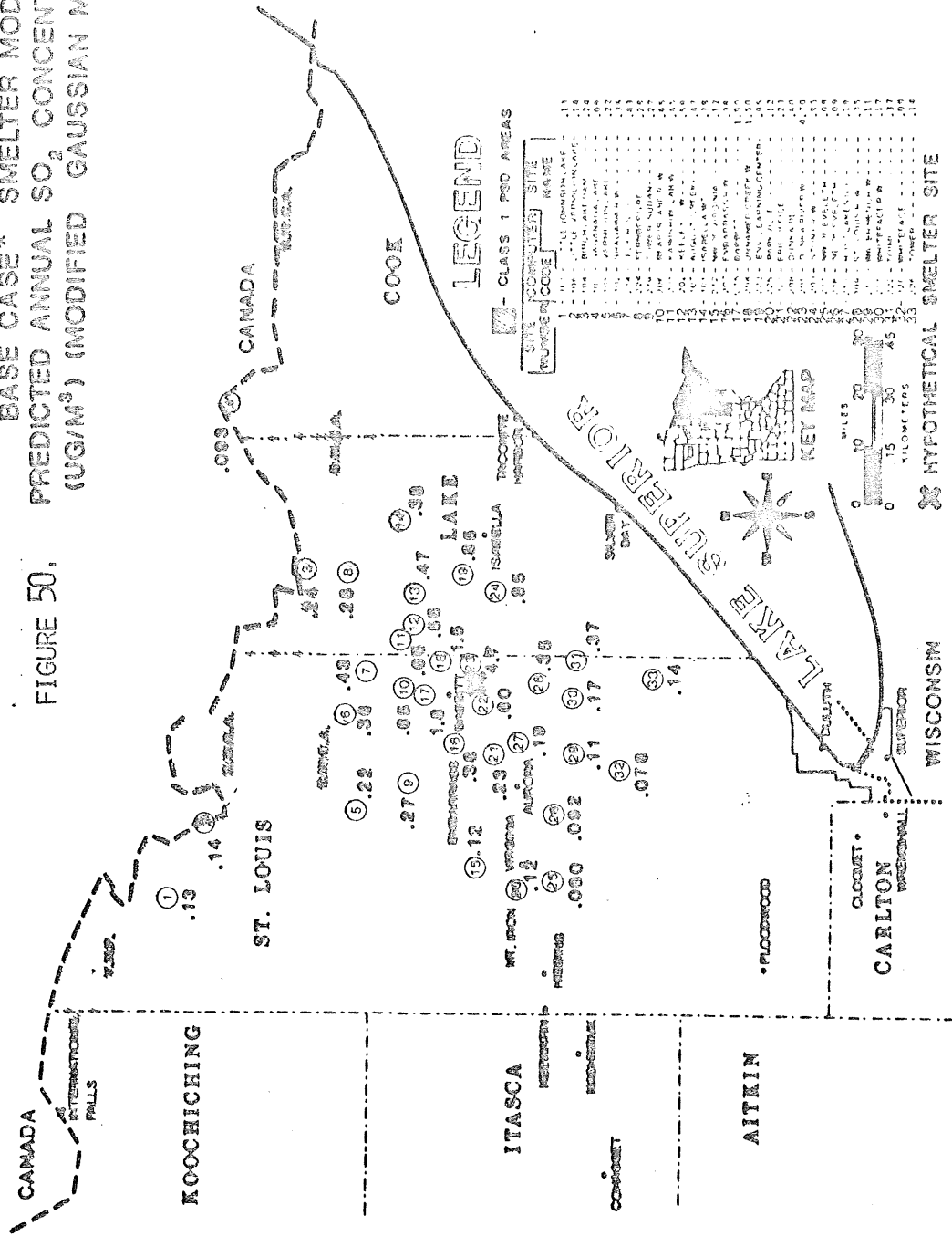


SITE NUMBER	COMPUTER CODE	SITE NAME
1	101	LITTLE JOHNSON LAKE
2	102	LITTLE VERMILION LAKE
3	103	BIRCH LAKE DAM
4	104	NAGANOGA LAKE
5	105	VERMILION LAKE
6	106	WARREN LAKE
7	107	ELM S
8	204	FERMEGARD
9	214	TOWER GARDEN
10	206	BRANT ISLAND R
11	204	HAWTHORNE LAKE
12	202	WELLEY C R
13	107	AUGUST CREEK
14	101	ISABELLA MT
15	212	RUN N VIRGINIA
16	207	EMPHYSOGR R
17	215	BAHMIT
18	204	UNNAMED CREEK W
19	203	ENV LEARNING CENTER
20	204	FRANKVILLE
21	207	ERIE OFFICE
22	208	DUNKARD
23	205	DUNKARD RIVER
24	203	STINK R
25	211	NE OF EVELETH
26	218	NE OF EVELETH
27	210	MOUNT LAKE G L
28	208	ST LOUIS A O
29	210	WALLENHOLM R
30	211	WHITEFACE R
31	202	TOWER
32	202	WHITEFACE
33	208	TOWER

-274-

BOUNDARY OF REGIONAL STUDY AREA

ATROGAN •
FIGURE 50. BASE CASE* SMELTER MODEL
 PREDICTED ANNUAL SO₂ CONCENTRATIONS
 (UG/M³) (MODIFIED GAUSSIAN MODEL)

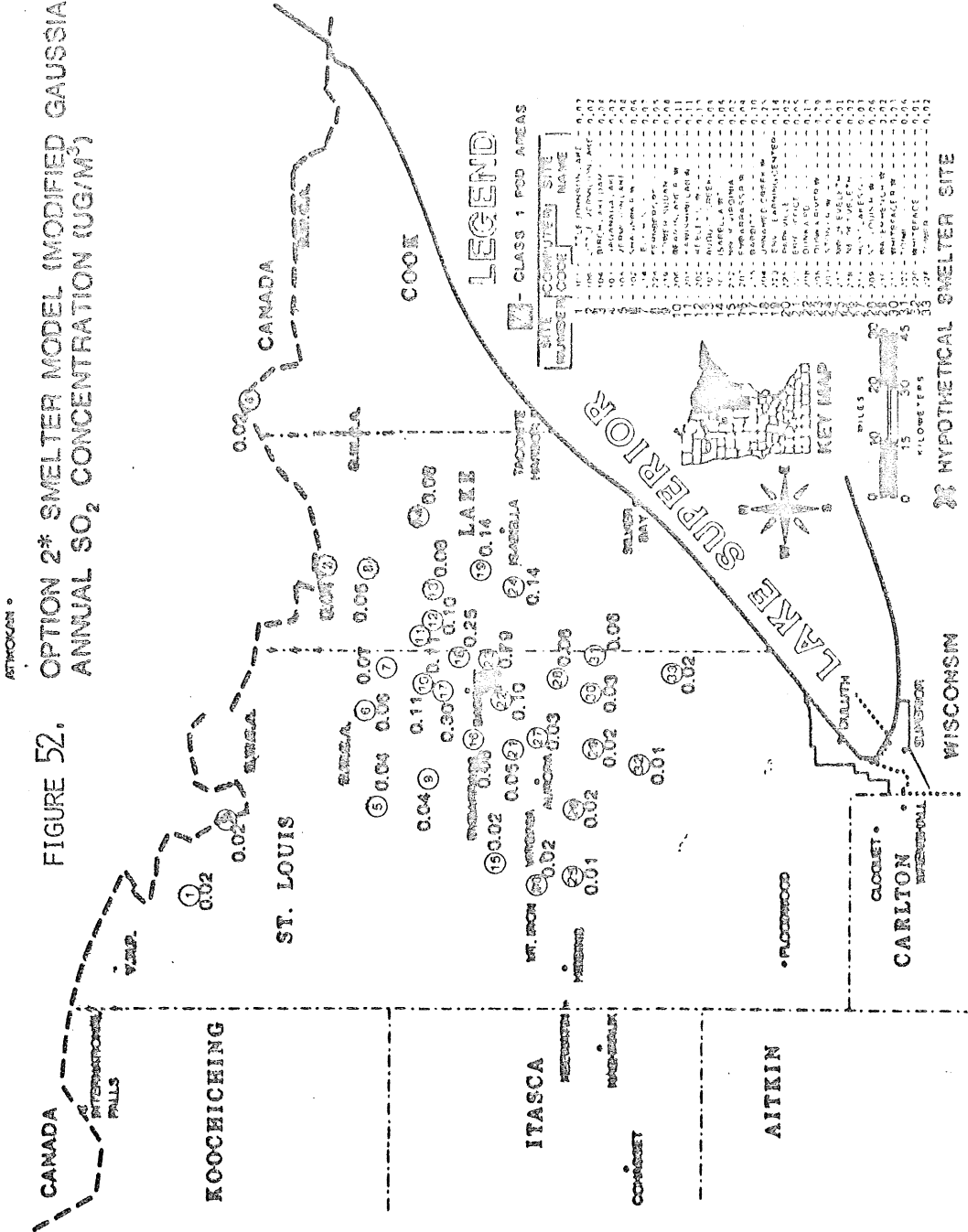


CLASS 1 PSD AREAS

SITE NUMBER	COMPUTER SITE NAME
1	LAKE SUPERIOR
2	LAKE SUPERIOR
3	LAKE SUPERIOR
4	LAKE SUPERIOR
5	LAKE SUPERIOR
6	LAKE SUPERIOR
7	LAKE SUPERIOR
8	LAKE SUPERIOR
9	LAKE SUPERIOR
10	LAKE SUPERIOR
11	LAKE SUPERIOR
12	LAKE SUPERIOR
13	LAKE SUPERIOR
14	LAKE SUPERIOR
15	LAKE SUPERIOR
16	LAKE SUPERIOR
17	LAKE SUPERIOR
18	LAKE SUPERIOR
19	LAKE SUPERIOR
20	LAKE SUPERIOR
21	LAKE SUPERIOR
22	LAKE SUPERIOR
23	LAKE SUPERIOR
24	LAKE SUPERIOR
25	LAKE SUPERIOR
26	LAKE SUPERIOR
27	LAKE SUPERIOR
28	LAKE SUPERIOR
29	LAKE SUPERIOR
30	LAKE SUPERIOR
31	LAKE SUPERIOR
32	LAKE SUPERIOR
33	LAKE SUPERIOR

* STACK SO₂ EMISSION RATE 300 GM/SEC.
 FUGITIVE SO₂ EMISSION RATE 31 GM/SEC.

FIGURE 52. OPTION 2* SMELTER MODEL (MODIFIED GAUSSIAN MODEL)
ANNUAL SO₂ CONCENTRATION (UG/M³)



* STACK SO₂ EMISSION RATE 32 QM/SEC.
FUGITIVE SO₂ EMISSION RATE 31 QM/SEC.

respectively. Assuming a factor of two error in the modeling results, neither of the annual PSD increments would be in jeopardy at more than 5 km from a smelter located at the site south of Babbitt. However, a receptor 5 km from the smelter might easily experience annual concentrations greater than the Class I increment if the base case or option 1 smelters were moved so that this receptor fell into a Class I area.

The predicted annual average SO₂ concentrations from a smelter must be considered in the context of other SO₂ sources in the region, since standards are exceeded or not exceeded as a result of combined contributions from all sources in the region. Therefore, the effect of adding a smelter (located 4.8 km south of Babbitt) to those sources expected in the region by 1985 was evaluated.

Modeling results are summarized for the following cases:

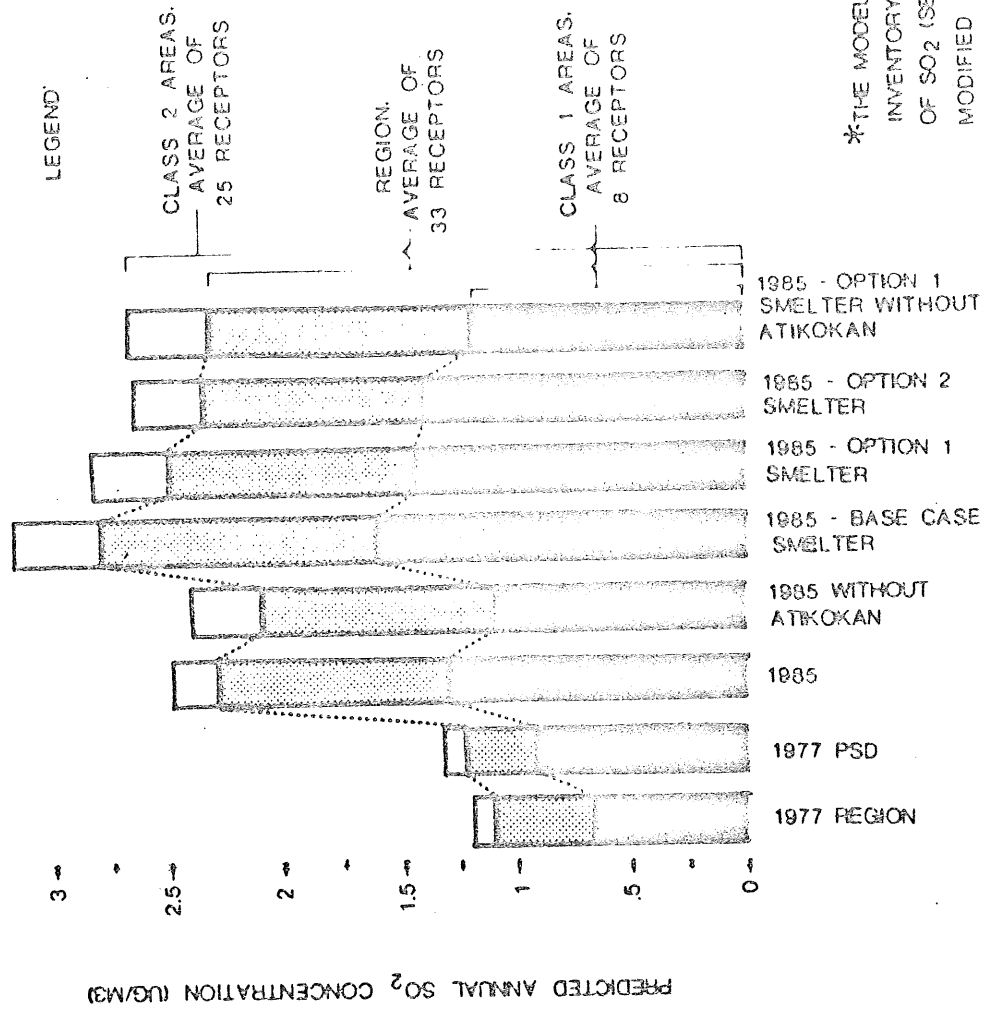
- 1) 1985 Region,
- 2) 1985 Region excluding the proposed Atikokan power plant,
- 3) 1985 Region with copper-nickel development: base case, option 1, and option 2 smelters, and
- 4) 1985 Region with option 1 smelter excluding the proposed Atikokan power plant.

Figure 53 shows the annual SO₂ averages for receptors in Class I areas, Class II areas, and all receptors in the region for the different cases. The predicted 1977 regional and PSD averages are also included for reference. Recall that the 1977 regional baseline differs slightly from the corresponding PSD baseline because it reflects slightly different values for the SO₂ point source emissions inventory.

The national annual primary SO₂ ambient air quality standard of 80 µg/m³ is not expected to be exceeded by any of the copper-nickel smelter configurations with anticipated regional growth by 1985. The

PREDICTED ANNUAL CLASS 1, CLASS 2 AND REGIONAL SO₂ AVERAGES WITH SELECTED SMELTER CASES (BASED ON A HYPOTHETICAL SMELTER SITE 3 MILES SOUTH OF BABBITT)*

FIGURE 53



*THE MODELING IS BASED ON THE EMISSIONS INVENTORY FOR LOCAL POINT SOURCES OF SO₂ (SEE SECTIONS 3.4.1.1). USING THE MODIFIED GAUSSIAN MODEL.

highest predicted annual SO₂ average (5.7 µg/m³ at Parkville) is less than about 7% of the standard. Substituting the option 1 or option 2 smelters into the simulations has little effect on the highest values. The regional sources predominate (with less than 10% effect from the smelter) in the southwest corner of the region from Parkville up to about 20 km from the smelter along the line of emission sources paralleling the Iron Range.

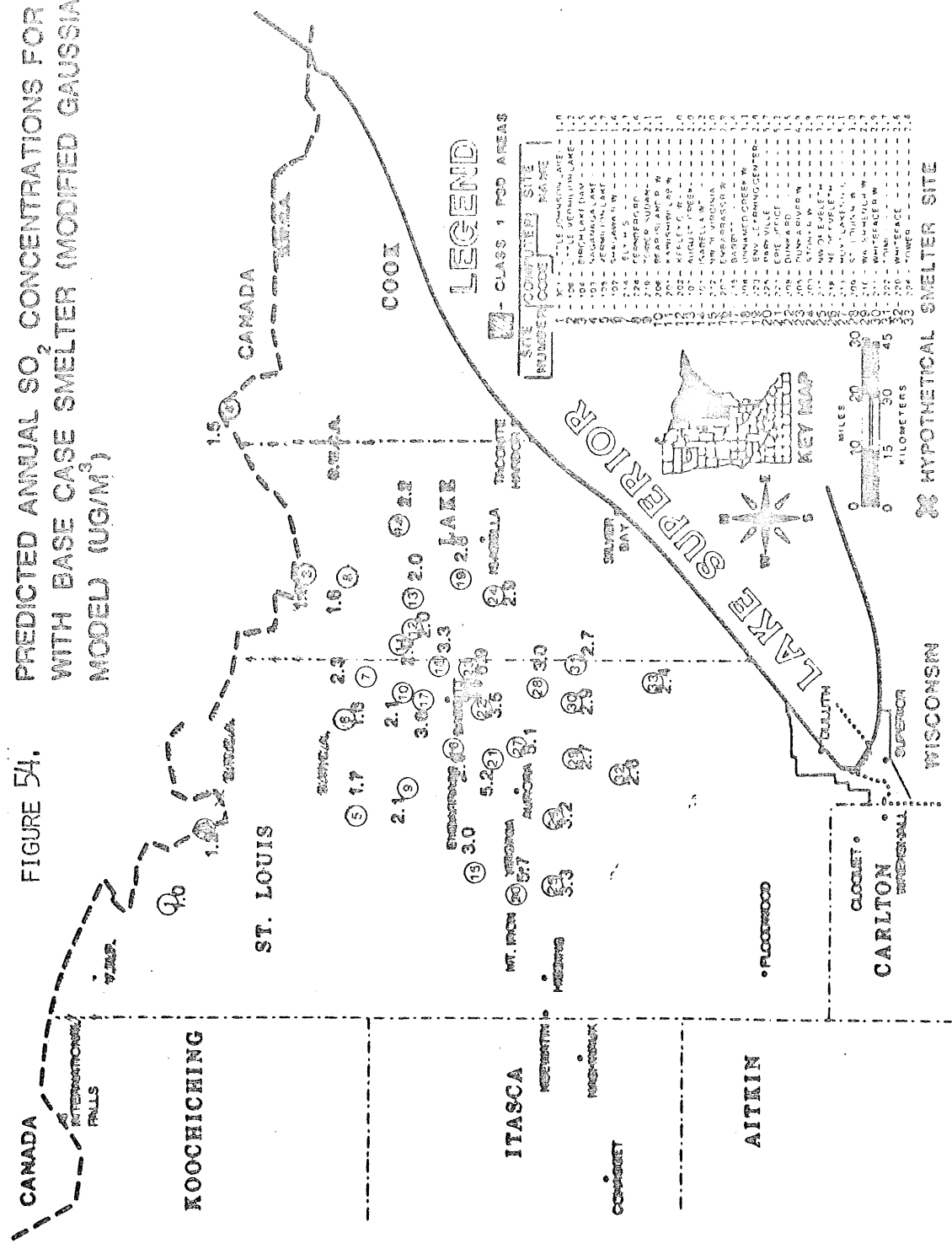
Figures 54,55,56, and 57, which show the predicted annual SO₂ concentrations at each receptor for the regional runs with copper-nickel development, are discussed below.

The option 1 smelter results in a regional annual SO₂ average (2.5 ug/m³) that is about 9% higher than without copper-nickel development. The annual averages in Class I and Class II areas are 1.4 µg/m³ and 2.8 µg/m³, respectively, compared to 1.3 µg/m³ and 2.5 µg/m³, respectively, without copper-nickel development.

The highest annual average SO₂ concentration with the option 1 smelter in Class I and Class II areas was 2.0 ug/m³ at Isabella Watershed and 5.6 µg/m³ at Parkville, respectively, compared to a high of 1.8 µg/m³ (at Isabella Watershed) and 5.6 µg/m³ (at Parkville) without copper-nickel development. The option 1 smelter has little effect on the annual concentrations in the Class II area except at sites located 20 km to the north and east, and sites located 30 km to the south and east. The most dramatic figures occur at Dunka River Watershed where the annual average is 4.3 µg/m³ with an option 1 development compared to 2.2 µg/m³ without copper-nickel development.

If a smelter uses state-of-the-art controls (option 2) then the

ATKINSON •
FIGURE 54. PREDICTED ANNUAL SO₂ CONCENTRATIONS FOR 1985 WITH BASE CASE SMELTER (MODIFIED GAUSSIAN MODEL) (UG/M³)



LEGEND

CLASS 1 FOOD AREAS

SITE NUMBER	COMPUTER SITE CODE	SITE NAME
1	X1	LEWIS AND CLARK
2	X2	LEWIS AND CLARK
3	X3	LEWIS AND CLARK
4	X4	LEWIS AND CLARK
5	X5	LEWIS AND CLARK
6	X6	LEWIS AND CLARK
7	X7	LEWIS AND CLARK
8	X8	LEWIS AND CLARK
9	X9	LEWIS AND CLARK
10	X10	LEWIS AND CLARK
11	X11	LEWIS AND CLARK
12	X12	LEWIS AND CLARK
13	X13	LEWIS AND CLARK
14	X14	LEWIS AND CLARK
15	X15	LEWIS AND CLARK
16	X16	LEWIS AND CLARK
17	X17	LEWIS AND CLARK
18	X18	LEWIS AND CLARK
19	X19	LEWIS AND CLARK
20	X20	LEWIS AND CLARK
21	X21	LEWIS AND CLARK
22	X22	LEWIS AND CLARK
23	X23	LEWIS AND CLARK
24	X24	LEWIS AND CLARK
25	X25	LEWIS AND CLARK
26	X26	LEWIS AND CLARK
27	X27	LEWIS AND CLARK
28	X28	LEWIS AND CLARK
29	X29	LEWIS AND CLARK
30	X30	LEWIS AND CLARK
31	X31	LEWIS AND CLARK
32	X32	LEWIS AND CLARK
33	X33	LEWIS AND CLARK
34	X34	LEWIS AND CLARK
35	X35	LEWIS AND CLARK

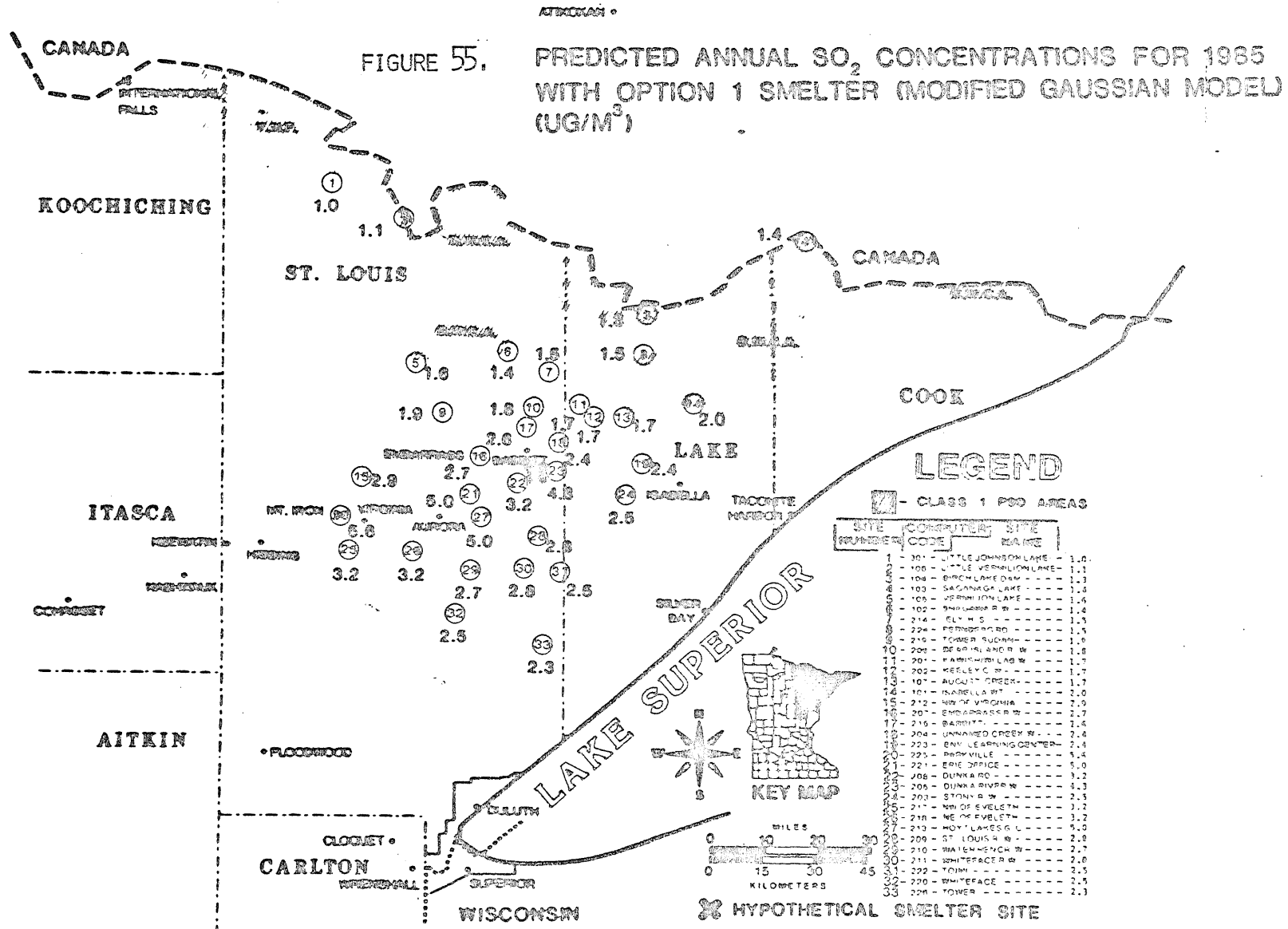
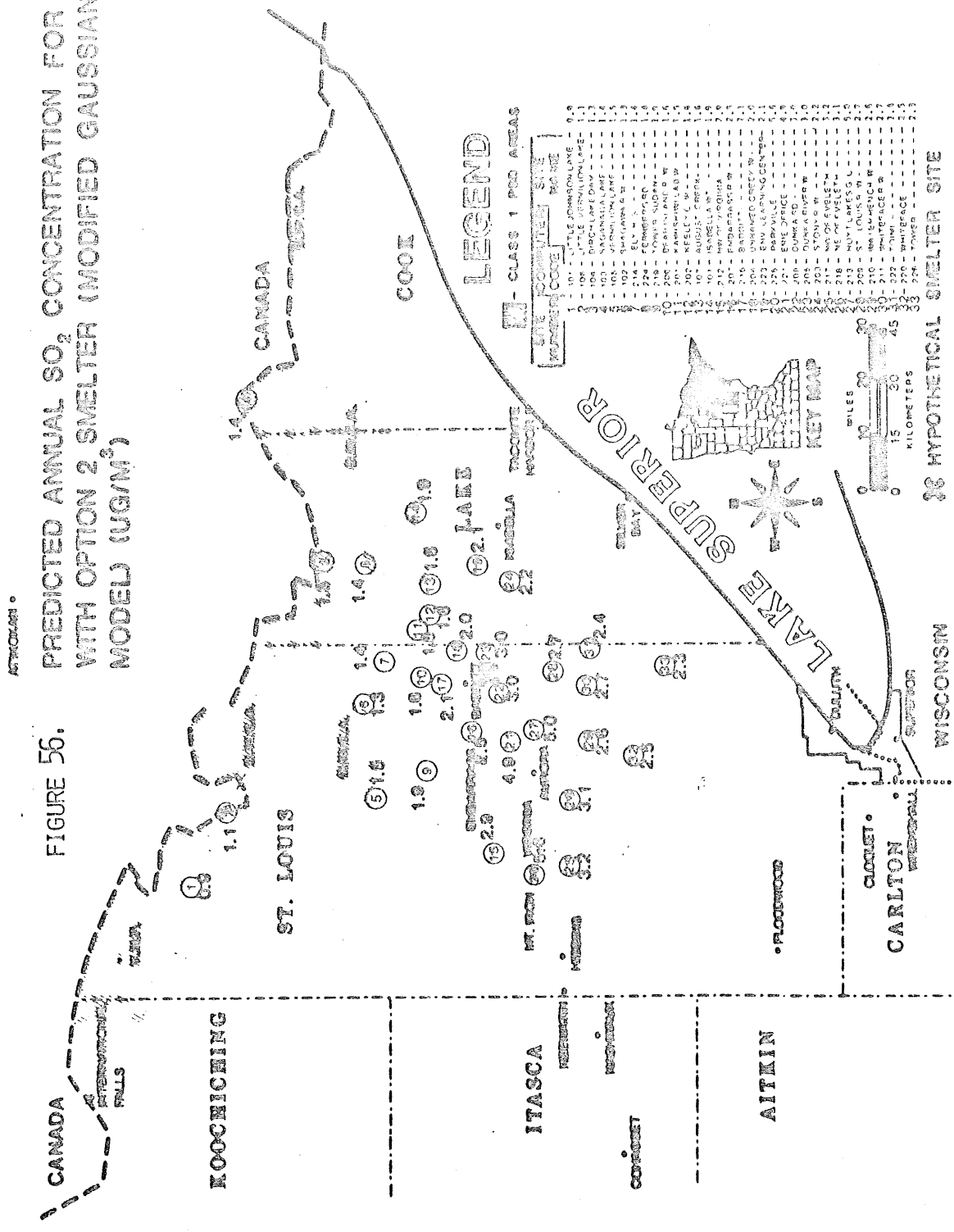
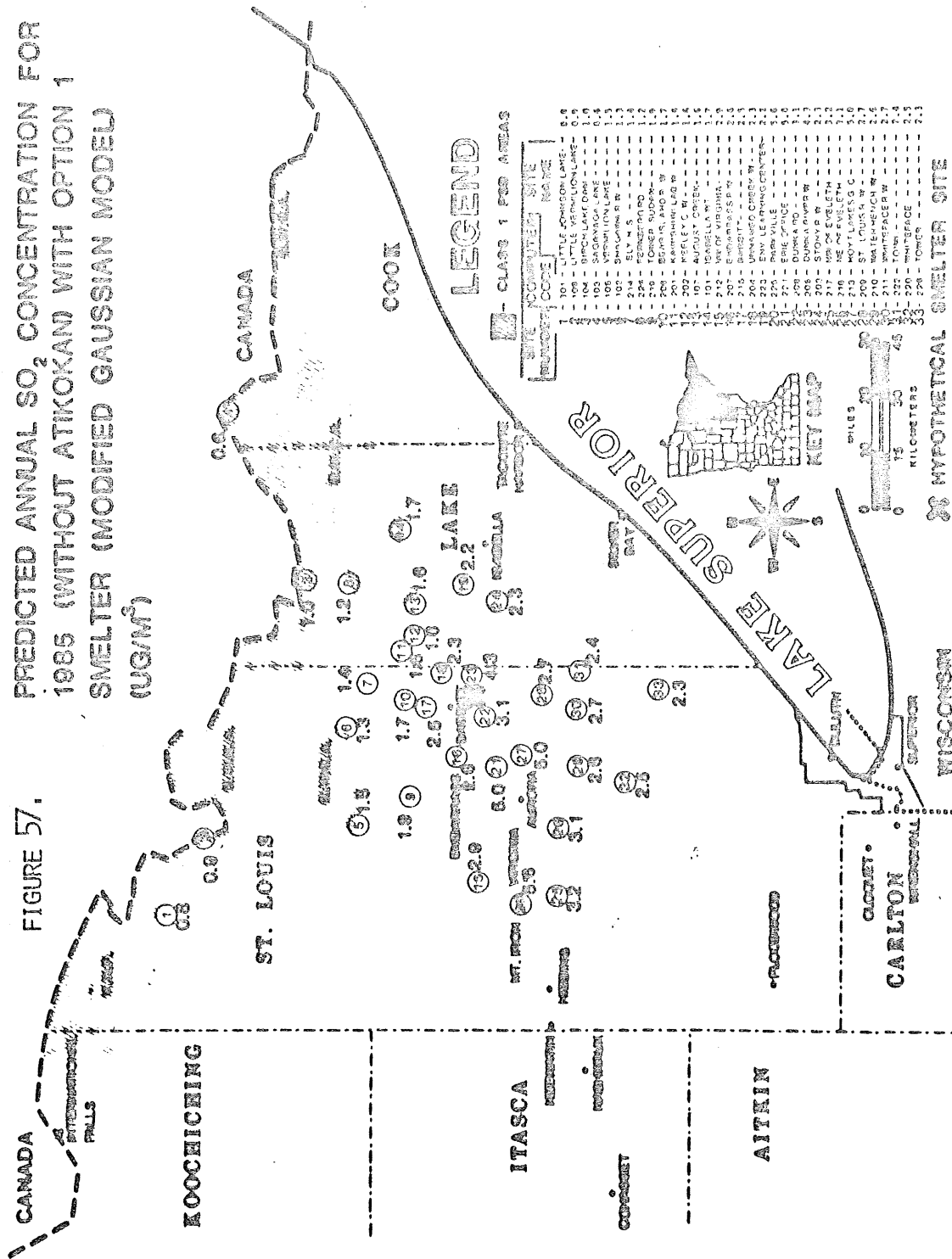


FIGURE 56. PREDICTED ANNUAL SO₂ CONCENTRATION FOR 1985 WITH OPTION 2 SMELTER (MODIFIED GAUSSIAN MODEL) (UG/M³)



ATKOKAN •
FIGURE 57.
PREDICTED ANNUAL SO₂ CONCENTRATION FOR
1985 (WITHOUT ATKOKAN WITH OPTION 1
SMELTER (MODIFIED GAUSSIAN MODEL
(UG/M³)



annual regional, Class I, and Class II averages decrease slightly below the option 1 levels.

If the smelter is controlled only to the level of the base case smelter, then the regional, Class I, and Class II averages increase over the option 1 levels by about 12%.

Removing the proposed Atikokan power plant (assumed to be 800 MW) from the annual regional runs with the option 1 smelter decreases the annual Class I SO₂ average by about 14% to 1.2 µg/m³. The annual Class II average remains about the same at 2.7 µg/m³, and the regional average decreases slightly to 2.3 µg/m³.

Annual SO₂ averages for the 1985 simulations with the three copper-nickel smelter models are summarized for sites showing the most variation in concentrations in Table 70.

Irrespective of the smelter site location, none of the three smelters in combination with other regional sources appear likely to exceed the allowed annual PSD Class II increment.

This conclusion does not apply to the Class I areas where the distance between any smelter site and the Class I area will be a major factor in the ability of a smelter to meet annual PSD Class I SO₂ increments.

Siting limitations based on annual averages will not be discussed further since the next section will show that the 24-hour PSD increments will place even more stringent restrictions on smelter siting.

8.1.2. 24-hour concentrations.

The discussion of 24-hour concentrations will be presented in two parts. First, in parallel with the previous discussion of annual average SO₂ concentrations, the focus will be on a hypothetical smelter site

Table 70. Summary of annual SO₂ concentration at selected sites for the various copper-nickel development cases₃ with a comparison to 1977 and 1985 predictions without copper-nickel development, µg/m³.

Receptor Site No.	Receptor Site Name	Receptor Relation To Hypothetical Smelter Site	1977 PSD/Region	1985	1985 + Base Case	1985 + Option 1	1985 + Option 2	
11	Kawishiwi Laboratory	22 km NE	0.79	0.75	1.5	2.0	1.7	1.5
24	Stony River W.	26 km E,SE	1.2	1.2	2.1	2.9	2.5	2.0
18	Unnamed Creek W.	9 km NE	0.93	0.87	1.7	3.3	2.4	2.0
23	Dunka River W.	5 km E	1.2	1.2	2.2	6.9	4.3	3.0
10	Bear Island River W.	18 km N	0.82	0.77	1.5	2.1	1.8	1.6
22	Dunka Road	7 km SW	1.3	1.2	2.9	3.5	3.2	3.0
19	Env. Learning C.	28 km E	1.2	1.1	2.0	2.8	2.4	2.1
Region Average (based on 33 sites)		---	1.2	1.1	2.3	2.8	2.5	2.3

located south of Babbitt. The smelters will be discussed in combination with other sources expected in the region by 1985. Second, since the Babbitt site is used only as a reference point, a non-site-specific discussion follows, with general conclusions about the potential restrictions to smelter siting based on the Class I 24-hour PSD increment.

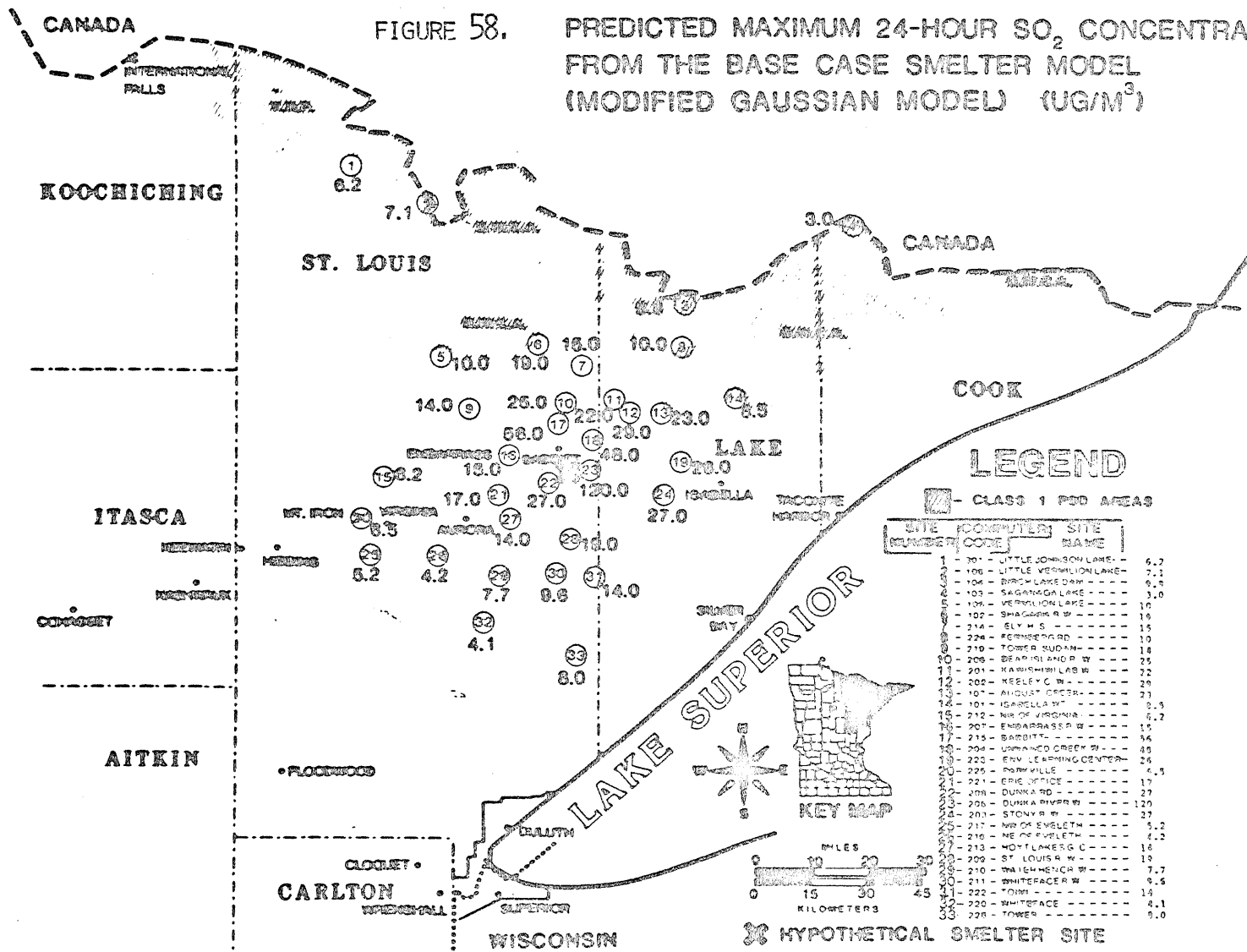
Figures 58, 59, and 60 show the predicted maximum 24-hour SO₂ concentrations resulting from the base case, option 1 and option 2 smelters when they are located south of Babbitt. The results indicate that the federal ambient standards are not predicted to be exceeded at any of the regional receptors using any of the smelters in the simulations. However, one site in the base case smelter run shows a 24-hour SO₂ concentration of 120 µg/m³ (Dunka River Watershed) which, considering the model accuracy, raises the possibility that the state ambient standard of 260 µg/m³ could be exceeded close to the smelter site. This problem does not appear to exist for the option 1 or option 2 smelters.

The modified gaussian model predicts that the 24-hour PSD increments will be exceeded. It is predicted that the base case smelter will exceed the maximum 24-hour PSD increment at 7 of 8 Class I receptors and 1 of 25 Class II receptors. The maximum predicted concentration in the Class I area is 23 µg/m³ at August Creek (29 km from the source) followed by a second high of 19 µg/m³ at Shagawa River Watershed (35 km from the source). The highest SO₂ concentration in the Class II area is 120 µg/m³ at Dunka River Watershed (5 km from the source). A second high of 99 µg/m³ also occurred at that site.

ATKOKAM •

FIGURE 58. PREDICTED MAXIMUM 24-HOUR SO₂ CONCENTRATIONS FROM THE BASE CASE SMELTER MODEL (MODIFIED GAUSSIAN MODEL) (UG/M³)

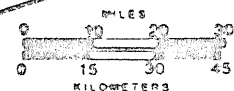
-288-



LEGEND

■ - CLASS 1 PDD AREAS

SITE NUMBER	CONVENTOR CODE	SITE NAME	CONCENTRATION
1	201	LITTLE JOHNSON LAKE	6.2
2	106	LITTLE VERMILION LAKE	7.1
3	104	BIRCH LAKE DAM	9.2
4	103	SAGAMOGA LAKE	3.0
5	104	VERMILION LAKE	10
6	102	SHAGBARK R W	10
7	214	SLY H S	15
8	224	FERNSBURD	10
9	210	TOWER SUDAN	14
10	206	BEAR ISLAND R W	25
11	201	KAMISHIBI LAS W	22
12	202	KEELY C W	20
13	101	AUGUST CREEK	21
14	101	ISABELLA W	2.5
15	212	NE OF VIRGINIA	6.2
16	207	EMBARRASSED W	15
17	215	BARDITT	56
18	204	UNWIND OREG W	40
19	222	FRY LEARNING CENTER	24
20	225	POBYVILLE	4.5
21	221	ERIE OFFICE	17
22	208	DUNN RD	27
23	206	DURKA RIVER W	120
24	201	STONY R W	27
25	217	NE OF EVELETH	5.2
26	210	NE OF EVELETH	4.2
27	213	HOT LAKES G C	18
28	209	ST LOUIS R W	19
29	210	WILKINSON R W	7.7
30	211	WHITEFACE R W	9.5
31	222	TOWN	14
32	220	WHITEFACE	4.1
33	228	TOWER	9.0



KEY MAP

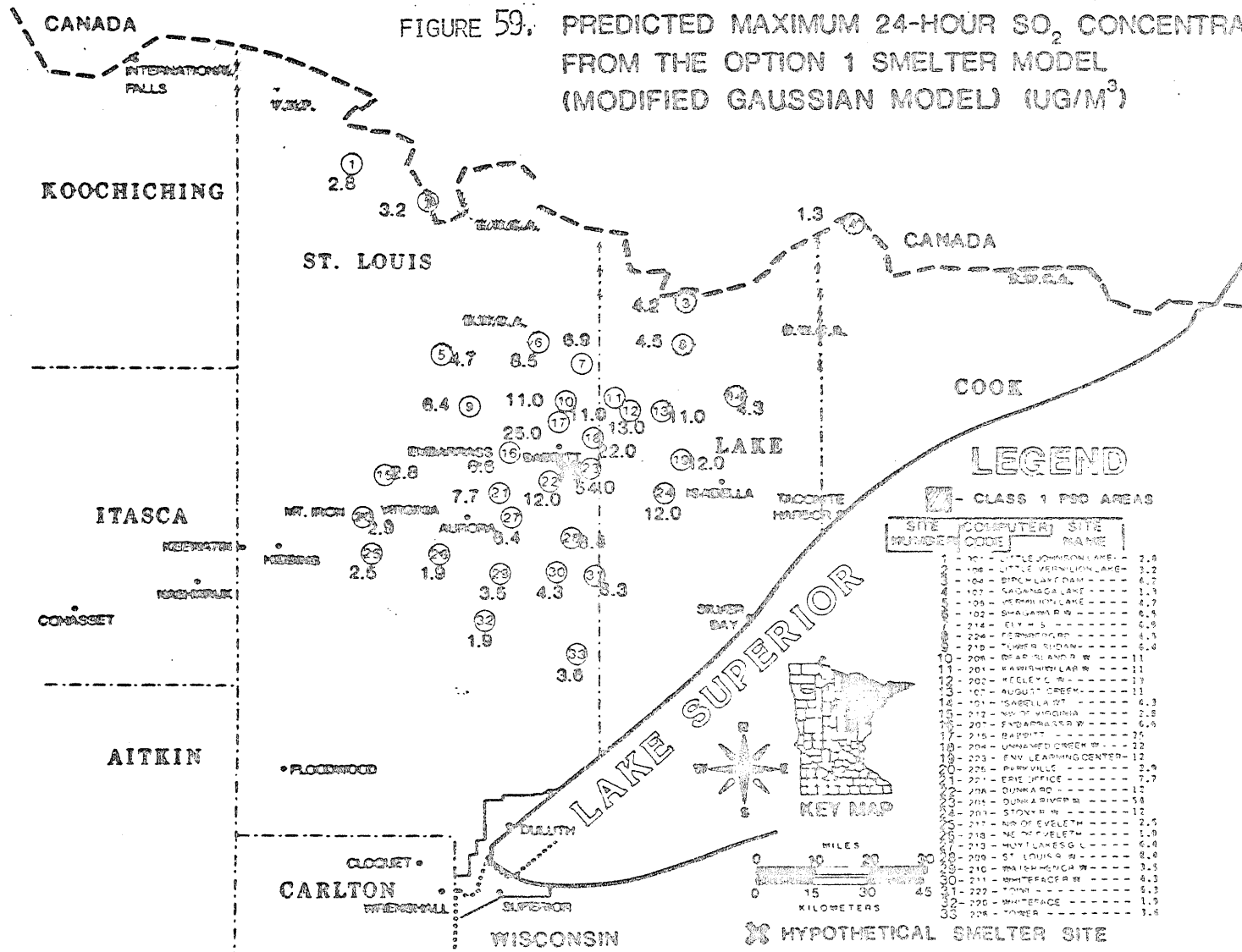
0 15 30 45
KILOMETERS

0 10 20 30
MILES

⊗ HYPOTHETICAL SMELTER SITE

ATKOKAN •

FIGURE 59. PREDICTED MAXIMUM 24-HOUR SO₂ CONCENTRATIONS FROM THE OPTION 1 SMELTER MODEL (MODIFIED GAUSSIAN MODEL) (UG/M³)



LEGEND

☐ - CLASS 1 PDD AREAS

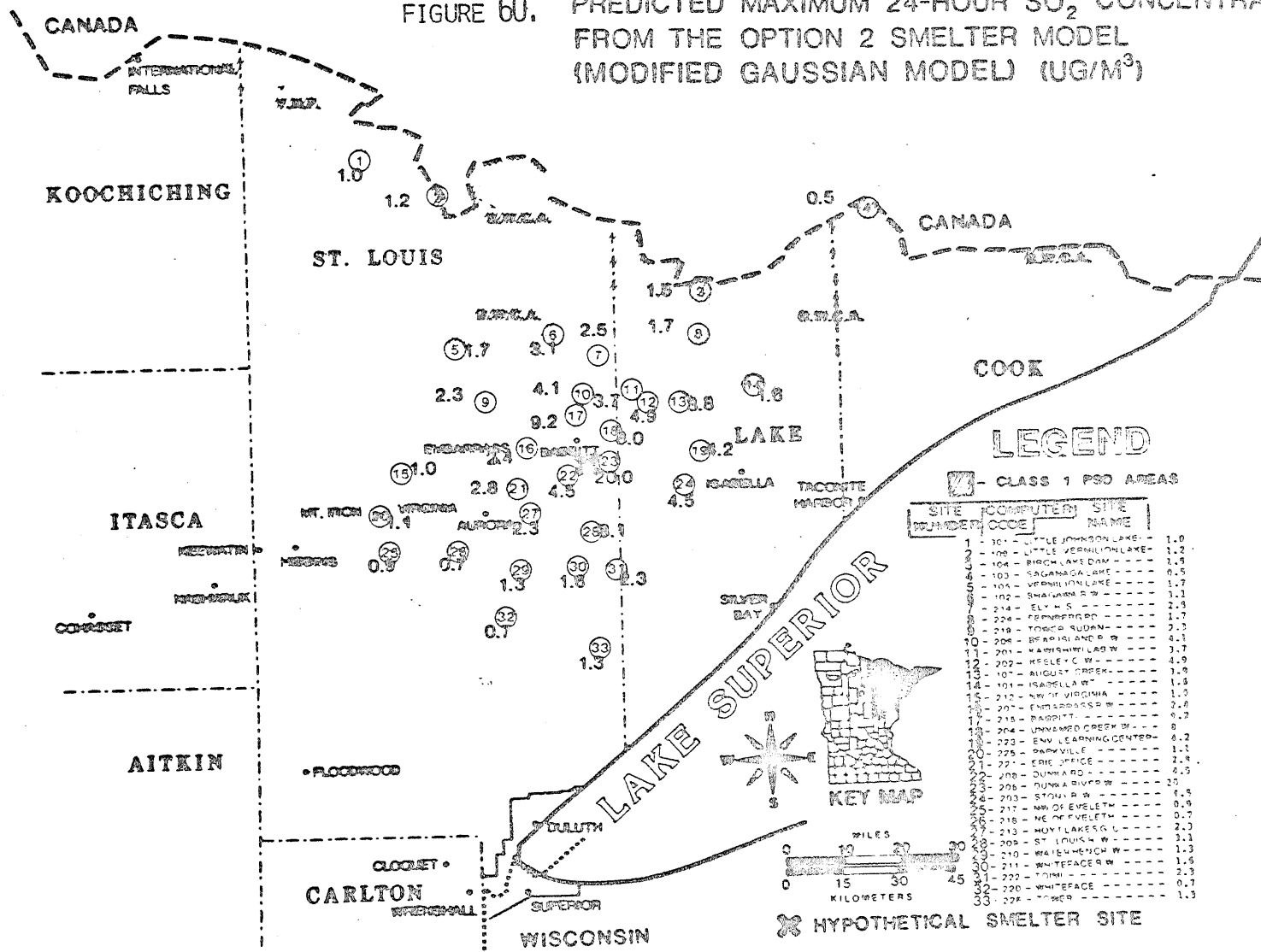
SITE NUMBER	COMPUTER CODE	SITE NAME	CONCENTRATION (UG/M ³)
1	101	LITTLE JOHNSON LAKE	2.8
2	108	LITTLE VERNILION LAKE	3.2
3	104	BIRCH LAKE DAM	6.7
4	107	KADANSKA LAKE	11.3
5	105	VERMILION LAKE	6.9
6	102	SHALAMON R.	6.5
7	214	CITY - S	6.8
8	224	FERMONT RD.	6.3
9	210	WOLF SHOALS	6.0
10	208	DEAR SIR AND R. W.	11
11	201	KARIBONHILAR W.	11
12	202	KEELEY C. W.	13
13	107	AUGUST CREEK	11
14	101	ISABELLA ST.	6.3
15	212	W. OF VIRGINIA	2.8
16	207	KADANSKA R. W.	6.0
17	215	BAUDUIT	26
18	204	UNNAMED CREEK W.	22
19	223	ENV. LEARNING CENTER	12
20	226	PARKVILLE	2.9
21	221	EYE OFFICE	7.7
22	206	DUNKA RD.	12
23	205	DUNKA RIVER W.	58
24	203	STONK R. W.	12
25	217	RD. OF EVELETH	2.9
26	218	NE. OF EVELETH	1.0
27	213	HUTVILANES G. L.	6.0
28	200	ST. LOUIS R. W.	8.0
29	210	WATSON MENCH W.	3.5
30	211	WHITEFACE R.	6.3
31	222	TOWN	6.3
32	220	WHITEFACE	1.9
33	208	TOWNS	3.5

☒ HYPOTHETICAL SMELTER SITE

ATKOKAN •

FIGURE 60. PREDICTED MAXIMUM 24-HOUR SO₂ CONCENTRATIONS FROM THE OPTION 2 SMELTER MODEL (MODIFIED GAUSSIAN MODEL) (UG/M³)

-290-



Ambient SO₂ 24-hour concentrations are about 55% lower for the option 1 smelter than for the base case smelter, and the PSD increments are expected to be exceeded at only two of 8 Class I receptors. The Class II increment is not exceeded. Further control of the smelter gases to reach the option 2 smelter results in an 84% reduction in ambient concentrations compared to the base case levels. None of the PSD increments are predicted to be exceeded on the basis of absolute numbers by the option 2 smelter, but uncertainties in the modeling results (factor of two) could jeopardize the Class I increment.

The previous comments apply to concentrations resulting from the individual smelter models. These are now placed into perspective against the background of predicted 1985 concentrations due to other regional sources. Figures 61, 62, 63, and 64 show the predicted maximum 24-hour concentrations resulting from the three smelter cases along with 1985 regional growth.

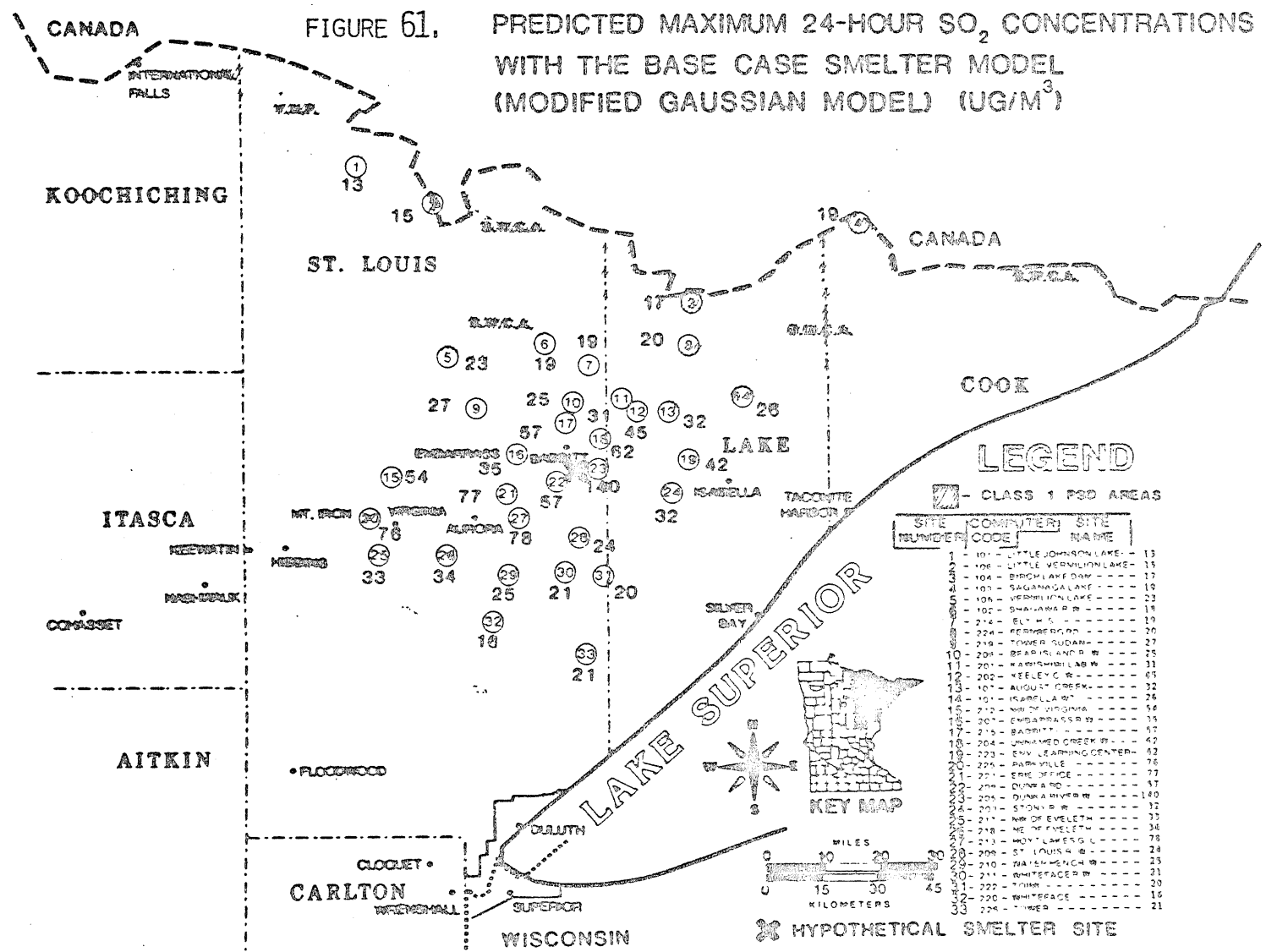
Again, neither the federal (365 $\mu\text{g}/\text{m}^3$) nor the state (260 $\mu\text{g}/\text{m}^3$) 24-hour ambient standards are predicted to be exceeded at the regional receptors. A possible exception is the Dunka River Watershed site where the modeling error makes it impossible to rule-out concentrations higher than the state ambient standard when the base case smelter is included in the 1985 simulations. The highest predicted 24-hour SO₂ concentration for the base case smelter with 1985 sources is 140 $\mu\text{g}/\text{m}^3$ at the Dunka River Watershed receptor.

Substituting the option 1 smelter into the simulation decreases the maximum 24-hour concentration by about 50% to 78 $\mu\text{g}/\text{m}^3$ at Dunka River Watershed. A second site, Hoyt Lakes Golf Course, is also predicted to

ATKOKAN •

FIGURE 61. PREDICTED MAXIMUM 24-HOUR SO₂ CONCENTRATIONS IN 1985 WITH THE BASE CASE SMELTER MODEL (MODIFIED GAUSSIAN MODEL) (UG/M³)

-292-



LEGEND

☐ - CLASS 1 PSD AREAS

SITE NUMBER	COMPUTER CODE	SITE NAME
1	101	LITTLE JOHNSON LAKE - 13
2	108	LITTLE VERMILION LAKE - 15
3	104	BIRCH LAKE DAM - 17
4	103	SAGANAGA LAKE - 19
5	106	VERMILION LAKE - 23
6	102	SHAWANA R R - 18
7	214	ELY H S - 19
8	224	FERRBERG RD - 20
9	219	TOWER ROAD - 27
10	204	BEAR RIVER R - 25
11	201	WATKINSVILLE R - 31
12	202	KEELEY C R - 45
13	107	AUGUST CREEK - 32
14	101	ISABELLA ST - 26
15	212	NW OF VERMILION - 16
16	207	EMBARRAS R R - 25
17	215	BADWITZ - 47
18	204	UNION CREEK R - 42
19	223	ENV LEARNING CENTER - 62
20	225	PARKVILLE - 76
21	221	ERIE OFFICE - 73
22	226	QUINN RD - 75
23	224	DUNN RIVER R - 140
24	201	STONY R R - 32
25	211	NW OF EVELETH - 35
26	218	ME OF EVELETH - 36
27	213	MOY LAKE S C - 28
28	208	ST LOUIS R - 21
29	210	WALSHMACH R - 23
30	211	WHITEFACE R - 21
31	222	TOWER - 20
32	220	WHITEFACE - 16
33	224	TOWER - 21

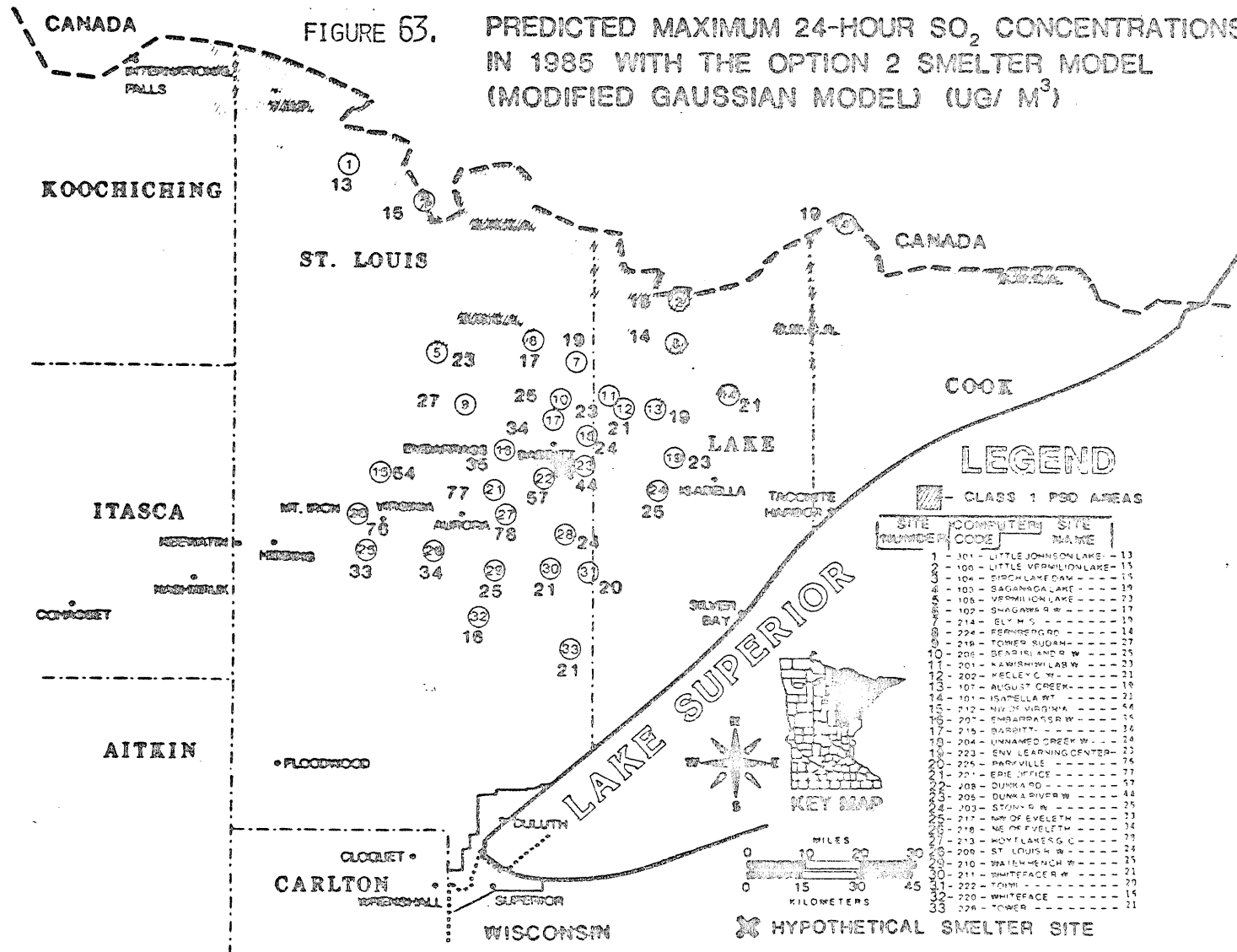


☒ HYPOTHETICAL SMELTER SITE

ATKIN

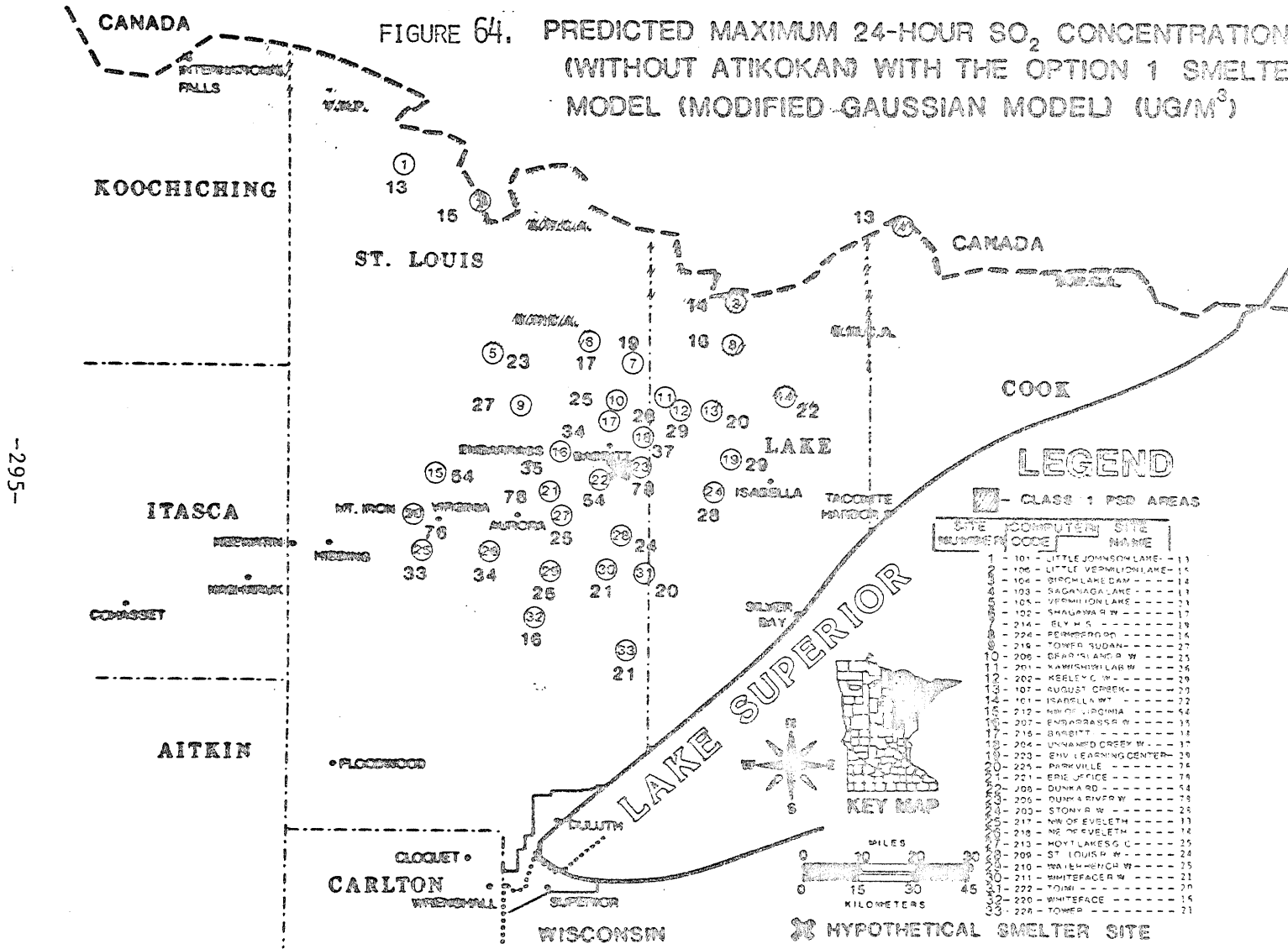
FIGURE 63.

PREDICTED MAXIMUM 24-HOUR SO₂ CONCENTRATIONS
IN 1985 WITH THE OPTION 2 SMELTER MODEL
(MODIFIED GAUSSIAN MODEL) (UG/ M³)



ATIKOKAN

FIGURE 64. PREDICTED MAXIMUM 24-HOUR SO₂ CONCENTRATIONS IN 1985 (WITHOUT ATIKOKAN) WITH THE OPTION 1 SMELTER MODEL (MODIFIED GAUSSIAN MODEL) (UG/M³)



LEGEND

■ - CLASS 1 FOD AREAS

SITE NUMBER	COMPUTER CODE	SITE NAME
1	101	LITTLE JOHNSON LAKE
2	106	LITTLE VERMILION LAKE
3	104	BIRCH LAKE DAM
4	103	SAGANAGA LAKE
5	105	VERMILION LAKE
6	102	SHAGAWA W
7	214	ELY W
8	224	PERMISSEPOO
9	216	TOWER SUDAN
10	206	DEAR ISLAND W
11	201	WAMISHOILAR W
12	202	KEELY C W
13	107	AUGUST CREEK
14	101	ISABELLA W
15	217	NW OF VIRGINIA
16	207	EMBARRASS W
17	215	BABBITT
18	204	UNWASO CREEK W
19	223	ENV LEARNING CENTER
20	225	PARKVILLE
21	221	ERIE OFFICE
22	209	DUNKARD
23	205	DUNKARD SMPR W
24	203	STONEY W
25	217	NW OF EVELETH
26	218	NE OF EVELETH
27	213	HOYT LAKES C
28	209	ST LOUIS W
29	210	WATERBENCH W
30	211	WHITEFACE W
31	222	TOIN
32	220	WHITEFACE
33	224	TOWER

⊗ HYPOTHETICAL SMELTER SITE

-295-

have a high of $78 \mu\text{g}/\text{m}^3$.

Substituting the option 2 smelter into the simulation further decreases the maximum 24-hour concentration at Dunka River Watershed to $44 \mu\text{g}/\text{m}^3$, but does not affect the predicted concentration of $78 \mu\text{g}/\text{m}^3$ at Hoyt Lakes Golf Course.

In summary, Figure 65 shows the general areas impacted by the three smelter cases. These are areas where maximum 24-hour concentrations are different from the 1985 simulation without a copper-nickel smelter. Table 71 summarizes the maximum and second high 24-hour concentrations for those sites showing the most variation for the three smelter cases.

Predicted maximum 24-hour and second high concentrations at receptors in Class I and Class II areas for the different modeling simulations are shown in Figure 66; the 1977 regional, 1977 PSD and 1985 values are also included for comparison.

The maximum and second high 24-hour concentrations for the base case smelter in the Class I area are $32 \mu\text{g}/\text{m}^3$ (August Creek) and $26 \mu\text{g}/\text{m}^3$ (Isabella Watershed), respectively. These values are about a third higher than the maximum and second high values predicted for 1985 without copper-nickel development-- $23 \mu\text{g}/\text{m}^3$ at Vermillion Lake and $20 \mu\text{g}/\text{m}^3$ at Isabella Watershed.

In the Class II area the maximum and second high values are $140 \mu\text{g}/\text{m}^3$ (Dunka River Watershed) and $125 \mu\text{g}/\text{m}^3$ (Dunka River Watershed), respectively, for the base case smelter. These values are about 80% and 55% higher than the maximum and second high concentrations predicted for 1985 without copper-nickel development-- $78 \mu\text{g}/\text{m}^3$ at Hoyt Lakes

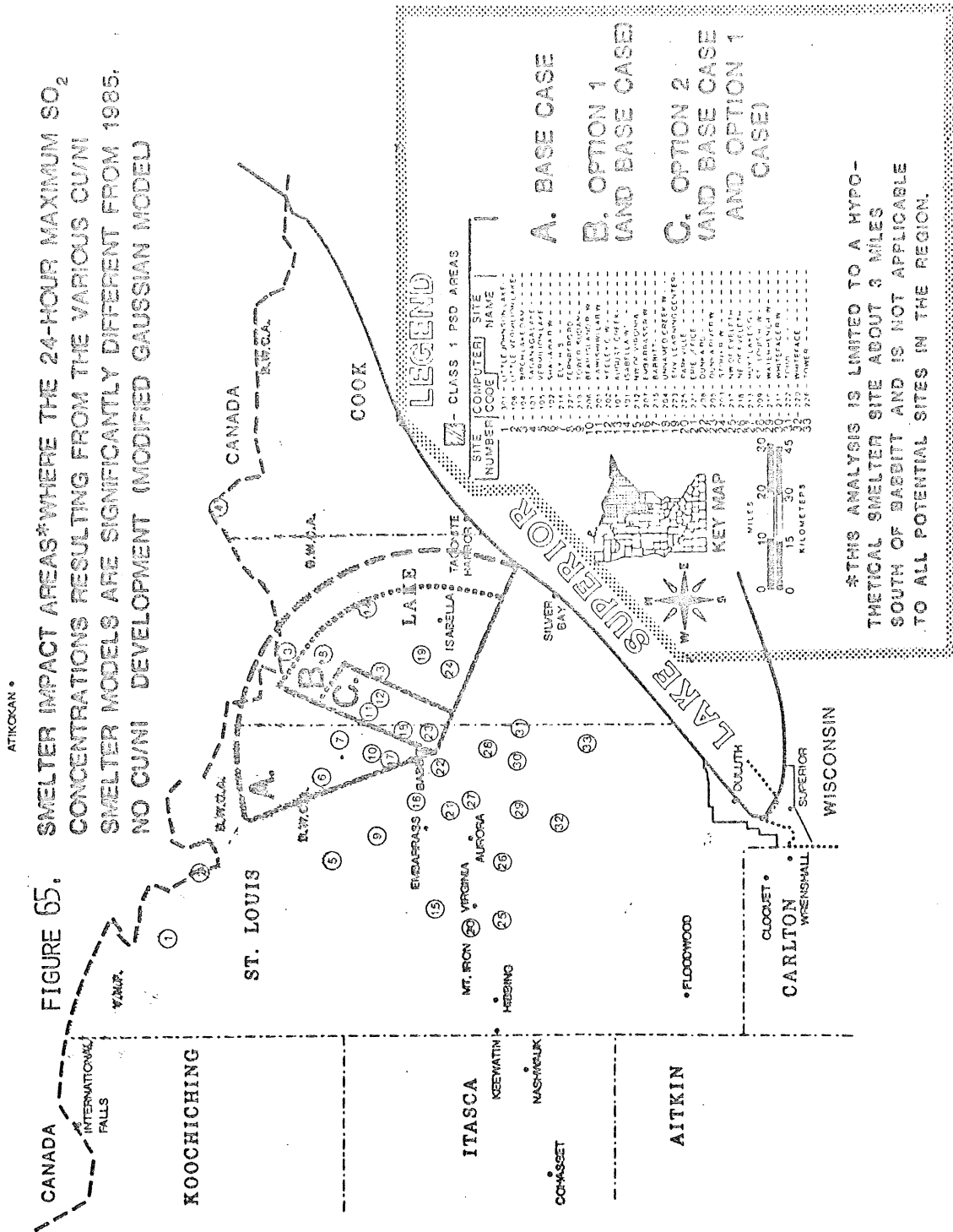
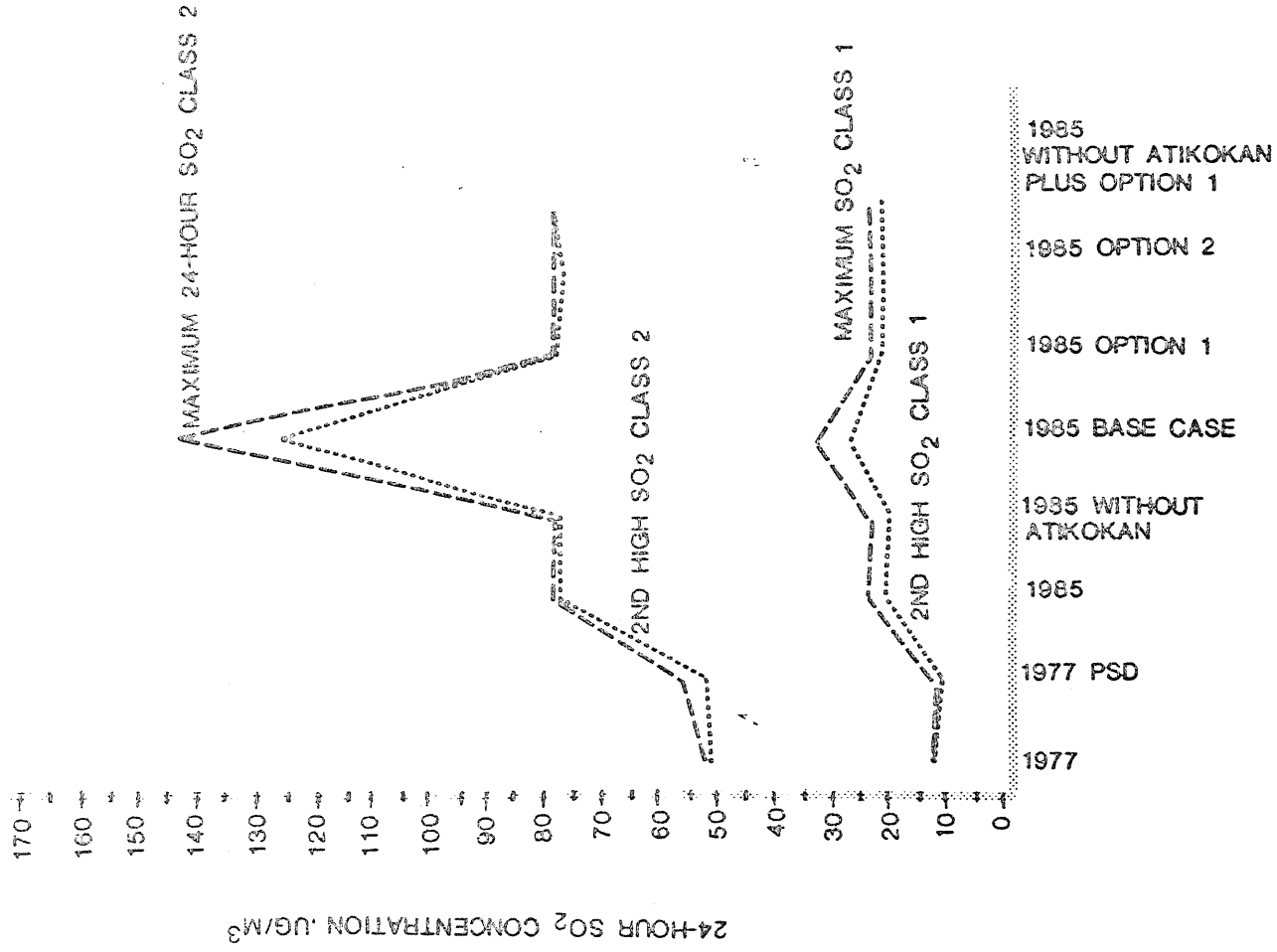


Table 71. Summary of 24-hour maximum and second high SO₂ concentrations at selected sites for copper-nickel development cases in 1985 (smelter location is 4.8 km south of Babbitt), $\mu\text{g}/\text{m}^3$.

site no.	receptor name	1985+base case		1985+option 1		1985+option 2	
		high	2nd high	high	2nd high	high	2nd high
11	Kawishiwi Lab	31	30	26	20	23	18
24	Stony River W.	32	30	28	22	24	23
18	Unnamed Creek W.	62	53	37	27	24	23
23	Dunka River W.	143	125	78	71	44	43
10	Bear Island R.W.	25	25	25	21	25	21
22	Dunka Road	57	40	57	40	57	40
19	Env. Learning C.	42	41	29	27	23	23

FIGURE 66

SUMMARY OF HIGHEST AND 2ND HIGHEST 24-HOUR SO₂ CONCENTRATION PREDICTED AT ANY RECEPTOR IN CLASS 1 AND CLASS 2 AREAS, RESPECTIVELY, FOR VARIOUS SCENARIOS (MODIFIED GAUSSIAN MODEL)



Golf Course and $77 \mu\text{g}/\text{m}^3$ at the Erie Office, respectively.

Substituting the option 1 smelter into the simulation results in a high of $23 \mu\text{g}/\text{m}^3$ (Vermillion Lake) followed by a second high of $22 \mu\text{g}/\text{m}^3$ (August Creek) in the Class I areas. In the Class II area the high and second high are both $78 \mu\text{g}/\text{m}^3$ (Dunka River Watershed, Hoyt Lakes Golf Course). These values are about the same as in the simulation without copper-nickel development.

Substituting the option 2 smelter has little effect on the concentrations that are predicted for the 1985 case without copper-nickel development.

Removing the Atikokan power plant from the analysis with the option 1 smelter results in maximum and second high 24-hour concentrations in the Class I and Class II areas that are essentially unchanged. Maximum concentrations are decreased at only two sites on the Minnesota-Canada border.

In terms of the PSD increments, both the 24-hour Class I increment ($5 \mu\text{g}/\text{m}^3$) and the Class II increment ($91 \mu\text{g}/\text{m}^3$) are predicted to be exceeded by one or more of the modeled smelter cases together with other sources expected by 1985. The predicted values greater than the increments are listed in Table 72.

Using the maximum 24-hour concentration, the Class I increment is exceeded at 8 sites for the base case smelter, and at 7 sites each for the option 1 and option 2 smelters. These numbers drop to 6 and 4, respectively, when the second high is used. If Atikokan is excluded from the 1985 plus option 1 smelter emissions inventory, then the increment is exceeded at 6 sites using the maximum concentration and

Table 72. A summary of the predicted concentrations greater than the Class I and Class II 24-hour PSD increments in 1985 with the various smelter models ($\mu\text{g}/\text{m}^3$).^a

Receptor Site No.	Receptor Site Name	Base Case Smelter, 1985		Option 1 Smelter, 1985		Option 2 Smelter, 1985		Option 1 Smelter, 1985 without Atikokan	
		High	2nd High	High	2nd High	High	2nd High	High	2nd High
<u>Class I</u>									
14	Isabella W.	14	8	10	(4) ^b	9	(3)	10	(4)
6	Shagawa River W.	11.2	9.2	9.2	8.2	9.2	8.2	9.2	8.2
4	Saganaga Lake	7	(4) ^b	7	(4)	7	(4)	(1)	(0)
3	Birch Lake Dam	6	5	(4)	(3)	(4)	(2)	(3)	(1)
5	Vermillion Lake	15.6	9.6	15.6	9.6	15.6	9.6	15.6	9.6
2	Little Vermillion L.	9.1	5.1	9.1	5.1	9.1	5.1	9.1	(4.1)
13	August Creek	23.3	17.3	11.3	10.3	10.3	7.3	11.3	10.3
1	Little Johnson Lake	5.7	(3.7)	5.7	(3.7)	5.7	(3.7)	5.7	(3.7)
<u>Class II</u>									
23	Dunka River W.	128	110	(63)	(56)	(29)	(28)	(63)	(56)

^aThe values shown are the differences between the highest (or second highest) value predicted for the modeling case and the 1977 PSD baseline value.

^bValues shown in parenthesis do not exceed the increments ($5\mu\text{g}/\text{m}^3$ -Class I; $91\mu\text{g}/\text{m}^3$ -Class II).

at three sites using the second high. The Class II increment is exceeded at only one site and only for the base case smelter.

In order to determine the magnitude of the values greater than the PSD increment just highlighted, the PSD analysis was made for each day of the year at each site rather than just using the high or second high values at each site in the region. For example, the calculated SO₂ concentration on January 1, 1977 was subtracted from the predicted concentration on January 1, 1985 and so forth for each day in the year, using the same weather for both years. Figures 67 through 71 show the resulting SO₂ concentration increments which were greater than the PSD Class I allowed increment. The data are plotted for each of the Class I sites, and 1985 data without copper-nickel development are included for comparison (Figure 67).

Regional point source growth in 1985 is predicted to result in a total of 91 twenty-four hour values which exceed the PSD increment over the 8 Class I sites without copper-nickel development (Figure 67). Most of the values greater than the increment are concentrated in the range of 5-6 µg/m³ but go as high as 14 and 17 µg/m³. When the Atikokan power plant is removed from the inventory (Figure 68), the number of 24-hour values greater than the increment decreases by 34% to 60. The Class I sites that are most impacted by Atikokan are Birch Lake Dam, Saganaga Lake, and Isabella Watershed (site numbers 3,4, and 14, respectively).

When the base case is included in the simulation (Figure 69), the PSD Class I increment is exceeded 151 times, an increase of 66% over 1985 point source growth alone. With the option 1 smelter in the simulation (Figure 70) the number of values exceeding the Class I

FIGURE 67

24-AMBIENT SO₂ CONCENTRATIONS GREATER THAN THE CLASS 1 PSD INCREMENT, 1985 WITHOUT CU/NI DEVELOPMENT (MODIFIED GAUSSIAN MODEL)

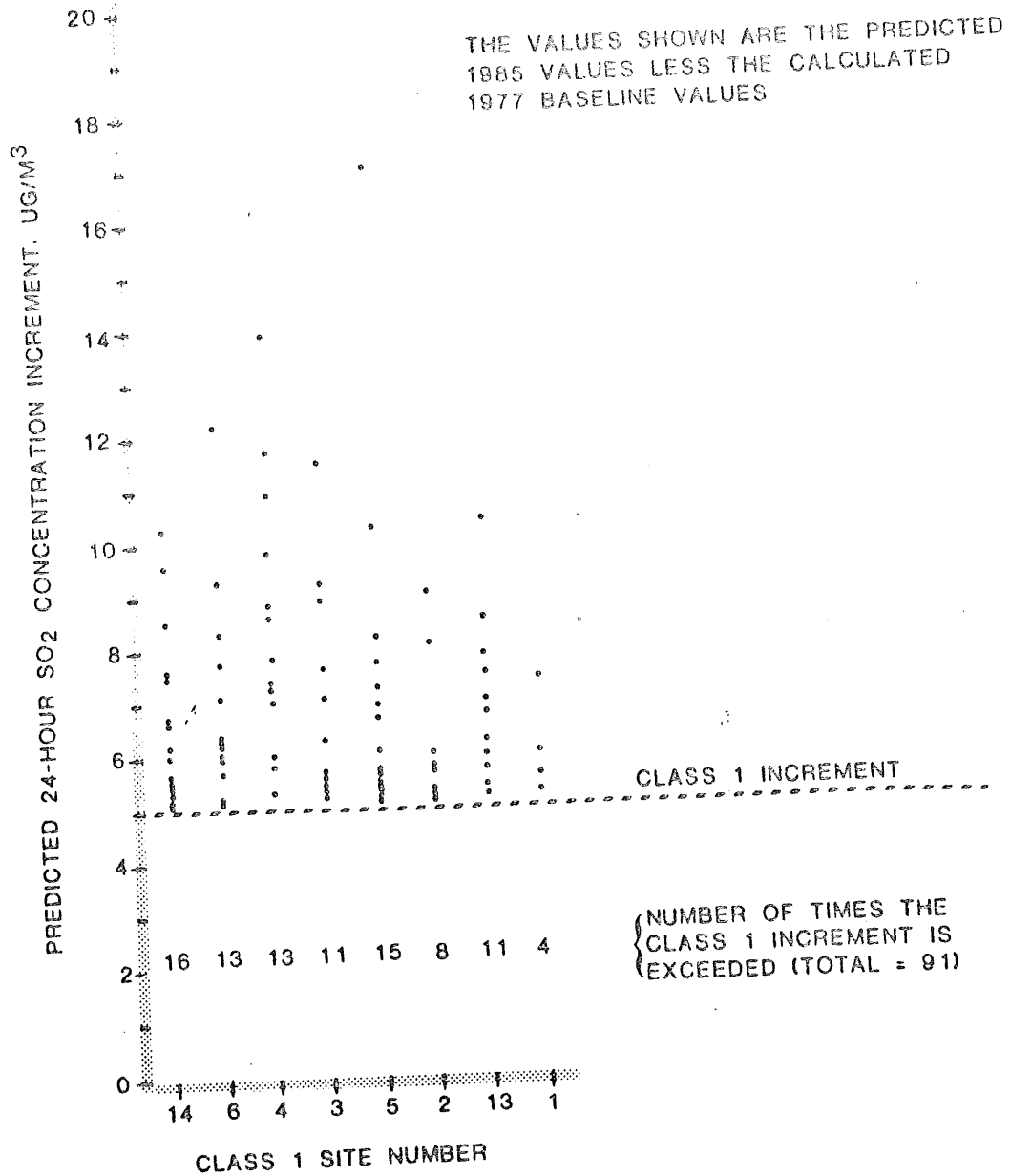


FIGURE 68

24-HOUR AMBIENT SO₂ CONCENTRATIONS GREATER THAN THE CLASS 1 PSD INCREMENT, 1985 EXCLUDING ATIKOKAN (MODIFIED GAUSSIAN MODEL)

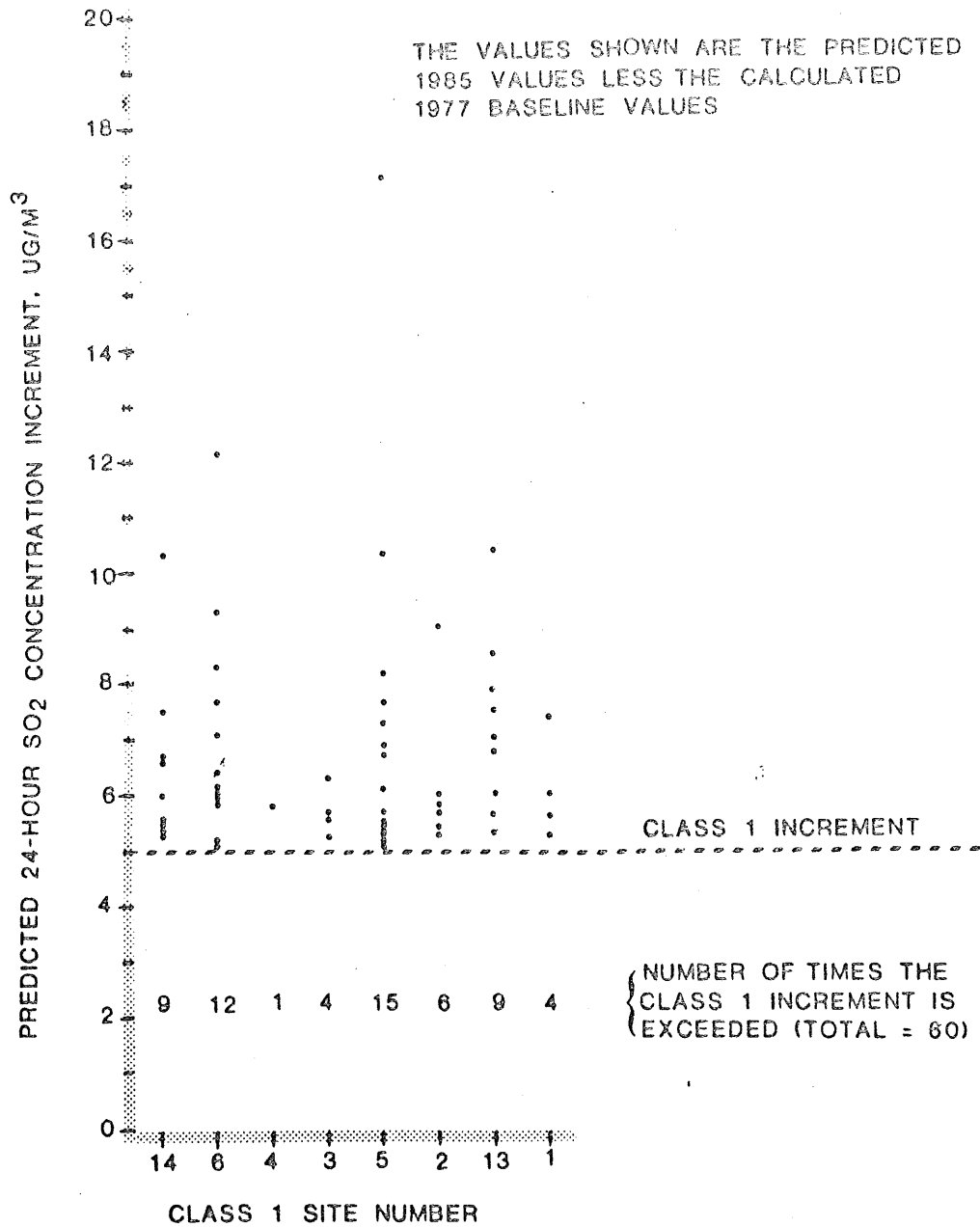


FIGURE 69

24-HOUR AMBIENT SO₂ CONCENTRATIONS GREATER THAN
THE CLASS 1 PSD INCREMENT, 1985 WITH BASE CASE
SMELTER MODEL
(MODIFIED GAUSSIAN MODEL)

THE VALUES SHOWN ARE THE PREDICTED
1985 VALUES LESS THE CALCULATED
1977 BASELINE VALUES

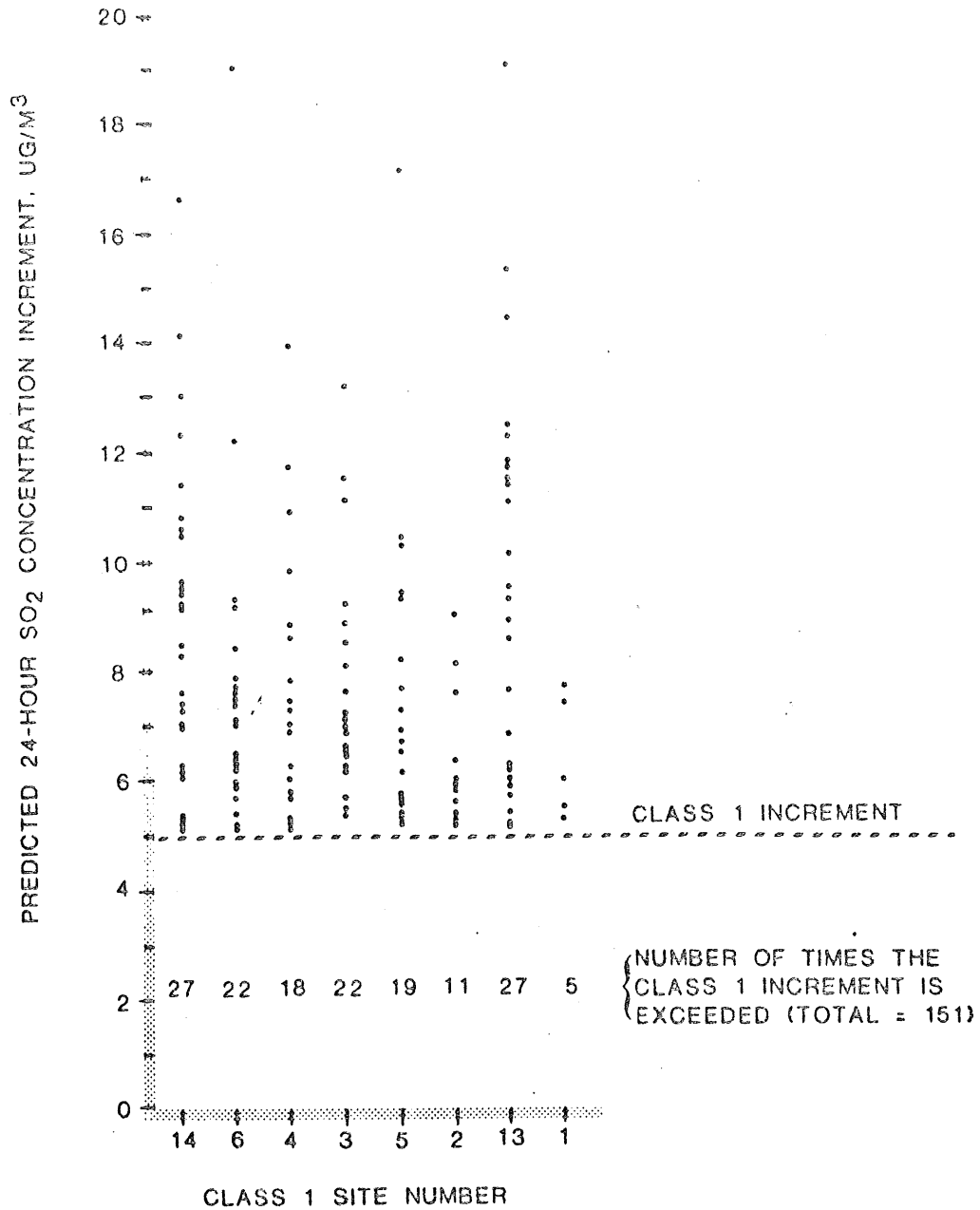


FIGURE 70

24-HOUR AMBIENT SO₂ CONCENTRATIONS GREATER THAN THE CLASS 1 PSD INCREMENT, 1985 WITH OPTION 1 SMELTER MODEL (MODIFIED GAUSSIAN MODEL)

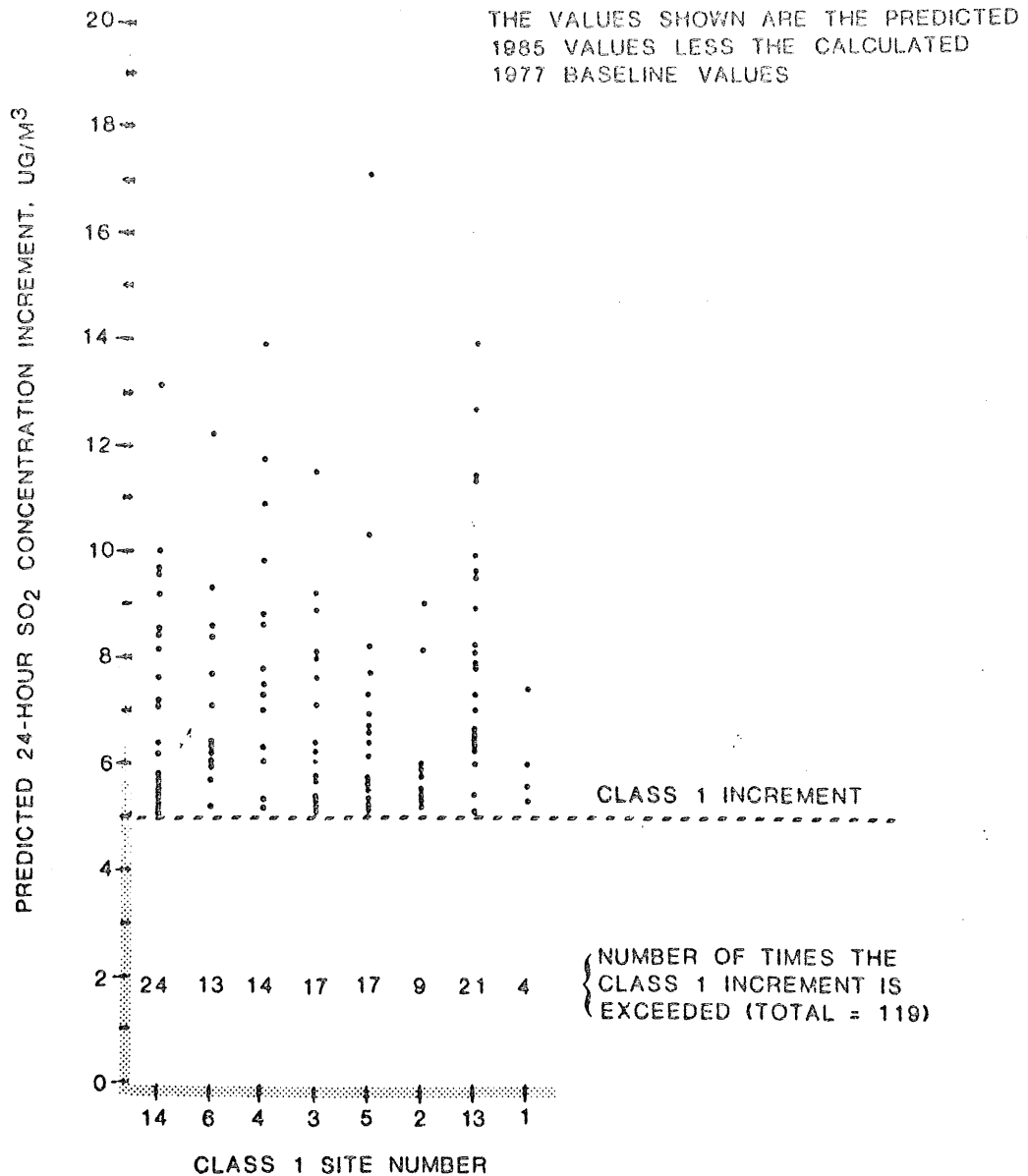
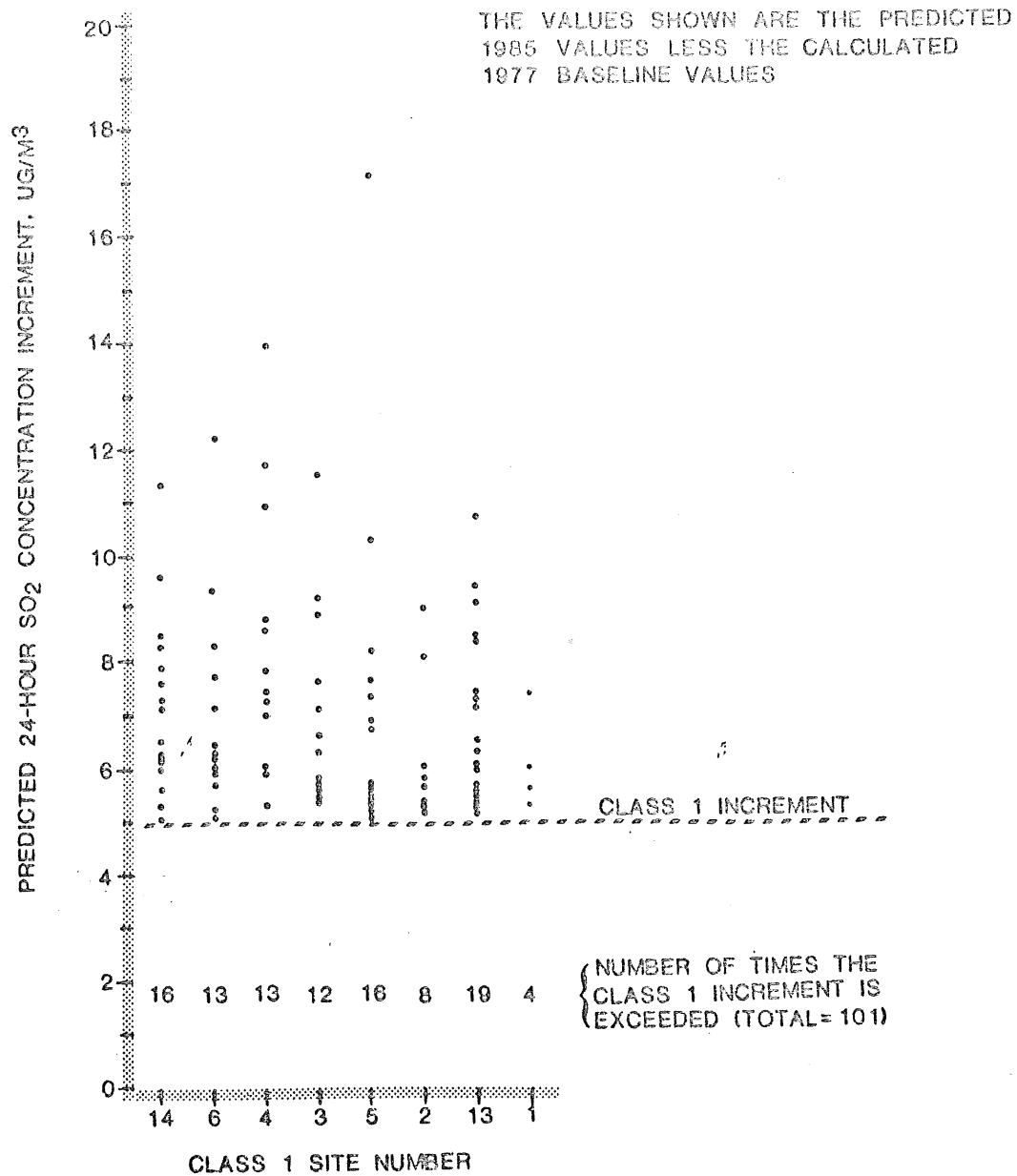


FIGURE 71

24-HOUR AMBIENT SO₂ CONCENTRATIONS GREATER THAN THE CLASS 1 PSD INCREMENT, 1985 WITH OPTION 2 SMELTER MODEL (MODIFIED GAUSSIAN MODEL)



increment is 119, a 31% increase over those due to 1985 regional point source growth alone. Most of the values greater than the increment are in the 5-7 $\mu\text{g}/\text{m}^3$ range. The impact of the option 1 smelter is greatest at Birch Lake Dam, August Creek (site no. 13), and Isabella Watershed which are east and northeast of the smelter.

The option 2 smelter (Figure 71) results in only 101 values greater than the Class I increment, an increase of only 11% over predicted 1985 point source growth.

Even though the PSD Class I increment is predicted to be exceeded several times at different sites with any of the smelter models, it is predicted to be exceeded in any case as a result of the projected growth in regional SO_2 point sources without copper-nickel development.

The 24-hour Class II increment is not predicted to be exceeded (using this difference method) at any of the sites in the Class II areas. The highest difference occurred (with the base case smelter) at Parkville, where a difference of 55 $\mu\text{g}/\text{m}^3$ is predicted. It should be noted that the discrepancy between this figure and the single value greater than the increment which was predicted previously is due to the method of computation. The single value was based on maximum concentrations rather than day-by-day comparisons. When the day-by-day method is used the meteorology remains the same for the baseline and projected years and only the emissions change. This results in high values occurring on the same day for both baseline and projected years which in effect decreases the spread between the values.

Table 73 presents a summary of the number of times the 24-hour increments are exceeded on a month-by-month and annual basis for each

Table 73. Summary of the number of times the 24-hour SO₂ Class I^a PSD increment is predicted to be exceeded by month at all Class I receptor sites based on day-by-day simulations.

	MONTH												ANNUAL TOTAL
	J	F	M	A	M	J	J	A	S	O	N	D	
1985-Baseline No Cu-Ni development	11	14	2	3	2	0	4	3	11	12	13	16	91
1985-Baseline Atikokan excluded	10	8	2	3	2	0	0	0	8	8	8	11	60
1985-Baseline with the base case smelter model	22	19	7	4	6	3	5	6	15	22	17	25	151
1985-Baseline with the option 1 smelter model	17	17	6	3	3	2	4	4	13	18	14	18	119
1985-Baseline with the option 2 smelter model	13	15	3	3	2	1	4	4	13	13	13	17	101

^aThe Class II 24-hour increment is not predicted to be exceeded.

of the modeling cases in the Class I and Class II areas. Most of the values greater than the increments (70-85%) occur during the fall and winter months when atmospheric conditions favor limited mixing and limited dispersion of pollutants.

The previous discussion, based on a hypothetical smelter site south of Babbitt, has shown that the 24-hour ambient SO₂ PSD increment is expected to be exceeded in Class I areas for all the smelter models, and that the increment is predicted to be exceeded by regional growth alone, without copper-nickel development. In terms of the smelter location, it

it is clear that its distance from the Class I areas will be a major factor in the ability of the facility to meet the PSD increments. This problem is considered further by computing the ambient 24-hour concentrations of SO₂ from a smelter simply as a function of distance from the source. Source location is not specified in these runs.

The meteorological input data for the 24-hour simulations (no specific smelter location) were selected from the Hibbing airport weather data to give worst case dispersion days. That is, those days causing the highest ground level concentrations were selected on the basis of wind persistence and lack of precipitation. Table 74 summarizes the meteorology of these single day simulations.

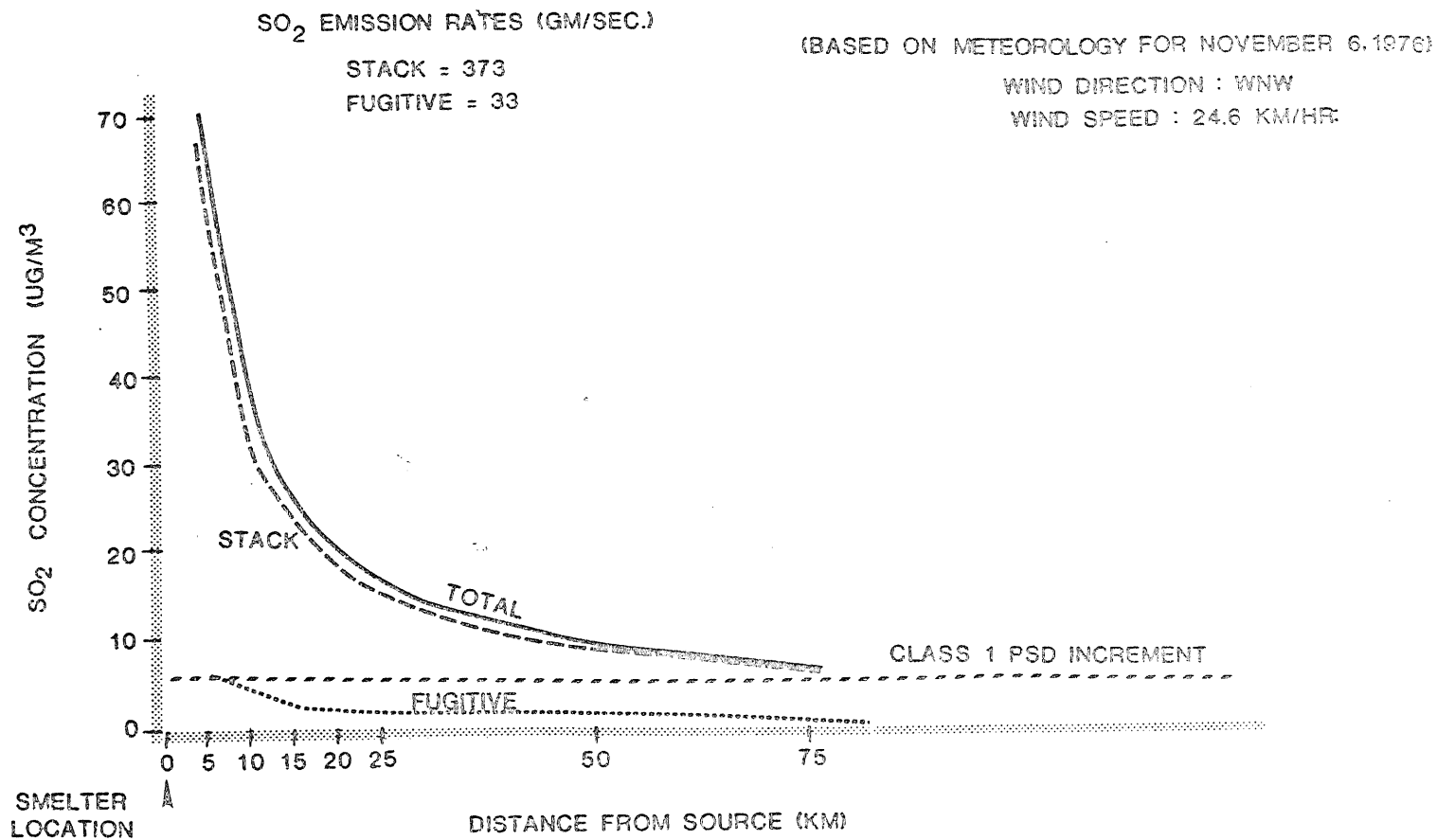
Table 74. Meteorology for selected single day runs of the modified gaussian model.

Date	Wind Direction	Wind Speed (km/hr)	Stability	Height (m)
10/28/76	SSW	22.2	neutral	1100
11/6/76	WNW	24.6	neutral	1100
12/20/76	NW	23.4	neutral	650
1/15/77	WNW	19.6	neutral	650
2/28/77	NW	16.9	neutral	1150

Figure 72 shows the results for one of the days (November 6, 1976) for the base case smelter. Identical runs were made using the standard short-range models.⁶¹ Both models clearly show that at 10 km from the source, the fugitive contribution from the smelter is very small relative to that of the stack. Total concentrations are in the range of 35-40 µg/m³ according to both models. This is typical of the results from all of the 5 days modeled.

MAXIMUM PREDICTED 24-HOUR SO₂ CONCENTRATIONS ALONG
THE COMBINED PLUME CENTERLINE FOR THE BASE CASE
SMELTER MODEL (MODIFIED GAUSSIAN MODEL)

FIGURE 72



Fugitive emissions are relatively more important for the option 1 and option 2 smelters. The stack and fugitive emissions are nearly equal for the option 2 smelter.

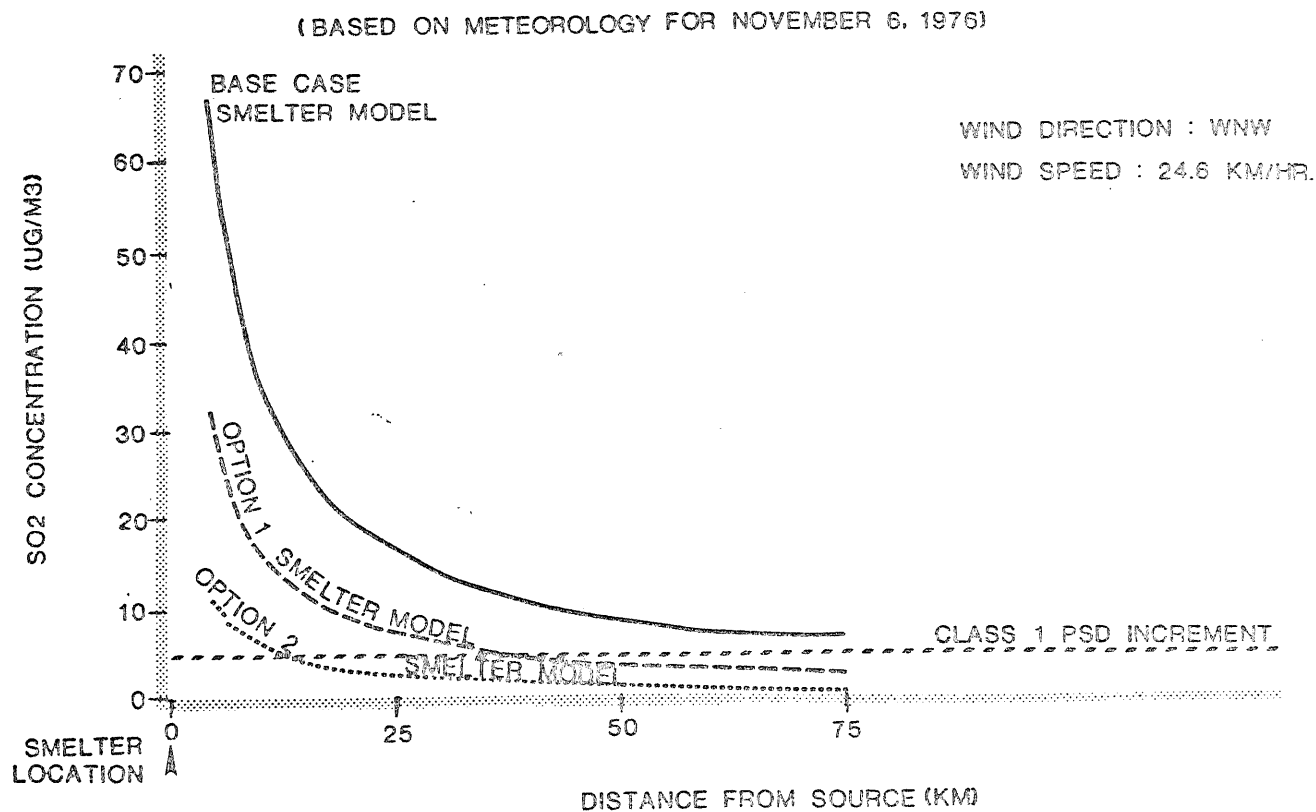
The modified gaussian model indicates that on three of the five days, the Class I SO₂ increment is exceeded even at 75 km from the source. On the remaining two days, the increment is exceeded up to 55 km from the source.

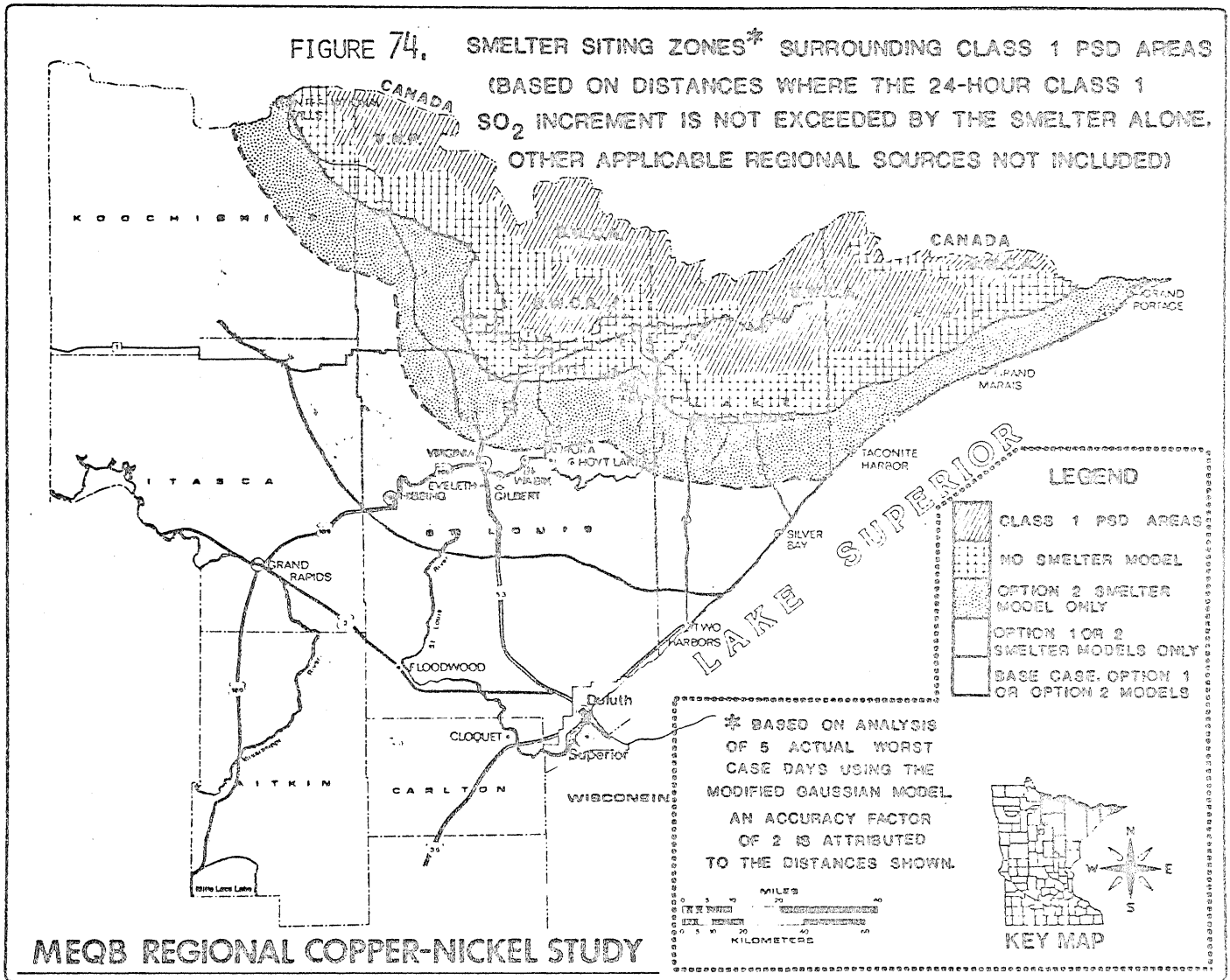
On the basis of these results it appears that a smelter with emissions similar to those in the base case smelter could not be sited within 75 km of a Class I area without causing the increment to be exceeded in that area. The spatial restrictions are reduced for the option 1 and option 2 smelter cases which have successively lower stack emission rates. Figure 73 shows the total predicted SO₂ concentrations for all three smelter cases, again using November 6, 1976 as a reference day. The results indicate that concentrations from the option 1 smelter model alone drop below the Class I increment at roughly 35 km, and concentrations from the option 2 smelter drop below the increment at about 13 km.

Based on these results, it is possible to rather generally zone the space surrounding the Class I areas. The zones refer only to the ability of a smelter facility to avoid exceeding the Class I 24-hour PSD increment when acting alone. The effect of other sources utilizing a portion of the increment would be to increase the distances needed between the Class I area and the smelter site. Figure 74 shows the zones based on the 5 single day runs of the modified gaussian model. These distances could be off by a factor of two based on model accuracy.

MAXIMUM PREDICTED 24-HOUR SO₂ CONCENTRATIONS RESULTING FROM
THREE MODEL SMELTER CASES (USING THE MODIFIED GAUSSIAN MODEL)

FIGURE 73





When these data are applied to the development zones for the ore body (Figure 75), none of the smelter models (acting alone) are predicted to be able to meet the 24-hour PSD Class I increment in zones 1 or 2. The option 2 smelter could meet requirements in zones 3 and 4, while the option 1 (and, of course, option 2) smelter could meet the increment in zones 5, 6, and 7. The base case smelter could not meet the increment in any of the development zones. Within the factor of 2 accuracy of the model, at worst, none of the smelters could meet the increment in zones 1, 2, 3, and 4, and only the option 2 smelter could be located in zones 5, 6, and 7. The other smelter models would not meet the PSD requirements for Class I areas in any of the zones. Again, the above discussion assumes that the entire increment would be available to the smelter alone.

As noted previously, the 24-hour Class I PSD increment is expected to be exceeded at several receptors even without copper-nickel development. Taking this into consideration, smelter siting would appear to be excluded in areas which are between the point sources along the Iron Range and any Class I areas. Thus, siting in development zones 1, 2, 3, and possibly 4 and 5 may be precluded due to this consideration. This conclusion is independent of the degree of SO₂ control that could be achieved by a smelter, since the increment is expected to be consumed by planned new or expanded SO₂ point sources. Sites which are located away from the Iron Range-Class I line may avoid this difficulty, making zones 6 and 7 look most promising.

The above discussion and associated zone designations are not intended to indicate the desirability or acceptability of a smelter site

in particular areas. This is a question that must be determined by the appropriate authorities. Rather, the discussion is intended to illustrate the major air quality factors which will have to be considered in making this determination. It is apparent that the 24-hour PSD increment in a Class I area is one of the standards that will have a major influence on smelter siting in northeastern Minnesota. The effect of other new SO₂ sources is also important since they may consume some or all of the allowed increment, potentially excluding a smelter from the region. Clearly, long-range planning is required for any future industrial development in northeastern Minnesota.

8.2. AMBIENT SULFATE CONCENTRATIONS

Measured average ambient sulfate concentrations (based on total sulfur) in the region are in the range of 1 to 3 $\mu\text{g}/\text{m}^3$. The modified gaussian model simulations indicated that local point sources of SO₂ contributed less than 1% of total measured sulfate in 1977. The modeling simulations, of course, consider only the sulfate which results from SO₂ oxidation. Sulfur emitted directly from the sources as sulfate is not included in the emissions inventory because the data were not available. However, direct source contributions of sulfate are not expected to be significant. Thus, the modeling results, along with the uniformity of the measured values at all sites, suggest that the bulk of the ambient sulfate in the region is transported from sources outside the region. The model predicts that expected increases in SO₂ emissions in the area by 1985 will increase the regional average ambient sulfate concentration to 84 ng/m^3 , a factor of 15 increase over the calculated 1977 local contribution. Recall that this increase occurs against a

background probably dominated by long-range transport which may double (to 2-6 $\mu\text{g}/\text{m}^3$) by 1985. It is in this context that the sulfate concentrations from a smelter in the region are considered.

The modified gaussian model was used to predict ambient sulfate concentrations from a smelter located south of Babbitt as previously discussed. The results are shown in Table 75 for the three smelter models along with the available measured data. Regional averages are also given for the smelter cases based on the 33 regional receptors. A comparison of the average of the predicted data at 8 sites to the average of the measured data at the same sites shows that the base case model smelter is predicted to contribute only about 4% of the measured atmospheric sulfur (assumed present as sulfate) in 1977. The corresponding values for the option 1 and option 2 models are less than 1%.

The above results indicate that the predicted contributions of a local smelter to ambient sulfate concentrations is quite small relative to the expected levels which seem to be attributable to remote sources. There is a large difference (approximately a factor of 6) between the base case smelter and the other two options. In terms of the calculated contribution due to local sources in 1977 (regional average of 5.4 ng/m^3) any of the smelter models would increase this local contribution several fold. The predicted 1985 local contribution (without copper-nickel) of 84 ng/m^3 would be increased 86%, 15%, and 10% for the base case, option 1, and option 2 smelter models, respectively. Although these average increases are a small part of the overall sulfate concentrations, increases are much larger in the immediate vicinity of the smelter.

Table 75. Predicted annual average sulfate concentrations for three smelter models located south of Babbitt and measured sulfate concentrations at selected sites.

Site	Sulfate Concentrations ($\mu\text{g}/\text{m}^3$)			Measured ^a Average
	Base Case Model	Option 1 Model	Option 2 Model	
Babbitt	0.25	0.048	0.038	2.09
Whiteface	0.0093	0.0015	0.0014	2.28
Hoyt Lakes	0.026	0.0047	0.0039	1.89
Erie	0.038	0.0067	0.0057	1.07
Dunka Road	0.085	0.016	0.013	1.97
Fernberg	0.034	0.0052	0.0051	2.12
Env. Learning C.	0.11	0.018	0.016	2.03
Toimi	0.049	0.008	0.007	1.40
Dunka River W.	0.65	0.12	0.099	---b
Average	0.075 ^c	0.014 ^c	0.011 ^c	1.85 ^d
Regional Average	0.072 ^e	0.013 ^e	0.012 ^e	

^aEisenreich, Hollod, and Langevin (1978)

^bMeasured data are not available for the Dunka River W. site. The data from this site are included to show the predicted concentrations at the receptor closest to the smelter.

^cAverage of predicted data from 8 sites (Dunka River W. is not included in the average).

^dAverage of measured data from 8 sites.

^eAverage of predicted data from 33 regional receptors.

For example, a concentration of $0.65 \mu\text{g}/\text{m}^3$ is predicted at the Dunka River Watershed receptor using the base case smelter. This value is about a factor of seven larger than the predicted 1985 regional average (based on 33 receptors), and it is about 35% of the measured regional average.

Atmospheric sulfate is of interest because it provides a source of sulfate deposition onto land and water surfaces. Increased deposition

is important, particularly in the BWCA, because many of the weakly buffered lakes in the area are already susceptible to acidification. As a result, it may not be possible to dismiss the importance of any new SO₂ source (and sulfate source) in the area. The specific location is also important in this respect.

8.3. SULFATE DEPOSITION

As in the previous section, the potential contribution of a smelter to sulfate deposition in northeastern Minnesota must be considered in the context of the existing and predicted deposition rates in the absence of copper-nickel development. Recall that the measured geometric mean deposition rate for the region was 14.4 kg/ha/yr based on bulk deposition data. The calculated dry deposition rate based on measurements of ambient sulfate concentrations was 1.78 kg/ha/yr. Calculations using the modified gaussian model indicated that the bulk of the local contribution (about 91-96%) occurs as dry deposition, and this generally corresponds to the calculated dry deposition rate based on ambient air concentrations. Predicted deposition (wet and dry from local sources) for the region was 2.2 kg/ha/yr from 1977 point sources and 4.6 kg/ha/yr from projected 1985 sources.

Against this background, the sulfate deposition rates from the three smelter models (sited south of Babbitt) were predicted using the modified gaussian model. Table 76 presents the results of these simulations along with measured and predicted deposition rates without copper-nickel development for reference.

It appears that the regional base case deposition rates would be comparable to the present dry deposition rate of 1.8 kg/ha/yr in the

Table 76. Predicted annual average sulfate deposition rates for three smelter models located south of Babbitt; rates without a smelter are included for comparison.

Site	Sulfate deposition rates (kg/ha/yr)				Calculated ^a Dry Deposition (1977-78)
	Predicted (modified gaussian model)			1985 (no smelter)	
	Base Case Model	Option 1 Model	Option 2 Model		
Babbitt	4.7	2.0	0.77	3.8	1.98
Whiteface	0.24	0.10	0.04	4.5	2.13
Hoyt Lakes	0.63	0.27	0.10	8.8	1.79
Erie Office	0.73	0.32	0.12	11	1.01
Dunka Road	2.1	0.86	0.34	5.5	1.86
Fernberg Road	0.58	0.26	0.096	3.5	2.01
Env. Learning Center	1.5	0.65	0.24	4.1	1.92
Toimi	0.98	0.43	0.16	4.1	1.32
Dunka River W.	8.2	3.6	1.4	4.3	---b
Average	1.4 ^c	0.61 ^c	0.23 ^c	5.7 ^c	1.8 ^d
Regional Average	1.2 ^e	0.52 ^e	0.25 ^e	4.7 ^e	

^aBased on ambient air concentration measurements.

^bMeasured data are not available at the Dunka River W. site. The data from this site are included to show the predicted concentration at the receptor closest to the smelter.

^cAverage of predicted data from 8 sites (Dunka River W. is not included in the average).

^dAverage of measured data from 8 sites.

^eAverage of predicted data from 33 regional receptors.

region. Recall that the dry deposition rate essentially represents the contribution from local SO₂ point sources. The local input (based on the same 8 sites as the measured data) is predicted to increase to 5.7 kg/ha/yr by 1985. Using the predicted 1985 deposition rate as a reference, the averages shown in Table 76 for the three smelter models represent increases of 25%, 10%, and 1% for the base case, option 1, and option 2 smelters, respectively. These local source contribution increases occur against the background bulk deposition rate in the region that is in the range of 14-15 kg/ha/yr. The bulk deposition rate is dominated by wet deposition and appears to be the result of transport from distance sources, probably to the south and east. Regional bulk deposition is expected to possibly double by 1985.

Sulfate deposition is a major concern for water quality. It appears that regional deposition will continue to be dominated by wet deposition from distant sources. Nevertheless, any new sources in the area will simply aggravate existing problems. Further, site specific impacts are again an important consideration.

The Dunka River Watershed receptor located 5 km east of the hypothetical smelter site shows a predicted deposition rate that is almost 6 times the average rate from the 33 receptors, and is double the average rate recorded by the bulk samplers during the baseline period. Although this increase is reduced to 25% and 10% for the option 1 and option 2 smelters, respectively, these increases are substantial.

Sensitive lakes that receive a large portion of their inflow from areas surrounding the smelter might experience serious acidification

) impacts from increased sulfate deposition. The water quality impacts of increased sulfate deposition are considered in Chapter 10.

Predicted annual sulfate deposition is summarized for the different smelter cases in Table 77.

Table 77. Predicted annual sulfate deposition resulting from the three smelter models, 1977 regional sources, and 1985 regional sources, kg/ha/yr.

SITE NO.	NAME	BASE CASE	OPTION 1	OPTION 2	1977 REGION	1985 REGION
1	Little Johnson Lake	0.36	0.16	0.060	1.1	2.1
2	Little Vermillion Lake	0.36	0.16	0.060	1.1	2.4
3	Birch Lake Dam	0.47	0.21	0.078	1.6	3.0
4	Saganaga Lake	0.18	0.081	0.030	1.1	2.5
5	Vermillion Lake	0.65	0.29	0.11	1.4	3.2
6	Shagawa R. W.	0.81	0.36	0.13	1.4	2.7
7	Ely High School	0.85	0.38	0.14	1.5	2.9
8	Fernberg Road	0.58	0.26	0.096	2.2	3.5
9	Tower-Sudan	0.75	0.33	0.12	1.8	3.9
10	Bear Island R. W.	1.3	0.59	0.22	1.7	3.2
11	Kawishiwi Lab W.	1.3	0.58	0.22	1.7	3.1
12	Keeley Creek W.	1.2	0.54	0.20	1.8	3.2
13	August Creek	0.99	0.44	0.16	1.9	3.4
14	Isabella Watershed	0.74	0.36	0.12	3.0	4.3
15	NW of Virginia	0.35	0.15	0.58	2.2	6.2
16	Embarrass R.W.	1.4	0.61	0.23	2.2	4.9
17	Babbitt	4.7	2.0	0.77	1.9	3.8
18	Unnamed Creek W.	3.1	1.4	0.52	1.9	3.7
19	Environ. Learning C.	1.5	0.65	0.24	2.5	4.1
20	Parkville	0.30	0.13	0.049	2.9	9.7
21	Erie Office	0.73	0.32	0.12	4.0	11
22	Dunka Road	2.1	0.86	0.34	2.5	5.5
23	Dunka River W.	8.2	3.6	1.4	2.2	4.3
24	Stony River W.	1.5	0.68	0.25	2.6	4.2
25	NW of Eveleth	0.24	0.10	0.039	2.9	7.0
26	NE of Eveleth	0.31	0.13	0.051	2.5	5.9
27	Hoyt Lakes Golf C.	0.63	0.27	0.10	5.5	8.8
28	St. Louis R. W.	1.1	0.46	0.17	2.4	4.7
29	Waterhen Creek W.	0.38	0.16	0.62	2.4	4.9
30	Whiteface River W.	0.45	0.20	0.74	2.3	4.6
31	Toimi	0.98	0.43	0.16	2.1	4.1
32	Whiteface	0.24	0.10	0.04	2.1	4.5
33	Tower	0.41	0.18	0.068	1.8	3.9

CHAPTER 9. IMPACT ANALYSIS FOR PARTICULATE EMISSIONS

This section presents the ambient air concentrations and surface deposition rates for particulates (TSP) likely to result from copper-nickel development in the region.

9.1. AMBIENT PARTICULATE CONCENTRATIONS

Particulates from a copper-nickel development may be released from both point and area sources. Point source emissions will result from smelting operations, and for this discussion will be treated as area sources. Modeled particulate increases from smelting and regional growth occur in the context of measured TSP concentrations ranging from $10 \mu\text{g}/\text{m}^3$ (background for the region) to means above $50 \mu\text{g}/\text{m}^3$ (population centers near mining operations). Short-term concentrations (24-hour) of several hundred $\mu\text{g}/\text{m}^3$ occur in the region, particularly adjacent to local sources such as mining operations.

The smelter facility as a potential point source of atmospheric particulates was discussed in Chapter 3. Two models were presented for smelter stack emissions representing two levels of emissions controls. The base case smelter model was assigned an emission rate of 2385 mtpy of particulates. The option 1 and option 2 smelter models have identical particulate removal efficiencies and constitute one particulate emissions model which releases 358 mtpy of particulates.

Estimates of fugitive particulate emissions were also presented in Chapter 3. These emissions are treated as a low-level point source. This is a reasonable assumption, for example, where the major dust-producing operations are enclosed in a single large building with a roof vent and fan to maintain a good working environment for smelter

personnel. Fugitive particulate emissions were estimated to be 1500 mtpy for both models.

A mass median particle diameter of 1.1 microns was used for both particulate stack and fugitive emissions based on EPA studies of smelter emissions.²³⁸ This size will vary depending on the specific source of particulates within the smelter operation. If the mass median diameter is larger, fugitive particulates would tend to settle faster. Further, fugitive particulate emissions are only about 40% of the total base case emissions, but are 80% of the total option 1 and option 2 smelter emissions. Uncertainties in the size and character of the fugitive emissions estimates, therefore, have a greater effect on the predicted air quality impacts from the option 1-option 2 smelter than from the base case smelter.

The modified gaussian model was used to predict annual and maximum 24-hour particulate concentrations resulting from a smelter located 4.8 km south of Babbitt. The highest predicted annual average concentrations for the base case smelter (10^{-4} to 10^{-3} $\mu\text{g}/\text{m}^3$) are negligible relative to both the ambient air quality standards and PSD increments. It does not appear that annual ambient particulate concentrations will be a factor in smelter siting.

Predicted maximum 24-hour particulate concentrations for the two smelter models are presented in Figures 76 and 77. The maximum 24-hour predicted particulate concentrations for the base case model are $5.6 \mu\text{g}/\text{m}^3$ at August Creek (Class I area) and $36 \mu\text{g}/\text{m}^3$ at Dunka River Watershed (Class II area). These values are 56% and 92%, respectively, of the Class I and Class II increments. The corresponding values for

the option 1-option 2 model are $2.7 \mu\text{g}/\text{m}^3$ at August Creek (27% of the Class I increment) and $18 \mu\text{g}/\text{m}^3$ at Dunka River Watershed (49% of the Class II increment). Generally, the concentrations from the option 1-option 2 model are half those from the base case model.

From these data it appears that the Class II increment would probably be exceeded by the base case model, but not by the option 1-option 2 model.

In order to generalize the above results, 24-hour particulate concentrations were also predicted for a non-site specific case for five days likely to result in high ambient concentrations. Figure 78 presents the results for the base case smelter model using meteorology data for November 6, 1976. Particulate (TSP) concentrations fall below the Class I increment at about 15 km from the smelter. This distance is reduced to about 6 km for the option 1-option 2 smelters where the fugitive emissions component dominates. Applying the factor of two modeling accuracy to these results could increase the distances from the source at which the Class I increment is met to about 30 km for the base case model and 12 km for the option 1-option 2 model.

The above results for the smelter alone are now placed into perspective in the context of particulate concentrations expected from other point sources in the region. Modeling simulations of point sources expected in the region by 1985 without copper-nickel development showed that the Class I increment was not expected to be exceeded, but the Class II increment was expected to be exceeded at two receptors, Erie and Parkville. These results show that new sources of particulates planned for the region by 1985 may be important factors in siting plans

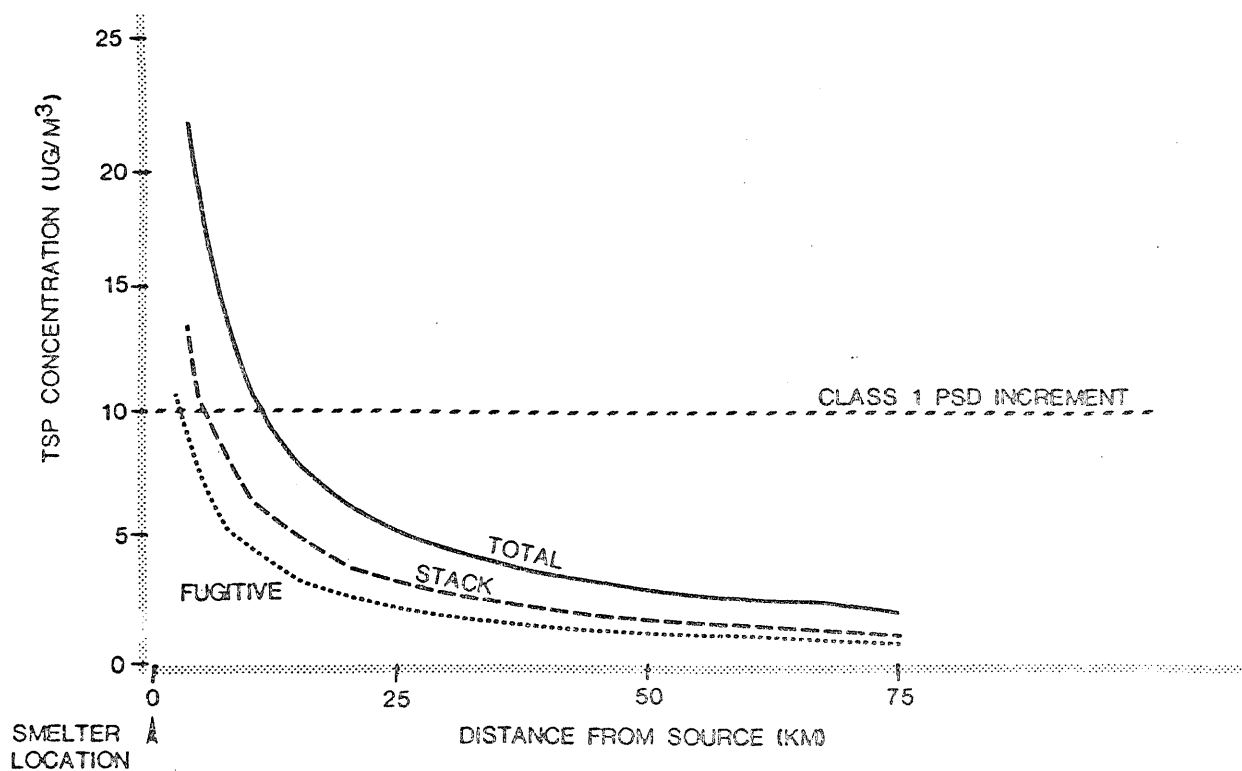
PREDICTED STACK AND FUGITIVE CONTRIBUTIONS TO 24-HOUR TSP CONCENTRATIONS
ALONG A COMBINED PLUME CENTERLINE FOR THE BASE CASE SMELTER MODEL
(USING THE MODIFIED GAUSSIAN MODEL)

FIGURE 78

(BASED ON METEOROLOGICAL DATA FOR NOVEMBER 6, 1976)

WIND DIRECTION : WMW

WIND SPEED : 24.6 KM/HR.



for a smelter in the Class II area.

When the smelter models, sited south of Babbitt, are included along with the 1985 particulate point source emissions inventory, the resulting particulate concentrations are not predicted to exceed either the annual ambient air quality standards or the annual PSD increments.

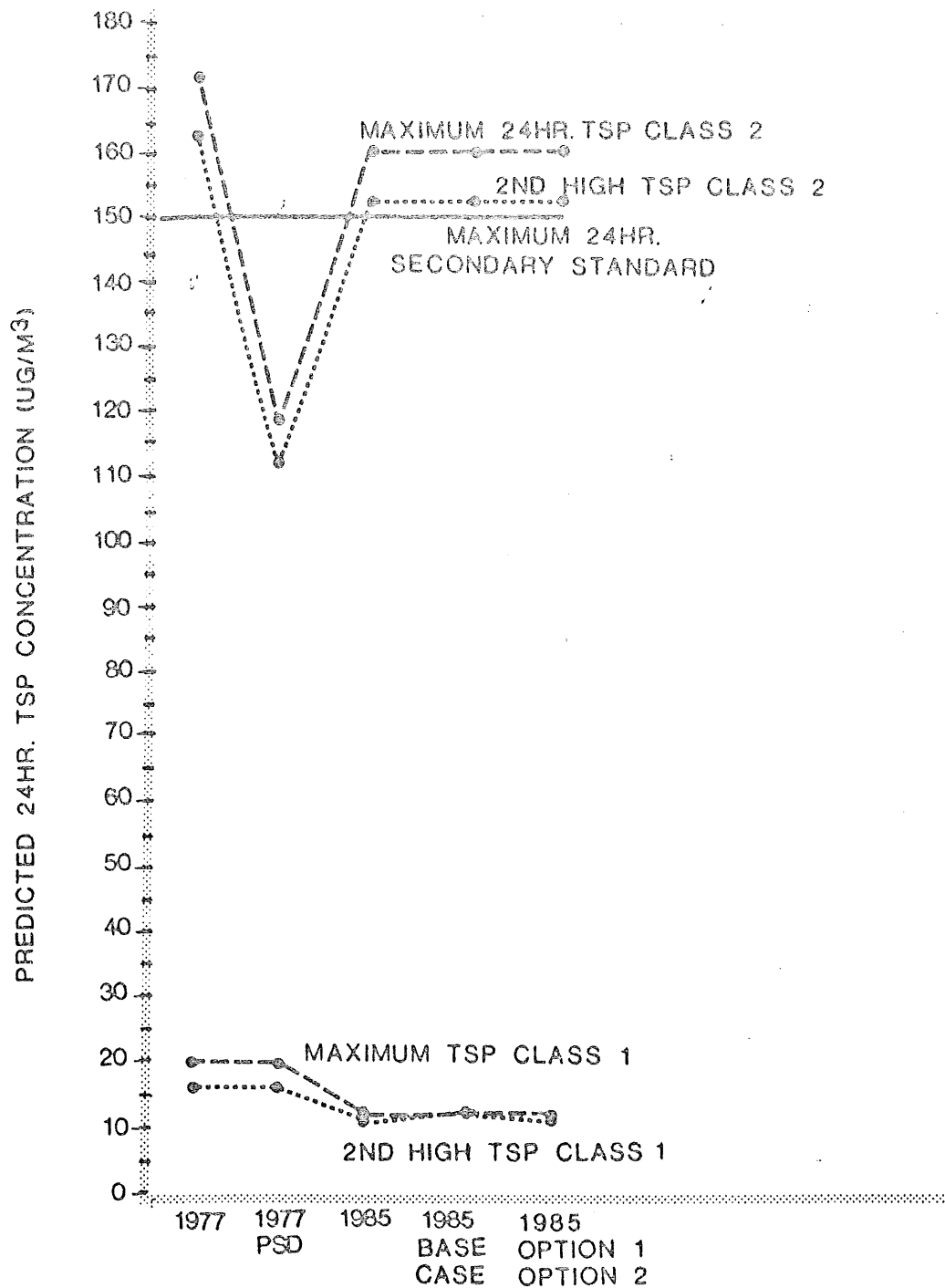
Therefore, the focus, again, is on the predicted 24-hour concentrations. Figure 79 shows both the predicted maximum and second high 24-hour particulate concentrations for the Class I and Class II areas. The 1977 regional and PSD baselines are also shown, along with 1985 concentrations with and without copper-nickel development.

The data indicate that the maximum concentrations in the Class I area are predicted to decrease about $6-8 \mu\text{g}/\text{m}^3$ by 1985, with or without the modeled smelter sources. The ambient air quality standards are not exceeded in the Class I area. However, the 24-hour secondary standard of $150 \mu\text{g}/\text{m}^3$ is predicted to be exceeded by both the maximum ($160 \mu\text{g}/\text{m}^3$) and second high ($152 \mu\text{g}/\text{m}^3$) concentrations predicted for the Erie receptor in the Class II area. Neither smelter model affects these concentrations. Also note that the computed 1977 PSD baseline at the Erie receptor is considerably lower than the 1977 regional baseline, resulting in the prediction that the Class II PSD increment will be exceeded.

The absence of a smelter effect in the above results is an important point to understand. The maximum 24-hour concentrations predicted earlier for the base case smelter alone was $5.3 \mu\text{g}/\text{m}^3$ at the Erie receptor. However, the juxtaposition of the smelter site south of Babbitt with respect to the other sources was such that when the

PREDICTED 24-HOUR MAXIMUM AND 2ND HIGH TSP CONCENTRATIONS IN CLASS 1 AND CLASS 2 AREAS FOR SELECTED RECEPTORS (MODIFIED GAUSSIAN MODEL)

FIGURE 79



highest concentrations occurred at Erie, the wind was not blowing in directions that allowed the smelter to contribute much to those concentrations. The relative orientation of point sources with respect to receptor sites plays a major role in the resulting short-term concentrations. This consideration would indicate that locating several point sources along a single line, particularly oriented along major wind axes, should be avoided if ambient particulate concentrations downwind of the sources are to be minimized.

The area impacted by the smelter particulate emissions is the sector to the NE and SE of the facility. The modeling predicts that the maximum 24-hour particulate concentrations due to base case development at the Dunka River Watershed is $60 \mu\text{g}/\text{m}^3$ (40% of the secondary standard; 23% of the primary standard) compared to $24 \mu\text{g}/\text{m}^3$ without development. The option 1-option 2 model results in a maximum 24-hour concentration of $41 \mu\text{g}/\text{m}^3$, a 32% decrease over the base case smelter.

The next highest 24-hour concentration in the area impacted by the smelter is at the Unnamed Creek Watershed receptor. The base case smelter results in a maximum 24-hour concentration of $23 \mu\text{g}/\text{m}^3$ compared to $19 \mu\text{g}/\text{m}^3$ with no copper-nickel development, about a 20% difference. The option 1-option 2 model results in a concentration of $19 \mu\text{g}/\text{m}^3$ which is the same as the concentration resulting from 1985 sources without copper-nickel development.

In summary, total particulate emissions from a smelter present a problem in terms of short-term averaging periods when PSD increments might be exceeded close to the smelter. Distances of 15-30 km from the Class I areas for the base case smelter model appear to be adequate

to prevent the increment from being exceeded. This distance is less restrictive than that imposed by SO₂ emissions from the same smelter model.

9.2. METALS

Since metals emissions data were not available for the regional sources, it was not possible to compare predicted concentrations or deposition rates resulting from regional development to existing levels. The general approach is to compare predicted levels resulting from a copper-nickel smelting operation to existing background levels and literature values in order to identify elemental constituents which may pose environmental or health problems.

The predicted elemental concentrations and deposition rates are more uncertain than SO₂ estimates as a result of uncertainty in the distribution of elements during various stages of smelting and pollution control. For example, volatiles such as arsenic are modeled as particulates and are assumed to be well controlled. As more information becomes available, it may be shown that these elements are distributed differently than assumed in the mass balances and that they are not released as particulates.

The analysis for metals is based on the option 1-option 2 smelter model which has emissions, and therefore concentrations, roughly half those of the base case smelter.

9.2.1. Ambient air concentrations.

Ambient air concentrations of Cu, Ni, As, Cd, Pb and Hg were measured at eight sites in the region. Table 78 presents a comparison between the measured and predicted concentrations resulting from the

Table 78. Comparison between measured^c and predicted ambient air concentrations of selected metal species, ng/m³.

Location	COPPER		NICKEL		ARSENIC		CADMIUM		LEAD		MERCURY	
	Meas	Pred	Meas	Pred	Meas	Pred	Meas	Pred	Meas	Pred	Meas	Pred
Region	4.1 ^a	13 ^b	1.7 ^a	2.9 ^b	4.6 ^a	0.006 ^b	2.1 ^a	0.004 ^b	38 ^a	0.007 ^b	1.0	0.002
Babbitt	2.8±2.3	45	2.6±2.5	10	7.2±7.6	0.020	1.6±3.3	0.012	136±80	0.023	0.86±0.054	0.0053
Whiteface	3.0±2.4	1.5	1.2±0.91	0.37	3.7±4.3	0.0008	0.57±0.54	0.005	31±25	0.0009	1.2±1.1	0.0002
Hoyt Lakes	3.3±2.5	4.6	1.1±0.96	1.0	7.7±9.6	0.0021	1.6±1.1	0.0013	34±36	0.0024	0.74±0.86	0.0006
Erie	2.5±2.6	6.8	0.71±1.9	1.5	4.5±11	0.0031	0.40±0.55	0.0019	33±33	0.0036	1.4±0.96	0.0009
Dunka Road	7.6±11	15	4.0±5.6	3.4	4.6±4.2	0.0066	5.4±22	0.0041	22±22	0.0076	0.85±0.97	0.0017
Fernberg Rd.	5.7±9.9	5.3	2.5±5.7	1.3	3.1±3.1	0.0030	6.0±16	0.0019	19±25	0.0035	0.78±0.83	0.0009
Env. Learning C.	2.4±1.7	18	1.3±	4.2	3.3±	0.0092	1.2±	0.0058	19±	0.011	1.0±	0.0026
Toimi	5.7±8.5	8.5	0.36±0.51	2.0	2.8±2.8	0.0042	0.22±0.44	0.0026	13±14	0.0048	1.2±0.93	0.0012
Dunka R. W. ^d		130		28		0.054		0.034		0.063		0.014

^a based on 8 sites

^b based on 33 sites

^c measured data from Thingvold et al. (1979)

^d measurements were not available at this site; predicted data are included for worst-case comparison.

the option 1-option 2 smelter.

The concentrations of these pollutants which were measured in north-eastern Minnesota are typical of concentrations measured in remote areas: Cu, 0.4-100 ng/m³; Ni-0.4-10 ng/m³; As, 0.3-5.0 ng/m³, Cd, 0.01-4.0 ng/m³; Pb, 0.3-200 ng/m³; Hg, 0.06-0.4 ng/m³.⁵⁹

A comparison of measured and predicted data at each receptor site shows that the option 1-option 2 smelter would result in ambient air concentrations of Hg, Pb, As, and Cd that are 2-3 orders of magnitude lower than existing levels. Concentrations of Cu and Ni, however, are expected to be the same order of magnitude or higher. A comparison of predicted concentrations at Dunka River Watershed to the measured values shows that the predicted concentrations of Cu, Ni, and Cd are within an order of magnitude of currently measured regional concentrations.

Maximum 24-hour concentrations of these six metals were estimated on the basis of the elemental composition of the concentrate and total particulate concentration predicted using meteorology from November 6, 1976 (Figure 78). It was assumed that the elements were present in total particulate in the same ratio as in the concentrate. The analysis is not site specific, and concentrations are calculated at 5 km, 20 km, and 50 km downwind from the source. The resulting concentrations for the option 1-option 2 smelter are shown in Table 79 along with measured regional average 24-hour and maximum 24-hour concentrations. Concentrations resulting from the base case smelter can be obtained by doubling the predicted concentrations. The values in Table 79 probably represent an order of magnitude estimate because of underlying assumptions. The results, however, generally agree with the site specific modeling runs.

Table 79. Maximum predicted 24-hour ambient concentrations of metals in particulates downwind of the option 1-option 2 smelter model, assuming particulates have the elemental composition of the concentrate, compared to measured values in the region, ng/m³.

Element	24-Hour Concentrations Measured in the Region ^a		Predicted Maximum 24-Hour Concentration Downwind Of the Option 1-Option 2 Smelter ^f		
	Average ^b	Maximum	5 km ^c	20 km ^d	50 km ^e
Cu	12	109	1500	480	210
Ni	4	27	290	93	40
As	7	51	0.34	0.11	0.05
Cd	9	132	0.44	0.14	0.06
Pb	59	734	0.65	0.21	0.09
Hg	3	11	0.0019	0.0006	0.0003

^a data from analysis of 24-hour membrane samples (Eisenreich, Hollod, and Langevin 1978).

^b average for all stations, with non-detectable data omitted

^c Based on total particulate concentrations of 22 ug/m³ at 5 km downwind.

^d Based on total particulate concentration of 7 ug/m³ at 20 km downwind.

^e Based on total particulate concentration of 3 ug/m³ at 50 km downwind.

^f Based on meteorology of November 6, 1976 and no specific smelter location; values are rounded.

The predicted ambient air concentrations on both an annual and a 24-hour basis are far below those levels associated with measurable health effects in Chapter 4.

9.2.2. Deposition.

Table 80 presents a compilation of measured metals deposition data in the study region and from other areas. These values provide a basis of comparison to determine whether or not deposition loadings from a copper-nickel smelter would approach existing or reported values. In general, the measured dry deposition rates are typical of remote,

mid-continental areas.⁵⁹

Metal loadings at the regional sampling sites are calculated as dry deposition rates using ambient air concentrations measured in the region and the dry deposition velocities from Chilton, England.³² For comparison the predicted values at Dunka River Watershed and the average from the 33 receptors are also included in Table 80.

A comparison of the data shows that the option 1-option 2 smelter will result in Cu and Ni deposition rates comparable to existing rates.

Deposition of As, Cd, Pb, and Hg is expected to be at least 2 orders of magnitude lower at each of the sites. When predicted deposition rates at Dunka River Watershed are compared to the measured values, levels of Cu and Ni are predicted to be elevated, and cadmium is within an order of magnitude of the measured value.

Predicted deposition rates of metals for the option 1-option 2 smelter are given in Table 81.

The impact of metals desposition on the area's soils and waters is considered further in Chapter 10.

Table 80. Mean annual measured and predicted deposition rates for the option 1-option 2 smelter at regional receptors.
(g/ha/yr)

Location	COPPER		NICKEL		ARSENIC		CADMIUM		LEAD		MERCURY	
	Meas	Pred	Meas	Pred	Meas	Pred	Meas	Pred	Meas	Pred	Meas	Pred
Fernberg ^a	15	31	11	5.2	1.9	0.002	7.6	0.001	18	0.003		0
Env. Learn. C. ^a	6.0	100	5.7	17	1.9	0.007	1.6	0.004	18	0.01		0.0001
Dunka Road ^a	19	180	18	26	2.8	0.021	6.9	0.011	20	0.022		0.003
Toimi ^a	15	52	1.6	8.8	1.9	0.005	0.32	0.002	13	0.006		0
Erie ^a	6.3	42	3.2	6.8	2.8	0.003	0.63	0.002	32	0.004		0
Hoyt Lakes ^a	8.2	39	5.0	6.0	4.7	0.004	1.9	0.002	32	0.005		0
Whiteface ^a	7.6	22	5.4	3.7	2.2	0.002	0.63	0.0009	130	0.002		0
Dunka R.W. ^d		760		117		0.050				0.065		0.015
Region, dry ^a	10	80	7.6	13	2.8	0.006	2.5	0.003	34	0.008		<0.001
Region, bulk ^b	11		<14		<11		3.0		77			
Urban ^c	270- 1400		1720				40		1650- 4750			
Remote Urban ^c	18- 230		91				1.0		19- 246		1-3	
Oceans & Lakes ^c	40- 570		14- 68				6.0- 11		77- 130			

^a measured data calculated using Chilton's deposition velocities (Cawse, 1974) and regional ambient air data.

^b bulk deposition data

^c Eisenreich *et al.* 1978

^d measurements were not available at this site; predicted data are included for worst-case comparison.

Table 81. Predicted annual metal deposition rates for the option 1-
option 2 smelter.

Site No.	Name	g/ha/yr.		mg/ha/yr			
		Cu	Ni	As	Cd	Pb	Hg
1	Little Johnson Lake	13	2.2	1.0	0.5	1.0	0
2	Little Vermillion Lake	13	2.3	1.0	0.6	2.0	0
3	Birch Lake Dam	25	4.3	2.0	0.9	3.0	0
4	Saganaga Lake	7.8	1.4	0.7	0.3	1.0	0
5	Vermillion Lake	26	4.4	2.0	1.0	3.0	0
6	Shagawa R. W.	41	7.0	4.0	2.0	5.0	0
7	Ely High School	56	9.1	4.0	2.0	5.0	0
8	Fernberg Road	31	5.2	2.0	1.0	3.0	0
9	Tower-Sudan	36	5.9	3.0	2.0	4.0	0
10	Bear Island R.W.	90	14	6.0	3.0	9.0	1.0
11	Kawishiwi LaB W.	87	14	5.0	3.0	8.0	1.0
12	Keeley Creek W.	74	12	6.0	3.0	8.0	1.0
13	August Creek	55	9.3	4.0	2.0	6.0	0
14	Isabella Watershed	40	7.0	3.0	2.0	5.0	0
15	NW of Virginia	15	2.7	2.0	0.8	2.0	0
16	Embarrass R.W.	77	12	7.0	4.0	9.0	0
17	Babbitt	290	48	29	15	35	2.0
18	Unnamed Creek W.	230	36	14	7.0	20	2.0
19	Environ. Learning C.	100	17	7.0	4.0	10	1.0
20	Parkville	14	2.4	1.0	0.6	2.0	0
21	Erie Office	42	6.8	3.0	2.0	4.0	0
22	Dunka Road	180	26	21	11	22	3.0
23	Dunka River W.	760	117	50	24	65	15
24	Stony River W.	110	18	7.0	4.0	10	1.0
25	NW of Eveleth	10	1.9	1.0	0.8	2.0	0
26	NE of Eveleth	16	2.8	2.0	1.0	3.0	0
27	Hoyt Lakes Golf C.	39	6.0	4.0	2.0	5.0	0
28	St. Louis R.W.	54	9.2	5.0	3.0	7.0	0
29	Waterhen Creek W.	20	3.4	3.0	2.0	3.0	0
30	Whiteface River W.	22	3.7	2.0	0.9	2.0	0
31	Toimi	52	8.8	5.0	2.0	6.0	0
32	Whiteface	12	2.1	2.0	1.0	2.0	0
33	Tower	17	3.0	2.0	0.9	2.0	0

CHAPTER 10. SOIL AND WATER IMPACTS

This chapter will explore potential impacts of smelting in northeastern Minnesota on soils in terms of copper and nickel deposition, and impacts on surface waters in terms of sulfate and metal deposition. This is not intended to be an exhaustive study, but to highlight problem areas.

Detailed reports on potential ecosystem effects due to copper-nickel development have been prepared by Sather et al.²⁰⁸ Glass and Loucks⁸⁸ have prepared an extensive report documenting potential adverse effects on the BWCA-VNP area from the proposed Atikokan, Ontario power plant.

10.1. SOIL IMPACTS

The impact of heavy metals loading on soils is of concern in terms of soil productivity, leaching into the water system, and toxicity to soil microorganisms and plants.

Heavy metals contamination of soil and subsequent damage to vegetation has been reported by several investigators. Buchauer²⁷ reports that plant death occurred in the vicinity of a zinc smelter with zinc levels up to 80,000 ppm and cadmium levels up to 1,500 ppm. Djuric et al.⁵³ reported on soil contamination from a lead smelter in Yugoslavia.

The effects of metals on plants may be direct or indirect. Hutchinson and Whitby¹¹⁰ reported that root elongation of radish, cabbage, tomato, and lettuce was almost totally inhibited at all sites closer than 3.8 km from the Conniston smelter at Sudbury, irrespective of the depth from which the soil was obtained. A 50% reduction in root elongation was found at a distance of 10.4 km from the smelter when compared to controls at 50 km. In the tomato 2 ppm each of Ni, Al, Co, and Cu reduced root elongation by 70%, 80%, 60%, and 30%, respectively. Total

inhibition occurred at 10 ppm Ni, 4 ppm Al, 15 ppm Co, and 15 ppm Cu. Sulfate levels of 250 ppm were not found to be inhibitory.

Slowed decomposition resulting from heavy metal loading may produce litter layers that are poor seedbeds for species that require mineral soil for establishment such as red pine and jack pine.²⁰⁸ Field investigations by Jordan¹¹⁶ and Hutchinson and Whitby¹⁰⁹ suggest that heavy metals deposited near smelting operations have a tendency to remain in the humus of the forest floor rather than leaching into the mineral horizons of the soil.

The litter layer is important as a potential reservoir of plant nutrition, particularly of nitrogen and phosphorous. A lowering of primary productivity could result if the concentrations of nitrogen and phosphorous increase due to a lower decomposition and mineralization rate.

Tyler²⁵⁶ found that the biological activity of the soil decreases with increasing heavy metal content, and suggested that activity decreases long before the litter production of coniferous trees and their vitality are affected.

Ruhling and Tyler²⁰⁶ found that litter decomposition in forest surrounding metal processing industries is influenced by high concentrations of deposited metals. Their studies demonstrated significant decreases in CO₂ evolution with increasing concentrations of Cd, Cr, Cu, Fe, Ni, V, and Zn for partially disintegrated spruce needles.

Tyler²⁵⁵⁻²⁵⁹ studied the effects of heavy metal deposition (primarily Cu and Zn) from a brass mill in Sweden on soil biological processes and productivity in spruce forest soils. Cu and Zn deposition

were found to reduce the decomposition rate, the nitrogen mineralization rate, and phosphatase activity.

The conversion of organic nitrogen compounds of the litter layer into mineral nitrogen primarily by microbes is a primary process. Tyler²⁵⁵⁻²⁵⁷ reports that at copper concentrations greater than 30 ppm (about three times the background level) the nitrogen mineralization rate decreases rapidly with increasing copper content.

Organic phosphates in the soil are broken down by phosphate enzymes. A reduction in phosphatase activity has the eventual effect of slowing vegetation growth because organic nutrients are not directly taken up by plants. Phosphatase activity was found to significantly decrease at copper concentrations of 30 to 300 ppm, and a decrease in phosphatase activity was measured for copper concentrations as low as 15 ppm.²⁵⁶⁻²⁵⁷

Tyler^{254,256} also found that high metal concentrations caused an extensive reduction in urease activity.

Two stages of ecosystem disruption due to heavy metals accumulation were noted by Jackson and Watson:¹¹³ 1) an initial stage at 1.2-2.0 km from the stack characterized by accumulation but no measureable effects on soil litter biota, and 2) an advanced stage at 0.4-0.8 km from the stack characterized by depletion of soil and litter nutrient pools, and evidence of depressed decomposition communities and nutrient translocation.

Arthropod biomass was found to be significantly decreased ($p < 0.1$) at 0.8 km from a Pb smelter.¹¹³ Arthropods are responsible for the initial stages of litter decomposition by increasing substrate surface

area, and enrichment by gut passage, and inoculation of microbial decomposition.

Dissolved metals from the litter layer may leach into the underlying soil and may be assimilated by plant roots and translocated into above ground vegetation. Jackson and Watson¹¹³ demonstrated increased concentrations of Pb, Cd, Zn, and Cu in oak roots and leaves at 0.4 km from a lead smelter compared to controls at 21 km.

Because of the potential for decreased soil productivity and possible bioaccumulation of metals in the food chain, the impacts of copper and nickel smelter emissions on the litter layer was examined for three upland soil types in northeastern Minnesota. Predicted copper and nickel loadings after 25 years of smelter operation were added to existing levels taken from Patterson and Asseng¹⁸⁰ to provide an estimate of concentrations after development. This calculation depends on the forest floor weight; that is, for a given concentration, higher soil weight results in higher loadings.

Although this analysis does not consider build-up or loss of the litter layer, leaching of metals, or any changes in litter weight due to metals build-up, it should provide a worst-case comparison between present and projected metals loadings.

The analysis is limited to three soil associations (Newfound-Newfound, Mesabo-Barto, Toivola-Unnamed Cloquet) with two plots each of aspen vegetation.²⁰⁸ Receptor sites were selected near the field plots, and the predicted annual depositions (based on a smelter located south of Babbitt) were calculated as 25 year loadings at each of the receptors. Figure 80 shows the field plots and receptor locations.

FIGURE 80. FIELD PLOT AND RECEPTOR LOCATION FOR AIR/SOIL IMPACT ANALYSIS

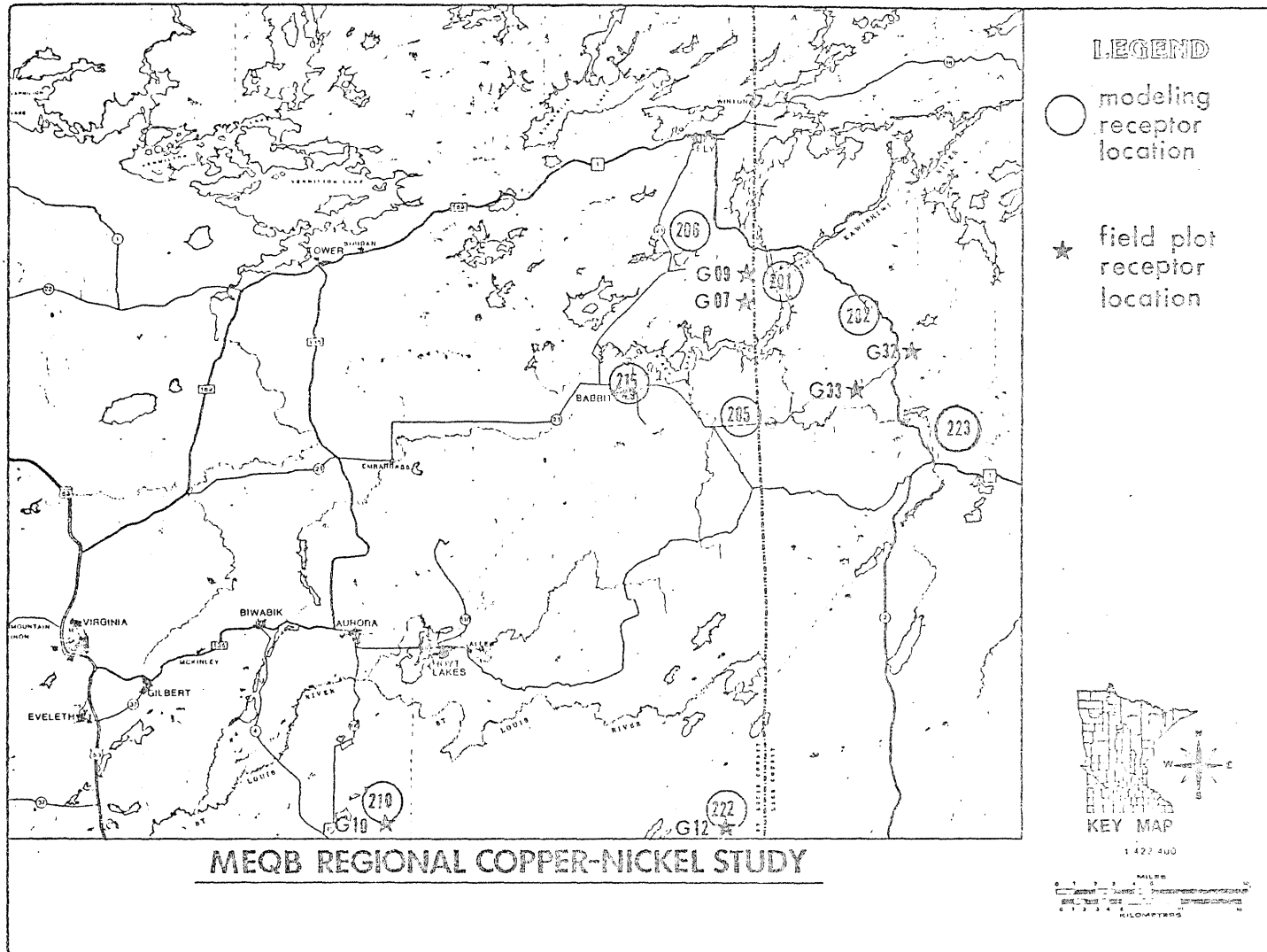


Table 82 shows a comparison between the measured background Cu and Ni soil concentrations and projected loadings after 25 years of option 1 smelter operation. The average of the measured data, 14.0 ppm Cu and 7.0 ppm Ni, is below world-wide average values of 15 to 40 ppm Cu and 15 to 25 ppm Ni given by Aubert and Pinta.⁵

The option 1 smelter operating for twenty-five years could have the effect of increasing the background concentrations of copper at the six selected plots from 2 to 40 times; nickel concentrations could be increased from about 2 to 500 times. These estimates include the deposition rates from the Dunka River Watershed receptor which is the site most impacted by the smelter.

The impact of Cu and Ni loading from a 25 year smelter operation can be further examined by calculating changes in litter decomposition rates.²⁰⁸

This calculation is made using Freedman's⁷⁷ data on heavy metals and litter decomposition along a transect downwind of the Copper Cliff smelter at Sudbury. Litter decomposition half-life and 95% loss time for aspen litter were calculated by Freedman. Since decomposition rates in northeastern Minnesota were measured by the same method, it seems reasonable to compare the two measurements to evaluate the effect of a smelter on litter decomposition rates.

Copper soil concentrations (Table 82) after twenty-five years of option 1 smelter operation were compared to soil concentrations measured at 30 km and 40 km from the Copper Cliff smelter at Sudbury. Predicted copper concentrations at the six sites in northeastern Minnesota range from 35 to 540 ppm compared to 200 ± 80 ppm measured at

Table 82. Comparison between background and predicted Cu and Ni concentrations in soils after 25 years of option 1 smelter operation.

Soil Association	% of Area	Plot and Vegetation	Measured data ^a		Predicted loading after 25 years of option 1 smelter, g/ha		Predicted soil conc. background + smelter, ppm		litter depth cm	litter weight g/m ²	
			Cu g/ha	Ni (ppm)	Cu g/ha	Ni g/ha	Cu ppm	Ni ppm			
Newfound	#5	13.5	G10, Aspen	150 (13)	12 (10)	1300 (110)	220 (19)	120	19	1.2	1190
Newfound			G12, Aspen	107 (18)	72 (12)	500 (86)	85 (15)	100	27	0.9	581
Toivola Unnamed Creek	#7	11.2	G32, Aspen	560 (13)	460 (10)	2580 (58)	430 (9.6)	70	38	3.4	4470
			G33, Aspen	450 (12)	1270 (16)	1850 (23)	300 (3.8)	35	20	4.4	7910
Mesaba Barto	#8	12.7	G07, Aspen	210 (13)	20 (<1.0) ^d	10700 ^c (530)	1670 ^c (83)	540	<84	1.2	2020
			G09, Aspen	730 (13)	76 (1.3)	2220 ^b (530)	350 ^b (6.0)	51	7.0	5.9	5830

^aPatterson, III and Asseng (1978)

^baverage of 2 sites

^caverage of 3 sites

^dresults reported as zero; a less than of 1.0 ppm used in the calculation

40 km from the Copper Cliff smelter and 400 ± 400 ppm at 30 km. Predicted nickel concentrations which range from 7 to 83 ppm are less than half of the Copper Cliff data, 160 ± 40 ppm, at 40 km. The time required for 95% decomposition of aspen litter was calculated to be 6.52 years at 30 km and 1.25 years at 40 km from the Copper Cliff smelter.⁷⁷ The 95% loss time at each of the regional sites were calculated to be 5.7 years at G07, 5.1 years at G09, 4.4 years at G10, 5.0 years at G12, 5.4 years at G32, and 4.3 years at G33; the average 95% loss time for these sites is 4.65 years.¹⁷⁹ These data suggest that after 25 years of smelter operation, projected metals loadings could reduce litter decomposition rates from a tenth to over a factor of 2. An average decrease of about 30% is calculated over the six regional receptors.

10.2. WATER IMPACTS

The impact of metals and acid forming species on the study region's lakes and streams is of vital interest. Many of the lakes and streams in the area are already susceptible to acidification based on buffering capacity (Table 83). The deleterious effects of acidic precipitation are well documented.⁵⁴ Some of these effects include mobilization of toxic elements, bioaccumulation, changes in nutrient cycling, and a reduction in growth and reproduction of plant and animal species.

Glass and Loucks⁸⁸ report that about 75% of the 85 sampled BWCA-VNP lakes have a total alkalinity less than 15 mg/l as CaCO_3 , and about 23% have alkalinity less than 5 mg/l as CaCO_3 . Evidence suggests that some lakes in the BWCA are at or near the threshold of acidification serious enough to initial species depletion and lowered productivity.⁸⁸

The surface water quality impacts of the option 1 copper-nickel

Table 83. Susceptibility of lakes and streams to acidification.

LAKE SUSCEPTIBILITY		
<u>High</u>	<u>Medium</u>	<u>Low</u>
Greenwood	Gabbro	Colby
Clearwater	Brich	Bass
North McDougal	Sand	Wynne
South McDougal	White Iron	Tofte
Turtle	Fall	
Long	August	
Bear Head	State	
Perch	Pine	
Bear Island	Big	
Seven Beaver		

STREAM STATIONS		
Kawishiwi-6	Kawishiwi-1,2,3,4,5,7	Isabella-1
Bear Island-1	Keeley Creek-1	Dunka-2
Bob Bay-1	Partridge-4	Stoney River-1,2,3,4
Stoney River-5	St. Louis-3	St. Louis-1,2
Filson Creek-1		Partridge-1,2,3,5
		Embarrass-1,2
		Waterhen-1
		Whiteface-1,2

Source: Thingvold et al. (1979)

smelter were assessed by: 1) comparing measured snowpack concentrations calculated at selected watersheds to predicted snowpack concentrations calculated from winter deposition rates, 2) comparing predicted annual deposition to measured average stream and lake concentrations, and 3) determining the length of time required to neutralize a low and a high alkalinity lake.

10.2.1. Snowpack concentrations.

The atmospheric deposition of air pollutants onto surface waters occurs under two distinct sets of climatic conditions, summer and winter.

During the winter months when the ground is frozen and surface runoff is non-existent, air pollutants are deposited onto the snowpack, stored, and later released over a very short time interval (a few hours to several days) during the spring melt.¹ The time interval of release is a function of the suddenness of the spring thaw and the watershed size. Small watersheds respond more quickly than large watersheds.

The melt-freeze cycles that occur during the snowmelt can result in dramatic increases in the concentrations of pollutants in the meltwaters.^{87, 122} Johannessen et al.¹¹⁵ found that concentrations of H^+ , $SO_4^{=}$, NO_3^- , and heavy metals were two to three times greater in the first 30% of meltwater than in the snow samples during laboratory and field studies.

During the summer the deposition of air pollutants is a function of the pollutant type and concentration as well as the type of rain-storm. In northeastern Minnesota the ambient air concentrations of pollutants appear to be due to long-range transport, and the greatest loading of $SO_4^{=}$ and H^+ has been found to occur during the wet months, normally June and July.²⁴⁷ In 1977, however, the wet months were September and October.

Snowmelt enrichment tests were conducted in the study region during 1978, and these results generally confirm that about 50% to 70% of the 5 parameters analyzed (H^+ , $SO_4^{=}$, NO_3^- , Cl^- , F^-) are contained in the first 40% of the meltwater.²⁴⁷

The deposition rates predicted for the snow season (November 1-April 30) using the option 1 smelter were converted to snowpack concentrations using an average snow depth equivalent water content of 114 mm

which is about 90% of normal. It was assumed that everything that is deposited remains in the snow until melting.

Table 84 presents a summary between the predicted regional snowpack concentrations of selected species and the measured concentrations at five watersheds which are shown in Figure 81.

In the case of copper the predicted snowpack concentrations range from 15-390 $\mu\text{g}/\text{l}$ compared to a measured regional average concentration of 5.0 $\mu\text{g}/\text{l}$. Predicted nickel concentrations are also elevated, ranging from 2 $\mu\text{g}/\text{l}$ to 60 $\mu\text{g}/\text{l}$ compared to a measured regional average of 2.3 $\mu\text{g}/\text{l}$. Predicted sulfate concentrations in snow are estimated to be the same order of magnitude as the measured values, ranging from 0.05 to 1.0 mg/l for predicted values compared to 1.8 mg/l for measured values. Predicted Cd and Pb concentrations are 1 to 4 orders of magnitude below the measured values. Measured snowpack concentrations were not available for As and Hg.

If we assume that the average concentration in the snow can double or triple at the spring melt, then predicted concentrations would increase accordingly.

Table 85 presents a comparison between measured snowpack concentrations and measured stream concentrations at low flow, spring flow, and the highest concentration observed at six stream sites.

Predicted snowpack concentrations from the option 1 smelter could be substantially higher than measured maximum concentrations for Cu and Ni, assuming a 2-3 times increase at snowmelt. The impact of the smelter emissions would be greater in small systems such as Filson Creek (F-1) rather than large systems such as Kawishiwi (K-6). In large systems

FIGURE 81. WATERSHED AND RECEPTOR LOCATIONS

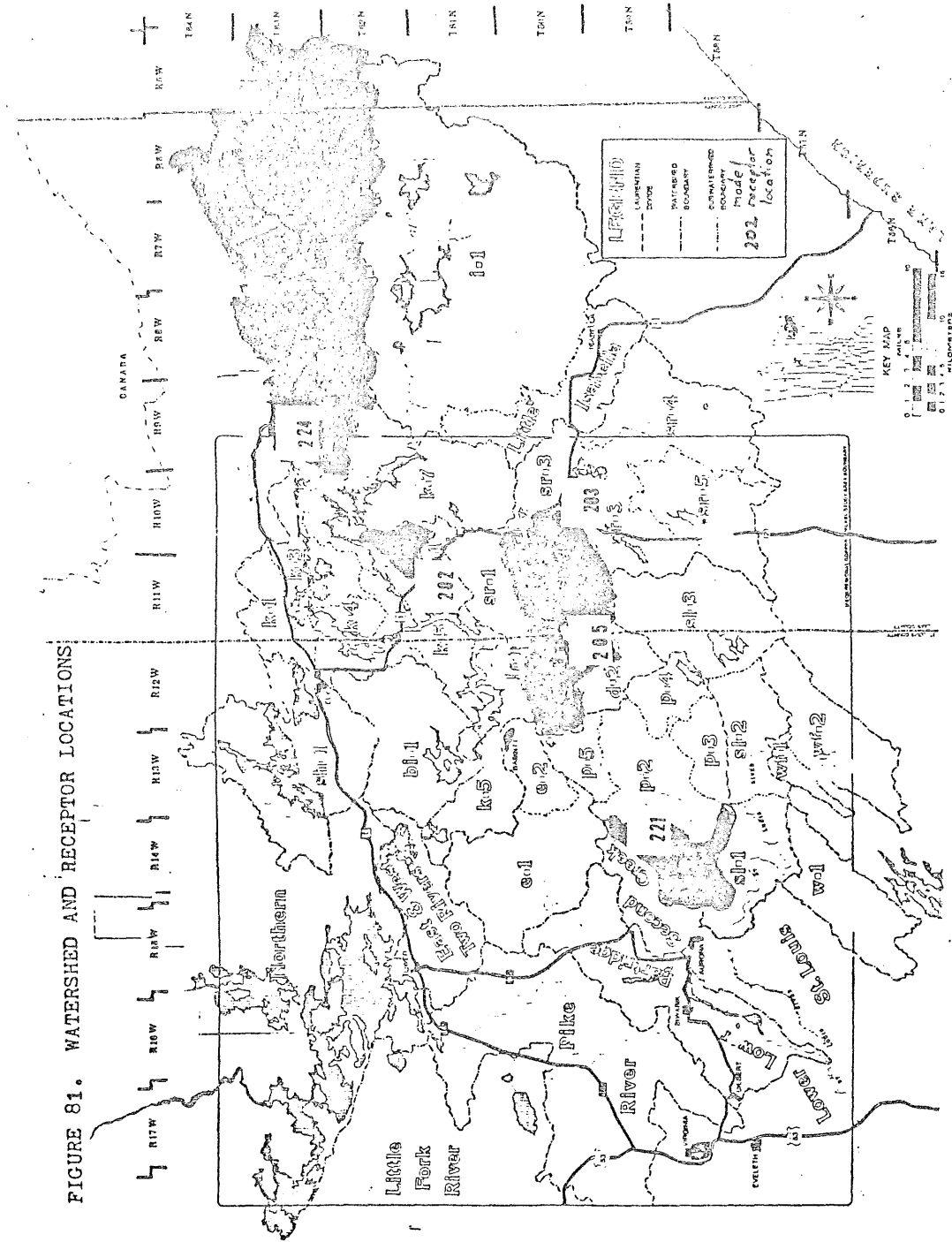


Table 84. Comparison between measured average snowpack concentrations and predicted snowpack concentrations of selected species.

Species	measured ^b average	Snowpack Concentration				
		F-1	P-1	D-1 ^a	SR-2	K-6
SO ₄ ⁼ mg/l	1.8	0.14	0.055	1.0	0.17	0.23
Cu μg/l	5.0	35	16	390	56	15
Ni μg/l	2.3	5.7	2.4	60	9.1	2.6
As μg/l		2x10 ⁻³	1x10 ⁻³	0.022	3.5x10 ⁻³	1x10 ⁻³
Cd μg/l	0.25	1.1x10 ⁻³	5x10 ⁻⁴	0.011	1.7x10 ⁻³	5.2x10 ⁻³
Pb μg/l	9.3	3.1x10 ⁻³	1.4x10 ⁻³	0.031	5.0x10 ⁻³	1.5x10 ⁻³
Hg μg/l		2.6x10 ⁻³	3.8x10 ⁻⁵	0.011	4.4x10 ⁻³	8.8x10 ⁻⁵

^areceptor at D-1 is Dunka River Watershed, site most impacted by

^ba smelter

Thingvold et al. (1979)

there is sufficient receiving water and subsequently buffering capacity to neutralize the effects of acidic snowmelt and provide adequate dilution. In a small system the snowmelt may account for the major portion of the stream flow.²⁴⁷

The concentration of most trace elements in the surface waters of the BWCA-VNP and the study region are generally low.^{88, 247} Increased concentrations of trace metals due to copper-nickel development or to regional growth will result in greater percentages of toxic metals available for mobilization and accumulation. Acidic runoff due to snowmelt is also important because it occurs during the spawning season when fish are more vulnerable.

10.2.2. Stream and lake concentrations.

The next step in the analysis was to attempt to relate the predicted annual depositions to average stream and lake concentrations of selected

Table 85. Summary comparison between snowpack concentration and stream concentration of selected species at low flow, spring flow, and the highest concentrations observed.^b

Species ^a	snowpack conc.	Stream Location								
		F-1			P-1			D-1		
		spring melt	low flow	max conc	spring melt	low flow	max conc	spring melt	low flow	max conc
SO ₄ ⁼ mg/l	1.8	7.9	5.4	15	63	190	260	9.5	13	70
Cu μg/l	5.0	8.7	5.5	12	4.0	4.0	5.9	2.3	1.7	6.1
Ni μg/l	2.3	8.0	6.0	8.0	6.0	7.0	7.0	2.0	2.0	10
Pb μg/l	9.3	1.2	0.7	6.4	0.7	0.4	2.6	1.0	0.6	46
Cd μg/l	0.25	0.05	0.02	0.18	0.08	0.43	0.18	0.05	0.08	0.15
pH	4.5	5.9	7.3	7.3	7.3	6.6	7.3	6.8	7.1	7.7

Species ^a	SR-2			K-6		
SO ₄ ⁼ mg/l	6.5	5.5	14	4.0	3.7	7.2
Cu μg/l	2.8	0.6	2.8	1.6	1.8	2.0
Ni μg/l	2.0	2.0	3.0	4.0	2.0	4.0
Pb μg/l	0.9	0.4	31	2.4	0.3	2.4
Cd μg/l	0.04	0.02	0.15	0.12	0.03	0.13
pH	5.8	6.8	7.5	6.4	6.5	7.0

^a measured data not available for As and Hg

^b Thingvold et al. (1979)

parameters. For this analysis the regional deposition data and a regional runoff value of 27.2 cm^{102} were used to calculate a regional concentrations of selected metals and sulfate in the watersheds. All of these calculations are based on the option 1 smelter located south of Babbitt.

It was assumed that the input into the stream or lake remained constant, and that removal by precipitation, plant uptake, weathering, and so forth does not occur.

Table 86 provides a comparison between the measured and predicted deposition rates, stream, and lake concentrations. A comparison between the measured deposition rates expressed as a concentration and the mean stream and lake concentrations is generally good for sulfate, copper, and nickel. Arsenic, cadmium, and lead depositions appear to be high compared to the measured lake and stream concentrations, and may indicate that these are being removed by chemical activity.

Since it seems reasonable to relate the measured deposition data to average stream and lake concentrations, the comparison was extended to include the predicted deposition data.

The predicted stream data include the average of those receptors in each watershed for the three stream groups. The measured data are separated into an impacted group A (primarily taconite mining related impacts), group B (moderately impacted by human activity), and group C (unimpacted). The predicted data indicate that streams which are now moderately impacted will receive the largest impacts from a smelter at Babbitt; the impacted area will of course change with the smelter location.

Table 86. Comparison between measured and predicted deposition rates, stream, and lake concentrations, from the option 1 smelter located at Babbitt.

species	deposition kg/ha/yr	conc units	dep rate as a conc ^a	measured data			lake conc ^b	
				mean stream conc			range	mean
				A	B	C		
SO ₄ ⁼	14.36	mg/l	5.28	97	27	7.1	<1-140	7.8
Cu	0.011	µg/l	4.04	3.0	2.7	4.2	0.2-10	1.8
Ni	0.014	µg/l	<4.9	24.8	2.1	3.5	0.4-6.0	1.4
As	<0.011	µg/l	<4.04	0.83	6.0	0.82	0.4-2.1	0.7
Cd	0.003	µg/l	1.1	0.055	0.061	0.046	0.008-0.8	0.05
Pb	0.007	µg/l	28.3	1.08	2.4	0.76	0.08-1.9	0.5

species	deposition, kg/ha/yr		conc units	mean stream concentration			average lake concentration
	range	mean		A	B	C	
	SO ₄ ⁼	0.16-3.6		0.97	mg/l	0.23	
Cu	0.02-0.76	0.17	µg/l	37	125	29	28
Ni	0.006-0.12	0.027	µg/l	5.9	19	4.8	2.7
As	(2-29)x10 ⁻⁶	1.3x10 ⁻⁵	µg/l	3.0x10 ⁻³	1.0x10 ⁻²	2.5x10 ⁻³	8.3x10 ⁻⁴
Cd	(2-24)x10 ⁻⁶	7.0x10 ⁻⁶	µg/l	1.5x10 ⁻³	4.8x10 ⁻³	1.5x10 ⁻³	1.2x10 ⁻⁴
Pb	(2-65)x10 ⁻⁶	1.7x10 ⁻⁵	µg/l	3.7x10 ⁻³	1.2x10 ⁻²	3.0x10 ⁻³	1.2x10 ⁻³

^a calculated using a regional runoff value of 27.2 cm

^b surface values only; Thingvoid et al. (1979)

A comparison of the measured to predicted data shows that As, Cd, and Pb would not pose a significant problem. Calculated stream and lake concentrations of these metals are negligible compared to the measured data. Sulfate contributions from the option 1 smelter are within an order of magnitude of the measured concentrations. Predicted Cu and Ni concentrations are elevated compared to the measured stream and lake concentrations.

10.2.3. Sulfate deposition onto area lakes.

Acid lakes are characterized by shifts in major ion composition that lower pH, and by changes in trace metal and organic components.

Comparison of the variations in lake pH observed among waters in northwestern Norway, southeastern Norway, and the Adirondacks at comparable calcium or total base forming cation levels indicates that the acid lakes (pH less than 5, alkalinity < 0) predominate in those regions where strong acid forming anion concentrations exceed the prevailing base forming cations. Sulfate appears to be the major acid forming anion and nitrate is also significant.²¹¹

Increased metals concentrations (Al, Mn, Zn, Cu, and Ni) have been reported in lake water from acidified areas.^{50, 51, 211} These increased concentrations may be due in part to increased atmospheric loading from specific sources, and to increased leaching from soils or lake sediments.

The ability of a lake to buffer acidic inputs is primarily a function of its bicarbonate content which in turn depends on the amount of calcium carbonate weathered from bedrock, overburden, and soils in the lake and its watershed.

Lakes with the smallest ratio of drainage area to lake volume in

any given geological substrate will have the poorest buffering due to the small area of substrate available for weathering. These lakes may not, however, be the most sensitive to increasing acidity because they have smaller areas exposed to deposition, and their greater depth allows for greater dilution.

In an attempt to characterize the impact of sulfate from a hypothetical smelter on pH in lake waters, the predicted sulfate concentrations resulting from sulfate deposition are titrated against existing alkalinity in a low alkalinity lake and a high alkalinity lake. Assumptions which were made include: 1) the major portion of acidity found in rainwater is attributed to sulfate,⁹² 2) the deposited sulfate is not buffered in transit, and 3) alkalinity is not replenished in the lake. The assumption of no replenishment in the lake has the effect of underestimating the time it will take to titrate the lake alkalinity. This error could be substantial for lakes with small flushing times.

Turtle Lake which is in the Kawishiwi River Watershed and Tofte Lake just north of the watershed were selected for the analysis. These lakes are shown in relation to the smelter in Figure 81. Neither of these headwater lakes is directly impacted by residential or industrial sources. Turtle Lake has an alkalinity of 6 mg/l as CaCO_3 compared to an alkalinity of 70 mg/l for Tofte Lake.

The alkalinity in each of these lakes is titrated against the acidity from the drainage and lake areas assuming no replenishment or buffering to pH 4.5.

Precipitation can be expressed as the sum of runoff, evapo-

transpiration, and changes in storage and underflow. Underflow and storage are both taken to be zero in northeastern Minnesota.^{86, 225}

The expression for precipitation can then be simplified and rearranged to give an expression for runoff:

$$\text{runoff} = \text{precipitation} - (\text{evapo-transpiration}) \quad (86)$$

Runoff for the region averages about 27.2 cm per year; about 58% of the average runoff occurs in April, May, and June, and most of this is due to snow melt.⁸⁶

Using this expression for runoff, the net water to the land drainage area was calculated from:

$$(P - ET_w) * (A_d - A_o) = \text{Net water}_{\text{land}}, \quad (87)$$

where p is the precipitation at Babbitt (72.6 cm), ET_w is the evapo-transpiration from drainage, A_d is the watershed drainage area, and A_o is the lake area.

The net water to the lake was calculated from:

$$(P - ET_l) * A_o = \text{Net water}_{\text{lake}}, \quad (88)$$

where ET_l is the evapo-transpiration from the lake (474 mm for small lakes²⁷⁸). Total water to the lake is then the sum of equations 87 and 88.

Results of the titration calculations are summarized in Table 87. The results show that a low alkalinity lake like Turtle Lake could be acidified in a relatively short period of time at present sulfate loadings, and that existing point sources are not as significant as sources from outside the region. The addition of new sources such as the option 1 smelter could be important in determining the productive life span of low alkalinity lakes. Time spans for acidification appear to

Table 87. Number of years required to titrate to pH 4.5 a low and a high alkalinity lake with strong acid input for selected cases.

lake data	Turtle lake ^a	Tofte lake ^b
alkalinity, ueq/l	120	1400
lake volume, m ³	1.55x10 ⁶	5.09x10 ⁶
drainage area, km ²	6.4	1.7
<u>selected cases</u>		
measured 1977 region (local + distant sources)		
SO ₄ loading, kg/ha	18.7	18.7
years to titrate	0.75	29
1985 region assuming doubling of 1977 input		
SO ₄ loading, kg/ha	37.4	37.4
years to titrate	0.37	14.5
predicted 1977 (local point sources only)		
SO ₄ loading, kg/ha	1.7	2.2
years to titrate	8.2	243
predicted 1985 (local point sources only)		
SO ₄ loading, kg/ha	3.1	3.5
years to titrate	4.5	153
predicted option 1 smelter		
SO ₄ loading, kg/ha	0.58	0.26
years to titrate	24.5	7900
predicted option 1 smelter with 1985 local sources		
years to titrate	3.9	144

^a predicted deposition from site 201

^b predicted deposition from site 224

be on the order of less than 10 years at present sulfate deposition rates, and perhaps 100 to 200 years for moderately high alkalinity lakes. These results represent a worst case approximation because of assumption made in the calculations. Even though the calculated numbers are not absolute, they, along with existing evidence, identify the urgency of the problem and the need for careful evaluation of any activities which could increase acidic input into the region.

BIBLIOGRAPHY

1. Air Pollution Across National Boundaries. Sweden's case study for the UN conference on the human environment. 1971. Stockholm, Sweden. 96pp. cited in Gorham 1975.
2. American Conference of Governmental Industrial Hygienists (ACGIH). 1978. TLVs. Threshold limit values for chemical substances in workroom air adopted by ACGIH for 1978. Cincinnati, Ohio.
3. American Meteorological Society. 1977. Committee on atmospheric turbulence and diffusion. Accuracy of dispersion models. Bull. Am. Meteorol. Soc., 59(8): 1025-1026.
4. Ashbrook, Peter. 1978. Arsenic and human health. Regional Copper-Nickel Study, Minneapolis, MN.
5. Aubert, H. and M. Pinta. 1977. "Trace elements in soils." Elsevier Scientific Publ. Co. Amsterdam, 1977.
6. Baer, R.L., D.L. Ramsey, and E. Biondi. 1973. The most common contact allergens. 1968-1970. Arch. Derm. 108: 74-78.
7. Baker, E.L., D.S. Folland, et al. 1977a. Lead poisoning in children of lead workers. New England J. of Med. 296: 260-61.
8. -----, C.G. Hayes, P. Landrigan, R.T. Leger, J.L. Handke and J.M. Harrington. 1977b. A nationwide survey of heavy metal absorption in children living near primary copper, lead and zinc smelters. Am. J. Epid. 106: 261-273.
9. Bakir, F., et al. 1973. Methylmercury poisoning in Iraq. Science, 181: 230-241.
10. Balsillie, D. 1978. Personal communication. Ontario Ministry of the Environment, Sudbury, Ontario.
11. Barard, M.L. (ed) 1958. Project prairie grass, a field program in diffusion. Geophys. Res. Pap. No 59, Vols 1 and 2. Rept. AFCRC-TR-58-235, AD-152572 and AD-152573. Air Force Cambridge Research Center, Hanscom AFB, Mass.
12. Barrie, L.A. and H.W. Georgii. 1976. An experimental investigation of the absorption of sulphur dioxide by water drops containing heavy metal ions. Atm Env. 10: 743-749.
13. Beamish, R.J. and H.H. Harvey. 1972. Acidification of the La Cloche Mountain Lakes, Ontario and resultant fish mortalities. J. Fish. Res. Bd. Canada. 29: 1131-1143.

14. Becker, Dennis. 1979. Personal communication. Division of Air Quality, Minnesota Pollution Control Agency, Roseville, MN.
15. Beton, D.C. et al. 1972. Acute cadmium fume poisoning. Brit. J. Ind. Med. 23: 292-301.
16. Bielke, S. and G. Gravenhorst. 1977. Heterogeneous SO₂ oxidation in the droplet phase. Presented at the Intl. Symp. on Sulfur in the Atm. Sept. 7-14, 1977. Dubrovnik, Yugoslavia.
17. -----, D. Lamb, and J. Miller. 1975. On the uncatalyzed oxidation of atmospheric SO₂ by oxygen in aqueous systems. Atm. Env. 9: 1083-1090.
18. Blanchard, D.C. 1967. "From raindrops to volcanoes." Doubleday, Garden City, NY 180 pp.
19. Blejer, H.P. 1976. Inorganic lead: biological indices of absorption -- biological threshold limit values. In: Carnow, B.W. (ed), Health effects of occupational lead and arsenic exposure--A symposium. HEW Publ. No. (NIOSH) 76-134. Washington, D.C. pp 165-177.
20. Blot, W.J. and J.F. Fraumeni. 1975. Arsenical air pollution and lung cancer. Lancet. 142-144.
21. Bowman, Joseph. 1978. Internal memo. Regional Copper-Nickel Study. Minneapolis, MN.
22. Boyer, David S. 1978. Ontario: Canada's Keystone. National Geographic. 154(6): 760-795.
23. Briggs, G.A. 1969. "Plume Rise," AEC Crit. Rev. Ser., TID-25075. USAEC, Div Tech. Inform., Est., Oak Ridge, Tennessee.
24. -----, 1971. Consequences of effluent release. Plume rise: A recent critical review. Nuclear Safety. 12(1): 15-24.
25. Brimblecombe, P. and D. J. Spedding. 1975. The dissolution of iron from ferric oxide and pulverized fuel ash. Atm. Env. 9: 835-838.
26. Bringfelt, B. 1969. A study of buoyant chimney plumes in neutral and stable atmospheres. Atm. Env. 3(6): 609-624.
27. Buchauer, M.J. 1971. Effects of zinc and cadmium pollution on vegetation and soils. Ph.D. thesis Rutgers University, New Brunswick, N.J. 103 pp.

28. Budney, Laurence J. 1977. Guidelines for air quality maintenance planning and analysis, Volume 10 (revised): Procedures for evaluating air quality impact of new stationary sources. EPA-450/4-77-001, Research Triangle Park, North Carolina.
29. Campbell, Ivor E. 1973. Sulfur dioxide control at the copper smelters in the United States. ECE Conference, Dubrovnik, Yugoslavia., November 19-24.
30. Calvert, Jack G., et al. 1977. Mechanism of the homogeneous oxidation of sulfur dioxide in the troposphere. Presented at the Intl. Symp. on Sulfur in the Atm. Dubrovnik, Yugoslavia. Sept. 7-14.
31. Carpenter, S.B., et al. 1971. Principal plume dispersion models: TVA power plants. J. Air Poll. Cont. Assoc. 21: 491-495.
32. Cawse, P.A. 1974. A survey of atmospheric trace elements in the U.K. (1972-73). AERE-R7669. AERE Harwell, Oxfordshire, England.
33. Chamberlain, A.C. 1966. Transport of gases to and from grass and grass-like surfaces. Proc. Roy. Soc. London, A. 290: 236-65.
34. -----, 1967. Transport of lycopodium spores and other small particles to rough surfaces. Proc. Roy. Soc. London, A. 296: 45-70.
35. -----, 1976. Response to: Approaches to evaluating dry deposition of atmospheric aerosol pollutant onto lake surfaces, by J.W. Winchester. Volume 2. Supp. 1. J. Great Lakes Research. pp 38-41.
36. Cheng, Robert T., John O. Frohlinger and Morton Corn. 1971a. Aerosol stabilization for laboratory studies of aerosol-gas interactions. J. Air Poll. Cont. Assoc. 21(3): 138-142.
37. -----, Morton Corn and John O. Frohlinger. 1971b. Contribution to the reaction kinetics of water soluble aerosols and SO₂ in air at ppm concentrations. Atm. Env. 5: 987-1008.
38. Coleman, Richard T., Jr. 1978. The behavior of minor and trace elements in a smelter treating copper/nickel concentrates from the Minnesota Duluth Gabbro complex. Draft Report. Radian Corporaton. DCN # 78-200-250-02. Austin, Texas.
39. Corn, Morton and Robert T. Cheng. 1972. Interactions of sulfur dioxide with insoluble suspended particulate matter. J. Air Poll. Cont. Assoc. 21 (11): 870-875.

40. Costescu, L.M. and T.C. Hutchinson. 1972. The ecological consequences of soil pollution by metallic dust from the Sudbury smelters. Proc. 18th Ann. Mtg. Inst. Env. Sci. New York. pg. 540-545.
41. Cox, R.A. and S.A. Penkett. 1971a. Photo-oxidation of atmospheric SO₂. Nature, 229: 486-488.
42. -----, 1971b. Oxidation of atmospheric SO₂ by products of the ozone-olefin reaction. Nature, 230: 321-322.
43. -----, 1972. Aerosol formation from sulfur dioxide in the presence of ozone and olefinic hydrocarbons. J. Chem. Soc. Faraday Trans. 68: 1735-1753.
44. Dana, Terry M., et al. 1973. Natural precipitation washout of sulfur compounds from plumes. EPA-R3-73-047. Research Triangle Park, N.C.
45. -----, J.M. Hales and M.A. Wolf. 1975. Rain scavenging of SO₂ and sulphate from power plant plumes. J. of Geophysical Research 80: 4119-4129.
46. Davis, D.D. and Gary Klauber. 1975. Atmospheric gas phase oxidation mechanisms for the molecule SO₂. Intl. J. Chem. Kin. 1: 543-556.
47. Davis, S.M. and J.H. Lunsford. 1976. Surface reactions of SO₂ with NO₂ on hydrated silica gel. J. Environ. Sci. Health A1(12): 735-741.
48. Daubendiek, Richard L. and Jack G. Calvert. 1975. A study of the N₂O₅ - SO₂-O₃ reaction system. Env. Letters, 8(2): 103-116.
49. DeMarrais, Gerard A. 1959. Wind speed profiles at Brookhaven National Laboratory. J. Meteorol. 16: 181-190.
50. Dickson, W. 1975. The acidification of Swedish Lakes. Inst. Fresh. Res. Drottningholm. Report No. 54, pp. 8-20.
51. Dillon, P.J., et al. 1977. Acidic precipitation in south central Ontario: Recent observations. Ont. Ministry of Env. Report, Sept. 1977. 24 p.
52. Dittenhoefer, Allen C. and Rosa G. de Pena. 1977. A study of production and growth of sulfate particles in coal operated power plant plumes. Presented at the International Symposium on Sulfur in the Atmosphere. Dubrovnik, Yugoslavia. Sept. 7-14, 1977.

53. Djuric, D., *et al.* 1973. Environmental contamination by lead from a mine and smelter. Arch Environ. Health, 23: 275-9.
54. Dochinger, L.S. and T.A. Seliga (eds). 1976. Proc. First. Intl. Symp. on Acid Precipitation and the Forest Ecosystem. USDA Forest Service Tech Rep. NE-23. Upper Darby, PA.
55. Doll, R., L.G. Morgan, and F.E. Speizer. 1970. Cancers of the lung and nasal sinuses in nickel workers. Brit. J. Cancer, 24: 623-632.
56. Dovland, Harald and Anton Eliassen. 1976. Dry deposition on a snow surface. Atm. Env. 10: 783-785.
57. Draxler, Roland R. and William P. Elliot. 1977. Long-range travel of airborne material subjected to dry deposition. Atm. Env. 11: 35-40.
58. Driesinger, B.R. 1970. SO₂ levels and vegetation injury in the Sudbury area during the 1969 season. Department of Energy and Resources Management, Province of Ontario, Canada. April, 1970. 45 pp.
59. Eisenreich, S.J., G.J. Hollod, and S. Langevin. 1978. Precipitation Chemistry and Atmospheric Deposition of Trace Elements in Northeastern Minnesota. University of Minnesota, Minneapolis, MN.
60. Endersen, William G. 1978. Personal Communication. Regional Copper-Nickel Study, Minneapolis, MN.
61. -----, 1979. Short range dispersion of sulfur dioxide from the smelter complex. Regional Copper-Nickel Study. Minneapolis, MN.
62. ----- and D. Feeney. 1979. Particulates in northeastern Minnesota, regional characterization. Regional Copper-Nickel Study. Minneapolis, MN.
63. Erikson, E. 1963. The yearly circulation of suflur in nature. J. Geophys. Res. 68: 4001-4008.
64. Fay, J.A., M. Escudier, and D.P. Hoult. 1970. A correlation of field observations of plume rise. J. Air Poll. Cont. Assoc. 20: 391-397.
65. Feeney, D. 1978. Statistical modeling of TSP data. Regional Copper-Nickel Study. Minneapolis, MN.

66. Finklea, J.F., et al. 1974. Frequency of acute lower respiratory disease in children: Retrospective survey of five Rocky Mountain communities, 1961-1970. pp. 3-55 to 3-56. In: US EPA Office of Research and Development. Health consequences of sulfur oxides: A report from CHESS, 1970-1971. EPA-650/1-74-004. Washington, D.C.
67. Fisheries and Environment Canada. 1976. Annual Meteorological Summary. Thunder Bay "A", Ontario. Atmospheric Environment. Downsview, Ontario.
68. Fisheries and Environment Canada. 1977. Annual Meteorological Summary. Thunder Bay "A", Ontario. Atmospheric Environment. Downsview, Ontario.
69. Flick, D.F., H.F. Kraybill and J.M. Dimitroff. 1971. Toxic effects of cadmium: A review. Env. Res. 4: 71-85.
70. Forrest, J. and L. Newman. 1977a. Further studies on the oxidation of sulfur dioxide in coal-fired power plant plumes. Atm. Env. 11: 465-474.
71. -----, 1977b. Oxidation of sulfur dioxide in the Sudbury smelter plume. Atm. Env. 11: 517-520.
72. Foster, P.M. 1969. The oxidation of sulphur dioxide in power station plumes. Atm. Env. 3: 157-175.
73. Fowler, D. and M.H. Unsworth. 1974. Dry deposition of sulphur dioxide on wheat. Nature. 249: 389-390.
74. Fraumeni, J.F., Jr. 1975. Remarks made during discussions following the carcinogenesis in the metal industry session at the Conference on Occupational Carcinogenesis, March 24-27. New York City, NY.
75. Freiberg, Johnny. 1974. Effects of relative humidity and temperature on iron-catalyzed oxidation of SO₂ in atmospheric aerosols. Env. Sci. Tech. 8(8): 731-734.
76. Friedlander, S.K. and H.F. Johnston. 1957. Deposition of suspended particulates from turbulent gas streams. Ind. Eng. Chem. 49: 1151-1156.
77. Friedman, W. 1978. Personal communication, unpublished data. Sudbury, Ontario.
78. Friend, J.P. 1973. "The global sulfur cycle; in Chemistry of the Lower Atmosphere." S.I. Rasool (ed.). Plenum, NY.

79. Fuller, E.C. and R. H. Crist. 1941. The rate of oxidation of sulfite ions by oxygen. J. Am. Chem. Soc. 63: 1644-1650.
80. Galloway, James N., G.E. Likens and E.S. Edgerton. 1976. Acid precipitation in the northeastern United States: pH and acidity. Science. 194: 722-724.
81. Garland, J.A. 1977. Dry and wet removal of sulfur from the atmosphere. Presented at the International symposium on sulfur in the atmosphere. Dubrovnik, Yugoslavia. Sept. 7-14.
82. -----, D.H.F. Atkins; C.J. Reading, S.J. Caughey. 1974. Deposition of gaseous sulphur dioxide to the ground. Atm. Env. 8: 75-79.
83. ----- and J.R. Branson. 1976. The mixing height and mass balance of SO₂ in the atmosphere above Great Britian. Atm. Env. 10: 353-362.
84. -----, W.S. Clough, D. Fowler. 1973. Deposition of sulfur dioixde on grass. Nature. 242: 256-257.
85. Gartrell, F.E., F.W. Thomas, S.B. Carpenter. 1963. Atmospheric oxidation of SO₂ in coal-burning power plant plumes. Am. I. Hyg. Assoc. J. 29: 113-120.
86. Garn, Gerbert S. 1975. Hydrology and water resources of the Superior National Forest. USDA Forest Service.
87. Gjessing, Egil T., et al. 1976. Effects of acid precipitation on freshwater chemistry. pp. 65-85. In: Finn H. Braekke, ed. Impact of acid precipitation on forest and freshwater ecosystems in Norway. SNSF Project, Aas, Norway.
88. Glass, Gary E. and Orie L. Loucks. (eds). 1979. Impacts of air pollutants on wilderness areas of northern Minnesota. US. EPA Env. Res. Lab., Duluth, MN.
89. Gleason, R.P. 1968. Exposure to copper dust. Amer. Ind. Hyg. Assoc. J. 29: 461-462.
90. Gorham, E. 1975. Acid precipitation and its influence upon aquatic ecosystems -- an overview. pp. 425-458. In: L.S. Dochinger and T.A. Selinga (eds). 1976.
91. ----- and A.G. Gordon. 1960. Some effects of smelter pollution north-east of Falconbridge, Ontario. Can. J. Bot. 38: 307-12.

92. Granat, L., R.O. Hallberg and H. Rodhe. 1976. The global sulphur cycle. In: Soderlund, R. and B.H. Svensson (eds). "Nitrogen, phosphorous, and sulphur--global cycles." SCOPE Rept. 7. Swed. Nat. Res. Council, Stockholm, Sweden. pp. 89-134.
93. Green, George. 1978. Personal communication. Public Service Company of Colorado. Denver, Colorado.
94. Hales, J.M. 1977. Wet removal of sulfur compounds from the atmosphere. International Symposium on Sulfur in the Atmosphere. Dubrovnik, Yugoslavia. Sept. 7-14.
95. Hales, J.M. and S.L. Sutter. 1973. Solubility of sulfur dioxide in water at low concentrations. Atm. Env. 7: 997-1001.
96. Hammerle, J.R. 1976. Chapter 17. Emission Inventory. In: Stern, Arthur, (ed), "Air Pollution Vol. 3. Measuring, monitoring, and surveillance of air pollution," 3rd edition. Academic Press, London, England.
97. Harrison, Mr. 1978. Personal communication. ASARCO. El Paso, Texas.
98. Haugen, D.A. (ed). 1959. Project prairie grass, a field program in diffusion. Geophys. Res. Pap. No. 59, Vol. 3. Rept. AFCRC-TR-58-235, AD-217076. Air Force Cambridge Research Center, Hanscom AFB, Mass.
99. Hernberg, S. 1976. Biochemical, subclinical and clinical responses to lead and their relation to different exposure levels, as indicated by the concentration of lead in blood. In: Nordberg, G.F. (ed). "Effects and dose-response relationship of toxic metals." Elsevier, Amsterdam.
100. Heuper, W.C. 1955. A quest into the environmental causes of cancer of the lung. Public Health Monograph No. 36. U.S. Dept. Health, Educ. and Welfare. pp 27-29.
101. -----, 1966. Occupational and environmental cancers of the respiratory system. Recent Results Cancer Research. 3: 85-93.
102. Hewitt, Martha. 1978. Personal Communication. Regional Copper-Nickel Study. Minneapolis, MN.
103. Hewson, E. Wendell, 1976. Chapter 11. Meteorological measurements. In: Stern, Arthur C. (ed). "Air Pollution, Volume 1. Air pollutants, their transformation and transport." 3rd edition. Academic Press. New York, NY.
104. Hill, B.A. 1966. "Principles of Medical Statistics." Lancet, London, England.

105. Hinds, W.T. 1970. Diffusion over coastal mountains of southern California. Atm. Env. 4: 107-124.
106. Holzworth, George C. 1972. Mixing heights, wind speeds, and potential for urban air pollution throughout the contiguous United States. EPA, Research Triangle Park, N.C. Office of Air Programs.
107. Horst, Thomas W. 1977. A surface depletion model for deposition from a gaussian plume. Atm. Env. 11: 41-46.
108. Huhn, Frank. 1978. Personal communication. Department of Geology, McMaster University, Hamilton, Ontario.
109. Hutchinson, E.C. and L.M. Whitby. 1974. Heavy-metal pollution in the Sudbury mining and smelting region of Canada, I. Soil and vegetataion contamination by nickel, copper and other metals. Environmental Conservation. 1(2): 123-132.
110. ----- . 1976. The effects of acid rainfall and heavy metal particulates on a boreal forest ecosystem near the Sudbury smelting region of Canada. Proceeding of the first Intl. Sym. on Acid Precip. and the Forest Ecosystem, USDA report NE-23.
111. International Joint Commission. 1977. Atmospheric loading of the Great Lakes and the Great Lakes drainage basin. Great Lakes Regional Office, 100 Ouelette Avenue, Windsor, Canada.
112. Islitzer, N. and D. Slade. 1968. Diffusion and transport experiments. Meteorology and Atomic Energy, 1968. D. Slade (ed). USAEC TID 24190. Germantown, Md.
113. Jackson, D.R. and A.P. Watson. 1977. Disruption of nutrient pools and transport of heavy metals in a forestred watershed near a lead smelter. J. of Env. Quality. 6(4): 331-338.
114. James, K.W. and P.M. Foster. 1976. Discussions. The application of an isotopic ratio technique to studies of the atmospheric oxidation of sulfur dioxide in the plumes from an oil-fired and coal-fired power plant - I and II. Atm. Env. 10: 671.
115. Johannessen, M., et al. 1975. Acid precipitation in Norway: The regional distribution of contaminants in snow and the chemical concentration processes during snow melt. Proc. Intl. Symp. Isotopes and Impurities in snow and ice, Intl. Assoc. Hydrolog. Sci., Grenoble, France. Aug. 1975. SNSF FA 4/75, SNSF Project, 1432 Aas-NLH, Norway.

116. Jordan, Marilyn J. 1975. Effects of zinc smelter emissions and fire on a chestnut oak woodland. Ecology. 56: pp 78-91.
117. Junge, C.E. and T.G. Ryan. 1958. Study of the SO₂ oxidation in solution and its rate in atmospheric chemistry. Quart. J. Roy Meteorol. Soc. 84: 46-55.
118. Kazantis, G. 1972. Chromium and Nickel. Ann. Occup. Hyg. 15: 25-29.
119. Kramer, J.r. 1960. The influence of smelter fumes upon the chemical composition of lake waters near Sudbury, Ontario and upon the surrounding vegetation. Can. J. Bot. 38: 477-87.
120. -----, 1973. Fate of atmospheric sulphur dioxide and related substances as indicated by chemistry of precipitation. Department of Geology, McMaster University, Hamilton, Ontario.
121. -----, 1975. Fate of atmospheric sulphur dioxide and related substances as indicated by chemistry of precipitation. Dept. of Geology, McMaster University, Hamilton, Ontario.
122. -----, 1976a. Assessment of the ecological effects of long-term atmospheric material deposition. Unpublished report. 83 pp. McMaster University, Hamilton, Ontario.
123. -----, 1976b. Fate of atmospheric sulphur dioxide and related substances as indicated by chemistry of precipitation. Dept. of Geology, McMaster University, Hamilton, Ontario.
124. Krupa, S.V., M.R. Coscio, Jr., and E.A. Wood. 1975. Evidence for multiple hydrogen ion donor systems in rain pp. 371-380. In: L.S. Dochinger and T.A. Seliga (eds). 1976. Proc. First Intl. Symp. on Acid Precip and the Forest Ecosystem. USDA Forest Service Tech Rept. NE-23. Upper Darby, PA.
125. Kuratsune, M., et al. 1974. Occupational lung cancer among copper smelters. Intl. J. Cancer. 13: 552-58.
126. Landigran, P.J., et al. 1975. Epidemic lead absorption near an ore smelter. New England J. Med. 292: 123-29.
127. Lane, R.E., et al. 1968. Diagnosis of inorganic lead poisoning: A statement. Brit. Med. J. 4: 501-.
128. Lemen, R.A., J.S. Lee, J.K. Wagoner and H.P. Blejer. 1976. Cancer mortality among cadmium production workers. Ann. New York Acad. Sci. 271: 273-279.

129. Levy, A., D.R. Drewes, and J.M. Hales. 1976. SO₂ oxidation in plumes: A review and assessment of relevant mechanistic and rate studies. EPA-450/3-76-022.
130. Likens, G.E. 1976. Acid precipitation. Chem. and Engr. News, 22: 29-44.
131. Logan, W.P.D. 1953. Mortality in London fog incident, 1952. Lancet, 1: 336-338.
132. Louria, Donald B., Morris M. Joselow, and Ann A. Browsder. 1972. The human toxicity of certain trace elements. Ann. of Int. Med. 76: 307-319.
133. Lusic, M.A. and K.G. Anlauf, L.A. Barrie and H.A. Wiebe. 1977. Plume chemistry studies at a northern Alberta power plant. Presented at the Alberta Sulphur Gas Research Workshop III. Nov. 17-18, 1977. University of Alberta, Edmonton, Alberta.
134. ----- and H.A. Wiebe. 1976. The rate of oxidation of sulfur dioxide in the plume of a nickel smelter stack. Atm. Env. 10: 793-798.
135. -----, H.A. Wiebe, and J.M.L. Gray. 1975. Further work on the measurement of the oxidation and dispersion of sulfur dioxide in chimney plumes. Report ARQA 17-75. Atmospheric Environment Service, Downsview, Ontario, Canada.
136. Lyons, W.A., J.C. Dooley, and K.T. Whitby. 1978. Satellite detection of long-range pollution transport and sulfate aerosol hazes. Atm. Env. 12: 621-631.
137. ----- and R.B. Husar. 1976. SMS/GOES visible images detect a synoptic-scale air pollution episode. Monthly Weather Review, 104: 1623-1626.
138. Mason, B.J. 1971. "The physics of clouds." 2nd ed.arendon Press, Oxford, England. 671 pp.
139. Matheson, K.H., Jr. 1978. Personal communication. Kennecott Copper Corporation, Ray Mines Division, Hayden, Arizona.
140. Matteson, Michael J., Werner Stöber and Horst Luther. 1969. Kinetics of the oxidation of sulfur dioxide by aerosols of manganese sulfate. 1969. Ind. Eng. Chem. Fund. 8(4): 677-687.
141. Maxwell, Christine. 1978. Iron Range air quality analysis. Midwest Research Institute Project No. 4523-L(2).
142. McCabe, L.J., J.M. Symons, R.D. Lee, G.G. Robeck. 1970. Survey of community water supply systems. J. Am. Water Works Assoc. 62: 670-687.

143. McElroy, James L. 1969. A comparative study of urban and rural dispersion. J. Appl. Meteorol. 8: 19-31.
144. McGovern, P.C. and D. Balsillie. 1974. Effects of sulphur dioxide and heavy metals on vegetation in the Sudbury Area (1973). Ontario Ministry of the Environment, Sudbury, Ontario.
145. -----, 1975. Effects of sulphur dioxide and heavy metals on vegetation in the Sudbury Area (1974). Ontario Ministry of the Environment, Sudbury, Ontario.
146. Milham, S., Jr. and T. Strong. 1974. Human arsenic exposure in relation to a copper smelter. Environ. Res. 7: 176-182.
147. Miller, D.F. 1977. Precursor effects on SO₂ oxidation. Presented at the Intl. Symp. on Sulfur in the Atmosphere. Sept. 7-14, 1977. Dubrovnik, Yugoslavia.
148. Miller, J.M. and Rosa G. De Pena. 1972. Contribution of scavenged sulfur dioxide to the sulfate content of rain water. J. Geophysical Research. 77(30): 5905-5916.
149. Minnesota Department of Health. 1976. Directory. Licensed & certified health care facilities. Minneapolis, MN 217 pp.
150. Minnesota Energy Agency. 1978a. The Minnesota coal study. In cooperation with the Dept. of Natural Resources, Dept. of Transportation, Pollution Control Agency, State Planning Agency. St. Paul, MN.
151. -----, 1978b. Data and analysis forecasting; energy coefficients and fuel substitution possibilities in the Copper-Nickel Area. Final Report. Minneapolis, MN.
152. -----, 1978c. Fuel consumption and fuel demand forecasting models, Copper-Nickel Study Area. Draft Interim Report, St. Paul, MN.
153. Minnesota Pollution Control Agency. 1978. Emissions inventory, 1975-76. Roseville, MN.
154. Montana State Board of Health and Dept. of Health, Educ. and Welfare. 1961-62. A study of air pollution in Montana. 94 pp.
155. Montgomery, T.L., et al. 1973. A simplified technique used to evaluate atmospheric dispersion of emissions from large power plants. J. Air Poll. Cont. Assoc. 23: 388-394.

156. Moses, Harry and Gordon Strom. 1961. A comparison of observed plume rises with values obtained from well-known formulas. J. Air Poll. Cont. Assoc. 11(10): 455-466.
157. National Research Council. 1972. Airborne lead in perspective. National Academy of Sciences. Washington, D.C.
158. -----, 1975. Medical and biological effects of environmental pollutants. Nickel. National Academy of Sciences. Washington, D.C.
159. -----, 1976. Recommendations for the prevention of lead poisoning in children. Nutrition Reviews, 34: 321-327.
160. -----, 1977a. Medical and biological effects of environmental pollutants. Arsenic. National Academy of Science, Washington, D.C.
161. -----, 1977b. Medical and Biological effects of environmental pollutants. Copper. National Academy of Sciences. Washington, D.C.
162. -----, 1978. An assessment of mercury in the environment. National Academy of Sciences, Washington, D.C.
163. National Oceanic and Atmospheric Administration. Environmental Data Service. Local Climatological Data 1976 and 1977 for Duluth and International Falls, Monthly Summaries. Ashville, NC.
164. National Oceanic and Atmospheric Administration, Environmental Data Service. Climatological data. Annual Summaries. Vol. 82, No. 13 and Vol. 83, No. 13. Ashville, NC.
165. Neal, R.C. 1978. Personal communication. State of New Mexico Health and Social Services Department. Sante Fe, New Mexico.
166. Nelson, W.C. and Company, INC. 1977. Prevention of significant deterioration analysis for AMAX copper processing facility, Braithwaite, Louisiana. New Orleans, LA.
167. Nelson, W. C., et al. 1974. Frequency of acute lower respiratory disease in children: Retrospective survey of Salt Lake Basin communities, 1967-1970. pp. 2-55 to 2-73. In: U.S. EPA Office of Research and Development. Health consequences of sulfur oxides: A report from CHESS, 1970-1971. EPA 650/1-74-004. Washington, D.C.

168. Newman, J.A., et al. 1975. Bronchiogenic carcinoma in the copper smelting and mining industry. Conference on Occupational Carcinogenesis. March 24-27. New York City, NY.
169. Newman, L., J. Forrest, and B. Hanowitz. 1975a. The application of an isotopic ratio technique to a study of the atmospheric oxidation of sulfur dioxide in the plume from an oil-fired power plant. Atm. Env. 9: 959-968.
170. -----, 1975b. The application of an isotopic ratio technique to a study of the atmospheric oxidation of sulfur dioxide in the plume from a coal-fired power plant. Atm. Env. 9: 969-977.
171. Nonhebel, G. 1960. Recommendations on heights for new industrial chimney stacks. Proc. Inst. Mech. Engr. 162: 355-367.
172. Novakov, T., S.G. Chang and A.B. Harker. 1974. Sulfates as pollution particulates: Catalytic formation on Carbon (soot) particles. Science 186: 259-261.
173. Office of State Demographer. 1979. Population estimates for Minnesota counties, 1978. State Planning Agency. St. Paul, MN. 14 pp.
174. Ohman, Stephen P. 1979. Volume 2. Technical Assessment. Chapter 2. Mineral extraction (mining). Regional Copper-Nickel Study, Minneapolis, MN.
175. Ott, M.G., B.B. Holder, H.L. Gordon. 1974. Respiratory cancer and occupational exposure to arsenicals. Arch. Environ. Health 29: 250-55.
176. Owens, M.J. and A.W. Powell. 1974. Deposition velocity of sulphur dioxide on land and water surfaces using a ³⁵S tracer method. Atm. Env. 8: 63-68.
177. Pasquill, F. 1961. The estimation of the dispersion of windborne material. Mct. Mag. 90: 33-49.
178. Pasquill, F. 1974. "Atmospheric Diffusion" 2nd ed. John Wiley, New York, NY.
179. Patterson, William A., III. 1978. Regional Copper-Nickel Study: Soil Decomposition Studies. Regional Copper-Nickel Study. Minneapolis, MN.
180. -----, and Norman E. Asseng. 1978. Regional Copper-Nickel Study: Soils of the area. Regional Copper-Nickel Study. Minneapolis, MN.

181. Paul, R. 1961. Silicosis in northern Rhodesia copper mines. Arch. Env. H. 2: 96-109.
182. Pedersen, E., A.C. Hogetveit, and A. Anderson. 1973. Cancer of respiratory organs among workers at a nickel refinery in Norway. Intl. J. Cancer. 12: 32-41.
183. Penkett, S.A. 1972. Oxidation of SO₂ and other atmospheric gases by ozone in the aqueous phase. Nature Physical Science. 240: 105-106.
184. -----, and J.A. Garland. 1974. Oxidation of sulphur dioxide in artificial fogs by ozone. Tellus 26(1-2): 284-289.
185. Pierson, D.H., P.A. Cawse and R.S. Cambray. 1974. Chemical uniformity of airborne particulate matter, and a maritime effect. Nature. 251: 675-679.
186. Pojar, Michael and Peter Kreisman. 1979. Volume 2. Technical Assessment. Chapter 4. Smelting and Refining. Regional Copper-Nickel Study. Minneapolis, MN.
187. Portelli, R.V. 1976. Mixing heights, wind speeds and air pollution potential from Canada. Atmospheric Environment Service, Downsview, Ontario.
188. -----, and D. Balsillie. 1976. Air quality monitoring report for the Sudbury Area (1975). Ontario Ministry of the Environment. Northeastern Region.
189. Potvin, R. Nov. 14, 1978. Personal Communication. Ontario Ministry of the Environment. Northeastern Region.
190. Potts, C.L. 1965. Cadmium proteinuria-the health of battery workers exposed to cadmium oxide dust. Ann. of Occupational Hygiene. 8: 55-61.
191. Prager, Manfred J., Edgar R. Stephens, and William E. Scott. 1960. Aerosol formation from gaseous air pollutants. Ind. Engr. Chem. 52(6): 521-524.
192. Ragland, Kenneth W., editor. 1972 "Particulate matter in the urban atmosphere." Midwest Universities Committee on Air Pollution.
193. -----, 1979. Impacts of air pollutants on wilderness areas of northern Minnesota. Section 3. Air quality in the Boundary Waters Canoe Area (BWCA). Ed: Gary E. Glass. Env. Res. Lab-Duluth, USEPA. Duluth, MN pp 12-48.

194. -----, and Robin L. Dennis. 1975. Point source atmospheric diffusion model with variable wind and diffusivity profiles. Air. Env. 9: 175-189.
195. Renzetti, N.A. and George J. Doyle. 1960. Photochemical aerosol formation in sulfur-dioxide-hydrocarbon systems. Int. J. Air Poll. 2: 327-345.
196. Ritchie, Ingrid. 1978. Sulfur dioxide conversion literature review. Regional Copper-Nickel Study, Minneapolis, MN.
197. -----, and Peter J. Kriesman. 1979. Volume 3. Physical Assessment. Chapter 3. Air Resources. Regional Copper-Nickel Study. Minneapolis, MN.
198. Roberts, Paul T. and Sheldon K. Friedlander. 1976. Photochemical aerosol formation SO₂, 1-heptene, and NO_x in ambient air. Env. Sci. Tech. 10(6): 573-580.
199. Roberts, T. M., et al. 1974. Lead contamination around secondary smelters: Estimation of dispersal and accumulation by humans. Science. 186: 1120-1123.
200. Robinson, E. and R.C. Robbins. 1970. Gaseous sulfur pollutants from urban and natural sources. J. Air Poll. Cont. Assoc. 20(4): 233-235.
201. -----, 1971. Emission concentrations and fate of atmospheric pollutants. Amer. Petroleum Inst. Publ. No. 4076.
202. Roe, F.J.C. and M.C. Lancaster. 1964. Natural, metallic and other substances as carcinogens. Brit. Med. Bull. 20: 127-133.
203. Roels, H., et al. 1976. Impact of air pollution by lead on the heme biosynthetic pathway in school-age children. Archives Env. Health. 31: 310-316.
204. Ross, R.D. 1972. "Air Pollution and Industry." van Nostrand Reinhold Company, New York, NY.
205. Rowe, Michael D., Samuel C. Morris and Leonard D. Hamilton. 1978. Potential ambient standards for atmospheric sulfates: An account of a workshop. J. Air Poll. Cont. Assoc. 28(8): 772-775.
206. Rühling, Ake and Germund Tyler. 1973. Heavy metal pollution and decomposition of spruce needle litter. Oikos. 24: 402-416.

207. Sanders, L.W. 1964. Tetraethyllead intoxication. Arch. of Env. H. 8: 270-277.
208. Sather, Nancy, Gerald Lieberman and William Patterson, III. 1979. Volume 4, Biological Environment, Chapter 2. Terrestrial Biology. Regional Copper-Nickel Study. Minneapolis, MN.
209. Sax, N.I. 1963. "Dangerous properties of industrial materials." Reinhold Publishing Co. N.Y.
210. Schrenk, H.H., et al. 1949. Air pollution in Donora, Pennsylvania. Pub. Health Bull. No. 306.
211. Schofield, C.L. 1976. Acidification of Adirondack lakes by atmospheric precipitation: Extent and magnitude of the problem. NY Dept. Env. Conserv. Final Rep. E-28-R, 42 p.
212. Schroeder, H.A. 1965. Cadmium as a factor in hypertension. J. Chronic disease. 18: 647-656.
213. -----, 1970. A sensible look at air pollution by metals. Arch. Env. H. 21: 798-806.
214. -----, and J.J. Balassa. 1966. Abnormal trace elements in man: Arsenic. J. Chron. Dis. 19: 85-106.
215. Schuman, Leonard M., Jack S. Mandel, Margot Hanson and Janet Nelms. 1977. Copper-nickel mining, smelting and refining as an environmental hazard to human health. A review of epidemiologic literature and study recommendations on sulfur dioxide and particulates. School of Public Health, University of Minnesota, Minneapolis, MN.
216. Schuman, Leonard M., Jack Mandel, Samuel Murray, Anna Lawler, Harold Weiss. 1976. Copper-nickel mining, smelting and refining as an environmental hazard to human health. A review of epidemiology literature and study recommendations. University of Minnesota, Minneapolis, MN.
217. Scott, B.C. 1978. Parameterization of sulfate removal by precipitation. Am. Meteorol. Soc. 17: 1375-1389.
218. -----, and M. Terry Dana. 1978. Wet removal rates for SO₂ gas and SO₄ aerosol. PNL-SA-7268. Richland, Washington.
219. Scott, W.D. and P.V. Hobbs. 1967. The formation of sulfate in water droplets. J. Atmos. Sci. 24: 54-57.

220. Sehmel, G.A. 1970. Particle deposition from turbulent air flow. J. Geophys. Res. 75(9): 1766-1781.
221. -----, 1971. Particle diffusivities and deposition velocities over a horizontal smooth surface. J. Colloid and Interface Science. 37(4): 891-906.
222. -----, 1972. Turbulent deposition of monodispersed particles on simulated grass. Chapter 2. In: Assessment of Airborne Particles, ed: Mercer, T.T., P.E. Morrow and W. Stöber. The Charles C. Thomas Publishing Company, Springfield, Ill. pp. 18-24.
223. -----, and S.L. Sutter. 1974. Particle deposition rates on a water surface as a function of particle diameter and air velocity. Journal de Recherches Atmosphériques. pg. 911-920.
224. -----, S.L. Sutter and M.T. Dana. 1973. Dry Deposition processes. In: Pacific Northwest Laboratory Annual Report for 1972 to the USAEC Division of Biomedical and Environmental Research. Volume II: Physical Sciences, Part I. Atmospheric Research. pg. 43-49. BNWL - 1751 PT 1, UC-53 Meteorology. Batelle Pacific Northwest Laboratories, Richland, Washington.
225. Siegel, Donald J. and Donald W. Erickson. 1978. Hydrology and ground-water quality of the copper-nickel study region. U.S. Geological Survey, St. Paul, MN.
226. Seltz, John. 1978. Personal Communication. Minnesota Pollution Control Agency, Roseville, MN.
227. -----, and M. West. 1976. Revised by L. King, D. Kelso, G.W. Endersen, D. Thingvold. 1977. Air quality program operations manual. Regional Copper-Nickel Study. Minneapolis, MN.
228. Semrau, Konrad. 1975. Controlling the industrial process sources of sulfur oxides. Advances in Chemistry Series. No. 139. Sulfur Removal and Recovery from Industrial Processes.
229. Shell Engineering and Associates. 1978. Dispersion modeling of the Iron Range from Grand Rapids to Buhl, Minnesota. Report prepared for the Hanna Mining Company.
230. Shepherd, J.C. 1977. Measurements of the direct deposition of sulphur dioxide onto grass and water by the profile method. Atm. Env. 8: 69-74.
231. Singer, Irving A., John A. Frizzola and Maynard W. Smith. 1966. A simplified method of estimating diffusion parameters. J. Air Poll. Cont. Assoc. 16: 594-596.

232. Slade, D.H., ed. 1968. Meteorology and atomic energy 1968. TID-24190. USAEC, Oak Ridge, Tennessee.
233. Slinn, W.G.N. 1974. The redistribution of a gas plume caused by reversible washout. Atm. Env. 8: 233-239.
234. -----, 1976. Some approximations for the wet and dry removal of particles and gases from the atmosphere. U.S. Dept. of Agriculture Forest Service, Tech Rept. NE-23, pp 857-894.
235. -----, and J.M. Hales. 1971. A reevaluation of the role of thermophoresis as a mechanism of in- and below- cloud scavenging. J. Atm. Sci. 28: 1465-71.
236. Smith, Maynard, E. and Irving A. Singer. 1966. An improved method of estimating concentrations and related phenomena from a point source emission. J. App. Meteorol. 5: 631-639.
237. Smith, Jerome P. and Paul Urone. 1974. Static studies of sulfur dioxide reactions. Effects of NO_2 , C_3H_6 and H_2O . Env. Sci. Tech. 8: 742-746.
238. Statnick, Robert M. 1974. Measurement of sulfur dioxide, particulate, and trace elements in copper smelter converter and roaster reverberatory gas streams. EPA-650/2-74-111.
239. Stern, Arthur C., et al. 1973. "Fundamentals of Air Pollution." Academic Press, New York, NY.
240. Stevens, S. 1978. Personal communication. July 19, Air Resources Branch, Ontario Ministry of the Environment.
241. Stokinger, H.E. and D.L. Coffin. 1968. Biologic effects of air pollution. In: Stern, A.C. (ed). "Air Pollution," pp 446-546. Academic Press, New York, NY.
242. Strom, Gordon H. 1976. Chapter 9. Transport and diffusion of stack effluents. In: Stern, Arthur C., (ed) "Air Pollution, Vol. 1 Air Pollutants, their transformation and transport," 3rd ed. Academic Press, New York, NY.
243. Summers, P.W. and P.M. Whelpdale. 1975. Acid precipitation in Canada. In: L.S. Dochinger and T.A. Seliga. 1976. pg. 411-421.
244. Sunderman, F.W., Jr., M.D. McNeely and M.W. Nehay. 1972. Measurements of nickel in serum and urine as indices of environmental exposure to nickel. Clinical Chem. 18: 992-5.

245. Sutherland, R.B. 1959. Respiratory cancer mortality in workers employed in an Ontario nickel refinery covering the period 1930-1957. Toronto: Report of the Div. of Ind. Hygiene, Ontario Dept. of Health.
246. Sutton, O.G. 1953. "Micrometeorology." McGraw-Hill, New York, NY.
247. Thingvold, Daryle. 1978. Personal Communication. Regional Copper-Nickel Study, Minneapolis, MN.
248. -----, R.W. Mustalish, B. Honetschlager and D.T. Feeney. 1979. Characterization of water resources of the Copper-Nickel Study Area. Regional Copper-Nickel Study, Minneapolis, MN.
249. Tsubaki, T. and K. Irukayama, eds. 1977. "Minamata disease (Methylmercury poisoning in Minamata and Niigata, Japan)." Elsevier Sci. Publ. Co., Kodansha, Ltd. New York.
250. Turner, Bruce D. 1969. Workbook of atmospheric diffusion. Pub Health Services Publ. No. 999-AP-26. Cincinnati, Ohio.
251. -----, 1970. Workbook of atmospheric dispersion estimates. U.S. Environmental Protection Agency, Office of Air Programs, Publication No. AP-26.
252. -----, 1979. Atmospheric dispersion modeling. A critical review. J. Air Poll. Cont. Assoc. 29(5): 502-519.
253. Tsuchiya, K. 1969. Causation of ouch-ouch disease (itai-itai byō). Keio J. of Medicine. 18: 181-211.
254. Tyler Germund. 1974. Heavy metal pollution and soil enzymatic activity. Plant and Soil. 41: 303-311.
255. -----, 1975a. Heavy metal pollution and mineralization of nitrogen in forest soils. Nature. 255 (5511): 701-702.
256. -----, 1975b. Effects of heavy metal pollution on decomposition in forest soils. I. Introduction investigations. Lund, Sweden. SNV PM 443E.
257. -----, 1975c. Effects of heavy metal pollution on decomposition in forest soils. II. Decomposition rate, mineralization of nitrogen and phosphorous, soil enzymatic activity. Lund, Sweden. SNV PM 542E.
258. -----, 1976. Heavy metal pollution, phosphatase activity, and mineralization of organic phosphorous in forest soils. Soil Biol. Biochem. 8: 327-332.

259. -----, 1978. Leaching rates of heavy metal ions in forest soils. Water, Air, and Soil Pollution, 9: 137-148.
260. Urone, Paul, et al., 1968. Static studies of sulfur dioxide reactions in air. Env. Sci. Tech. 2(8): 611-618.
261. U.S. Dept. of Health, Education, and Welfare, 1969. Air quality criteria for particulate matter. National Air Pollution Control Administration Publ. No. AP-49. Washington, D.C.
262. -----, 1975. Criteria for a recommended standard.... Occupational exposure to inorganic arsenic. New Criteria 1975. HEW Publ. No. (NIOSH) 75-149.
263. -----, 1976. Criteria for a recommended standard.... Occupational exposure to cadmium. HEW Publ. No. (NIOSH) 76-192.
264. U.S. Environmental Protection Agency, 1973. Guidelines for compiling a comprehensive emissions inventory. Rev. Publ. No. APTD-1135. Research Triangle Park, N.C.
265. -----, 1974. Background information for new source performance standards: Primary copper, zinc and lead smelters. Volume 1: Proposed Standards. U.S. EPA, Research Triangle Park, N.C.
266. -----, 1976a. National air quality and emissions trends report, 1975. Publ. No. 450/1-76-002. Office of Air and Waste Management, Research Triangle Park, N.C.
267. -----, 1976b. Standards of performance for new stationary sources. Primary copper, zinc, and lead smelters. Federal Register. 41(10): 2332-2341. Thursday, January 15.
268. -----, 1977a. Compilation of air pollutant emission factors. AP-42. Third edition (including supplements 1-7). Research Triangle Park, N.C.
269. -----, 1977b. Technical guidance for control of industrial process fugitive particulate emissions. EPA-450/3-77-010. Office of Air and Waste Management, Research Triangle Park, N.C.
270. -----, 1977c. Air quality data--1975 annual statistics including summaries with reference to standards. EPA-450/2-77-002. Research Triangle Park, N.C.
271. -----, 1978a. Federal Register, Vol. 43, No. 118, P. 26384.
272. -----, 1978b. Federal Register, Vol. 43, No. 99. pg. 29539.

273. -----, 1979. Federal Register Volume 44, No. 99, pg. 29539.
274. Veith, David L. 1979. Volume 2. Technical Assessment. Chapter 3, Mineral Processing. Regional Copper-Nickel Report, Minneapolis, MN.
275. Wang, Charles C., et al. 1975. Hydroxyl radical concentrations measured in ambient air. Science 189: 799-800.
276. Watson, B.F. 1976. Minnesota and environs. Weather almanac. 1976. Freshwater biological research foundation. Navarre, MN.
277. -----, 1978a. The climate of the Copper-Nickel Study Region of northeastern Minnesota. Part A: The long-term climatological record. Regional Copper-Nickel Study, Minneapolis, MN.
278. -----, 1978b. The climate of the Copper-Nickel Study Region of northeastern Minnesota. Part B: Weather during the project 1976-1978. Regional Copper-Nickel Study, Minneapolis, MN.
279. -----, 1979a. Meteorological considerations affecting dispersion of atmospheric constituents in the Duluth area. Regional Copper-Nickel Study, Minneapolis, MN.
280. -----, 1979b. Personal communication. Consulting meteorologist. Minneapolis, MN.
281. Weber, Erich. 1970. Determination of the life time of SO₂ by simultaneous CO₂ and SO₂ monitoring. Proc. 2nd Intl. Clean Air Congress. Washington, D.C. pp. 477-481.
282. Weisenberg, I.S. and J.C. Serne. 1976a. Design and operating parameters for emission control studies: White Pine Copper Smelter. EPA-600/2-76-036a.
283. -----, 1976b. Kennecott, Hayden, copper smelter. EPA-600/2-76-036b.
284. -----, 1976c. Kennecott, Hurley, copper smelter. EPA-600/2-76-036d.
285. -----, 1976d. Magma, San Manuel, copper smelter. EPA-600/2-76-036e.
286. -----, 1976e. Phelps Dodge, Ajo copper smelter. EPA-600/2-76-036f.
287. -----, 1976f. Phelps Dodge, Morenci copper smelter. EPA-600/2-76-036g.
288. -----, 1976g. Phelps Dodge, Douglas, copper smelter, EPA-600/2-76-036h.

289. -----, 1976h. Asarco, El Paso, copper smelter. EPA-600/2-76-036i.
290. -----, 1976i. Asarco, Hayden, copper smelter. EPA-600/2-76-036j.
291. -----, 1976j. Kennecott, McGill, copper smelter. EPA-600/2-76-036e.
292. Wendell, L.L., D.C. Powell, and R.L. Drake. 1976. A regional scale model for computing deposition and ground level air concentration of SO₂ and sulfates from elevated and ground sources. Third Symposium on Atmospheric Turbulence, Diffusion and Air Quality. pp. 318-324.
293. Weiss, R.E., et al. 1977. Sulfate aerosol: its geographical extent in the midwestern and southern United States. Science, 196: 979-980.
294. Whelpdale, D.M. and R. W. Shaw. 1974. Sulphur dioxide removal by turbulent transfer over grass, snow and water surfaces. Tellus, 26(1-2): 196-204.
295. Whitby, K.T., et al. 1977. Aerosol formation in a coal-fired power plant plume. Paper No. II. Particle Technology Laboratory Publication No. 335. Progress Report on Sulfur Aerosol Research of the Particle Technology Laboratory, Univ. of Minn., Minneapolis, MN. July 1977.
296. Whitby, L.M., et al. 1976. Ecological consequences of acidic and heavy metal discharges from the Sudbury smelters. Canadian Mineralogist, 14: 47-57.
297. Williamson, Samuel J. 1973. "Fundamentals of Air Pollution." Addison Wesley Publishing Company. Reading, Massachusetts.
298. Wilson, William E., Robert J. Charlson, Rudolf B. Husar, Kenneth I. Whitby, and Donald Blumenthal. 1976. Sulfates in the atmosphere. Presented at the 69th Annual Meeting of the Air Pollution Control Association. June 27 - July 1, 1976. Paper NO. 30.06. Portland, Oregon.
299. Wilson, Wm. E. and Arthur Levy. 1970a. A study of sulfur dioxide in photochemical smog. I. Effect of SO₂ and water upon concentrations in the 1-butene/NO_x/SO₂ system. J. Air Poll. Cont. Assoc. 20(6): 385-396.
300. -----, 1970b. A study of sulfur dioxide in photochemical smog. II. Effect of sulfur dioxide on oxidant formation in photochemical smog. APCA Paper #70-115. Presented at the 63rd Annual Meeting of the Air Pollution Control Association. June 14-18, 1970. St. Louis, Missouri.

301. Yakshina, L.I. and V. Makarov. 1966. Some results of antisilicosis measures at copper mines in the central Urals. Ryc. and Sanit. 31(1): 355-362.
302. Eatough, D.J., et al. 1978. The formation and stability of sulfite species in aerosols. Atm. Env. 12: 263-271.

19555

THE UNIVERSITY OF MINNESOTA

UNIVERSITY COMPUTER CENTER

```

          1 COS(W(1,1W)/57.3))
56. 047127B YSW = 111.1002*(RLAT = W(1,1W))
57. 047132B DST = SQRT(XSW**2 + YSW**2)
58. 047137B IF (ABS(DST).LT.0.0001) DST = 0.0001
59. 047143B WF(IW) = 1./DST
6. 047144B WFS = WFS + WF(IW)
61. 047146B 4.15 CONTINUE
62. 047151B DO 4.16 IW = 1,NW
63. 047152B W(K,J,IW) = WF(IW)/WFS
64. 047152B 4.16 CONTINUE
        C DETERMINE THE SOURCE TO RECEPTOR DIST AND ANG
65. 047163B XLA=55.5851*(SLONG(K)-RLONG(J))*COS(RLAT(J)/57.3)+COS(SLAT(K)
          1/57.3))
66. 047201B YLA = 111.1002*(RLAT(J)-SLAT(K))
67. 047204B SRDIST(K,J) = SQRT(XLA**2 + YLA**2)
68. 047214B 4.16 SRANG(K,J) = ATAN2(YLA,XLA)
        C DETERMINE THE WEATHER WEIGHTS AT THE RECEPTOR
69. 047227B DO 4.22 J = 1,NR
7. 047230B WFS = .0
71. 047230B DO 4.25 IW = 1,NW
72. 047233B XSW = 55.5851*(PLONG(J) - W(1,1W))*COS(RLAT(J)/57.3) +
          1 COS(W(1,1W)/57.3))
73. 047254B YSW = 111.1002*(RLAT(J) - W(1,1W))
74. 047257B DST = SQRT(XSW**2 + YSW**2)
75. 047264B IF (ABS(DST).LT.0.0001) DST = 0.0001
76. 047270B WF(IW) = 1./DST
77. 047271B WFS = WFS + WF(IW)
78. 047273B 4.25 CONTINUE
79. 047276B DO 4.26 IW = 1,NW
8. 047277B WWR(J,IW) = WF(IW)/WFS
81. 047277B 4.26 CONTINUE
82. 047306B 4.26 CONTINUE
        C PREP ZERO MAIN ARRAYS
83. 047310B DO 9.00 J=1, NR
84. 047311B III(J)=IIF(J)=0
85. 047311B DAYC(J)=SRAIN(J)*XMAX(J,1)*XMAX(J,2)*0.3
86. 047314B DO 45 I = 1,NM4
87. 047320B DO 45 L = 1,2
88. 047322B 45 DMXX(I,L,J) = 0.
89. 047334B DO 46 I = 1,16
9. 047336B DO 46 L = 1,4
91. 047340B WROSE(L,I,J) = 0.0
92. 047350B 4.00 CONTINUE
        C MAIN LOOP(9.0) ON DAYS FROM START OF THE WEATHER. II IS DAY COUNTER
93. 047353B II =
94. 047353B 9.1 CONTINUE
95. 047355B II=II+1
        C READ IN THE WEATHER FOR THE DAY
96. 047356B READ(7,536) (IW4(I),IW5(I),IW6(I),W(J,I),J=1,9),I=1,NW)
97. 047403B IF(IW4(1).EQ.0) STOP 1.00
98. 047405B IY=IW4(1) $ IM=IW5(1) $ IO=IW6(1)
101. 047417B IDATE = IY*1000 + IM*100 + IO
        C MAIN LOOP(2.00) ON RECEPTORS(J), UP TO 50 ALLOWED
102. 047414B DO 2.00 J=1,NR
        C ELIMINATION OF DAYS NOT TH MEASURED TIME PERIODS
103. 047417B IF(IY.EQ.IYRI(J).AND.IM.EQ.IMRI(J).AND.IO.EQ.IDRI(J)) III(J)=II
104. 047430B IF(III(J).EQ.0.OR.IIF(J).NE.0) GO TO 2.00
105. 047432B IF(IY.EQ.IYRF(J).AND.IM.EQ.IMRF(J).AND.IO.EQ.IDRF(J)) IIF(J)=II
106. 047442B MDAY = IM*100 + IO
107. 047444B ISSW = 0 $ IF(MDAY.LT.ISSUM.OR.MDAY.GT.IESUM) ISSW = 1
        C DO A WEIGHTED INVERSE DISTANCE AVERAGE OF THE WEATHER AT RECEPTOR
109. 047453B RT = OMR = TDR = XX = YY = SDVWR = SDMWR = 0.0
11. 047456B DO 2112 IW=1,NW
111. 047461B WB = WWR(J,IW) $ YT = W(6,IW) $ YTT = W(7,IW)
114. 047470B RT = RT + W(1,IW) * WG
115. 047473B OMP = OMR + W(2,IW)*WG

```

195537

THE UNIVERSITY OF MINNESOTA

UNIVERSITY COMPUTER CENTER

```

116. 474768 TOR = TOR + W(6,1W)*WG
117. 475018 XX = XX + TT*CCOS(TTT)*WG
118. 475118 YY = YY + TT*SIN(TTT)*WG
119. 475168 SOVWR = SOVWR + W(6,1W)*WG
12. 475218 SOVWR = SOVWR + W(9,1W)*WG
121. 475238 2122 CONTINUE
122. 475268 AVWR = SQRT(XX*XX + YY*YY)
123. 475338 AMWR = ATAN2(YY,XX)
124. 475358 SOVWR = SOVWR/SQRT(24.1)
124. 475378 C SUM THE TOTAL INCHES OF RAIN
SRAIN(J) = SRAIN(J) + RT
C COLLECT DATA NECESSARY FOR THE 16 FT WIND ROSE
126. 475428 A = 250.75 - AMWR*57.31
127. 475458 IF(A.GT.361.) A = A - 361.0
128. 475498 IA = IFIX(A/22.5) + 1
129. 475528 WRUSE(1,IA,J) = WRUSE(1,IA,J) + AVWR
13. 475558 WRUSE(2,IA,J) = WRUSE(2,IA,J) + 1.0
131. 475618 WRUSE(3,IA,J) = WRUSE(3,IA,J) + AVWR*AVWR
132. 475658 WRUSE(4,IA,J) = WRUSE(4,IA,J) + SOVWR
C CALCULATE MONTHLY MIXING HEIGHT FROM BEST SIN FIT TO SITE DATA
MMAX=1.07+0.51*CCSIN(IM-3.)*0.524
133. 475718 C COMPUTE DRY DEPOSITION AND SCAVAGING COEFFS
WCS04 = 46.*DMR**0.77/(300.*744.*DMR**0.15)
135. 476128 C1 = 2.88E-3*DMR/(377.*744.*DMR**1.05)*XKAL(IM)/ATMP(IM)
134. 476248 DO 56 I = 1,NM
137. 476278 56 WCM(I) = C1*WCM(I)
138. 476328 IF(ISSW.LT.1) THEN
134. 476348 C COMPUTE SUMMER DRY DEP + SCAVAGING COEFFS
QWCS02 = C1*WCS02
14. 476358 DFS02 = SDFS02 & DFS04 = SDFS04
142. 476418 ELSE
C COMPUTE WINTER DRY DEP + SCAVAGING COEFFS
143. 476428 WWS02 = ...
144. 476428 IF(DMR.GT.0.0001) WWS02 = WWS02*1.43E-3*DMR/(300.*744.*DMR
1*0.105)*XKAL(IM)/ATMP(IM)*(1.0-EXP(-2.0*(1.50+0.44*ALOG(DMR))))
145. 476728 DFS02 = WDFS02 & DFS04 = WDFS04
147. 476748 ENDIF
148. 476758 DO 55 I = 1,NM
149. 476778 55 CM(I) = DM(I) = .
C LOOP OVER THE SOURCES
15. 477128 DO 460 K=1,NSS
C DETERMINE THE WEATHER HALF-WAY BETWEEN THE SOURCE AND RECEPTOR FOR
C USE WITH LOSSES EN ROUTE AND THE BOX SIZE
151. 477158 TD = XX = YY = SOHW = .
152. 477178 DO 2122 IW = 1,NW
153. 477128 WG = WW(K,J,1W)
154. 477168 TT = W(6,1W) & TTT = W(7,1W)
155. 477238 TU = TD + W(4,1W)*WG
157. 477268 XX = XX + TT*CCOS(TTT)*WG
158. 477368 YY = YY + TT*SIN(TTT)*WG
159. 477418 SOHW = SOHW + W(1,1W)*WG
16. 477458 2122 CONTINUE
161. 477518 SOHW = SOHW * 1.2
162. 477518 AVW = SQRT(XX*XX + YY*YY)
163. 477568 AMW = ATAN2(YY,XX)
164. 477618 SHD = SRDIST(K,J) & ASR = SRANG(K,J) & QMOLD(2,K) = 0.0
C AUX ANGLE, RECEPTOR SOURCE TO WIND DIRECTION, STOP IF GT PIE/2
AUX=ABS(AMW-ASR) & IF(AUX.GT.3.14159)AUX=ABS(6.28318-AUX)
167. 477718 IF(AUX.GT.3.14159/2.) GO TO 4000
168. 477818 XSR = SRD*CCOS(AUX) & YSR = SRD*SIN(AUX)
17. 478018 C DETERMINE WIND SPEED AT STACK HEIGHT
TH = SHHEIGHT(K)/4.
172. 478018 AVX = LVW*(.03*TH**0.1 + .34*TH**0.15 + .091*TH**0.2 + .597
1*TH**0.25 + .275*TH**0.3)
173. 478138 C TIME TO REACH RECEPTOR DIST ALONG WIND HEADING(MOURS), STOP IF GT 24
T = XSR/AVX & IF(T.GT.24.) GO TO 4000

```



```

289. 0507200 C COMPUTE WIND ROSE FOR PRINTOUT. 1=AV. 2=FREQ. 3=5.0.
      RSUM = 0
290. 0507200 DO YA I = 1,16
291. 0507200 76 RSUM = RSUM + WROSE(2,I,J)
292. 0507300 DO J J = 1,16
293. 0507310 IF (WROSE(2,I,J).GT.0.) THEN
294. 0507360 WROSE(1,I,J) = WROSE(1,I,J)/WROSE(2,I,J)
295. 0507370 WROSE(4,I,J) = WROSE(4,I,J)/WROSE(2,I,J)
296. 0507400 ENDIF
297. 0507410 IF (WROSE(2,I,J).GT.0.) THEN
298. 0507430 WROSE(3,I,J) = SORT((WROSE(3,I,J)-WROSE(1,I,J)+2*WROSE(2,I,J))/
      1(WROSE(2,I,J)-1, 1))
299. 0507520 ELSE
300. 0507540 WROSE(3,I,J) = 0.0
301. 0507560 ENDIF
302. 0507560 77 WROSE(2,I,J) = WROSE(2,I,J)/RSUM
      C PRINT OUT THE PERIOD RESULTS
303. 0507620 WRITE(6,602) (NAMES(I),L=1,4),SRAT(J),RONS(J),
      1(YR(I),IMR(I),IDR(I),IYR(J),IMR(J),IDR(J))
304. 0510160 WRITE(6,604) SRAT(J)
305. 0510230 WRITE(6,605)
306. 0510260 WRITE(6,606) (WROSE(1,I,J),I=1,16),/(WROSE(3,I,J),I=1,16),/
      1(WROSE(4,I,J),I=1,16),/(WROSE(2,I,J),I=1,16)
307. 0510700 WRITE(6,607)
308. 0510770 WPLYR(6,608) ((NAMES(I),L=1,4),SRAT(J),SRANG(I,J),
      1(NAMES(I+1),L=1,4),SRD1ST(I+1,J),SRANG(I+1,J),I=1,NSS*2)
      WRITE(6,609) XMAX(J,2),NMAX(J,2),XMAX(J,1),NMAX(J,1)
309. 0511530 WRITE(6,610)
310. 0511660 IK = 2HS2 $ IIII = 2HS4
311. 0511710 WRITE(6,611) IK,DMAX(1,2,J),IIII,DMXX(2,2,J)
      1(METALN(I=5),DMXX(I,2,J),I=6,NM4)
312. 0511730 WRITE(6,611) IK,TOSA,IIII,PHA
      1(METALN(I=5),DMXX(I,1,J),I=6,NM4)
313. 0512230 WRITE(6,612)
314. 0512250 WRITE(6,611) IK,TOSA,IIII,PHA
315. 0512310 WRITE(6,632) TOS#,TOSD
316. 0512570 632 FORMAT(7,5X,4MET S04 =#F9.3+ DRY S04 =#F9.3)
317. 0512570 2000 CONTINUE
318. 0512610 GO TO 90
319. 0512610 599 FORMAT(1M1//# MODIFIED BOX MODEL FOR SULFUR AND METAL LOADING//)
320. 0512610 525 FORMAT(A13)
321. 0512610 531 FORMAT(2X,A2,4E11.4)
322. 0512610 531 FORMAT(2X,A2,4E11.4)
323. 0512610 532 FORMAT(15,3A10,2F9.4,F7.1,F5.2,7E11.4,/,5X,13E10.4)
324. 0512610 534 FORMAT(15,3A10,2F9.4,2X,3I2,2X,3I2)
325. 0512610 536 FORMAT(16X,3I2,F5.3,2F8.5,2F3.0,3X,4F7.4)
326. 0512610 603 FORMAT(1M1//,1X,15,2X,3A11,2X,#LATTITUDE =#F8.4# LONGITUDE =#
      1F8.4# START TIME =#I3,2I2# STOP TIME =#I3,2I2)
327. 0512610 604 FORMAT(7,5X,WIND ROSE(16 PYS,1,2,1,2,1,2,1,2,1,2,1,2,1,2)
      1#SSE S SSW SW WSW W ENE E ESE NW SE NNW#)
328. 0512610 607 FORMAT(7,5X,#SOURCE TO RECEPTOR DISTANCE(KM) AND HEADING #,
      1#ANGLE(C FROM EAST) FOR#I3# SOURCES#/)
329. 0512610 606 FORMAT(5X,#MEAN WIND(KM/H)#,16F7.2,/,5X,#WIND S.D.(KM/H)#
      1,16F7.2,/,5X,#MEAN WIND S.D.#,16F7.3,/,5X,#FREQUENCY #,16F7.4)
330. 0512610 608 FORMAT(2(5X,15,2X,3A11,2F8.2))
331. 0512610 609 FORMAT(7,5X,#MAXIMUM DAILY CONCENTRATION OF SO2 =#F9.3
      1#(UG/M3) ON#I7# = MAXIMUM DAILY DEPOSITION OF SO4 =#F9.3
      2#(KG/HA) ON#I7)
332. 0512610 610 FORMAT(7,5X,#PERIOD AVERAGE CONCENTRATIONS (SULFUR UG/M3): #,
      1*(METALS NG/M3)#)
      FORMAT(2(7,5X,9(A2##F9.3,2X)))
333. 0512610 612 FORMAT(7,5X,#PERIOD AVERAGE DEPOSITIONS (SULFATE KG/HA): #,
      1*(METALS G/HA)#)
334. 0512610 616 FORMAT(# NO.SOURCES=#I3# = NO.RECEPTORS=#I3# = NO.WEATHER STA=#I3
      1# = NO.METALS#I3# = START TIME #I3I2# = STOP TIME #I3I2)

```

UNIVERSITY COMPUTER CENTER 19554

```

341. 051261B 618 FORMAT(/IX#ELEMENTAL DATA = NAME = DRY DEPOSITION(CM/SEC) = WASHR
      051261B 620 WET RATIO = BACKGROUND CONCENTRATION(UG/CM3)A)
342. 051261B 621 FORMAT(/IX#SOURCE DATA = NAME = LONG = LAT = HEIGHT(M) = WIDTH (MM
      051261B 622 1) = HEAT RATE(CAL/SEC) = EMISSION OF SO2+SO3+METALS(LINE 2) = ALL I
      051261B 623 2N (GM/SEC)B)
343. 051261B 623 FORMAT(/IX# RECEPTOR DATA = NAME=IPX# = LONG = (LAT)
      051261B 624 1) = WEATHER = WIND = 250.0,3.0X#TOTAL S = 4F10.4)
344. 051261B 7.0
345. 051261B 7.0 FORMAT(0(5(2F.42,2E1.4),/))
346. 051262B
      END
  
```

```

1. 000000B FUNCTION ZWC502(CH12,DNR,QWCSO2,ISSW,HEX,HENRY,XKEQ)
2. 000000B DIMENSION T(12),P(12)
3. 000000B DATA IP,P/1.0,9.9,9.9,9.9,9.9,9.9,9.9,9.9,9.9,9.9,9.9,9.9/
4. 000000B DATA T/270.2,270.2,270.2,270.2,274.5,282.9,287.2,290.0,297.7,293.8,
5. 000000B 1276.8,270.2,270.2/
6. 000000B IF(CH12.LT.1.0E-10.0R.DNR.LT.1.0E-4) THEN
7. 0000360 ZWC502 = QWCSO2
8. 000041B RETURN
9. 000041B ENDF
10. 000041B HENRY = EXP(9.94 - 3.49.0/T(1M))/(.082*57.0/T(1M))
11. 0000560 XKEQ = EXP(-10.3 + 1781.0/T(1M))
12. 0000560 CH12 = CH12*1.0E-3 $ THEX = HEX*32.0
13. 000091B WASHR = (1.0/HENRY + THEX/CH12*(SORT(1.0 + CH12*XKEQ*64.0/
14. 000075B (HENRY*THEX**2))-1.0))
15. 0000770 IF (ISSW.LT.1) THEN
16. 0001070 ZWC502 = WASHR*DNR*1.0E-3/(300.0+744.0*DNR*.15)
17. 000110B ELSE
18. 000132B ZWC502 = WASHR*DNR*1.0E-3/(400.0+1488.0*DNR*.105)
19. 0001340 1(1.0 - EXP(-2.0*(1.5A*2.44*ALOG(DNR))))
20. 000132B ENDF
21. 0001340 IF (IP.LT.100) PRINT,CH12,DNR,WASHR,ZWC502,HENRY,XKEQ
22. 0001470 IP = IP + 1
23. 0001510 RETURN
24. 0001530 END
  
```

APPENDIX B

List of Abbreviations

ACGIH--American Conference of Government Industrial Hygienists
 BWCA--Boundary Waters Canoe Area
 CDM--Climatological Dispersion Model
 ESP--Electrostatic Precipitator
 LD--Lethal Dose
 MEQB--Minnesota Environmental Quality Board
 NIH--National Institutes of Health
 NSPS--New Source Performance Standards
 PSD--Prevention of Significant Deterioration
 STEL--Short-Term Exposure Limit
 TCA--Turbulent Contact Absorber
 TEM--Texas Episodic Model
 TLV--Threshold Limit Value
 TWA--Time Weighted Average
 VNP--Voyageurs National Park

Elements

As--Arsenic	Fe--Iron	Pb--Lead
Cd--Cadmium	Hg--Mercury	S --Sulfur
Cu--Copper	Ni--Nickel	SO ₂ --Sulfur Dioxide
TSP--Total Suspended Particulates		

Units

°C--Degrees Centigrade	gm/sec--Grams Per Second
°K--Degrees Kelvin	cal/sec--Calories Per Second
ppm--Parts Per Million	m ³ /sec--Cubic Meters Per Second
ppb--Parts Per Billion	m/sec--Meters Per Second
mtpy--Metric Tons Per Year	kg/ha/yr--Kilograms Per Hectare Per Year
um--Microns	g/ha/yr--Grams Per Hectare Per Year
ml--Milliliter	
km--Kilometer	
km/hr--Kilometers Per Hour	µg/l--Micrograms Per Liter
%/hr--Percent Per Hour	
ng/m ³ --Nanograms Per Cubic Meter	
µg/m ³ --Micrograms Per Cubic Meter	